LIVING TREES

AS

STRUCTURAL ELEMENTS

FOR

VERTICAL FOREST ENGINEERING

TESSA LIEVESTRO

LIVING TREES AS STRUCTURAL ELEMENTS FOR VERTICAL FOREST ENGINEERING

By

TESSA LIEVESTRO

In partial fulfilment of the requirements for the degree of
Master of Science
in Civil Engineering - Building Engineering
at the Delft University of Technology,
to be defended publicly on Wednesday, November 11, 2020, at 12:00.

Date   November 2, 2020
Student number   4378539

Thesis committee
Prof.dr.ir. J.W.G. (Jan-Willem) van de Kuilen | TU Delft
Drs. W.F. (Wolfgang) Gard | TU Delft
Ir. Hoessein Alkisaei | TU Delft
Ir. Pieter Timmerman | Arcadis
Ir. Xiuli Wang | TU Delft

An electronic version of this thesis is available at http://repository.tudelft.nl/.

PREFACE

This thesis report marks the end of my career as a student at the Delft University of Technology. The master thesis is part of the requirements to obtain a Master of Science Degree in Civil Engineering.

About a year ago, I read an article by Xiuli Wang in which she writes on the implementation of trees in building designs. I found this a fascinating concept and contacted her immediately to learn more about it. I got welcomed to the vertical forest family by Xiuli, Jan-Willem van de Kuilen, and Wolfgang Gard.

With lots of joy, I have dived into the wonderful world of trees, learned about their behaviour, strengths, and weaknesses. I would like to thank my committee members for accompanying me during this swim and providing useful criticism during meetings. Moreover, I would like to thank Hoessein Alkisaei for asking me: *Hoe gaat het?* and helping me prepare for the difficult questions.

Special thanks go to Pieter Timmerman and my other colleagues at *Arcadis* for helping me with the practical aspects of applying trees as structural elements to their *Wonderwoods* project. Furthermore, I am very grateful that *Arcadis* has provided financial support for carrying out winching tests. These tests added an essential part to my research and gave me one of the best learning experiences I have had.

Speaking of winching tests, I would also like to thank Dennis de Goederen from *Pius Floris Boomverzorging* with helping me carry out the tests. His knowledge about trees and their behaviour is mind-blowing. Moreover, I would like to thank Xiuli for helping me with the geometry measurements and the staff of the botanical garden for giving me the freedom to perform the tests as long as I did not harm the trees.

At last, I would like to thank my friends and family for all their help and putting everything in perspective. Oskar, my appreciation goes to you, for being locked up with me in one apartment supporting me regardless of my good or bad moods.

Tessa Sophia Prevestro

Delft, November 2020

ABSTRACT

The application of vertical forests in the building industry is a popular development with promising advantages regarding sustainability. However, placing trees along a façade gives additional loads which often results in extra material use. This is undesired concerning building design, costs, and the environment. To mitigate these adverse effects, trees could be used as load-bearing structural elements. To increase the stability of such elements, it might be advantageous to connect the trees to each other. Such connections can naturally be created with inosculations: self-growing connections in which the bark and inner tissue of two trees merge.

Applying living trees as structural elements requires a deeper understanding of both the botanical and structural behaviour of trees. Likewise, more must be known about the botanical and structural behaviour of self-growing connections. This research expands the knowledge on the topic of using living trees as structural elements, both as single tree elements and self-growing interconnected tree elements. This aim is reached by proposing a structural model of (interconnected) trees, which is verified by comparing the outcome of the model with the outcome of winching tests. Furthermore, a design is made in which living trees are used as structural elements in a vertical forest case study. This lays the groundwork on how to approach a living tree design, both from a structural and botanical point of view.

The structural model is verified by carrying out winching tests on the *Living Tree Pavilion,* including one single tree, one pair of cross-connected trees and one pair of parallel-connected trees. Additionally, winching tests are performed on a tree in an airpot, in which boundaries constrain the root system. During the winching tests, a force is applied to the tree system, and the elongation is measured on several locations of the tree, providing insight into the strain distribution. Additionally, the displacement of the trees is measured at the height of the force application. Based on geometry measurements, the trees are modelled as solids in a finite element software. From the models of the interconnected trees, a compound solid is created which behaves like a single solid. The winching load is applied to the models to allow for a comparison between the results of the winching tests and the models.

The geometry measurements show indications that leaning trees create an oval cross-section, which is influenced by the presence of inosculations. The winching tests show that an unconstrained root system is stiffer than a root system constrained by an airpot. Furthermore, the tests show that interconnected trees do not have favourable stiffness qualities compared to single trees. A comparison between the model and test results indicates that the finite element model is a plausible representation of reality for the single tree, the parallel-connected trees, and the out-of-plane results of the cross-connected trees. The finite element model fitted poorer with the in-plane winching test results of the cross-connected trees. More research is needed to determine whether diverging tree characteristics, in the direction that is rarely subjected to loads, could explain the discrepancy in measured and modelled behaviour.

Two designs are created in which living trees of the *Wonderwoods* vertical forest carry the loads of a plant container. There are three reasons why cross-connected trees are not favourable over a design with single trees. First, the single trees can bear the plant containers at a younger age. Second, the risk of trees not creating suitable inosculations is high. Third, as interconnected trees share one container, the competition for space can become fierce.

This research concludes that a system of interconnected trees as structural elements is not favourable over a system of single trees. This is mainly because no clear advantages in terms of strength and stability could be found in both the winching tests and the design for *Wonderwoods*.

TABLE OF CONTENTS

1 INTRODUCTION

Isn't it a pity that trees are always cut before they can be used as a building material while living trees have so many advantages for the environment? This thesis explores the possibilities of using trees in constructions whilst keeping them alive.

Figure 1.1 shows an example. It is an artwork by Karsten Födinger (2020) in which trees carry a concrete slab. Unfortunately, most of the trees cracked after a while because the concrete slab slipped over the bark and blocked the tree's nutrition transport.

This example illustrates the problem with using living trees as a structural element, which is the lack of knowledge on the growth behaviour and structural capacity of trees. The change of tree characteristics over time asks for a process-based approach for engineers and architects.

The same holds for inosculations, which are connections that trees can naturally create

Figure 1.1 Artwork by Karsten Födinger in La Vallée in France (Födinger, 2019)

between stems or branches when these are pressed together. Creating interconnected trees could increase the stability of living tree elements. This research investigates how this technique works and whether it is favourable for construction.

The basis for this research will be a literature study, followed by data gathered from winching tests in which both single and interconnected trees will be pulled. From these tests, the displacements and the distributions of strain through the (interconnected) trees will be observed. Based on these results, a method for creating a structural model of living trees and their inosculations will be proposed.

The concept of building with living trees will be applied to the Wonderwoods vertical forest project. This lays the groundwork on how to approach a living tree design, both from a structural and botanical point of view. A 'vertical forest' is a promising and popular design concept in which trees are placed on the balconies of a residential tower. Often these trees result in large loads on the structure, requiring extra material use. To mitigate these adverse side effects, the trees will be given a structural function. Designs with either single standing or interconnected trees will be compared.

The reader will be further introduced to the problem context in chapter 2, which will be followed by the research description, including the problem statement and research aim, in chapter 3. Chapters 4 and 5 contain a theoretical background about the botanical and structural behaviour of trees and self-growing connections. Chapter 6 describes the methodology of geometrical measurements and pulling tests carried out on both single standing and interconnected trees, which is followed by the results in chapter 7. In chapter 8, the theory will be applied to a case study design. The report finishes with a discussion and conclusion in chapter 9 and 10.

2 PROBLEM CONTEXT

Background information is required to form a good understanding of the research subject. In this chapter, several topics are discussed, starting with the current applications of vertical forests and followed by examples of structures that are built with living trees.

2.1 CURRENT APPLICATIONS OF VERTICAL FORESTS

A vertical forest can be defined as a large number of trees, planted along the façade of a high-rise structure. To be a 'forest', a variety of trees needs to be planted that can attract birds and insects. This creates an urban ecosystem and increases the biodiversity in a city.

The first vertical forest is the *Bosco Verticale* in Milan, Italy, which was finished in 2014. It is designed by the architect Stefano Boeri as a prototype for his vision of a new architectural biodiversity, in which he focusses on the relationship between humans and other living species (Boeri, 2016). Figure 2.1 shows a photo of the project, consisting of two towers stacked with 711 trees.

Boeri (2016) states several advantages of creating such buildings densely populated by nature and people. Firstly, vertical forest buildings reduce the pollution of the urban environment because the vegetation on the buildings can absorb fine particles and CO_2. Furthermore, the vegetation produces oxygen and act as a shield to noise pollution for the inhabitants. Additionally, placing vegetation in a city reduces the heat island effect and creates rich biodiversity. By placing vegetation on, or in front of a façade, the energy consumption of a building is reduced. At last, a vertical forest works as an anti-sprawl device. Up till now, living so close to trees could only be found in single-family homes with gardens in a suburban area. Stacking these homes and gardens saves space and thus creates extra land for nature (Boeri, 2016).

Figure 2.1 Bosco Verticale in Milan, Italy

After the completion of this prototype, many more vertical forests were designed and created. The idea of a vertical forest has also reached The Netherlands. An example is *The Valley*, a multifunctional building in Amsterdam, that is currently under construction. Other designs with a vertical forest are *Wonderwoods* in Utrecht, *Vertical* in Amsterdam, and *Trudo* in Eindhoven (Hannema, 2019).

2.1.1 Trees in structural design

In most vertical forest projects, the trees are placed at the outermost part of the balconies, requiring extra structural measures due to their considerable weight. Three projects are evaluated to get an idea of the magnitude of these loads. These are *The Valley*, *Bosco Verticale* and *Wonderwoods*.

The small trees and other plants used in *The Valley* put an extra burden to the structural design. *Van Rossum* engineers modelled all the trees and plants as deadloads on the construction. With the help of a landscape architect, reasonable loads were determined, which are in between 6 and 10 kN/m², consisting mainly of the weight of the planting containers and soil. Locally, this could increase the needed reinforcement with up to 25 to 50 per cent compared to balconies without any plants or trees (Brahmatewari, 2020).

Also in *Bosco Verticale*, the trees are placed on overhanging balconies. Just as in *The Valley*, the deadload of the trees mainly comes from the containers and soil. For plants up to three meters this deadload is 11kN/m, and for trees up to six meters this deadload is 13kN/m. Trees with a minimum base of three meters even have 7kN/m extra. The growth of the tree is incorporated in the design. For example, a six-meter-tall tree doubles its weight over its lifetime from 300 to 600kg. Furthermore, dynamic stresses from wind loads are added. For this, a geometric-dimensional study was carried out to determine the height of the trunk, the area and centre of gravity of the foliage, and the air permeability (Boeri, 2016).

In *Wonderwoods,* the trees are placed in containers with an inner area of 4,2 square meters filled with a soil layer of one meter deep. The trees and soil together create a load of 45kN per container. In this building, the trees are planted with a height of 4,5 meters. The trees can grow up to a height of two floors, which is six meters. In contrast to the other two buildings, the trees are not placed on the balconies but are directly connected to the load-bearing walls of the building (Cents T. , et al., 2018).

Table 2.1 shows a comparison of the trees and loads between the three mentioned vertical forest projects. It is assumed that the containers of the *Bosco Verticale* have a width of 1,5 meters.

Table 2.1 Tree + soil loads in three projects

Project	Deadload of tree container	Height of trees
The Valley	6-10 kN/m^2	2 m
Bosco Verticale	7-13 kN/m^2	3-6 m
Wonderwoods	11 kN/m^2	4,5-6,6 m

2.1.2   Anchoring

Because the deadloads of the tree system mainly come from the containers and soil, the designers attempt to keep the containers as small as possible. This, however, hinders the growth of the roots and negatively influences the tree's foundation. Thus, additional measures must be taken to ensure the stability of the trees. For example, in *Wonderwoods*, the root-balls are anchored to the container underneath by a steel basket (Telgen, 2018). The same goes for the trees in *Bosco Verticale* that are subjected to the highest wind loads (Boeri, 2016). All other trees in this project have a horizontal frame in the pot to prevent the tilting of the trunk away from the soil.

Connecting the trees with steel cables to the balcony above mitigates the risk of falling branches or tree parts. Additionally, it prevents the falling of the tree in unexpected extreme conditions (Boeri, 2016; Koninklijke Ginkel Groep, 2018).

2.2   CURRENT APPLICATIONS OF LIVING TREE STRUCTURES

This paragraph discusses the advantages of trees as construction elements, followed by examples of living tree structures. Living tree structures are structures in which the primary structural system consists of multiple trees.

2.2.1   Advantages of trees as structural elements

Trees have several structural advantageous characteristics compared to traditional construction elements such as steel and concrete. First, trees can repair weak spots themselves. They also do not have to be overdesigned, because they can adapt, although slowly, to changing loads. By creating the most optimal shape, the wood can make optimal use of its strength and durability qualities (Nuijten, 2011).

2.2.2   Advantages of natural connections between trees

Trees can naturally form a connection with non-living elements or with other trees; the latter is called inosculation. Back in 1884, the French botanist Philippe Van Tieghem observed that connections occur naturally between trees of the same species. In such a connection, the wood tissue of both trees is intertwined, and common rings are created around the two original stems (Nuijten, 2011). Van Tieghem noticed that if one of the trees is cut below the connection, the other tree provides the necessary resources to the cut tree (Millner, 1932; Van Tieghem, 1884). This proves that trees can exchange water and nutrients.

A connection between trees can help to reduce the stresses in individual trees which makes the total system more resilient to various load situations. Pulling tree tests have proven that the stiffness of interconnected trees is larger than the stiffness of single standing trees (Borská, 2018).

Connected trees are building components with valuable possibilities for living tree structures (Ludwig, 2012). Structurally, this building technique is advantageous because the connections can develop great mechanical load-carrying capacity. Furthermore, with this technique, smaller plants can be connected, creating a larger organism. This is further explained in paragraph 4.4.1 Speed up of living tree construction

Next to the structural advantages, connecting trees has aesthetical value. Connections perfectly show the interaction between nature and technique. The connections are naturally created, but this only happens because they are first technically jointed (Ludwig, 2012).

2.2.3   Examples of living tree structures

In the Meghalaya Mountains in India, the principle of interconnecting trees is already applied for many years in living tree bridges, see figure 2.2 on the top. These bridges are built by guiding and connecting the roots of the Indian Rubber Fig. First, a deadwood bridge is built, and one Fig tree is placed on either side of the bridge. The roots of the Fig, which can grow from both branches and stem, are guided over the bridge. When they find rocks, soil, or another tree, they start to thicken, forming rope-like wood to resist tension stress. When they grow older, they start creating normal wood, which makes them able to resist compression forces. Grafts are made to connect the roots and branches of the trees. After several years, the two Figs have grown the total span of the bridge. Remarkably, the circumference of the trees grows in an asymmetrical and non-circular shape, which is the result of a demand-driven addition of biomass (Hundert & Pfeiffer, 2019).

In Europe, examples of living tree structures are mainly built in Germany for recreational or research purposes by the research group *Baubotanik-Living Architecture* at the University of Stuttgart.

Figure 2.2 on the bottom shows *Der Steg*, a walkable canopy with columns made of living willows, constructed in 2005. First, several willows were bonded together to ensure its initial strength. Over time the willows grew together into interconnected elements.

Figure 2.2 Top: Living tree bridge (Hundert & Pfeiffer, 2019). Bottom: Der Steg one year after completion (Ludwig, 2014)

The *Baubotanik-Tower* is a living tree 'building', constructed in 2009. It is a rhombic structure of White Willows carrying three non-living floors as can be seen in figure 2.3 on the left. White Willows were chosen because of their moisture-resistance, which is necessary for the wet marsh-like meadow. Furthermore, willows grow very fast, which is favourable for the creation of connections between trees. The right image in figure 2.3 shows that

the willows are placed in pairs, encouraged to merge over their length. At the connection between the willows and the floors, the willows are encouraged by screws to create crosswise inosculations. Until the willows are large and strong enough, the structure is carried by a temporary steel structure. It was expected that it would cost about eight years before this structure could be removed (Ludwig, 2012; Nuijten, 2011).

Figure 2.3 Left: Baubotanik-Tower after completion, Middle: and one year later (Ludwig, 2014). Right: Willows around a connection (Ludwig, 2012)

The third structure by this research group is the *Plane-Tree-Cube* in Nagold, created in 2012, as shown in figure 2.4. It is the first building designed for public use, as it is supposed to act as a vertical pocket park for the inhabitants of the urban area.

In the Netherlands, a small-scale living tree structure is constructed in 2011 by the TU Delft student Anne Nuijten, see figure 2.4. She designed the *Living Tree Pavilion* in which a viewing platform is supposed to be carried by trees. Until the trees have the required strength, the platform is carried by timber columns. The trees itself are connected with ropes by parallel-, cross-, and grafted-connections to create a stable structure (Nuijten, 2011).

Figure 2.4 Left: Plane-Tree-Cube three years old and, Middle: visualization of future situation (Ludwig, 2014), Right: Design Living Tree Pavilion (Nuijten, 2011)

2.2.4 Research results of first living tree structures
As the structures mentioned above were created a couple of years ago, first observations of their growth are available.

Based on the findings of *Der Steg,* it can be concluded that the main geometry of the construction does not change over time, because only the top part of the tree increases in height. The older and lower parts, to which the construction is connected, only increases in thickness. Also, this

structure clearly shows that many of the bundled willows were dying, giving the stronger ones the chance to grow and replace them. A third observation is that mostly the diagonally placed willows did not perform well. This proves that it is unfavourable if trees deviate much from their natural vertical position (Ludwig, 2014).

Unfortunately, there are no promising results of the *Baubotanik-Tower*. The tower was located on an open field which made it possible for frost to get into the planting pots. This damaged the plants so much that they had to be replaced (Höpfl, 2020).

Seven years after the *Living Tree Pavilion* was created, its growth is observed by the student Helena Borská. Initially, it was expected that the trees could be fully load-bearing in 2021, after ten years of growth. Borská observed in 2018 that some trees had died and were replaced by newly planted trees. Furthermore, not all expected connections were created. She, therefore, adjusted the expected year that the structure will be load-bearing to 2023. She also performed pulling tree tests to determine the difference in stiffness of trees with and without connections. These tests showed that connections positively influence the stiffness in both the direction along the connection as the direction perpendicular to the connection (Borská, 2018).

3 RESEARCH DESCRIPTION

3.1 PROBLEM DEFINITION

The application of vertical forests in the building industry is a promising and popular development regarding sustainability. However, placing trees on balconies gives extra static and dynamic loads which usually results in extra material use in the stability structure of such buildings. This is undesired concerning building design, costs, and the environment.

What could help mitigate the adverse effects of the trees on the structural system is for the trees to carry part of the loads. The trees become a structural element which reduces the need for traditional structural elements. This, however, results in some new problems, mainly due to the lack of knowledge about tree strengths and growth patterns. Solutions must be found on how to deal with the fact that the strength of a tree varies over its lifetime, which might result in a tree not having the required strength when they are planted.

Connecting the trees with self-growing connections might be advantageous for their stability. Just as for the trees' strengths, there is also a lack of knowledge about the behaviour of connections and their capabilities.

Because the problem as mentioned above is too broad to research for all vertical forests, a case study has been chosen as a starting point. This case study is the *Wonderwoods* vertical forest. Along the façade of this building, there are containers with either plants or a single tree. The containers with a tree directly transfer their loads to the load-bearing walls. The containers with the plants, however, transfer their loads by use of consoles via the floors to the load-bearing walls. This requires extra reinforcement in the floors which hinders the construction sequence. Solutions should be found to improve this structural scheme by using living trees as structural elements.

3.2 RESEARCH OBJECTIVE AND QUESTIONS

This research aims to expand the knowledge on the topic of using living trees as structural elements, both as single tree elements and (self-growing) interconnected tree elements. The research delivers a proposal for a structural model of (interconnected) trees, which is compared to strain and deformation measurements of winching tests. Furthermore, the research delivers a comparison between single and interconnected tree systems, applied to the *Wonderwoods* case study. This comparison will be based on both the botanical and structural behaviour of the trees. In the botanical design, the tree species selection and the growth behaviour of the trees are included. The structural design includes the mechanical behaviour of the tree stem, the connections, and the applied loads.

This aim leads to the following research question:

What is the effect of using interconnected trees as structural elements compared to using single trees?

Concerning this main question, the following sub-questions are formulated:

- What is the botanical behaviour of (interconnected) trees?
- What is the structural behaviour of (interconnected) trees?
- How could (interconnected) trees be structurally modelled?
- How could (interconnected) trees be used as structural elements in *Wonderwoods*?

3.3 SCOPE

The research is limited to the following scope:

Comparison of structural model winching results

- The material properties in the structural model are simplified as homogeneous.
- The behaviour of the structural model will be compared with real trees that grow in the botanical garden of the *Delft University of Technology*.
- The comparison of the structural model with the winching results is limited to the strains and deformation. The measured root rotation during the winching tests will be used as input for the root stiffnesses of the models.
- The moisture content of the soil at the day of winching is registered to verify if the root system stiffness of several trees can be compared. Further analysis of the root system behaviour and the root-soil interaction is out of scope.

Case study design

- The research focusses on practices as can be found in The Netherlands or similar climates. This means the tree species that are investigated must be able to grow in The Netherlands. The selection will be narrowed to tree species that can grow in the *Wonderwoods* climate. From this selection, only one species is chosen to apply in the designs. This contradicts with the description of a vertical forest.
- The design will be based on the *Wonderwoods* vertical forest case study. Freedom is taken to change existing designs not to limit the possibilities of the living tree elements. Whether the design is satisfactorily for the architect is out of scope.
- The design will be made for the *Wonderwoods* south-west façade only.
- A system of interconnected trees will be limited to two trees.
- The design can be a combination of natural tree elements and artificial construction elements.
- Structural verification is based on the Dutch building code. However, this might not always be possible because living tree elements are not standardized in the code. In this case, reasonable assumptions will be made.
- The assumption is made that the design could be structurally verified if it can resist the applied forces in tension, compression, bending, shear, and a combination of these. Other structural verifications like buckling and torsion and the dynamic behaviour are out of scope.
- The growth of the trees is included in the structural design. However, only the most crucial time steps will be discussed in this report. This includes the time of planting, the time that the trees can fulfil their structural function, and at the envisioned end of the life-time of the trees.
- The influence of the trees on the building is out of scope; only the structural capacity of the trees themselves will be investigated.
- This research does not focus on the influence of the roots on structural stability. A reasonable assumption of the root stiffness will be made.
- The scope of this research does not include costs and environmental impact calculations.

Note: the European number format is used. A comma marks a decimal, and a dot marks a group of three digits.

4 Botanical Behaviour of Trees and Connections

To be able to use living trees as a structural element, it is necessary to understand their botanical behaviour. A tree can adapt to its environment, but this has its limits. Without respecting the natural growth behaviour and requirements of a tree, it is hindered to grow and will not give the desired structural capability. It is, therefore, crucial that these mechanisms are included in the design.

This chapter focusses on this growth behaviour and the trigger for trees to grow in a particular shape or direction. Additionally, it will be discussed how trees increase in strength, as the trees must grow stronger at the right location to be able to bear de required loads. This will be followed by an introduction to self-growing connections and how to make these. The chapter closes with remarks about designing with trees.

4.1 Tree growth behaviour

In this report, several tree components are mentioned. Figure 4.1 illustrates the definition of the tree anatomy that is used in this report.

Trees have very diverse ways of adapting and interacting with their environment. Just as for designing with steel or concrete, this behaviour should be known and should be considered in a design (Hundert & Pfeiffer, 2019).

Trees grow their construction material on-site mainly from water and CO_2, using sunlight as an energy source. This process is known as photosynthesis and is possible due to chlorophyll, existing in the leaves of the trees. The roots take up the essential water and nutrients for the tree. In natural forests these roots are often connected, this way glucose can be exchanged between trees, ensuring that also smaller trees, often shadowed by the larger

Figure 4.1 Description of tree anatomy (Encyclopaedia Britannica, 2012)

trees, receive enough energy to live. Trees benefit from surrounding trees, together they can create an ideal moist and windless climate, and by interconnecting the roots, they can resist stronger storms (Wohlleben, 2016). However, trees can also compete for space. When trees grow larger, they need an increasing amount of resources, so they need to occupy a larger area. If this is not available, the large trees can take up space of weaker trees (Ludwig, 2012).

Secondary growth is the increase of the stem in thickness. In literature, several theories can be found about the tree's triggers to increase its thickness at a specific location. According to Hundert and Pfeiffer (2019), a stem or branch increases the most in thickness if a large water transport capacity is needed or due to high mechanical stresses. This strikes with the axiom of uniform stress, which states that a tree increases in thickness in such a way that the bending stresses are, over time, averaged out (Mattheck, 1998). However, this theory is often questioned, for example by Duncan Slater (2016) who collected a series of scientific studies that prove that the axiom is not a logically consistent model for all the different shapes of trees.
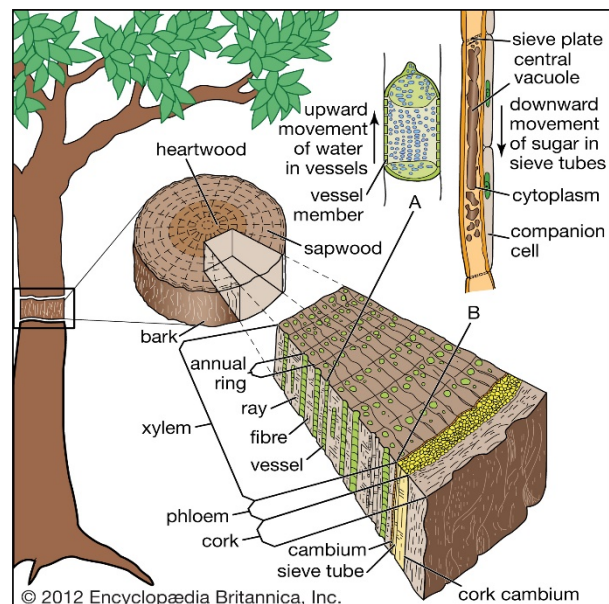
Another theory is the Pipe-Model theory as described by Shinozaki in 1960. In this theory every leaf has its own 'pipe' with a constant circumference, connecting the leaf with the roots. These components together create a plant or tree. The conical shape of a tree can be explained by the dead branches and leaves that still have their 'pipe' in the stem of the tree. This theory is illustrated in figure 4.2 on the left. However, this theory is often questioned, as well (Ludwig, 2012). Studies showed that the model is not valid as a general rule as they often find non-linear relationships between the amount of foliage and stem size (Lehnebach, Beyer, Letort, & Heuret, 2018).
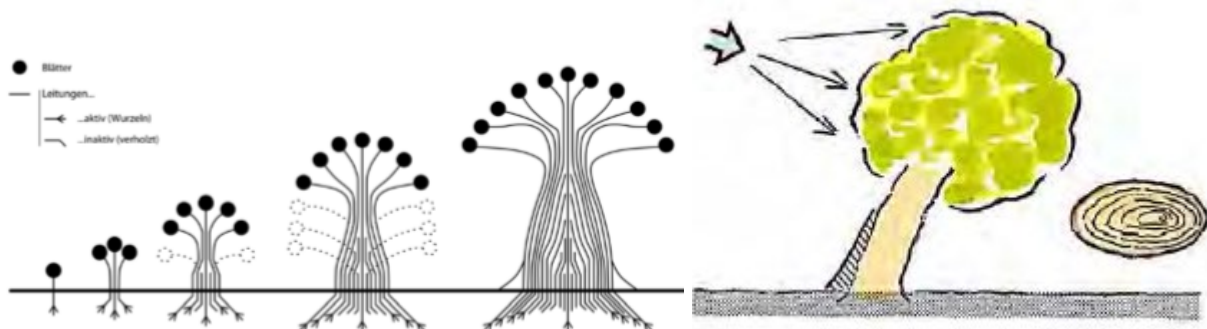

Figure 4.2 Left: Illustration of the Pipe-Model theory (Ludwig, 2012). Right: Illustration of a leaning broad-leaved tree (Wessolly & Erb, 2016)

There are several examples of trees forming secondary growth due to a gravitational or load stimulus (Wilson & Archer, 1977). One of these examples are branches that strengthen themselves for a downwards load by creating secondary growth on their underside (Wessolly & Erb, 2016). Another example is the relationship between the wind direction and an oval shape of the stems, as illustrated in figure 4.2 on the right. This is found in Larix and Poplar trees (Larson, 1965). The study on Poplar trees showed that due to the optimised oval shape of the stem, the tree has an equal strain all around the stem if it is subjected to wind from the prevailing direction (Wessolly & Erb, 2016).

4.2 FORMATION OF A CONNECTION

Inosculations often occur between the roots of the trees but could also occur between stems and branches. In Europe, such natural connections do not frequently occur as trees are only rarely firmly pressed onto each other. In other parts of the world, where the soil is more stone-like, the roots of the trees seek for cavities to grow in. This makes it more likely that trees meet and thus inosculate naturally (Ludwig, 2012).

From experiments carried out by Ludwig (2012), it can be concluded that the trees need a certain pressure before they start to connect. There are various views on what triggers the trees to start to grow towards each other and form a connection. Mattheck (1998) explains this by the axiom of uniform stress: a tree always tends to have the same amount of stress along its section. Due to the creation of material at the location of the pressure, the stress is reduced. Millner (1932), however, thinks that the process starts with the rupture of the bark tissue so that a natural connection can be described as the healing of two wounds.

How such an inosculation grows is also a topic of research. Back in 1932, Millner described this process for the Hedera helix, a common ivy in which inosculations can often be seen. He described inosculations as a two-step process: first, the bark tissue merges, followed by the wood tissue. The former happens if the bark tissue of two stems is pressed against each other, which causes cracks and pushes the bark outwards. Once this has happened, several layers of thin-walled cells underneath the bark start thickening and thus bulging outwards forming a hump of wound cork, see figure 4.3 on the left. In the meantime, the same happened in the other stem, so these humps

eventually touch each other and fuse. A new bonding layer of tissue is created rapidly by cell division which pushes out the wound cork. Now, the bark of both stems has merged while the xylem tissue is still separate, see figure 4.3 in the middle. At this stage, the plants can exchange assimilates and hormones that are transported via the bark. Water and nutrients are not yet exchanged, and the connection does not have much mechanical strength.

Millner (1932) states that the inosculation process will now proceed to the second step, the merging of the xylem tissue. An increase in cell division happens in the cambium, which creates another hump, pressing itself through the earlier described bark tissue. Once these humps touch each other, they start to merge, and the cambium cells transform into regular parenchyma cells, leaving a continuous cambium ring between both stems. In the centre of this ring, a mass of loose parenchyma cells remains. Now xylem and phloem cells start to differentiate, eventually creating the first common growth ring. As the cambium is more active in the region of the connection, over the years, the two trees get a rounder shape.

Millner (1932) was able to prove that interconnected trees can exchange resources by cutting one of the stems just below the connection and thus separating this stem from its roots. The stem and branches were then kept alive via the connection to the other tree.
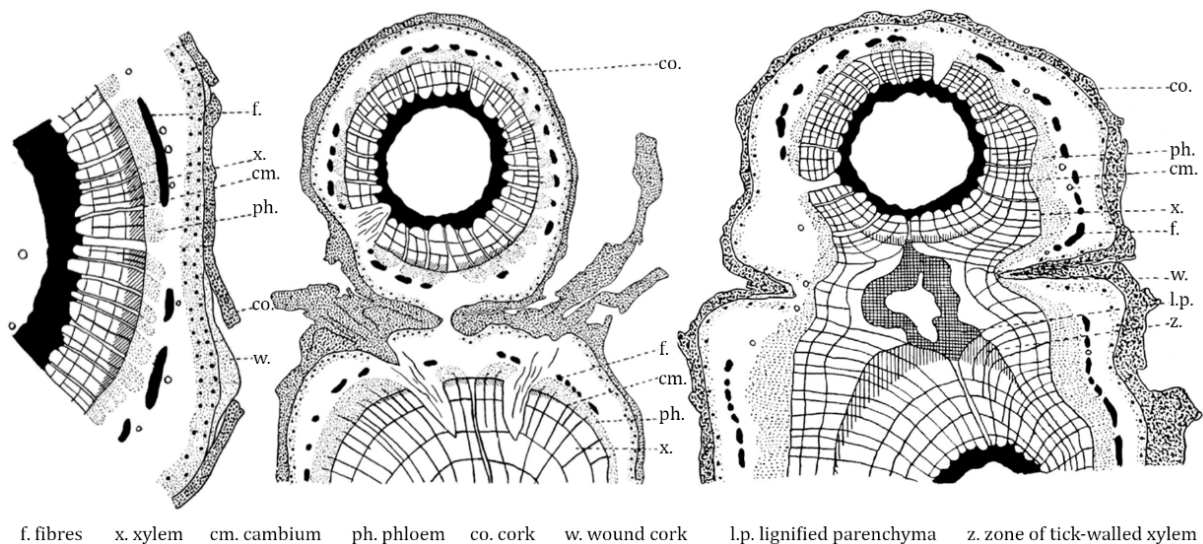

f. fibres   x. xylem   cm. cambium   ph. phloem   co. cork   w. wound cork   l.p. lignified parenchyma   z. zone of tick-walled xylem

Figure 4.3 Left: Drawings of creation of wound cork. Middle: Fusion of bark tissue. Right: Connection with common growth ring (Millner, 1932)

Recently, Winterman (2020) found the same results as Millner (1932). She observed inosculations in a Ficus tree with a CT-scan, see figure 4.4. It shows a similar shape with similar components as described by Millner.
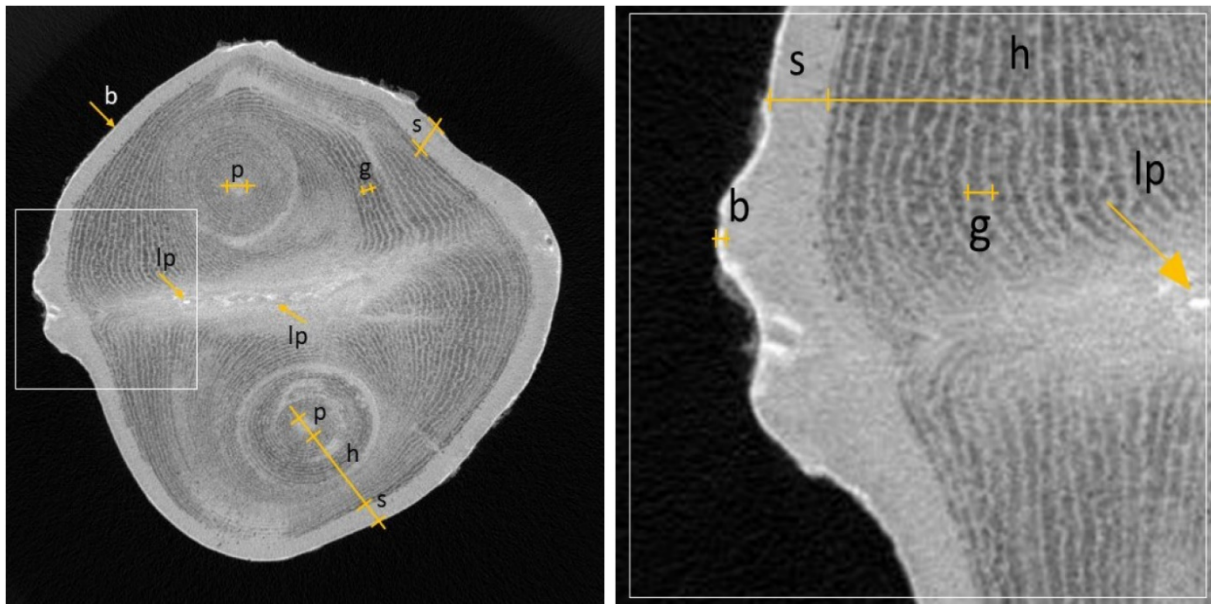
Figure 4.4 Left: CT-scan of a Ficus inosculation. Right: Zoomed selection. Bark (b), lost parenchymatous cells (lp), sapwood (s), heartwood (h), growth ring (g), pith (p) (Winterman, 2020)

4.3 CONNECTION TYPE AND TECHNIQUES

The type of connections that can be created can be categorized into three groups: parallel welds, cross welds, and grafts (Nuijten, 2011). Parallel welds are connections in the longitudinal direction of two trees. A schematic drawing of the creation of such a weld in the longitudinal can be seen in figure 4.5 on the left. Cross welds are connections between two trees in a transverse direction, so the direction of the fibres of these trees are different. As can be seen in the middle of figure 4.5, if a continuous ring is formed around the connection, it has the same fibre orientation as the dominant thicker tree. Human-made grafts cannot be made naturally. Grafts are created by removing half of both trees and placing the remaining halves together. The contact area in these connections is large, which makes it possible to transfer large compression forces in an earlier stage compared to naturally created welds. Disadvantages of this technique are the necessity of the trees being of the same species and the high infection risks during the time that the trees have an open wound. Differences between parallel welds and grafts can be seen in figure 4.5 on the right.
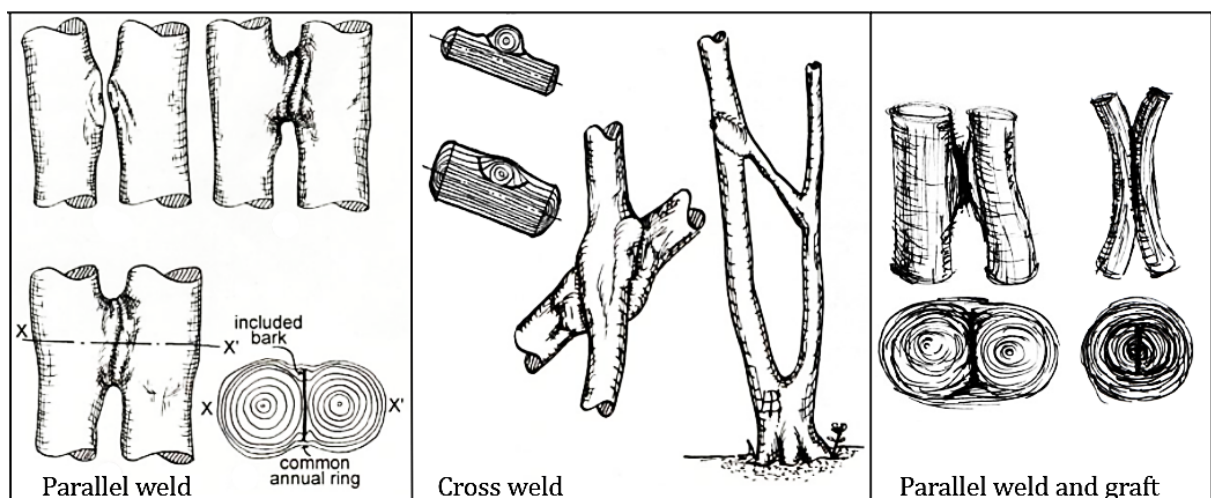

Figure 4.5 Left: Formation of an parallel weld (Mattheck, Design in Nature - Learning from trees, 1998), Middle: Formation of a cross weld (Mattheck, 1998), Right: Difference parallel weld and graft (Nuijten, 2011)

Once the xylem of two trees has fused, the connection has mechanical capacity. However, before this has happened, an adequate technique needs to give a certain pressure to let the trees start growing towards each other. A poor connecting technique can negatively influence the growth of the trees. For example, obstruction of assimilate transport leads to uneven growth and can result in a jump in diameter. Important to note is that any type of damage to the tissue leads to a mechanical weakness. Until a tree has repaired these wounds, this weak point increases the risk of failures. An ideal connection technique would, therefore, gradually give enough pressure with the least amount of negative consequences (Ludwig, 2012).

Transferring the pressures from the connecting equipment to the interface of the trees can be achieved in two ways: originating outside or inside the tree. The former is usually carried out with ropes or wires, tied around both stems. An advantage of this technique is that it does not unavoidably damage the tree. However, it cannot introduce large forces as this might strangle the tree, stopping its assimilate transport. If this strangling lasts too long, the neighbouring tissue might die. The other technique, introducing the connecting pressures from the inside of the tree, can, for example, be done by screws. This technique does not strangle the trees and is especially advantageous for harder wood species. The disadvantage is that it unavoidably damages the bark and usually also the xylem tissue. In general, the risk of infections increases by larger wounded areas (Ludwig, 2012).

The previously mentioned *Baubotanik* research group has carried out tests to examine different types of joining techniques and their applicability to different European tree species and joint geometries (parallel and cross). The three tested techniques are:

- Tying trees together with wide and pliable ties that lay over the bark
- Thin ropes that cut into the bark if the tree grows
- Connecting by screws that penetrate the wooden core of the stems

This research concludes that connecting the trees by screws is the most practical, reliable and plant compatible solution. Furthermore, it concludes that connections can be created the best in robust plants with a high ability for wound healing and a thin bark which is poor in fibres. From the ten tested species, the London Plane was the most applicable for all three joining techniques because it formed fast and qualitative joints (Hundert & Pfeiffer, 2019).

It depends on the tree species at what age the trees can be connected most easily. Millner (1932) observed that the Hedera Helix, for example, does not naturally connect if the tree is older than eight years. Furthermore, he found that the age difference between two connected stems is usually two or three years with a maximum of six years. This makes it impossible for younger branches to connect to much older ones.

4.4   REMARKS ABOUT DESIGNING WITH TREES

Some remarks are interesting to mention as they might be useful to apply in a living tree design.

4.4.1   Speed up of living tree construction

Using trees as a structural element in a rapidly developing world has its drawbacks because it takes decades for trees to mature. One technique to solve this problem is applied in *Der Steg*, where several willows were bundled together to
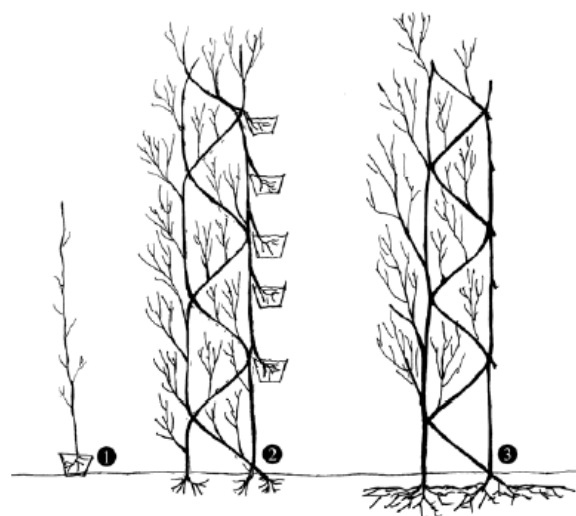

Figure 4.6 Plant addition technique (Ludwig, 2012)

18

ensure an initial strength. After a while, some willows will grow stronger, taking over the position of the weaker willows. Plant addition is another technique, developed by Ludwig (2012), where young trees are arranged in a framework and connected to each other. The idea is that after a while, the trees merge into a single organism which can share organs, ensuring that not all trees need their roots and leaves anymore. The organism then thickens, creating enough strength to remove the temporary scaffold system. This 'plant addition' technique makes it possible to create living buildings which already have the size of a mature tree. This technique is used in the *Baubotanik* tower, as described in paragraph 2.2.3 (Ludwig, 2012).

4.4.2   Application in the field of architecture

In case living-tree elements are used as construction elements, some characteristics of trees must be considered:

- It is unavoidable that some trees die, so this has to be included in the design concept (Ludwig, 2014).
- Trees do not increase their strength at locations where other elements support them. If this supporting element is then removed, the tree has an increased probability of failure (Mattheck, 1998).
- Trees should not deviate too much from their natural upright position and should not be bent too much. If the main shoot of the tree is placed horizontally, this shoot might lose its apical dominance and that another vertically growing shoot becomes the main shoot. To prevent this, it is preferred to create vertical structures over horizontal structures (Ludwig, 2012).
- As a follow up to the previous point: if trees are interconnected, and one tree is more inclined than other trees, the less inclined trees need to be pruned actively. Otherwise, less inclined trees will have more growing power and take over the inclined trees. It is therefore preferred to give all trees the same angle deviation (Ludwig, 2012).
- If two parallel axes of interconnected trees do not have the same length, the thickness of the shorter axis will increase more than the thickness of the longer axis. The Pipe-Model-Theory could explain this: water flows through both axes of the interconnected tree. However, the shorter axis has a lower resistance than the longer axis, and thus more water will flow through the shorter axis. According to the theory, if the water flow is too large for the area it flows through, this area will be enlarged, and the tree will increase in diameter. If it is undesired that one axis has a larger thickness increase than the other, parallel-connected axes should be given the same length (Ludwig, 2012).
- According to the same Pipe-Model-Theory: if structures need to have a high load-bearing capacity, they must be designed in such a way that the expected water flow corresponds to the main force flow. This way, the mechanically stressed axes increase in thickness and thus achieve the desired load-bearing capacity (Ludwig, 2012).
- Designing with elements that are alive is something different than what most architects and engineers are used to. The design is not a single static object but changes over time. As is described by Ferdinand Ludwig in 2014*: "This process-based thinking is a completely new field for architects that are used to create finalized objects and leave the project when the construction is completed. Here it has to be said that the idea of buildings as static objects is a widespread self-delusion of architects that ignore that their buildings are always exposed to changes."*

5 STRUCTURAL BEHAVIOUR OF TREES AND CONNECTIONS

Making a structural design requires information on three subjects: the load combinations, the limits of allowable stresses and strain, and the material and its mechanical properties (Viguier, Jehl, Collet, Bleron, & Meriaudeau, 2015). The first two are generally determined by the Eurocode and are discussed in paragraph 8.8. The third one is usually determined by the material's supplier, which is problematic in the case of living tree structures. Although tree nurseries do have much qualitative knowledge about the behaviour and the capacities of trees, the quantitative data available on the mechanical properties of tree species is limited.

This chapter starts with describing several failure types and the most critical loads on living trees. In paragraph 5.2.4, the current state of knowledge of the tree's mechanical properties is discussed. In paragraph 5.4, the same is done for the connections between trees.

5.1 FAILURE TYPES

According to Kane (2014), the most common failure types are uprooting, breakage of the union of co-dominant stems, failure in the trunk due to extant decay, and failure in the crown in the vicinity of branches. He concludes that the crown width is the best predictor for the maximum bending moment trees could resist before they failed by uprooting. The best predictor for the maximum bending moment of trees that failed in the crown is the second moment of area at the location of the failure.

Breakage of the stem occurs as follows: first, the outer fibres of the leeward side fail due to high compression forces, then the fibres next to those closer to the pith fail. This continues until the pith is reached. The more fibres fail in compression, the more tension the fibres at the windward side must resist. If this tension becomes too much, the outer fibres at the windward side break, resulting in total stem breakage (Wessolly & Erb, 2016).

Other failure types worth mentioning are torsional failure and delamination. The first is more likely to occur if a tree has large openings in its stem. Delamination is a vertical crack due to horizontal forces and occurs if the bonding between the fibres fails (Wessolly & Erb, 2016). As this happens particularly between co-dominant stems, it is likely also a failure mechanism in interconnected trees.

5.2 GENERAL LOADS ON LIVING TREES

The most common loads on a tree can be categorized into vertical and horizontal loads.

Vertical loads are mainly self-weight and precipitation. According to tree expert Dennis de Goederen, the amount of self-weight can be determined by measuring the volume of the stem and the five largest branches. About 10% should be added to this volume for the remaining smaller branches. The total volume should then be multiplied with the volumetric weight of green trees according to the *Stuttgarter Festigkeitskatalog* (Wessolly & Erb, 2016). The volume of one stem can be calculated by measuring the area at breast height and multiplying this with the height times 0,7 for the tapered shape. Self-weight results in principle in normal stresses in a tree, but deviations in tree shape can result in other stresses. This is explained in paragraph 5.2.3. Precipitation is, for example, rain or snow. According to Bob Ursem, director of the Botanical Garden of the TU Delft, about 50% of the precipitation stays on the leaves (Ursem, 2020). If the horizontal crown area is known, the weight of the precipitation can be calculated.

The most important horizontal load is wind load, which will be described in paragraph 5.2.1. The natural frequency of a tree plays an important role in the reaction of a tree to wind gusts. This will be explained in paragraph 5.2.2.

Not only external loads result in stresses in the tree. Internal mechanisms, like stresses due to unequal growth, are described in paragraph 5.2.4.

5.2.1 Wind load

Trees sway when subjected to wind loads, which creates bending stresses (James K. , 2003). Failure is assumed to occur when the induced moments exceed the moment capacity of the tree's cross-section (Ciftci, Kane, Brena, & Arwade, 2013).

According to James (2003), there are two failure mechanisms of trees subjected to wind load:

1. Windthrow. The tree fails at the interaction of the root plate and the soil.
2. Major stem or branch failure. The tree fails because a local stress exceeds the strength of the material. The local stress is usually the result of too high tension or compression forces in the outer fibres due to bending.

If windthrow is critical, it is possible to prevent tilting by placing horizontal frames over the root-balls. The second failure mechanism of stem or branch breakage is more complicated to prevent. According to several experts in the field of vertical forests, this is the main issue concerning safety (Beining, 2020; Cents, 2020).

Wind loading affects not only the behaviour of the tree itself but also the structure behind the tree in two ways. The first effect is the change of shape of the building due to the tree cover; this influences the drag of the building and thus the overall wind load. The second effect is the change in vibration. The vibrations of the trees and the structure are coupled, and thus the dynamic responses influence each other. Wang (2018) claims that the trees could act as a set of small dampers. With a mathematical model of a fifty-story structure with trees along the façade, he showed that tree cover significantly reduces the vibration of the host structure.

The magnitude of the load depends on the wind force at the location of the tree, the crown area, and the drag coefficient of the tree. The latter is a function of the magnitude of the wind force. Due to a higher wind load, a tree bends in the direction of the wind. This reduces its drag coefficient, as can be seen in figure 5.1. From wind force of 9 Bft and higher, the drag coefficient stabilizes, usually to a value of 0,25. If a tree has lost all its leaves, the drag coefficient drops to a value of 0,1 (Wessolly & Erb, 2016).
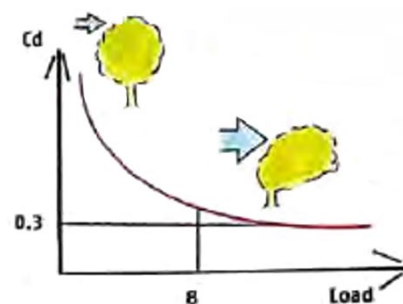

Figure 5.1 Change of drag coefficient with wind load (Wessolly & Erb, 2016)

Wind load does not only result in bending moments. If only a small part of the crown area catches wind, it can result in torsional stresses (Wessolly & Erb, 2016).

5.2.2 Tree dynamics

Wind load is not a constant, static load. It has a somewhat arbitrary nature as it changes velocities and direction all the time. The tree's behaviour to dynamic loads, such as wind gusts, is different from its behaviour to static or gradually applied loads.

A dynamic amplification factor is a value for the relation between the deflection, or stresses caused by a dynamic load, compared with the deflection or stresses caused by a static load. This amplification factor is influenced by the stem diameter, the number and slenderness of branches

in the crown, the elastic modulus of the stem and branches, and the damping ratio (Ciftci, Brena, Kane, & Arwade, 2013). As the presence of large branches influences the sway response of a tree, the way of pruning the trees can help to reduce the risk of failure (Ciftci, Brena, Kane, & Arwade, 2013). This is acknowledged by James et al. (2014), who states that the form of a tree has a more significant influence on the tree dynamics than the material properties.

Excurrent trees, in other words; trees with one dominant stem, have a higher natural frequency than decurrent trees, which have several co-dominant stems. If an excurrent tree is pruned in summer, this increases its natural frequency. The tree shape and pruning, however, has little effect on the damping ratio. Decurrent trees are subjected to larger wind stress compared to excurrent trees because they have a larger percentage of their branch mass in the top half of the crown (Miesbauer, Gilman, & Giurcanu, 2014).

Slender trees have a lower natural frequency; they sway with the direction of the wind, see figure 5.2. Ideally, the next wind gust catches them when they are swinging back. When the tree moves back along its rest position, it has maximum speed and thus maximum kinetic energy. The wind gust has about the same amount of energy, and thus the movement is reduced. Despite the great gust speed and tree speed in the crown, the trunk and the root system do not have to resist any load. However, if the second wind gust catches the tree when it is again swinging in the direction of the wind, the load of the second gust is added to the load

Figure 5.2 Natural frequency of trees (Wessolly & Erb, 2016)

of the first gust. If the sequence of the wind gusts corresponds with the natural frequency of the tree, it resonates, and failure is likely to occur (Wessolly & Erb, 2016).
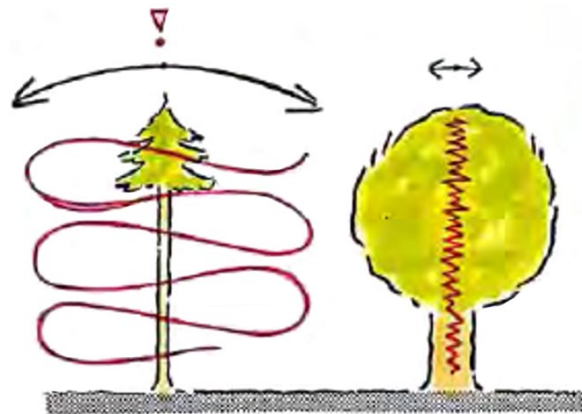
More compact trees have a higher natural frequency and contain a good oscillation damping. This oscillation damping is the result of a heavily branched shape with many leaves which all have their own natural frequency, opposing the main natural frequency. The tree is therefore not able to translate wind energy into movements, making it independent from dynamic effects (Wessolly & Erb, 2016).

In summary: young and slender trees can transform wind energy into movements, reducing the forces acting on the stem and root system. Older and compacter trees take up the wind forces by their structure. It can do this due to their thicker and stiffer stem and root system.

5.2.3 Divergent tree shapes

If a tree were a single straight stem, without any branches or other deviations, the flow of forces through a tree would be very straightforward. This is, however, never the case, resulting in additional stresses within a tree.

The most apparent deviation are branches. Every branch is subjected to its own load, which has to be transferred to a larger branch, or the main stem. Within a branch or trunk, the direction of forces is parallel to the fibres. At a branching point, this direction must be changed, giving a higher strain. A tree compensates for this effect by secondary growth: material is added at the bottom of

the branching point. This ensures that the growth rings of the branch are interlocked with the growth rings of the trunk (Wessolly & Erb, 2016).

Next to branches, the leaning of a tree also gives additional bending stresses, due to the eccentricity of its self-weight. If a tree has an asymmetrical tree crown, this can be a source of torsional stresses. If a curved tree catches wind load, this will result in horizontal forces perpendicular to the fibres. This is illustrated in figure 5.3. Additionally, such curved trees can also get torsional stresses.

Figure 5.3 Load distribution in curved trees (Wessolly & Erb, 2016)

Interconnecting trees gives large diverging tree shapes. Just as for curved trees, this results in stresses perpendicular to the grain. It is therefore essential, for the design of interconnected trees, to choose species that have decent wood properties perpendicular to the grain. The expectation is that the mechanisms that act on such a connection can be compared to the mechanisms that take place at a tree fork. Such tree forks are also subjected to higher perpendicular stresses. The ins and outs of this mechanism will be explained in paragraph 5.4.

5.2.4   Stresses

Loads on a tree can give axial stress, bending stress and torsional stress (Wessolly & Erb, 2016). Axial stress is mainly the result of the tree's self-weight, giving a uniformly distributed compressive stress along the axis. The leading cause for bending stresses is wind loading. If a tree is deflected due to, for example, the wind force, the self-weight of the tree gives additional bending stresses (Kane, 2014). This can contribute about 10 to 25% of the maximum bending moment, as has been proven with tests on Norway spruce by Lundström, Jonsson and Kalberer (2007). Torsional stress can be the result of wind only catching part of the leaf area, due to leaning of a tree or due to an asymmetric crown shape. Interconnected trees might be particularly vulnerable to torsional stress. The twisting of trees is especially dangerous if trees have an open cross-section (Wessolly & Erb, 2016). According to James et al. (2014), this topic is not yet been investigated, and no method has been developed on how to measure the dynamic torsional loads of trees.
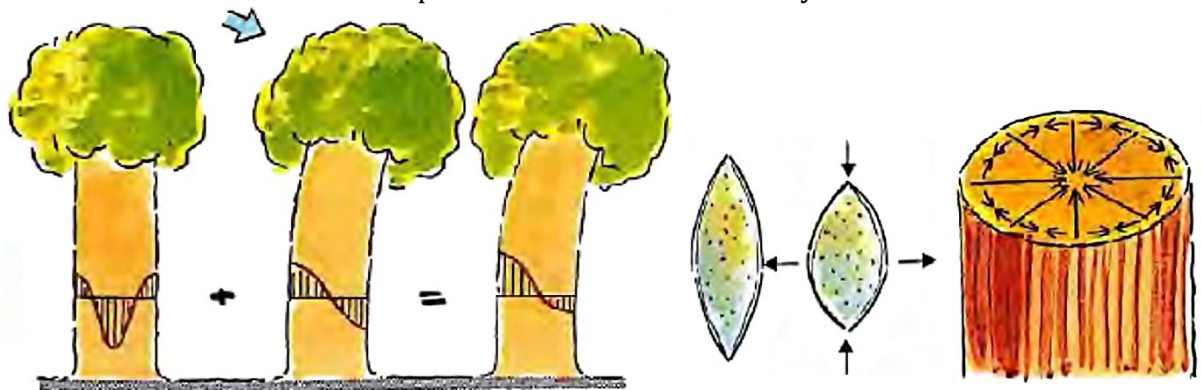

Figure 5.4 Left: Growth stresses which act as pretensioning to resist bending stresses (Wessolly & Erb, 2016), Middle: Shortening and thickening of maturing cell (Wessolly & Erb, 2016), Right: Prestress in transverse direction (Wessolly & Erb, 2016)

Next to the stresses resulting from external loads, there might be axial growth stresses present in the tree's cross-section. These stresses are compressive near the pith and tensile at the circumference, as can be seen in the left tree of figure 5.4. They are a result of the maturing of the wood cells, in which they shorten and thicken. The shortening gives longitudinal tension stress, and the thickening gives lateral compressive stress (Wessolly & Erb, 2016). This mechanism results in pretensioning, which gives smaller compressive stresses if the tree is subjected to bending. This is favourable because a tree is more prone to compression failure than to tension

failure, as will be explained in paragraph 5.3.1.1. Thus, the distribution of stress is more optimized, resulting in a higher load-bearing capacity. A disadvantage of reaching the elastic limit of both the tensile and compression side is that the tree can break without warning because a tree does not deform plastically in tension. What is important to note is that pretensioning can only occur if a tree is solid, which might not be the case for older trees. Luckily, this is not a problem as mainly young trees rely on the pretensioning mechanism. Without this mechanism, they would not be able to carry their enormous crowns in proportion to their slender stems (Wessolly & Erb, 2016).

If bending forces occur on curved parts of a tree, this gives tension stresses perpendicular to the grain, a direction in which the tree is very weak. Luckily, also in transverse direction a tree has a prestress mechanism. As can be seen in figure 5.4 on the right, this works like a bicycle wheel with compression forces in the outer ring and tensile forces on the spokes. The compressive force first needs to be released before the fibres are subjected to a tension load perpendicular to the grain (Wessolly & Erb, 2016).

5.3 GENERAL MECHANICAL PROPERTIES OF LIVING TREES

Biomechanics is the study of biological organisms from a mechanical perspective (Dahle, James, Kane, Grabosky, & Detter, 2017). This means that it tries to apply mechanical theories, known from, for example, the steel or concrete field of study, on plants. Although this gives guidance in describing and understanding the behaviour of plants, attention should be given that these simplifications do not always hold for the diverseness in plant architecture.

Three factors are determining the statics of a tree: the loads, the geometry, and the material. The loads acting on a tree have been discussed in paragraph 5.2. The geometry and the material together need to resist this load and will be described in this paragraph.

5.3.1 Material properties

5.3.1.1 Tension and compression

The tension and compression strength of wood can be explained by the straw model, see figure 5.5 on the left (Ravenshorst, 2019). The wood fibres can be imagined as a bundle of straws. When wood is subjected to a compressive force, parallel to the straws, these straws will buckle and deform plastically. If the straws are pulled in parallel direction, they are not able to deform plastically and will suddenly break. In other words: it behaves brittle. As can be seen in figure 5.5 bottom left, wood fibres are in general stronger in tension than in compression. According to Wessolly and Erb (2016), the tension resistance is about twice the compression resistance. Mattheck and Breloer (1994) and Dahle (2017) agree that the compression strength is normative.

Perpendicular to the grain angle, the load-bearing capacity of a tree is notably different between species. In general, the strength is much lower than parallel to the grain angle. This can once again be explained by the straw model in which it is much easier to deform the straws in the perpendicular direction. In compression the grains show some plastic deformation, in tension, the grains show a brittle failure.

An important note must be made that the behaviour of green wood is different from the behaviour of dry wood, as is shown in figure 5.5 bottom right. Greenwood has a lower compression strength, but it does show plastic deformation before failure (Wessolly & Erb, 2016).
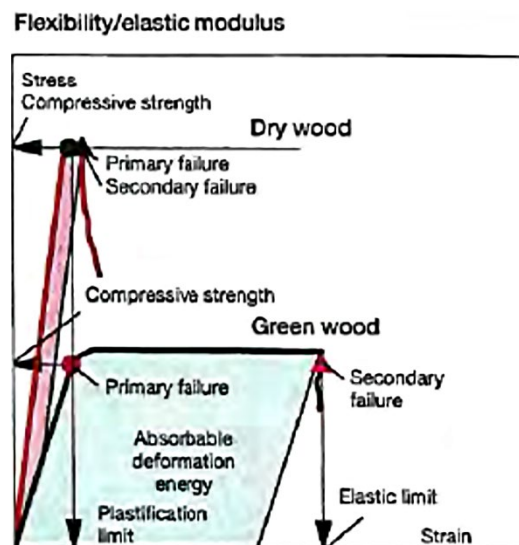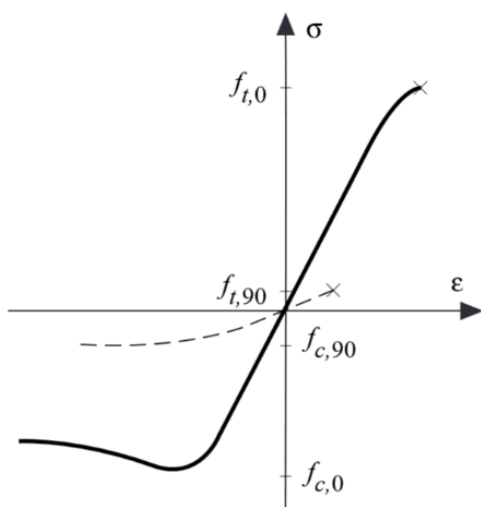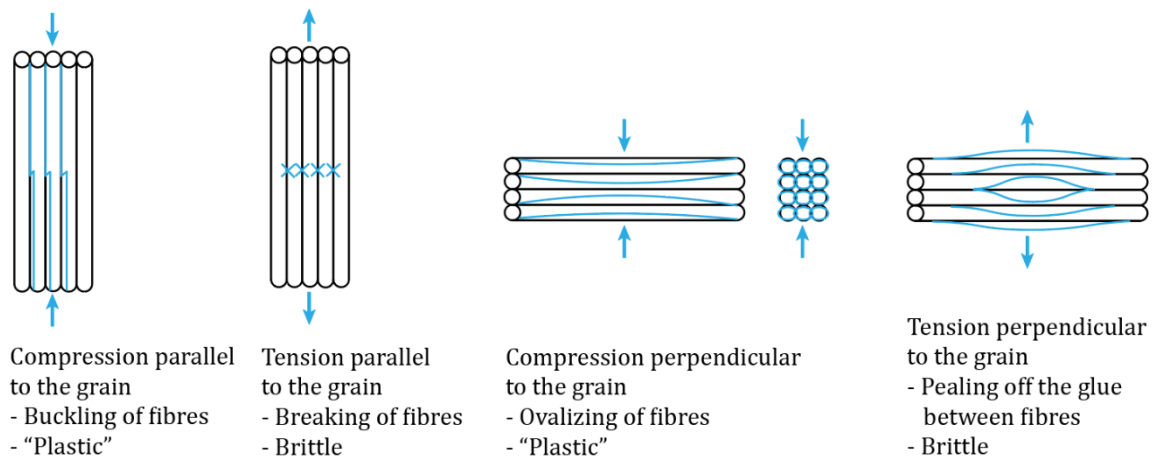
Figure 5.5 Top: Straw model, copy of (Ravenshorst, 2019), Bottom left: Stress-strain-curve of clear wood subjected to tensile and compression stress, parallel to the grain (solid line) and perpendicular to the grain (dashed line) (Blaß & Sandhaas, 2017), Bottom right: Different material behaviour dry and green wood (Wessolly & Erb, 2016)

5.3.1.2   Elasticity and plasticity

Elasticity is the resistance of a material to deform elastically. It is often referred to with the terms Young's Modulus, E-modulus, or MOE and is the ratio of stress to strain. Figure 5.5 on the bottom right shows that the elastic modulus of green wood is lower than that of dry wood.

In contrast to the elastic modulus, the elastic deformation limit does not differ for dry or greenwood. Moreover, the elastic limit does not change over the height of the tree, while strength and stiffness values might change (Wessolly & Erb, 2016).

How a tree behaves once the elastic limit is reached differs per tree species. Some species can deform plastically, which makes them able to take up some deformation energy, while other species have a more brittle failure behaviour. A clear overview can be seen in figure 5.6 on the left.
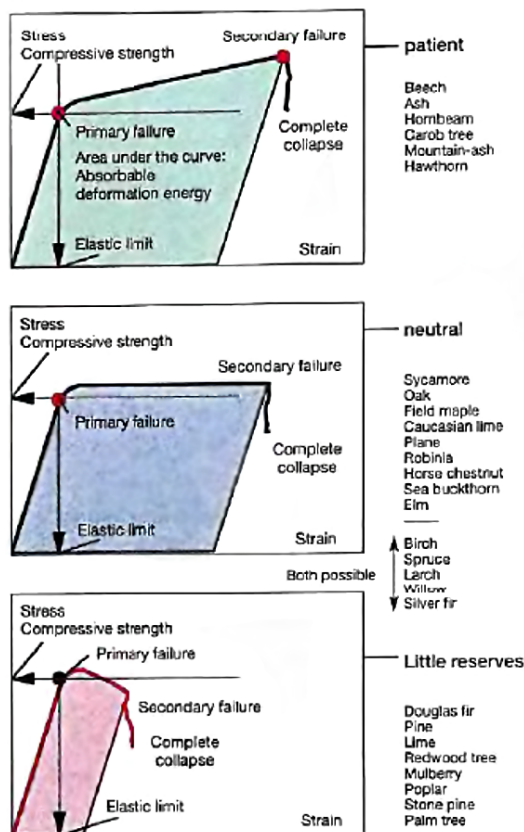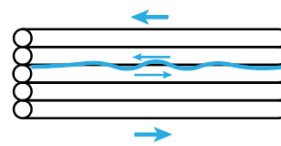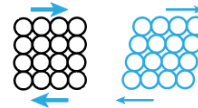
Figure 5.6 Left: Plastic behaviour of several tree species (Wessolly & Erb, 2016). Right: Shear stress copy of (Ravenshorst, 2019)

5.3.1.3   Shear

The resistance of wood to shear stress in several directions can once again be explained with the straw model, as seen in figure 5.6 on the right. If the shear stress is parallel to the fibres, it wants to peel off the 'glue' in between the fibres, which can be done quite easily. Perpendicular to the fibre, shear stress has to break all the fibres, which makes this direction much stronger. Next to parallel and perpendicular shear stress, there exists rolling shear stress, to which wood is very susceptible (Ravenshorst, 2019).

5.3.2   Geometry

Not only the material determines a tree's capacity to resist the loads, but the geometry is also even so important. Compression and tension forces on the tree are divided over the area of the cross-section. The geometry has even more influence concerning the stiffness, which can be defined as the resistance to bending and is calculated as the modulus of elasticity (E) times the moment of inertia (I). The moment of inertia for a solid circle is calculated as (Hartsuijker, 2014):

$$I = \frac{1}{4}\pi * radius^4$$

Which means that if the radius of the tree is doubled, that the tree can transfer sixteen times as much bending force.

5.3.3   Factors influencing the mechanical properties

The mentioned properties differ between tree species, between trees and even within a tree (Sterken, 2005). The properties can also change over the lifetime of a tree. Factors that influence

these properties are, for example, moisture content, age, and decay. These will be discussed in this paragraph.

5.3.3.1 Moisture content

An important factor influencing the mechanical properties is the moisture content. In general, wood has better mechanical properties if it has a lower moisture content (Niklas & Spatz, 2010). As most mechanical tests are carried out on dried wood with a moisture content of 12 per cent, these are not representative for living trees, which can have a moisture content in a range from 30 to more than 200 per cent (Dahle, James, Kane, Grabosky, & Detter, 2017; Glass & Zelinka, 2010).

Figure 5.7 shows a graph, published by Kretschmann (2010), in which the influence of the moisture content is shown on several
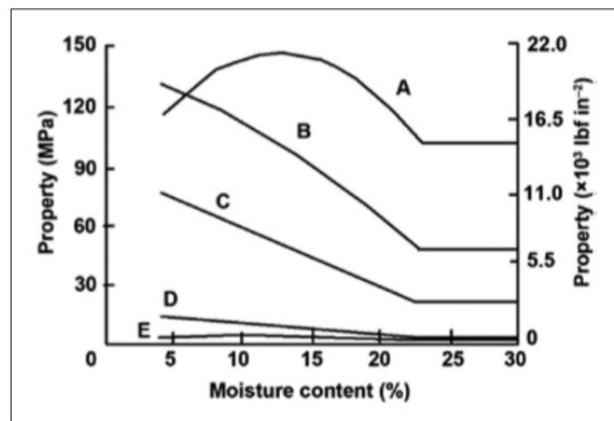

Figure 5.7 Effect of moisture content on wood strength properties. A: tension parallel to grain, B: bending, C: compression parallel to grain, D: compression perpendicular to grain, E: tension perpendicular to grain (Kretschmann, 2010).

strength properties. It clearly shows that above a specific moisture content, the properties do not change much. This moisture content is called the fibre saturation point and is typically around 28% of the moisture content (Blaß & Sandhaas, 2017).

When it is required to know the strength properties of a piece of wood which is tested with a different moisture content, the properties can be adjusted according to EN384. This code describes that the compressive strength values should be adjusted with 3% for every percentage point difference in moisture content. Similarly, the modulus of elasticity should be changed with 2% and the density with 0.5% (NEN, 2018; Ranta-Maunus, 2000).
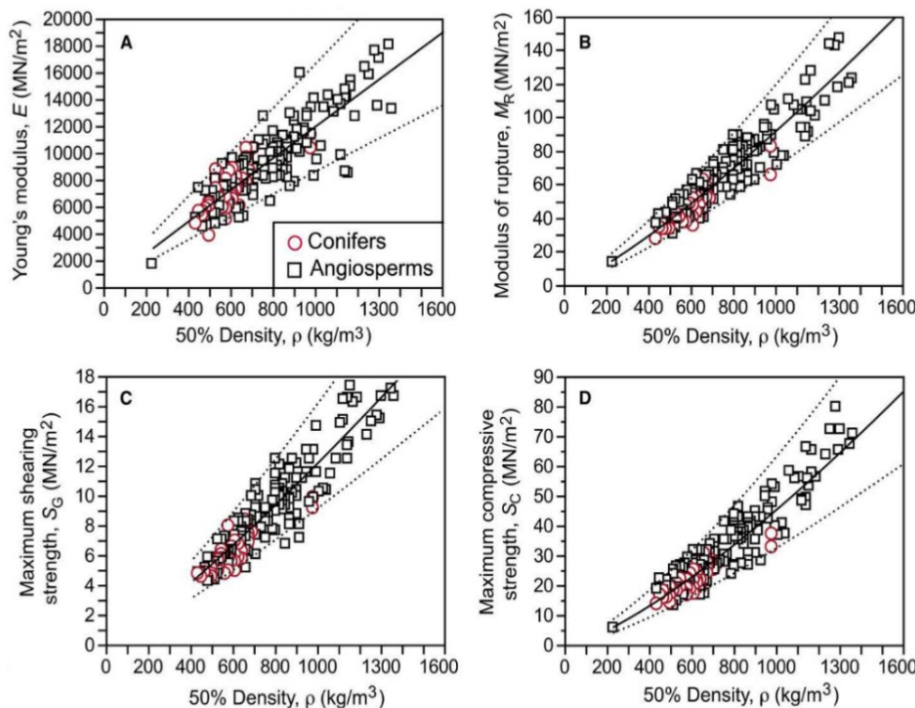

Figure 5.8 Relationship between four mechanical properties and the density of wood with 50% MC for a total of 161 conifer and angiosperm tree species (Niklas & Spatz, 2010).

Many researchers are convinced that density is an essential indicator for the mechanical properties of wood (Blaß & Sandhaas, 2017; Dahle, James, Kane, Grabosky, & Detter, 2017; Niklas & Spatz, 2010; Ranta-Maunus, 2000). Although Bao et al. (2001) agrees, he argues that the microfibril angle is a better indicator for the mechanical properties.

Niklas and Spatz (2010), studied the correlation between greenwood density and mechanical properties. Their test samples had a moisture content of 50 per cent. This moisture content is chosen because the wood properties do not differ significantly at higher moisture contents. They tested 161 soft- and hardwood species and found that the mechanical properties increase disproportionately with the density, as can be seen in figure 5.8.

The *Wood Handbook* of Kretschmann (2010) gives formulas for the relation between mechanical properties and the specific gravity of clear, straight-grained wood. See table 5.1. These relations are based on test results of 70 North American tree species. G is the specific gravity, which is the ratio of the wood density to water density at 4 °C which is 1.000 kg/m^3. For example, if a material has a density of 5000 kg/m^3, it has a specific gravity of 5.

Table 5.1 Functions relating mechanical properties to the specific gravity of clear, straight-grained wood (Kretschmann, 2010)

	Hardwood - Greenwood	Hardwood – 12%MC
Static bending – MOR [kPa]	$118.700 * G^{1,16}$	$171.300 * G^{1,13}$
Static bending – MOE [MPa]	$13.900 * G^{0,72}$	$16.500 * G^{0,70}$
Compression parallel [kPa]	$49.000 * G^{1,11}$	$76.000 * G^{0,89}$
Compression perpendicular [kPa]	$18.500 * G^{2,48}$	$21.600 * G^{2,09}$
Shear parallel [kPa]	$17.800 * G^{1,24}$	$21.900 * G^{1,13}$
Tension perpendicular [kPa]	$10.500 * G^{1,37}$	$10.100 * G^{1,30}$

It is generally accepted that trees can adapt their properties and shape during their lifetime, depending on the external influences (Dahle, James, Kane, Grabosky, & Detter, 2017).

The modulus of elasticity in trees varies over time; it increases until a certain age after which it remains almost constant. In other words, younger trees are more flexible than older ones (James K. , 2003). This can be explained by the larger portion of juvenile wood in younger stems and branches. Juvenile wood has shorter cells with thinner cell walls, and it has lower MOE and MOR[1] values (Dahle, James, Kane, Grabosky, & Detter, 2017). The more distal parts of a tree are in principle also younger, which makes them more flexible. This gives the tree the capability to bend and reconfigure the crown shape during high wind loads. The stiff base parts are then able to carry the bending and torsional moments, additionally to the self-weight (Dahle, James, Kane, Grabosky, & Detter, 2017).

Studies carried out on Finnish Birchwood showed that the density within a cross-section increases with the distance from the pith (Heräjärvi, 2004). As mentioned before, this means that the MOE and MOR increase from the pith outwards. This is also proven by a study on Sugar Maples, which mentions that the MOE of clear wood next to the bark is 14,5% higher than at 50% of the radius (Duchesne, Vincent, Wang, Ung, & Swift, 2016). Similarly, it states that the MOR increases

---

[1] Modulus of Elasticity (MOE) describes the resistance to deformation. Modulus of Rupture (MOR) describes the critical stress at which the wood breaks.

with 5,8% from half of the radius to the bark. Rais, Van de Kuilen and Pretzsch (2020) studied European beech and got the same conclusion. They tested 1907 sawn timber pieces from 100 Beech trees. When the MOE of each piece was plotted against its cambial age, ranging from zero to 140 years, a linear increase was found of 0,103% per year. It is assumed that this relationship is similar in other hardwood species.

Within a cross-section, there is also an unequal contribution to the tree's properties. The wood furthest from the centre contributes most to the second moment of area. This has the effect that the outer growth rings contribute disproportionally to the stiffness, although they only occupy a small area of the cross-section (Dahle, James, Kane, Grabosky, & Detter, 2017). Similarly, it could be argued that the sapwood influences the structural stiffness more than the heartwood (James K. , 2003). As a result, the most effective method to increase the flexural stiffness (EI) of a tree, is to increase the diameter (I) rather than increasing the stiffness (E). Remarkably, a branch starts increasing its diameter once it has reached a certain length, which is, for example, three meters for Norway maple. This reduces the branches' slenderness and ensures its structural function (Dahle, James, Kane, Grabosky, & Detter, 2017). One could say that the branch matures.

Ranta-Maunus (2000) agrees that small-diameter trees have a considerably lower strength because of their large proportion of juvenile wood. However, he says, in timber engineering, it is common to use size factors that decrease the properties of timber if it has a larger size. In his opinion, this contradicts each other. To investigate this phenomenon, he tested coniferous trees and found that the modulus of elasticity increases with increasing diameter, but that other properties as the modulus of elasticity in compression, the bending strength and the compression strength do not have positive or negative size effect. Furthermore, he concludes that the effect of juvenile wood is only weakening the modulus of elasticity in compression and does not weaken the other properties.

5.3.3.4   Decay
As expected, a decayed tree has a higher failure probability. However, a big part of a tree needs to be decayed before this holds true. Several papers refer to a maintenance guide written by Coder (1989) stating that, if the loss of the second moment of area is in between 20 and 45%, the tree should be treated with caution and that if the loss is more than 45% the tree is in danger (Ciftci, Kane, Brena, & Arwade, 2013; Dahle, James, Kane, Grabosky, & Detter, 2017; Kane, 2014; Smiley & Fraedrich, 1992). This seems to be consistent with several tests that have been performed. For example, winching tests of Kane (2014) showed that the loss of the second moment of area should be more than 20% before a tree is more likely to fail at the decayed location. Smiley and Fraedrich (1992) also agreed with this threshold, after they investigated which oak trees did and which did not stand a particular hurricane.

If 70% of the stem is decayed, this results in only a 30% increase of stress at the surface compared with a non-decayed cross-section (Ruel, Achim, Herrera, & Cloutier, 2010). This can be explained by the fact that a tree usually decays is in the middle of its cross-section. As the bending stress is greatest on the perimeter, this decay has little influence on the stress in this outer part (Dahle, James, Kane, Grabosky, & Detter, 2017).

5.3.4   Testing mechanical properties and strength class
There are several methods to determine the bending stiffness of a tree, both destructive and non-destructive (Kane, 2014).

- Winching test in the elastic range. In this test, a tree is pulled at a certain height, and the strain is measured. The stress at this location is the sum of the induced axial and bending stresses. Within the elastic range, the stress-strain curve could be modelled as linear, and

thus the modulus of elasticity can be determined (Clair, Fournier, Prevost, Beauchene, & Bardet, 2003).

- Winching test up to failure. This test is similar to the previous test, but the tree is pulled until failure. With this test, the maximum bending moment at the point of failure can be determined. The stress at this point is the sum of axial and bending stress. It gives information about failure modes and about the non-linear stress-strain curve that leads to failure (Clair, Fournier, Prevost, Beauchene, & Bardet, 2003). If trees fail in shear instead of bending, the shear stress at the point of failure can be calculated.
- Bending test. A commonly used method of predicting the bending strength of an element is the three or four-point bending test. This method could also be used on trees; however, only if they are logged (Ruel, Achim, Herrera, & Cloutier, 2010).

Most of these tests have been carried out on plantation-grown conifers for which predictions have been developed for the failure probability of these trees. It is, however, important to mention that these relationships cannot one-to-one be applied to open-grown trees. Kane (2014) has tried to develop mechanistic models to predict tree failure for open-grown trees, but to come up with good predictions, he stated that much more research is required.

In many winching tests, the modulus of elasticity is simplified as a constant. This simplification is questionable because winching tests give different results of moduli of elasticity for different pulling heights. This coincides with the statement of Dahle et al. (2017), that the modulus of elasticity, just as the modulus of rupture, decreases with the trunk height and branch length. Ruel (2010) mentions that it would be better to pull the tree at a greater height, in his research ideally at 80% of the height. If the tree would be pulled lower, this could induce high stresses at about 10% of the tree height, which influences the winching results.

5.3.4.1 Scaling from timber strength class to roundwood

European standards explain how to assign a piece of traditional timber to a predefined strength class. This can be done with either visual or with machine strength grading. Visual grading includes looking at the slope of the grain, the annual ring width, the knots, the wane and the decay. Machine grading focuses mostly on stiffness measurements, which is correlated to the strength. There are two standard methods to determine the modulus of elasticity. The first method applies a load to a piece of timber and measures the cross-sectional dimensions and deformation. The second method uses the relationship between the frequency of a freely vibrating piece of timber and its modulus of elasticity. This method is especially applicable if the cross-sectional dimensions vary over the length (Vries & Gard, 1998). According to De Vries and Gard (1998), these methods are also suitable for roundwood, although with some correction factors. Whether these methods are also applicable to living roundwood is, however, questionable because of the higher moisture content. That is why researchers attempt to use other grading methods such as the previously explained winching tests. A frequently observed complain is that more research is needed to determine the material properties of living trees, including variations in species and location (Dahle, James, Kane, Grabosky, & Detter, 2017).

Ruel et al. (2010) have tried to come up with correction factors to relate the mechanical strength of roundwood stems to values obtained from defect-free wood samples, as they are tested for traditional timber. They called this factor f_{knot} as is a commonly used factor for scaling timber strength properties. Ruel mentioned six papers that came up with a correction factor ranging from 0,7 to 1,0. For winching tests, the scaling of MOR values was based on a paper by Gardiner et al. (2000) and calculated with:

$$f_{knot} = \frac{32 * M_{crit}}{\pi * MOR * diameter^3}$$

In which:

M_{crit} is the critical bending moment for stem breakage [Nm]

MOR is the modulus of rupture determined from the small clear wood samples [Pa]

$diameter$ is the diameter at the point of rupture [m]

Ruel found that a correction factor should vary with species and that knowledge about cracks would help in selecting an appropriate factor.

Similarly, Ruel calculated the correction factor for the MOR values in three-point bending tests with:

$$f_{knot} = \frac{L*S}{\pi*MOR*radius^3}$$

In which:

L is the maximum load applied at breakage [N]

S is the span between supports [m]

From the three-point bending tests, he concluded that the correction factor to scale up from clear wood specimens to full logs is not enormous as it is around 0,93. The correction factor is, therefore, relatively insensitive to knots and decay (Ruel, Achim, Herrera, & Cloutier, 2010).

Overall, he failed in finding a satisfactory correction factor for the several tested tree species. In Ruel's opinion, this would probably be the case because there are other defects, not measured in this study, influencing the results.

Similarly, Niklas (1997) discussed that scaling results from small to large trees and the other way around is difficult. Firstly, due to the non-linear relationships between several mechanical parameters and tree size. Secondly, due to the change in material properties over the lifetime of a tree. If, for example, the modulus of elasticity is tested for a specimen, and then upscaled to an entire tree, this results in large errors (Dahle, James, Kane, Grabosky, & Detter, 2017; Kane, 2014).

5.4   GENERAL MECHANICAL PROPERTIES OF SELF-GROWING CONNECTIONS
At the time of writing, research is carried out into the strength of the fused area of inosculations by Xiuli Wang. She is a PhD candidate at the research group of *Bio-based Structures and Materials* at the *Delft University of Technology*. Although no conclusions are formulated yet, it seems that the fused area has similar mechanical properties as normal stem wood tissue. When this holds true, the strength of the connection between the trees is not governing. In other words, the trees can be modelled as if they are glued together with a glue which is stronger than the wood itself. To assume the capacity of the connection, it has to be determined which parts of the connection can take up certain loads. In figure 5.9, parts of the trees are shown that might contribute to certain mechanical characteristics. The two original stems are coloured in dark grey; the common growth rings are coloured in lighter grey (Nuijten, 2011).

- Bending: Just after the trees are planted there is no common ring which can transfer moments, so the connection is a hinge. Once common rings are formed, these can contribute to the bending strength, and the connection becomes rigid.
- Compression parallel: Both the original stems and the common rings contribute to the compressive strength.
- Compression perpendicular: Both the original stems and the common rings contribute to the compressive strength.
- Tension parallel: Both the original stems and the common rings contribute to the tensile strength.
- Tension perpendicular: Both the original stems and the common rings contribute to the tensile strength.
- Shear: Just after the trees are planted there is no common ring which can transfer shear forces. Once common rings are formed, these can contribute to the shear strength.
- Torsion: The torsional capacity depends on the shape of the cross-section, which could be simplified as an ellipse. It is expected that only the common rings contribute to the torsional capacity.
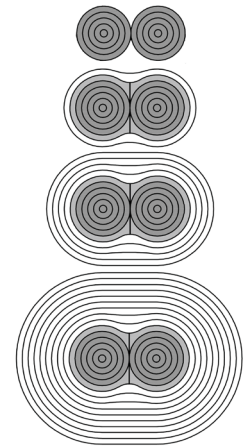

Figure 5.9 Parts of parallel connections that contribute to mechanical characteristics, growth from 0 to 10 years (Nuijten, 2011)

Helena Borská (2018) has carried out pulling tree tests on connected trees that are growing in the botanical garden of the TU Delft. From these tests, she concluded that the deflections are smaller for interconnected trees, which is mostly visible for trees with cross welds. Furthermore, if there is a parallel weld just above ground level, this can reduce the deflection approximately four times. These results are visible in both tangential and radial direction, but mostly in the tangential direction, which is the in-plane direction parallel to the connection.

A deviation in grain angle can cause a high reduction of the mechanical properties (MOR and MOE) of wood (Viguier, Jehl, Collet, Bleron, & Meriaudeau, 2015). It is, therefore, useful to have a look at the fibre deviation in connections. Winterman (2020) analysed CT-scans of cross-connections in Ficus trees. She found that the main fibre orientation of common growth rings is in the same direction as these rings. This would probably make the common growth rings the strongest part of the connection.

If the grains deviate from the main direction, the material properties can be calculated with a Hankinson-type formula: $N = \frac{P*Q}{P*\sin(\theta)^n + Q*\cos(\theta)^n}$. In which P stands for the strength parallel to the grain, Q for the strength perpendicular to the grain and θ for the angle. With table 5.2, n can be found, which is an empirically gained constant (Kretschmann, 2010). This procedure is visualised in figure 5.10.

Table 5.2 Constants for calculating wood properties under an angle (Kretschmann, 2010)

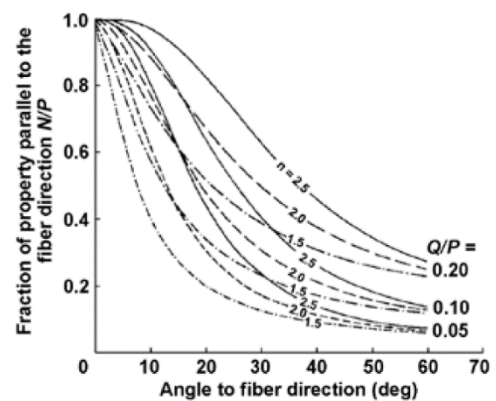| Property	n	Q/P
Tensile strength	1.5–2	0.04–0.07
Compression strength	2–2.5	0.03–0.40
Bending strength	1.5–2	0.04–0.10
Modulus of elasticity	2	0.04–0.12
Toughness	1.5–2	0.06–0.10

Figure 5.10 Effect of grain angle on mechanical properties of clear wood (Kretschmann, 2010)

5.4.1 Branches and co-dominant stems

To get a broader understanding of the mechanisms happening in connections, much could be learned from branch and co-dominant stem unions, which are extensively discussed in literature.

Kane carried out winching tests on 55 red oaks which showed that if the tree crown fails, this is often due to shear failure rather than bending. The shear stress needed to introduce this failure at the branches is about 100 times smaller than values obtained from specimen tests (Forest Products Laboratory, 2010). Kane argues that this proves that branches on decurrent trees are defects.

Slater (2013), however, argues that not all branches or tree forks should by default be considered a defect. In his research with 106 forked and wet hazel trees, he had a closer look at the fibres around the junction of co-dominant stems. He mentions three parts of wood tissue that contribute to the tensile strength of the fork, as shown in figure 5.11. Component 1 is the centre. It has a tortuous wood grain pattern and has, in the tests of Slater, a 19% higher density than the other parts. He explains that the tortuous wood grain pattern ensures that some grains are parallel aligned with the direction of the tension force in the fork. Component 2 is located in the junction plane, outside of component 1. Component 3 is located adjacent to the smaller stem. He found that component 1 contributes to one-third of the strength, although its size is only one-fifth. The results from a three-point bending test suggest that the tree forks can be almost as strong as its individual stems. He proved that intact forks have around 74% of the maximum bending strength of the smaller stem (Slater & Ennos, 2013).
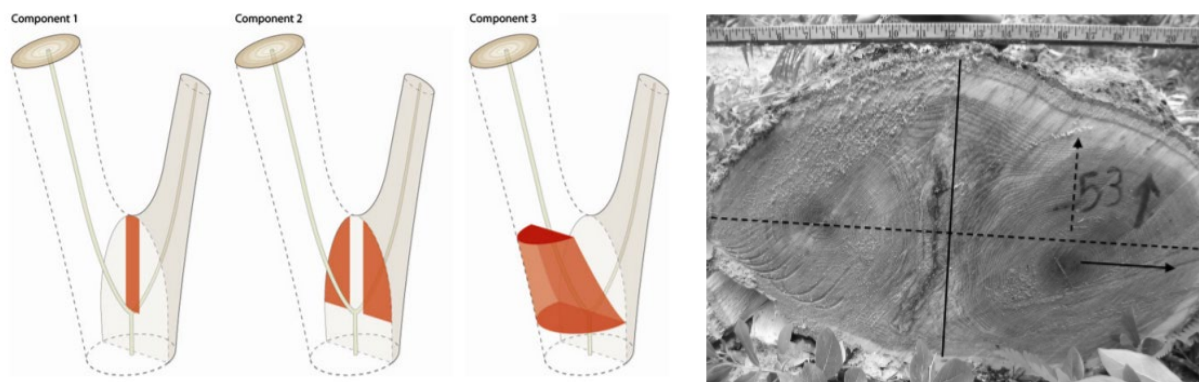

Figure 5.11 Left: Three components that contribute to the mechanical strength of a fork (Slater & Ennos, 2013). Right: Cross section of co-dominant stems, indicating the direction of loading (arrows) and the neutral axes (lines) (Kane, 2014)

The union between stems and branches, or between co-dominant stems, could be vulnerable, depending on three factors. The first is the ratio of the diameter of the branches or co-dominant stems. According to research by Kane et al. (2008), the ratio of diameters of the two stems is the best predictor of the strength of a junction.

The second factor influencing the vulnerability of unions is the inclusion of bark (Kane, 2014). When bark is included in the junction, this significantly weakens its strength. However, research shows that a tree can adapt their growth around the included bark. This makes that a junction with bark, is still stronger than if a hole would have been drilled (Slater & Ennos, 2013).

The third factor influencing the vulnerability of unions is the shape of the junction. This can be classified as U-shaped in which a bark ridge is visible, or V-shaped in which such a ridge cannot be observed, see figure 5.12. A U-shape is favourable, seeing as the fibres of the two stems are able to interlock making them capable of resisting larger horizontal forces as can be seen in the right drawing of figure 5.12. Additionally, the area over which the forces have to be transferred is larger, as is indicated by the red lines in figure 5.12. A V-shape often lacks this interlocking, which

can be the result of included bark, or simply because it has no space for secondary growth. The connection is thus only made by the adhesion on the sides of the vertical fibres, which is very vulnerable to horizontal tension load (Wessolly & Erb, 2016).
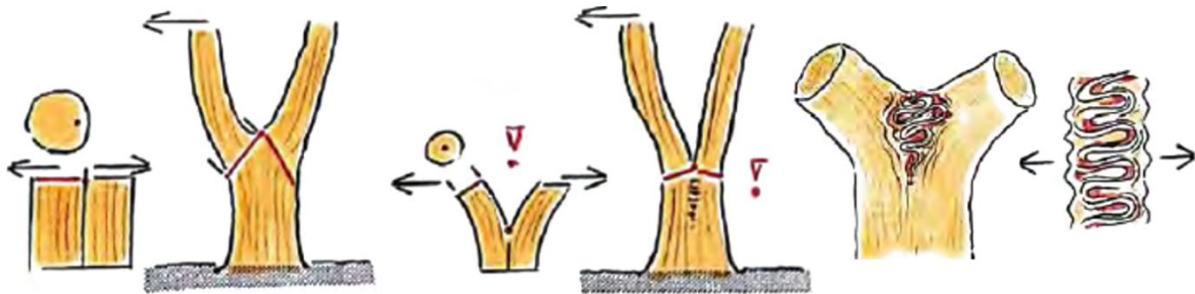

Figure 5.12 Left: U-shaped fork, Middle: V-shaped fork, Right: Interlocking of fibers (Wessolly & Erb, 2016)

Pulling tests on co-dominant stems showed that when the stems are both pulled in the same direction, it is more likely that the tree does not fail at the union, but somewhere else in the tree (Kane, 2014). When pushing the stems together, the absence of fibres in the middle has no influence. When pulling the stems apart, the absence of fibres is a weak spot for the introduced tension stresses, and the tree usually fails at the union. Pulling one of the stems in the direction of the dashed arrow, as indicated in figure 5.11 on the right, has a lower failure probability than pulling the stems in the direction of the solid arrow. This is due to the different influence of included bark for both pulling directions. When the tree is pulled in the direction of the dashed arrow, then the width of the included bark is perpendicular to the neutral axis (dashed line), this makes the effect minimal. When the tree is pulled in the direction of the solid arrow, then the width of the included bark is along the neutral axis (solid line), so the effect is significant (Kane, 2014).

6 METHODOLOGY LIVING TREE PAVILION AND AIRPOT TESTS

From the previous chapters came evident that there is a lack of knowledge about the behaviour of trees with self-growing connections. To be able to make a structural design in which connected trees are used, a way of modelling such a connection has to be found.

The *Living Tree Pavilion* and a tree in an airpot are chosen as study objects. Both are standing in the Botanical Garden of the TU Delft. In 2017 the *Living Tree Pavilion* was studied by Helena Borská (2018). She performed several measurements on the geometry of the trees. Furthermore, she performed winching tests to determine the influence of a connection on the displacement. Her results are used as a base for the expected results of this test.

The geometry measurements are performed again to get insight into the growth behaviour of trees and connections.

The main goal of the winching experiment is to create a dataset that can be used to validate models of a single standing, a cross-connected, and a parallel-connected tree. Subgoals are tot:

- Get insight into the rotational stiffness of the root system, to differentiate between deformation due to the root system and deformation due to the stem.
- Get an estimation of the root system stiffness of trees in airpots compared to unconstrained root systems.
- Get insight into the distribution of the modulus of elasticity over the height of the tree.
- Get insight into stress distribution due to a cross and parallel connection.
- Get a comparison of system stiffnesses based on deformation results.

There are two reasons for doing the winching tests again. First, the use of more advanced equipment makes it possible to measure root rotation and strain while Borská only measured the global deformation of the trees. This might give more insight into the distribution of stresses within trees and connections. Second, Borská found a scatter in the results that she could not interpret. It is tried to take away the possible reasons for this scatter. Borská suggested several reasons, which are:

- The deflections were very minimal. It is therefore advised to use a larger pulling force.
- The setup itself showed deformation because the used material was not strong enough.
- The pulling rope prolonged due to the attached weight.
- The deformation of the root system was not considered.

Based on observations of Borská, it is expected that the deflections of interconnected trees are smaller than the deflections of single standing trees. This will mostly be visible for the cross-connected trees as they have a connection higher up in the tree. The displacement reducing effect of connections will be visible in both radial and tangential direction.

Furthermore, it is expected that the trees have a modulus of elasticity of 6.250N/mm², as is stated in the *Stuttgarter Festigkeitskatalog* for Ash trees (Wessolly & Erb, 2016). This catalogue contains elastic moduli of living trees, determined immediately after a tree is felled by measuring the strain during compression tests on 4x4x40cm wood pieces. These pieces are sawn perpendicular to the surface of a one-meter high trunk, evenly distributed over the area.

This chapter starts with a description of the test pieces in paragraph 6.1. This is followed by the methodology of the tree characteristic measurements in paragraph 6.2, the methodology of the winching tests in paragraph 6.3, and the set-up of the finite element model in paragraph 6.4.

6.1 STUDY AREA

There are two test pieces, both located at the Botanical Garden of the TU Delft.

The first is a single elm tree (*Ulmus 'Clusius'*) which is standing in an airpot with a volume of 1,5m². This tree was planted in December 2018. See figure 6.1.

Figure 6.1 Ulmus 'Clusius' tree in the Botanical Garden of the TU Delft. Left: Photo of the tree during the winching test. Middle: Photo of the tree during the winching test. Right: Photo of the airpot. Photos taken on the 25th of June 2020.

The second test piece is the *Living Tree Pavilion* which is introduced in paragraph 2.2.3. Figure 6.2 includes a photo of this pavilion and a computer model of the original design by Nuijten (2011). The curved lines represent trees which are connected at ground level with natural growing parallel connections and have natural growing cross-connections higher up in the trees. Construction of the pavilion started in November 2010, and it opened in spring 2011.

Figure 6.2 Left: Photo of the Living Tree Pavilion, taken in June 2020. Right: 3D model of the Living Tree Pavilion (Nuijten, 2011)

Originally twenty-four ash trees (*Fraxinus Excelsior L.*) [2] were planted, of which twelve are still

---

[2] Correction: The reports of Nuijten (2011) and Borská (2018) state that ash trees are planted. However, when comparing the leaves, the pavilion is built with common lime trees (*Tilia x Europaea*).

standing at the time of testing. Figure 6.3 shows an illustration of these twelve trees, together with the connections between the trees.
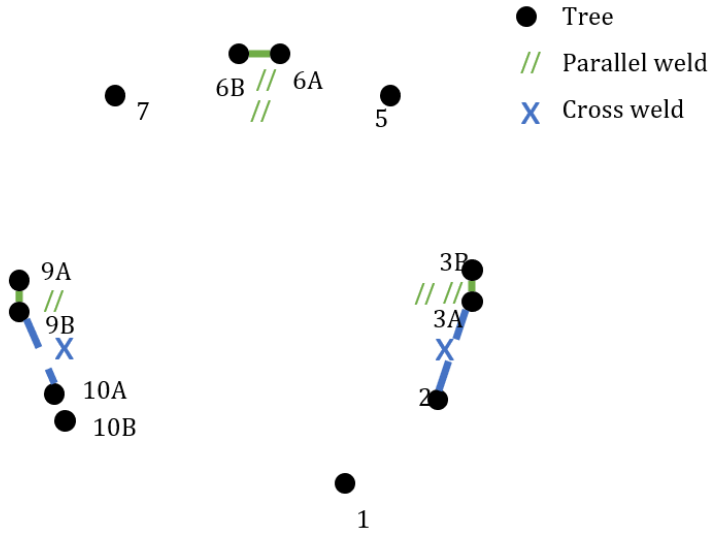

Figure 6.3 Top view illustration of the trees and their connections

Figure 6.4 shows the largest connections of the pavilion, which are the cross-connection between tree 9B and 10A and the parallel connection between tree 6A and 6B.

Figure 6.4 Left: Detailed view of cross connection tree 9B-10A. Right: Detailed view of parallel connection tree 6A-6B. Photos taken in June 2020.

Appendix B.1 contains more photos of the positioning of all trees and the connections.

6.2 Tree characteristic measurements

The equipment that is used during the measurements is listed in appendix B.2.

6.2.1 Tree growth – circumference increase

The circumference of all pavilion trees is measured in 2017 by Borská (2018). This procedure is followed so the results can be compared.

The circumference of the trees is measured at one meter of length of the trees, measured on the side of the tree that faces the middle of the pavilion. The one meter of length is measured with a soft ruler and marked with a waterproof marker. The circumference is measured with a soft ruler, perpendicular to the axis of the tree, see figure 6.5.

The measurements are performed on the 10th of June.

Figure 6.5 Left: Photo of circumference measurement with a soft ruler. Right: Illustration of the circumference measurement method

6.2.2 Connection growth

The dimensions of the connections are measured in December 2017 by Borská (2018). The same procedure is followed so the results can be compared. Figure 6.6 on the left shows which trees she has measured, and on the right, the figure shows the measured dimensions of the connections.
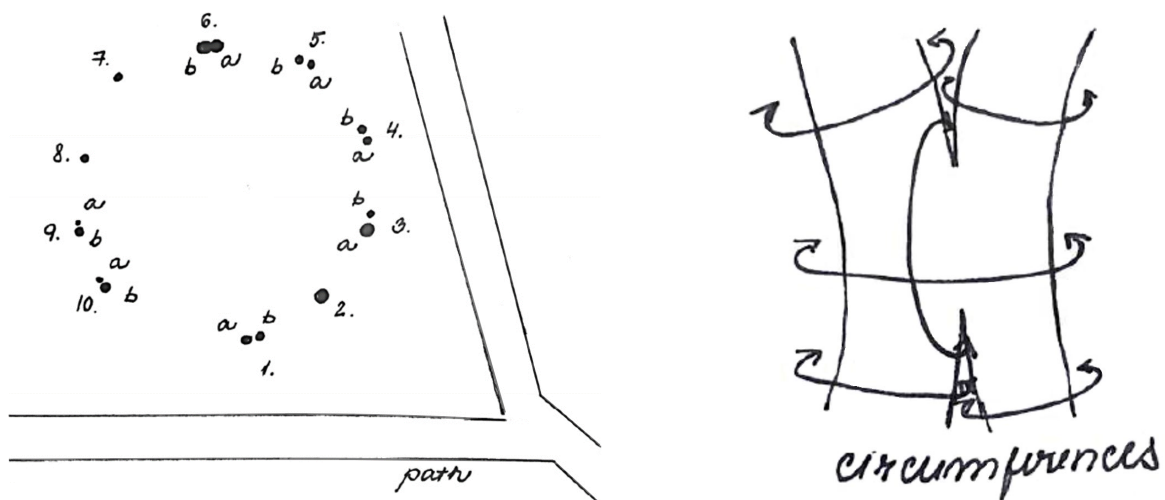

Figure 6.6 Left: Position of trees in 2017. Right: Measurements circumferences of connections (Borská, 2018)

The measurements are carried out twice, first on the 19th of March 2020, second on the 24th of June 2020.

6.2.3 Influence of connection on stem circumference

The circumference of the trees is measured at every half a meter of length up till 2,5 meters, measured on the side of the tree that faces the middle of the pavilion. Trees 6A, 6B, 9B, 10A, and 10B are measured with intervals of ten centimetres, because of their use in the winching tests. The length of the tree is measured with a soft ruler, and the measure locations are marked with a waterproof marker. The circumference is measured with a soft ruler, perpendicular to the angle of the tree, similar as explained in paragraph 6.2.1.

The measurements are performed on the 10th of June.

6.2.4 Ovalisation due to leaning of trees

With a calliper, the width of the tree stem in radial and tangential thickness is measured at every half a meter of length up till a length of two meters. This width is measured perpendicular to the direction of the stem. The comparison of the radial and tangential width is based on the average of the measurements over the two meters of length. The leaning of the tree and its magnitude is estimated by sight.

The measurements are performed on the 10th of June.

6.2.5 Tree geometry as input for the finite element model

The geometry is measured on the 10th, 15th, and 24th of June, and the 2nd and 3rd of July 2020.

The geometries of trees 6A, 6B, 9B, 10A, and 10B are measured based on their own coordinate system in which the radial axis is directed towards the middle of the pavilion, and the tangential axis is directed perpendicular to this. This is shown in figure 6.7 on the left.

At every 10cm of tree length, on the side facing the middle of the pavilion, a mark is written. At all these spots, the following is measured:

- Height. This is measured by holding a rope with a weight at the measurement location. The weight should just touch the ground level. The length of this rope is then measured with a steel retractable meter.
- Radial and tangential coordinates. The same rope with weight is used to measure the radial and tangential location of the marked points. One lath with a steel retractable meter is positioned towards the middle of the pavilion; another is positioned perpendicular to this. Two smaller laths, glued perpendicular to each other, are then placed below this weight to read the radial and tangential location at the bigger laths. At all times, the perpendicular angles are checked with a triangle ruler. To determine the radial and tangential coordinates of the middle point of the tree, the measured value is modified with the radii of the tree at the measured level and the bottom. This is illustrated in figure 6.7 on the right.
- Radial and tangential thickness. With a calliper, the width of the tree stem in radial and tangential direction is measured. This width is measured perpendicular to the direction of the stem.
- Circumference. The circumference is measured with a soft ruler, perpendicular to the direction of the stem.
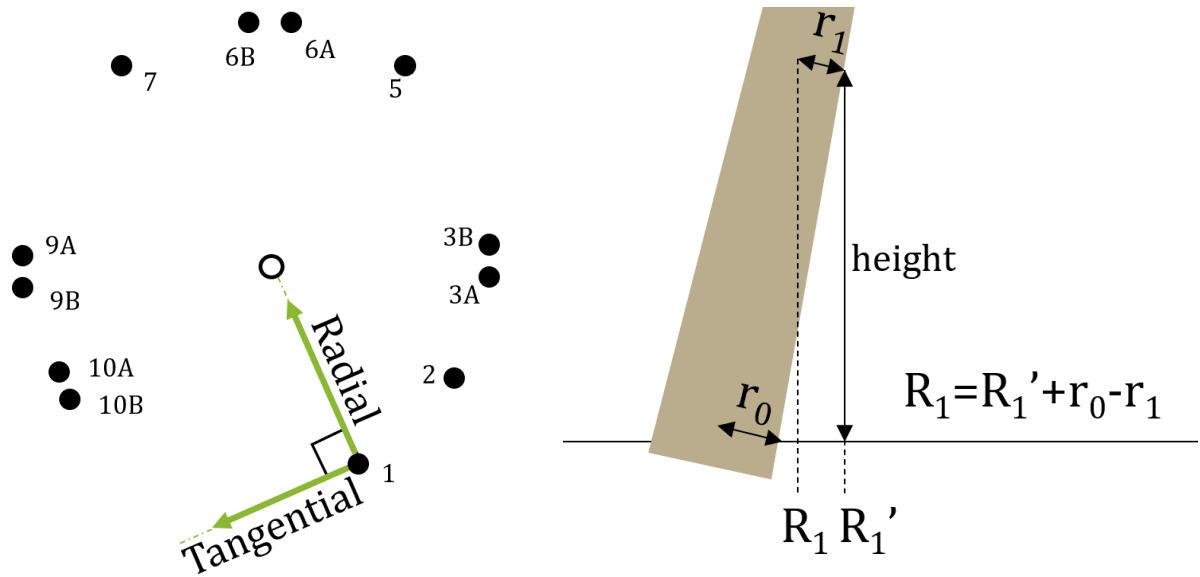
Figure 6.8 shows photos of the measurements.

Figure 6.7 Left: Coordinate system shown for tree 1. Right: Illustration of calculation after measuring the coordinates of several points on the tree.

Figure 6.8 Geometry measurements. Top left: Measuring the height. Top right: Measuring the tangential width. Bottom: Measuring the radial and tangential coordinates.

6.3 WINCHING TESTS

On the 25th of June 2020, winching tests are performed in collaboration with Dennis de Goederen, who is part of *Pius Floris Boomverzorging*. Figure 6.9 shows a photo of a winching test. During such tests, a force is applied on a tree by spanning a steel cable between the tree and an anchor point, in this test the towbar of a van. A winch stresses the steel cable. During one measurement cycle, the applied force, the strain on the marginal fibres of the tree at three locations and the tilting of the root plate at two locations is measured. Furthermore, the height of the application of the cable on the tree and the inclination of this cable is measured. The length of the cable is measured before and after winching.
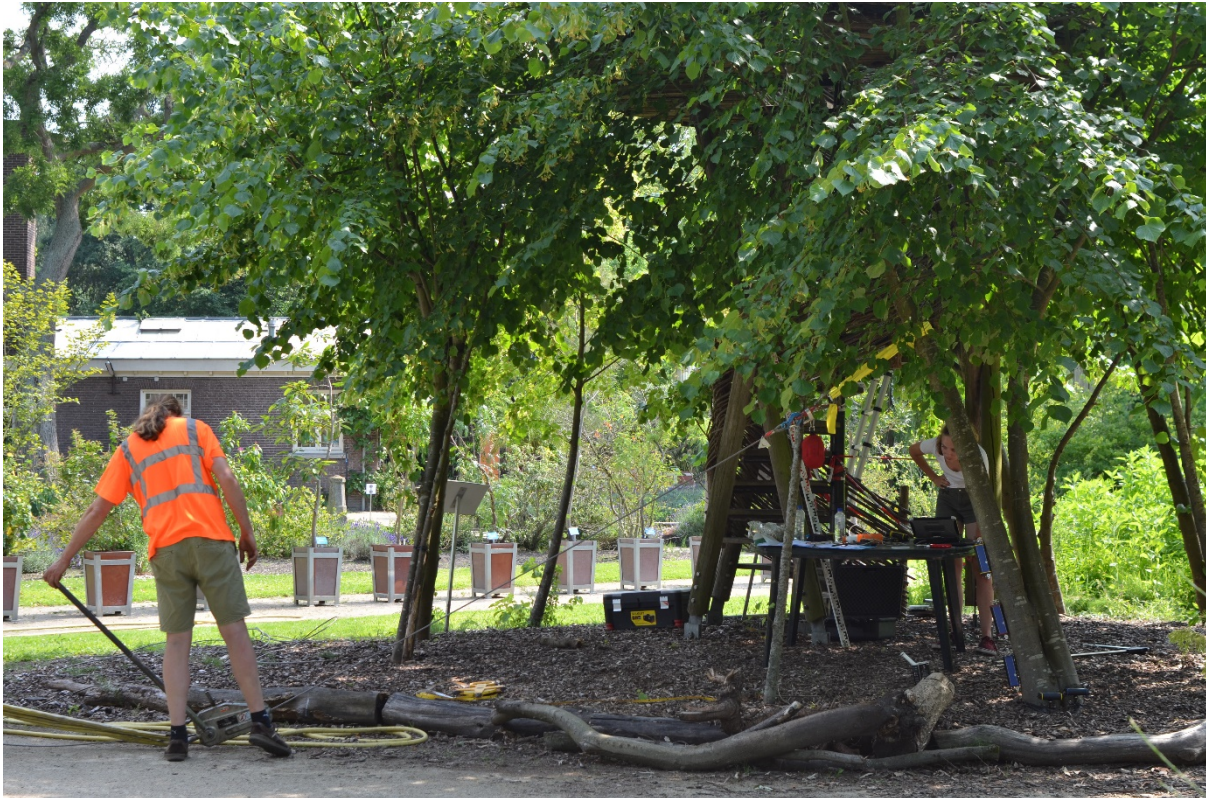
Figure 6.9 Photo of winching test trees 6A and 6B

The tested trees are described in paragraph 6.1. The trees that have been tested are:

- Single tree 10B
- Cross-connected trees 9B and 10A
- Parallel-connected trees 6A and 6B
- Single tree in an airpot

An overview of these trees, including their test directions and elastometer locations, is given in appendix B.3. As an example, the procedure for one of the tests on the parallel-connected trees 6A and 6B will be explained.

First three elastometers are placed on the tree, in the same line as the direction of the force application. The length of the tree at the locations of the elastometers is indicated in the right illustration of figure 6.10, in this case: 0,15, 0,45, and 0,75m. Two inclinometers are placed at the bottom of the tree, on the side perpendicular to the force direction. Each one is placed on another tree. In figure 6.10, this is illustrated with yellow and blue circular arrows. The cable is attached to the tree and the van, passing through a winch and force registration equipment. The height of

the cable is measured with a ruler lath, which is in this case, 1,9 meter. After pulling the cable a little bit, the angle is measured with a laser hypsometer with a built-in inclinometer. The angle is indicated in the illustration with 19,2°. The length of the cable is measured with a soft ruler. Then, force is applied to the tree by winching the cable until a specific strain or rotation is measured. This value is determined by Dennis de Goederen and could be read from a portable computer. At maximum stress, the length of the cable is measured again.

Later, not on the field, the horizontal angle of the cable with the radial direction is measured by drawing two lines in an air photo and measuring the angle. The first line from the tree to the middle of the pavilion, the second line from the tree to the location of the van. Figure 6.10 on the left illustrates this angle, which is 89°.
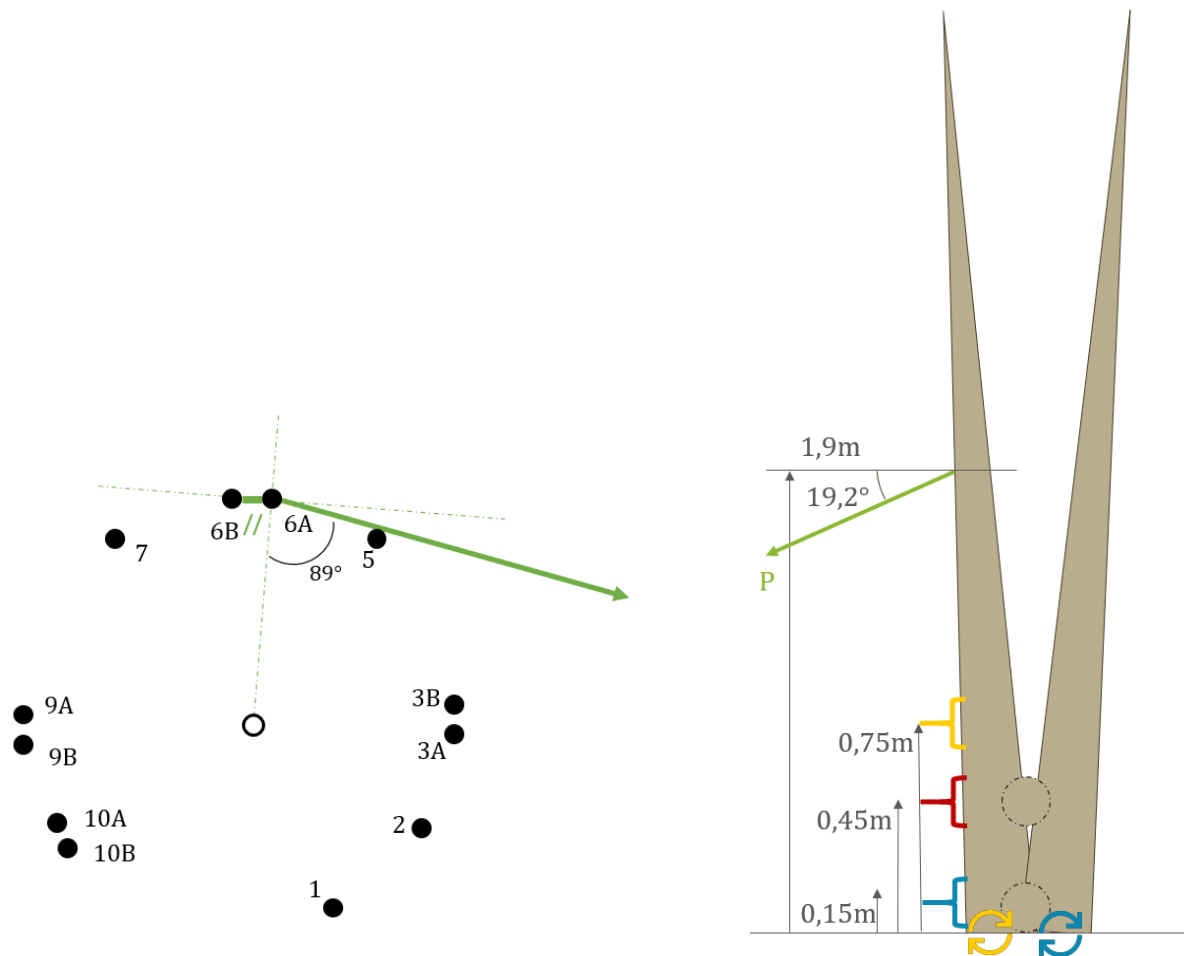
Figure 6.10 Illustrations of one measurement round of winching test trees 6A and 6B. Left: Top view of all trees with indication of horizontal force angle with the radial axis. Right: Trees 6A and 6B with yellow, red, and blue elastometers and yellow and blue inclinometers. Indicated are vertical angle of the cable and the heights of the elastometers and the cable.

Furthermore, the soil moisture content is measured according to the gravimetric method (The Editors of Encyclopaedia Britannica, 2018). These tests are performed by Marc Friebel, part of *Geoscience & Engineering Laboratory TU Delft*. At three locations a soil sample is taken: next to tree 6A, next to tree 10A, and in the airpot. With a shovel, a bit of soil is dug and put in a plastic bag. The three bags are closed airtight, marked with a number, and stored in the fridge. The latter was necessary because the soil samples were taken on the 26th of June (Friday), but the Geosciences laboratory opened on the 29th of June (Monday). On the 29th, aluminium containers were weighed, then the soil samples were put in, and the containers were weighed again. After they have been in an oven at 105°C for 24 hours, they were weighed one last time. The soil moisture content is not included in the winching analysis. The registration is carried out in case the winching results will be further investigated by a root or soil specialist.
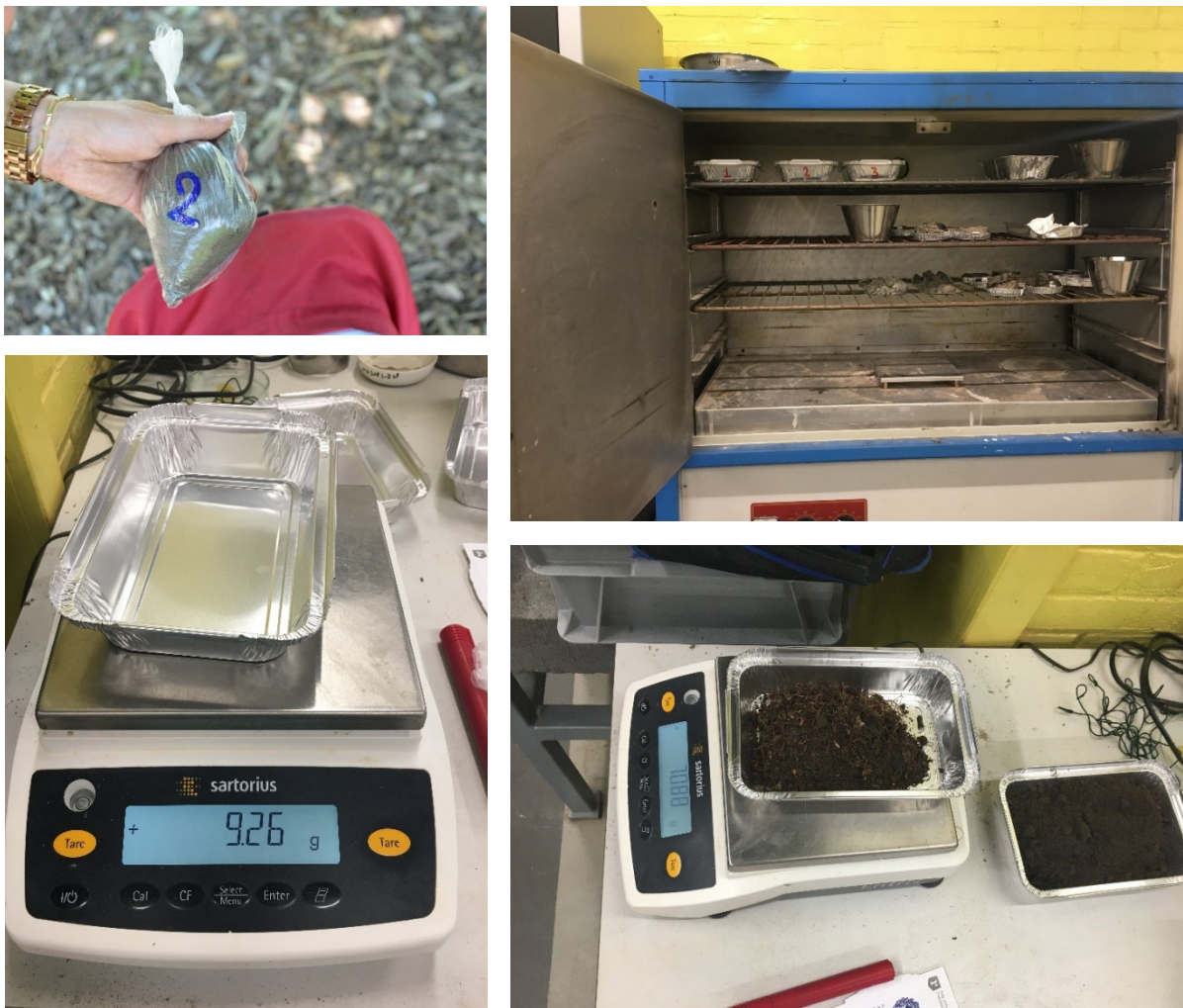

Figure 6.11 Soil moisture content. Top left: Soil sample. Top right: Three samples in an oven of 105°C. Bottom left: Weighting aluminium container. Bottom right: Weighting aluminium container with soil sample

6.4 FINITE ELEMENT MODEL

Based on the results from the geometry measurements, 3D finite element models are created of the single tree 10B, the cross-connected trees 9B-10A and the parallel-connected trees 6A-6B. The software *Dlubal RFEM 5.21* is used. Figure 6.12 shows that the trees are modelled as a solid, with an ellipse-shaped cross-section with intervals of 10cm of length, according to the measurements as described in paragraph 6.2.5. A geometrical linear analysis is carried out.
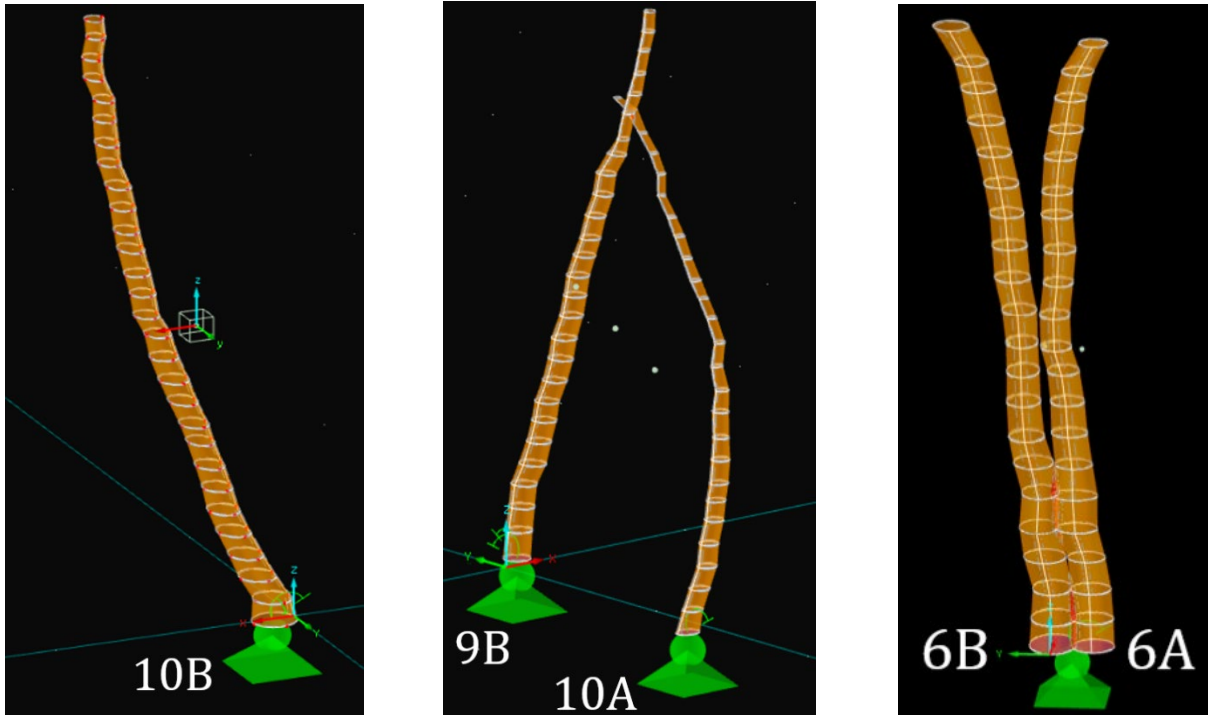

Figure 6.12 Finite element model of trees 10B, 9B-10A, and 6A-6B

The trees are rotated such that the x-direction of the models coincides with the direction of radial forces, and the y-direction coincides with the direction of tangential forces. The applied force during the tests is placed on the model, decomposed in a horizontal and vertical direction.
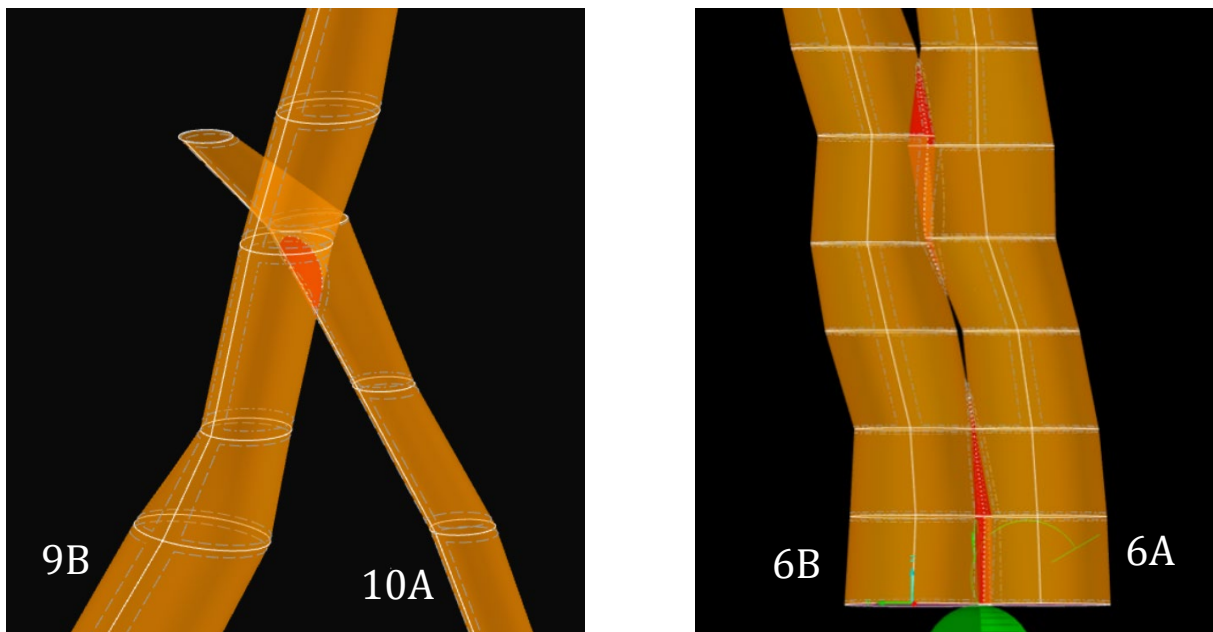

Figure 6.13 Left: Detail of connection tree 9B and tree 10A. Right: Detail of connection tree 6B and 6A

Trees 9B-10A and 6A-6B intersect each other in the model, see figure 6.13 for a close-up. The trees are first created as separate solids, after which one compound solid is created ensuring the two trees behave as one single solid. This way of modelling creates a rigid connection. The hypothesis is that this gives the proper distribution of stresses between the trees. This is based on the fact that the connection shows common growth rings, which, as explained in paragraph 5.4, makes the transfer of bending moments possible. Furthermore, during the winching tests, no movement within the connection was visible on eyesight. The hypothesis is tested by comparing the elastometer results from the winching tests with the strain results from the finite element model.

The base plates of the trees are rigid. Underneath the base plates, a nodal support is placed with a spring stiffness in both radial and tangential direction. The magnitude of the spring stiffness of single tree 10B is derived from the measured force and rotation during the winching tests. This derivation will be shown in paragraph 7.2.2. Likewise, the spring stiffness of trees 6A and 6B can be determined as these trees share one support. Modelling them with a single support is chosen because both trees show identical root rotation during the winching tests, as can be seen in the inclinometer results of appendix C.2.6. Trees 9B and 10A both have their own support.

Consequently, their spring stiffnesses cannot directly be determined from the measured force and rotation. The stiffnesses are determined with three iterations, starting with the average spring stiffness of tree 10B. Then, the stiffnesses are adjusted, based on the bending moment result from the finite element model and the measured root rotation of the winching tests. The final spring stiffness results in similar root rotations as measured during the winching tests.

The applied force on the model is the average of the force registration, from the moment that the increase of force application stops. Figure 6.14 illustrates an example of this. However, as the force measurement is not calibrated to 0kN at the beginning of the force registration, the blue line in the graph is adjusted to zero. The green line illustrates this.
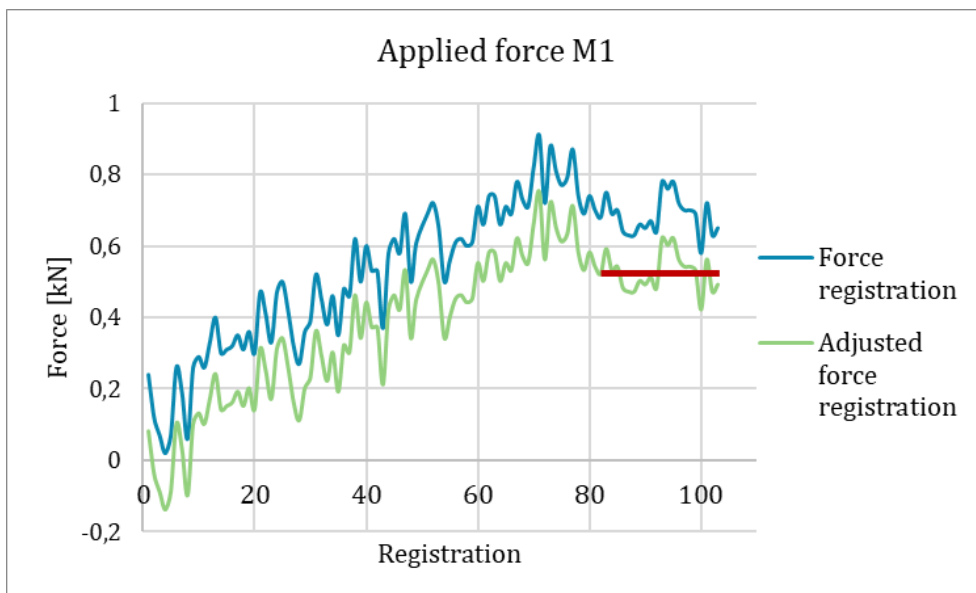

Figure 6.14 Registration of force during measurement 1 of tree 10B (blue line), adjusted to start at 0kN (green line). The red line indicates the registration of forces from the moment the increase of force application stops.

Table 6.1 shows the finite element model input values that are equal for the single tree, the cross-connected trees, and the parallel-connected trees. The parallel modulus of elasticity is the greenwood modulus of elasticity of Ash trees according to the *Stuttgarter Festigkeitskatalog* (Wessolly & Erb, 2016). The parallel direction in the model is defined as the vertical direction along the stem length. The perpendicular modulus of elasticity and the shear modulus are stated in the norm NEN-EN384 for hardwood timber (NEN, 2018). The Poisson's ratio is the ratio between the modulus of elasticity and the shear modulus.

Table 6.1 Input values for finite element model of tree 10B, 9B&10A, and 6A&6B

Material properties	
Modulus of elasticity parallel [N/mm²]	6.250
Modulus of elasticity perpendicular [N/mm²]	417
Shear modulus [N/mm²]	391
Poisson's ratio	0,0625
Loads	
Method of analysis	Geometrically linear analysis
Mesh settings	
Target length of finite elements [mm]	25,0
Solids FE mesh refinements [mm]	25,0

As explained, the results of the winching tests are the input values for the nodal support stiffness and forces in the finite element model. Table 6.2 shows a summary of these input values for the single tree 10B.

Table 6.2 Input values FE model of tree 10B

Measure-ment	Force application		Magnitude of force [kN]			Nodal support stiffness [kNm/rad]
	At length [mm]	Direction	P_x	P_y	P_z	φ_x and φ_y
1	2800	Radial	0,510	0	0,113	178,5
2	2800	Radial	0,553	0	0,124	149,9
3	2800	Radial	0,686	0	0,153	165,7

Similarly, table 6.3 summarizes the input values for the forces on the models of trees 9B and 10A, during seven measurement rounds.

Table 6.3 Input load cases in the FE model of trees 9B and 10A

Measure-ment	Force application			Magnitude of force [kN]		
	Description	At length[1] [mm]	Direction	Px	Py	Pz
1	At connection	2100	Radial	0,490	0	0,091
2	At connection	2100	Radial	0,408	0	0,076
3	Above connection	2600	Radial	0,157	0	0,049
4	Above connection	2600	Radial	0,150	0	0,042
5	Above connection	2600	Vertical	0	0	0,185
6	Above connection	2600	Tangential	0	0,228	0,127
7	Above connection	2600	Tangential	0	0,218	0,122

[1]Applied at tree 9B

Table 6.4 shows the nodal support stiffnesses of tree 9B and 10A, which are the same for all measurement rounds.

Table 6.4 Input values nodal support stiffness FE model of trees 9B and 10A

	Nodal support stiffness [kNm/rad]	
	φ_x	φ_y
Tree 9B	619	92
Tree 10A	40	69

Two measurement rounds are applied on trees 6A and 6B, both in tangential direction. The force magnitude applied to the finite element model is stated in table 6.5. The table also shows the nodal support stiffness for trees 6A and 6B, which share one support.

Table 6.5 Input values FE model of trees 6A and 6B

Measure-ment	Force application			Magnitude of force [kN]			Nodal support stiffness [kNm/rad]
	Description	At length[1] [mm]	Direction	Px	Py	Pz	φ_x and φ_y
1	Above connection	2000	Tangential	0	0,871	0,303	490
2	Above connection	2000	Tangential	0	1,043	0,363	490

[1]Applied at tree 6A

7 RESULTS LIVING TREE PAVILION AND AIRPOT TESTS

This chapter shows the results of the tests performed on the *Living Tree Pavilion* and the airpot tree. The same structure is used as in chapter 6 *Methodology Living Tree Pavilion and Airpot Tests*, starting with the measurements of tree characteristics in paragraph 7.1. This includes the growth in circumference and the growth of the connections. Additionally, the influence of a connection on the stem circumference is discussed after which it is investigated whether a connection influences the ovality growth of a stem. Paragraph 7.2 shows the results of the winching tests and presents the resulting root stiffness and bending stiffness of the total system. In paragraph 7.3, the winching results are compared with the finite element models.

7.1 TREE CHARACTERISTIC MEASUREMENTS

7.1.1 Tree growth – circumference increase

Appendix C.1.1 contains the measurement results of the circumference of the trees. Figure 7.1 shows a graph of the results, together with the measurement results of Borská (2018), six years after planting. At year 0, the circumferences are not measured but described in the design of Nuijten (2011). Whether the planted trees had the same thickness as designed is unknown.

Furthermore, Nuijten expected that the circumference of the trees increases with 20mm per year. This prognosis is included in the graph.
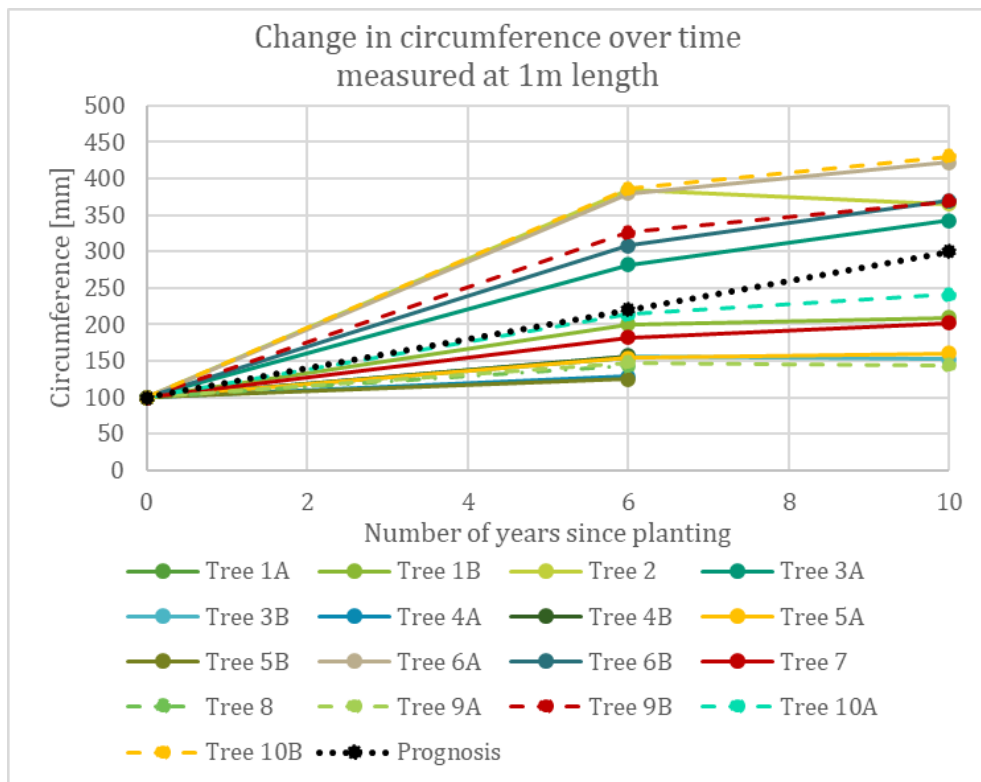
Figure 7.1 Change in circumference at 1m length over time. Including the designed circumference at 0 years after planting, the measurement results of Borská (2018) at 6 years after planting, and the measurement results at 10 years after planting. Additionally, it shows a prognosis by Nuijten (2011) for the increase in circumference over time.

Trees number 1B, 4A, 4B, 5A, and 8 are removed from the *Living Tree Pavilion*.

All trees increase in circumference except for trees 2, 3B, and 9A. For tree 3B, this can be explained by the death of the tree. A possible reason for a decrease in circumference measurement of the other two trees is the change in surface level. This level is variable as wood chips are scattered occasionally over the surface. This results in different heights at which the measurements are carried out, compared with the measurements of Borská (2018).

The circumference growth rate in the first six years is on average 21mm per year, in line with the expectation of Nuijten (2011). The growth rate decreases to 6mm per year in the last four years. According to Ernst Kamphuis, a gardener of the Botanical Garden, during the last years the tree growth is hindered by several floods and very wet soil.

7.1.2   Connection growth

Figure 7.2 shows the growth of the connection circumference in horizontal and vertical direction over ten growing seasons. Year zero is the expected circumference in the design of Nuijten (2011). Year six are measurements carried out by Borská (2018). Year nine is measured in March 2020, and year ten is measured in June 2020. Appendix C.1.2 contains tables with numerical values.
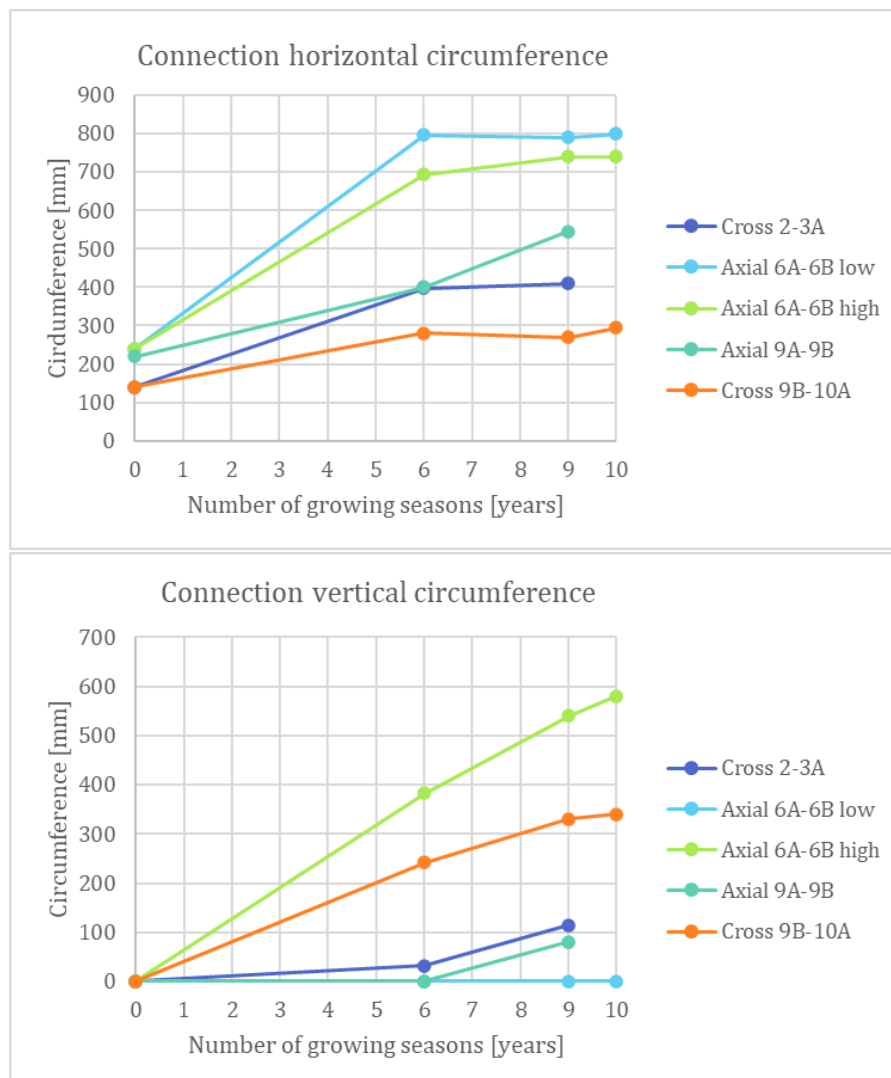
Figure 7.2 Growth in circumference of the connections in the Living Tree Pavilion. Measured during year 9 and 10. Year 0 is a prognosis by Nuijten (2011), year 6 is measured by Borská (2018). Top: Horizontal circumference. Bottom: Vertical circumference

After nine growth years, the same connections were observed as after six growth years, plus a parallel connection at the base of trees 9A and 9B. Almost all dimensions shown in the figures increased. Borská (2018) also measured the dimensions of the connection between tree 3A and tree 3B. Because tree 3B died, these results are not included in the graphs.

The measurements during the tenth growing season have either increased or are similar to the measurements of year nine.

7.1.3 Influence of connection on stem circumference

Trees may show less secondary growth just below a connection because of the stabilizing effect of this connection. This is checked for the pavilion trees with cross-connections, which are trees 2-3A and 9B-10A.

Figure 7.3 presents the results of the circumference measurements. Some trees are measured every 10cm of length, others every 50cm of length. The trees that have a cross-connection are coloured green or blue. A horizontal line indicates the length of the tree at the location of the connection. Although no clear trend can be seen, the sudden decrease in the circumference of tree 3A and 9B just below the connection could be the result of the stabilizing effect of the connection.
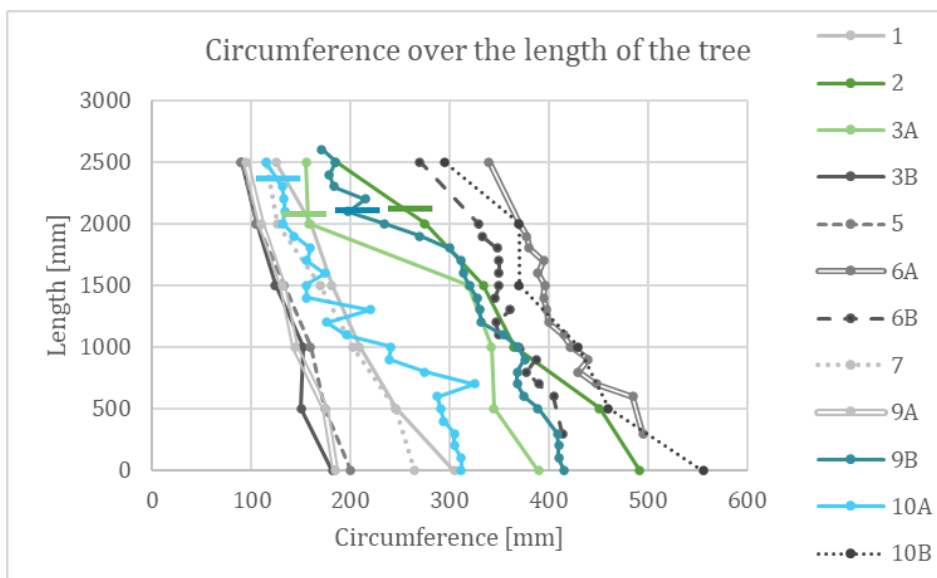
Figure 7.3 Change in circumference over the length of the trees. Cross connected trees are coloured. The location of a connection is marked with a line.

7.1.4 Ovalisation due to leaning of trees

As explained in paragraph 4.1, Wessolly and Erb (2016) observed that leaning broad-leaved trees, which the trees in the pavilion are, develop secondary growth on the tensile side of the tree. This is checked for the pavilion trees.

Based on the radial and tangential thickness, the cross-section of the trees is drawn in figure 7.4. The red lines indicate the direction in which the trees lean. The length of the line indicates the magnitude of the leaning of the tree. These values are estimated by sight, so no dimension indication is given.
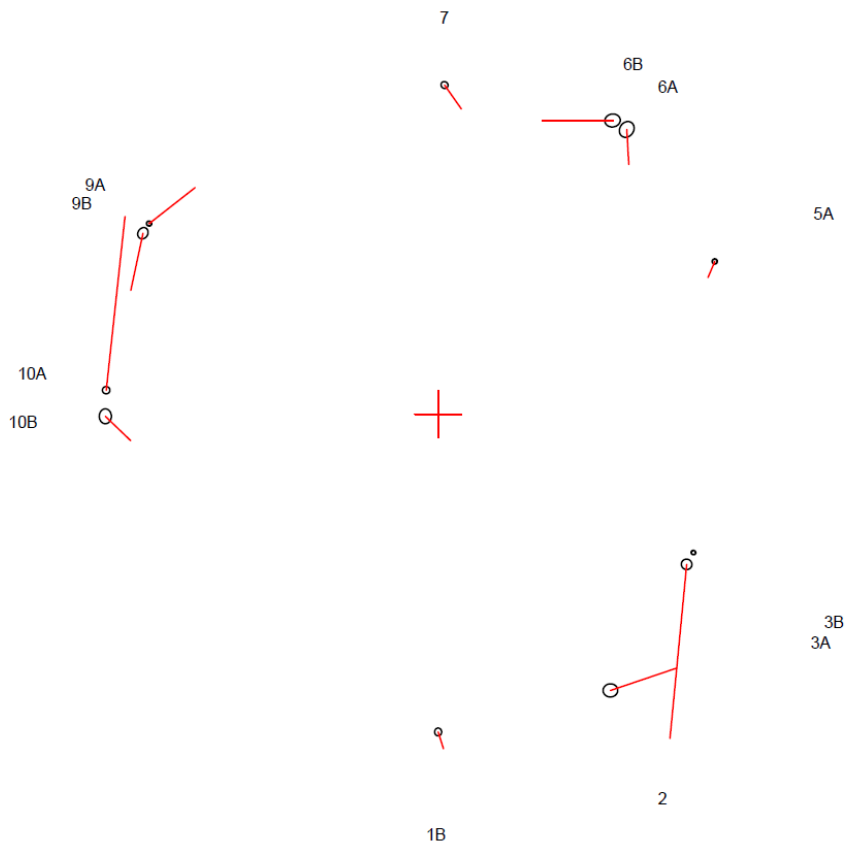
Figure 7.4 Ovalisation of trees. The red lines indicate the direction of the tree's centre of self-weight and the amount of eccentricity from the base of the stem.

The amount of ovalisation in the direction in which the tree leans is calculated with:

$$\frac{diameter\ in\ leaning\ direction - diameter\ perpendicular\ to\ leaning\ direction}{diameter\ perpendicular\ to\ leaning\ direction} \times 100\%\ (NEN, 2006)$$

A positive value indicates that there is ovalisation in the leaning direction of the tree.

Tree 1:	8,4	Tree 6B:	19,4
Tree 2:	13,7	Tree 7:	9,6
Tree 3A:	-3,7	Tree 9A:	0,7
Tree 3B:	X (dead)	Tree 9B:	13,4
Tree 5A:	2,3	Tree 10A:	-2,8
Tree 6A:	6,5	Tree 10B:	-0,1

Although minimal, most of the trees show ovalisation in the direction in which they are leaning. It is expected that once the trees grow larger, the influence of self-weight becomes more significant, increasing the ovalisation.

Remarkably, the trees that are leaning the most, trees 3A and 10A, have a negative ovalisation in the leaning direction. This may be due to their cross-connection to another tree. This stabilizing effect could take away the need of developing stiffness in the leaning direction.

7.2 WINCHING TESTS

7.2.1 Test registration

The registration of the force meters, elastometers and inclinometers can be found in the appendix C.2. In this appendix also the weather conditions and the results of the soil moisture content are given.

7.2.2 Root stiffness

During the three measurement rounds on the single tree 10B, the rotation of the root system in radial and tangential direction is measured with an inclinometer. The moment at the tree base, as illustrated in figure 7.5 on the left, is calculated with [3]:

$$M = F_{horizontal} \times h + F_{vertical} \times b$$
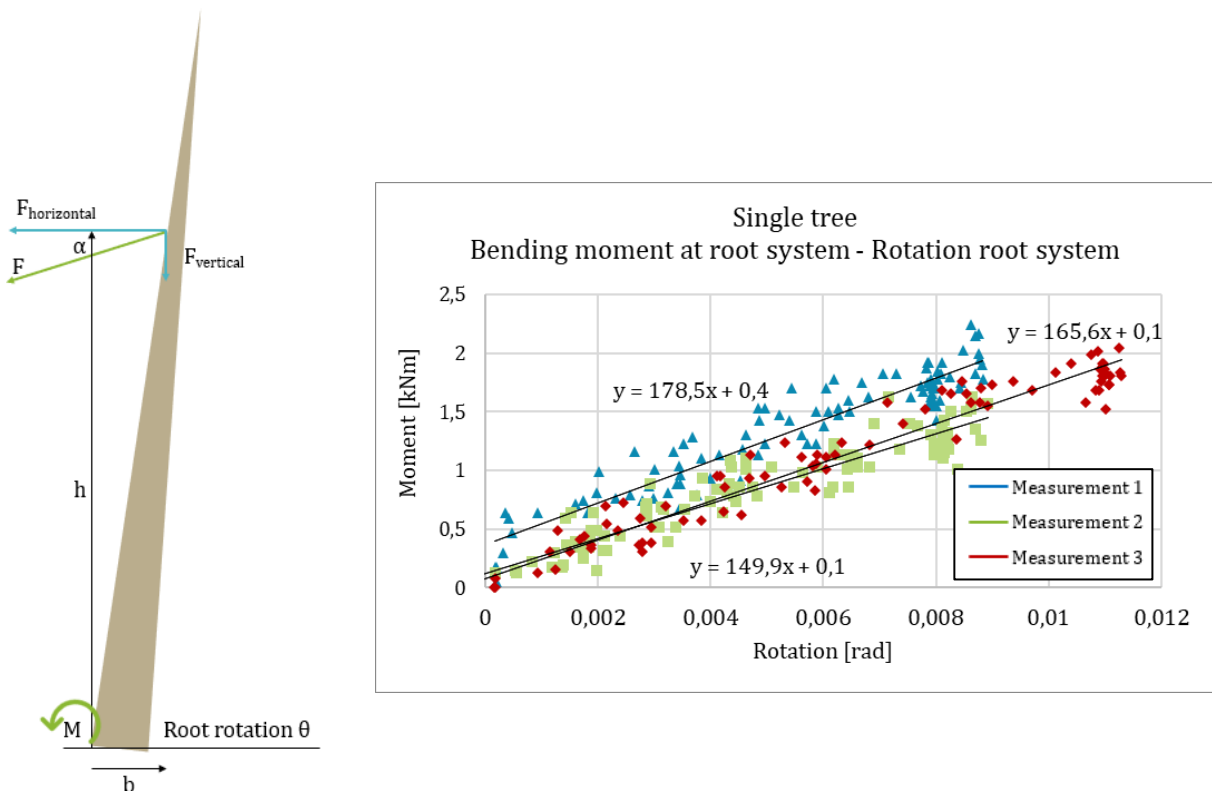
Figure 7.5 Left: Calculation of bending moment at the root system. Right: Graph of the bending moment at the base of tree 10B, versus the measured root rotation in the direction of the force (radial). A linear regression is drawn through the data points, the formulas are shown in the graph.

Because the tree is pulled within its elastic range, the root system stiffness can be calculated with:

$$k = \frac{M}{\theta}$$

Table 7.1 Results root system stiffness of tree 10B

Measurement	k [kNm/rad]
1	178,5
2	149,9
3	165,7
Average	164,7

This relationship is plotted as a linear regression through the data points in the graph of figure 7.5. The formulas of these regression lines are written in the graph. Table 7.1 summarizes the resulting root system stiffnesses.

---

[3] Carefully determine the positive and negative values based on the chosen coordinate system.

Following the same procedure as for tree 10B, the root system stiffness of the tree in an airpot is determined, see figure 7.6. The root system stiffness for this measurement is 24,4 kNm/rad.
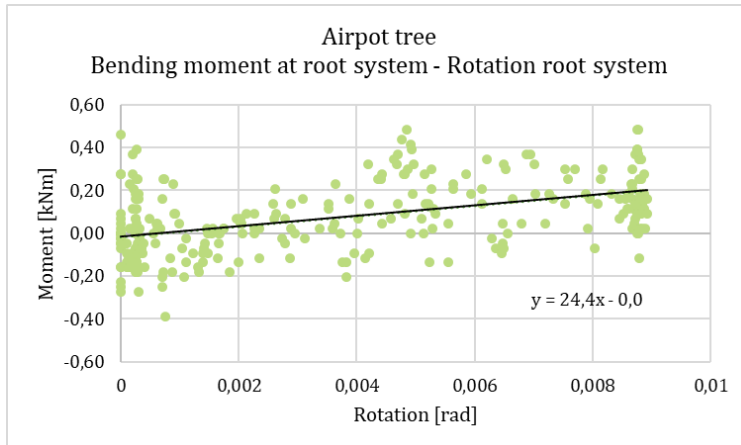

Figure 7.6 Graph of the moment at the base of the tree versus the measured rotation in radial direction, tree in airpot. A linear regression is drawn through the data points, the formula is shown in the graph.

7.2.3 Total system bending stiffness

To get an understanding of the bending stiffness of the tree systems, their measured displacement is compared to the applied force. Figure 7.7 shows a schematization of this system as a beam with a rigid support on one side. The bending stiffness of the total system, expressed as EI, is calculated with:

$$w_h = \frac{F_h * L^3}{3 * EI} + \theta * L$$

$$EI = \frac{F_h * L^3}{3(w_h - \theta * L)}$$

Table 7.2 summarizes the results. Although differently expected, the single tree has the highest bending stiffness. In table 7.3, the results of the bending stiffness are compared per volume of tree below the attached cable. It shows that the single tree still has the highest stiffness. Furthermore, the cross-connected trees have a higher bending stiffness in radial direction than in tangential direction. The parallel-connected trees have a low bending stiffness in the tangential direction.
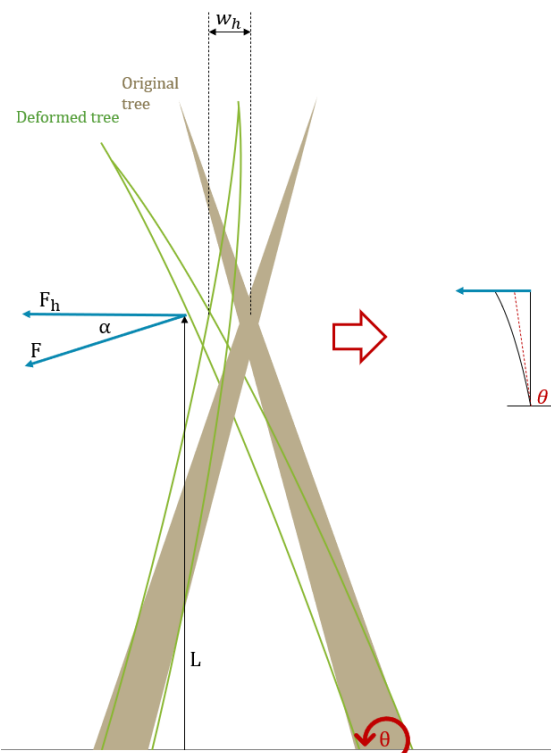

Figure 7.7 Schematization of a tree system into a beam with a rigid support on one side

Table 7.2 Total system bending stiffness

Tree	Connection	Force direction	L [m]	F_h [kN]	w_h [m]	$\theta*L$ [m]	EI [kNm²]
10B	No	Radial	2,8	0,6	0,26	0,03	18,4
9B-10A	Cross	Radial at connection	2,1	0,5	0,14	0,01	10,6
9B-10A	Cross	Radial above connection	2,6	0,2	0,09	0,00	9,8
9B-10A	Cross	Tangential above connection	2,6	0,3	0,27	0,00	4,8
6A-6B	Parallel	Tangential	2,0	1,0	0,53	0,01	4,9

Table 7.3 Total system bending stiffness per volume

Tree	Connection	Force direction	V [m³]	EI/V [kN/m]
10B	No	Radial	0,025	733
9B-10A	Cross	Radial at connection	0,023	464
9B-10A	Cross	Radial above connection	0,024	411
9B-10A	Cross	Tangential above connection	0,024	199
6A-6B	Parallel	Tangential	0,042	116

Table 7.4 shows that the results do not correspond to the results that Borská obtained in 2017. In general, she applied similar loads but measured smaller displacements. There are, of course, differences in the measuring method. Borská did not take root rotation into account, but as seen in table 7.2, its influence is small. Furthermore, the height of the cable application is not the same at all tests. This might give a difference in the obtained bending stiffness because of a deviating modulus of elasticity over the height of a tree. However, the most striking result is the difference in ratios between the results. The single tree 10B, for example, has a low bending stiffness according to Borská while in the recent test it has the highest bending stiffness. The opposite holds for the parallel connected trees which have a high bending stiffness according to Borská while in recent tests they have a low bending stiffness.

Table 7.4 Winching results Borská (2018)

Tree	Connection	Force direction	L [m]	EI [kNm²]
10B	No	Radial	2,0	83,7
9B-10A	Cross	Radial	2,0	26,1
9B-10A	Cross	Tangential	2,0	313,3
6A-6B	Parallel	Tangential	2,0	470,7

Errors in the displacement measuring method could be a cause for the unexpected low bending stiffness of the tangentially pulled cross-connected and parallel-connected trees. During the winching tests of tree 10B, trees 9B-10A in tangential direction, and trees 6A-6B, the winch got lifted off the ground. This was not the case for trees 9B-10A pulled in radial direction. Figure 7.8 illustrates that the winch lift gives a shortening of the cable without deformation of the tree. The height of the lifted winch is estimated based on photos of the winching test. Table 7.5 contains the adjusted results in which the estimated winch lift is included.
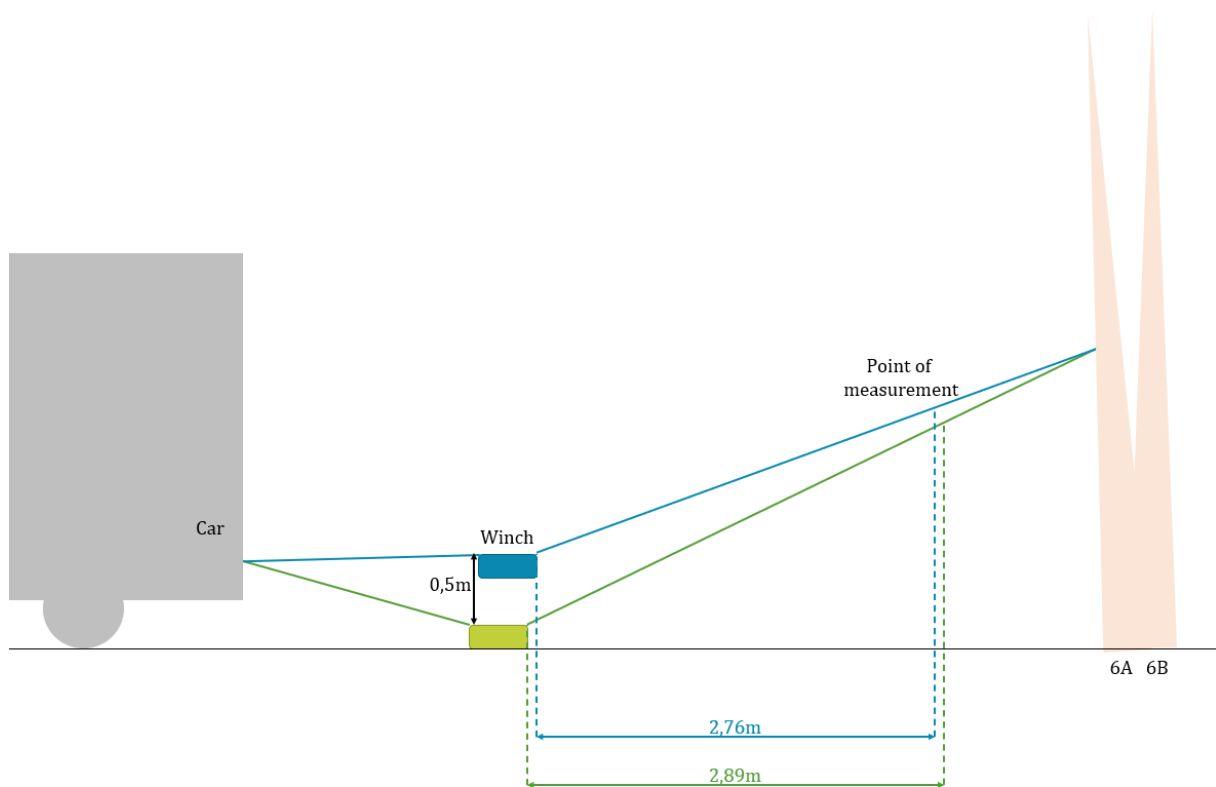
Figure 7.8 Shortening of the winching cable due to lifting of the winch. Illustrated for trees 6A-6B

Table 7.5 Total system bending stiffness including the lifting of the winch

Tree	Connection	Force direction	$w_{h,old}$ [m]	Lift [m]	$w_{h,lift}$ [m]	$w_{h,old}$-$w_{h,lift}$ [m]	EI [kNm²]
10B	No	Radial	0,26	0,1	0,02	0,24	20,2
9B-10A	Cross	Radial at connection	0,14	0,0	0,00	0,14	10,6
9B-10A	Cross	Radial above connection	0,09	0,0	0,00	0,09	9,8
9B-10A	Cross	Tangential above connection	0,27	0,4	0,11	0,16	8,7
6A-6B	Parallel	Tangential	0,53	0,5	0,13	0,40	6,8

As can be seen, the influence of this error is considerable. However, trees 9B-10A in tangential direction and trees 6A-6B remain the systems with the lowest bending stiffness.

Figure 7.9 contains photos of the cross-connection of trees 9B-10A. When having a closer look, small yellow cracks can be seen in the bark, indicated with white circles. According to Dennis de Goederen, this shows where a tree is often subjected to stress and therefore wants to create secondary growth. The central figures show the finite element model of the same connection when the trees are subjected to a radial force. In the figures on the right, the model is subjected to a tangential force. Clearly, the trees subjected to a radial force show more similarities with the bark cracks. Probably, the real trees are more often exposed to radial forces, resulting in an increase of stiffness in that direction. This might be an explanation for the difference in displacement results in the two directions of trees 9B-10A.
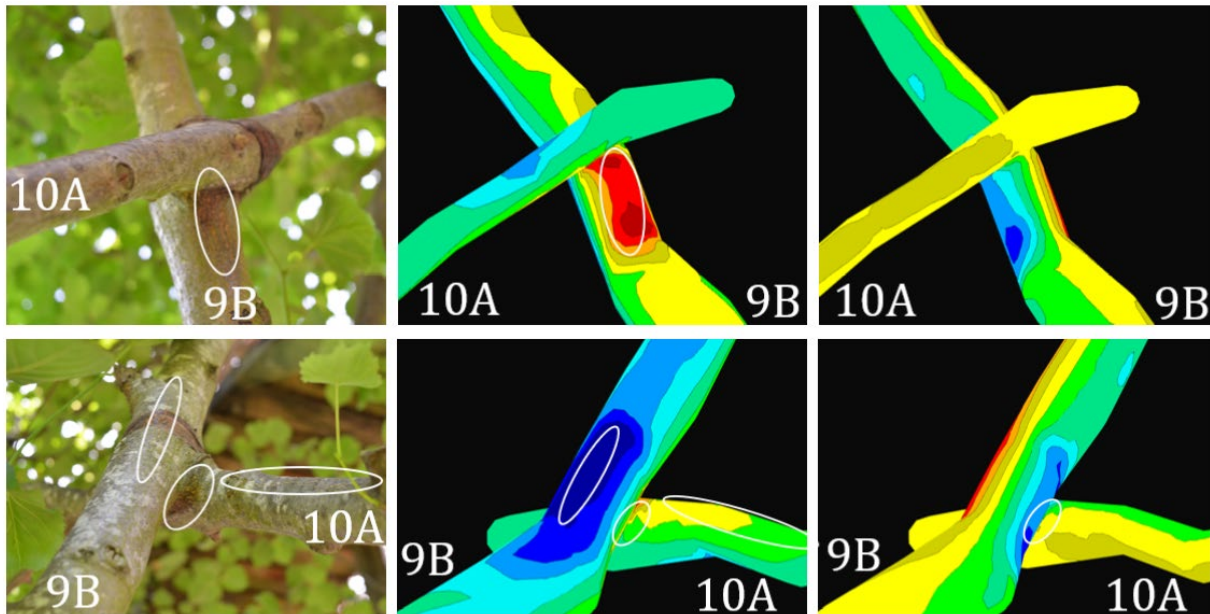
Figure 7.9 Left: Photos of the cross connection, white circles indicate cracks in the bark. Middle: Stress when subjected to radial force. Right: Stress when subjected to tangential force.

7.3 FINITE ELEMENT MODEL

The strain and displacement results of the winching tests are compared with the results from the finite element model.

7.3.1 Stress distribution single tree

Figure 7.10 shows the comparison between the actual measured strain results during the winching tests and the prediction of strain results by the finite element model for the single tree 10B. Appendix C.3.1 contains figures with numerical results, indicated at the location of the elastometers.
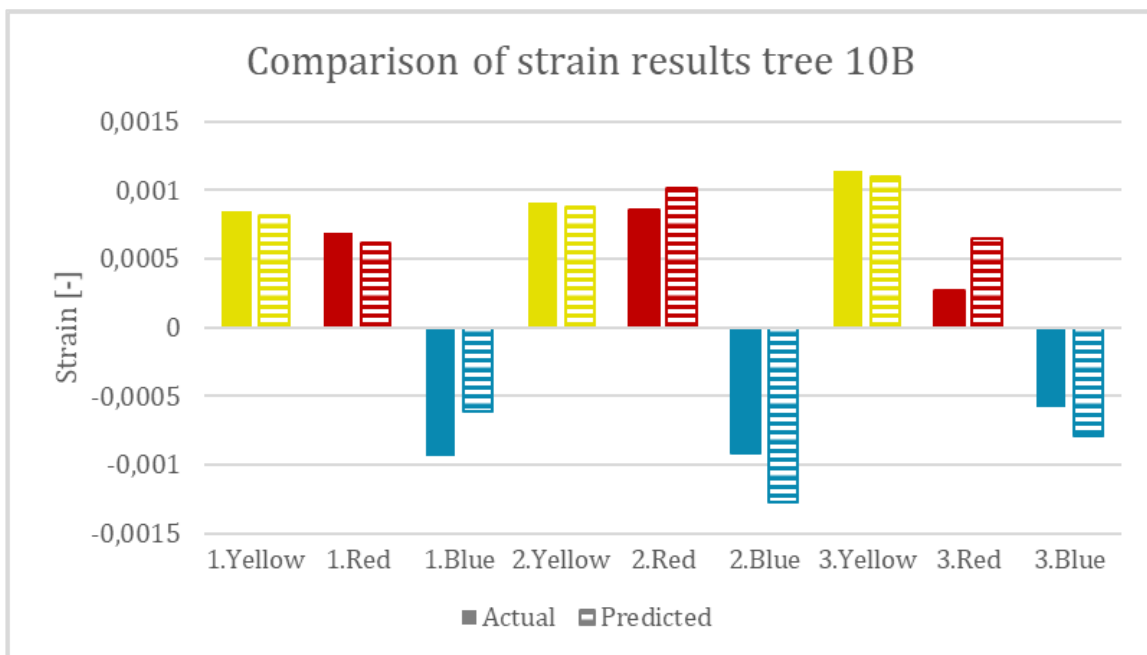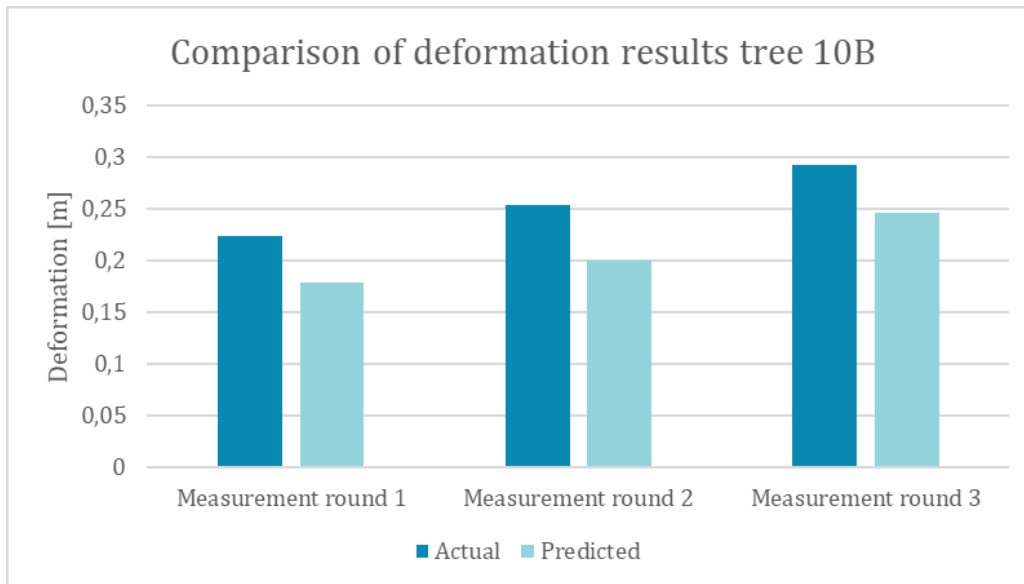

Figure 7.10 Histogram presenting the 'actual' strain results from the three elastometers during three winching rounds. These are compared with the 'predicted' strain results from the finite element model.

The position of the yellow elastometer did not change during the three tests. The graph shows that the measured strain corresponds with the strain in the model. During the first measurement rounds, the red and blue elastometers were positioned at the base of the tree, where the measured strain is larger than the strain in the model. During the second and third measurement round, the red and blue elastometers were placed higher in the tree. Here the measured strain is smaller than the strain in the model.

Figure 7.11 shows a comparison between the measured displacements during the three rounds of the winching tests and the predicted displacements of the finite element model. The displacements are measured in horizontal direction on 2,7m length of the tree, where the cable is attached to the tree. Appendix C.3.1 contains figures with numerical results.

Figure 7.11 Histogram presenting the 'actual' deformation results at 2,7m length of the tree during three winching rounds. These are compared with the 'predicted' deformation results from the finite element model.

From figure 7.11 can be concluded that the tree should be modelled with a lower modulus of elasticity, as this would increase the deformation. Iteratively is found that a modulus of elasticity of 5.000N/mm² fits the measured deformation the best. However, this modulus worsens the fit with the strain results. How this is possible can be explained by the literature study of paragraph 5.3.3.3, which describes that the modulus of elasticity changes within the tree's cross-section and over the tree's length. The deformation results are influenced by the entire range of elastic moduli over the tree's length, as the deformation is solely measured higher up in the tree, at the location of the force application. The strain results, on the other hand, indicate the elastic moduli solely at the location of the elastometer. Suppose the trees are modelled with a homogeneous modulus of elasticity, which they are in this research. In that case, one modulus may fit the deformation results the best, while another modulus fits the strain results the best. It is therefore expected that to fit both the strain and deformation measurements the best, the tree should be modelled with an inhomogeneous modulus of elasticity.

To get an idea of the distribution of the modulus of elasticity over the height, the local modulus of elasticity is calculated based on the stress-strain behaviour parallel to the grain, which in wood can be simplified into (Clair, Fournier, Prevost, Beauchene, & Bardet, 2003):

$$\sigma_L(x,y,z) = E_L(x,y,z)\varepsilon_L(x,y,z)$$

The local modulus of elasticity is calculated with:

$$E_L(z) = \frac{\sigma_L(z)}{\varepsilon_L(z)}$$

In this study, $\sigma_L(z)$ is the stress at the length z of the tree, predicted by the finite element model with a global modulus of elasticity of 6.250N/mm². $\varepsilon_L(z)$ is the measured strain from the winching test at length z.

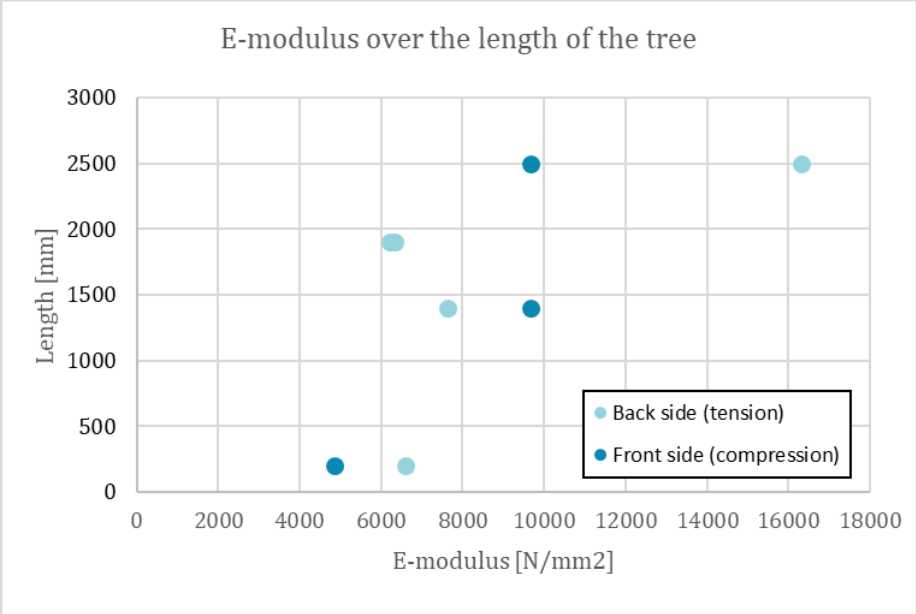The resulting moduli of elasticity are graphically displayed in figure 7.12. Appendix C.3.1 contains tables with numerical results.

Figure 7.12 Distribution of the local modulus of elasticity over the length of tree 10B. Determined according to Clair, Fournier, Prevost, Beauchene, and Bardet (2003) in which the stress is predicted by a finite element model with a modulus of elasticity of 6.250N/mm².

7.3.2 Stress distribution due to connection – cross connection

Figure 7.13 shows a comparison between the actual measured strain results during the winching tests and the prediction of strain results by the finite element model for cross-connected trees 9B and 10A. Appendix C.3.2 contains figures of the finite element model with numerical results, indicated at the locations of the measurements.
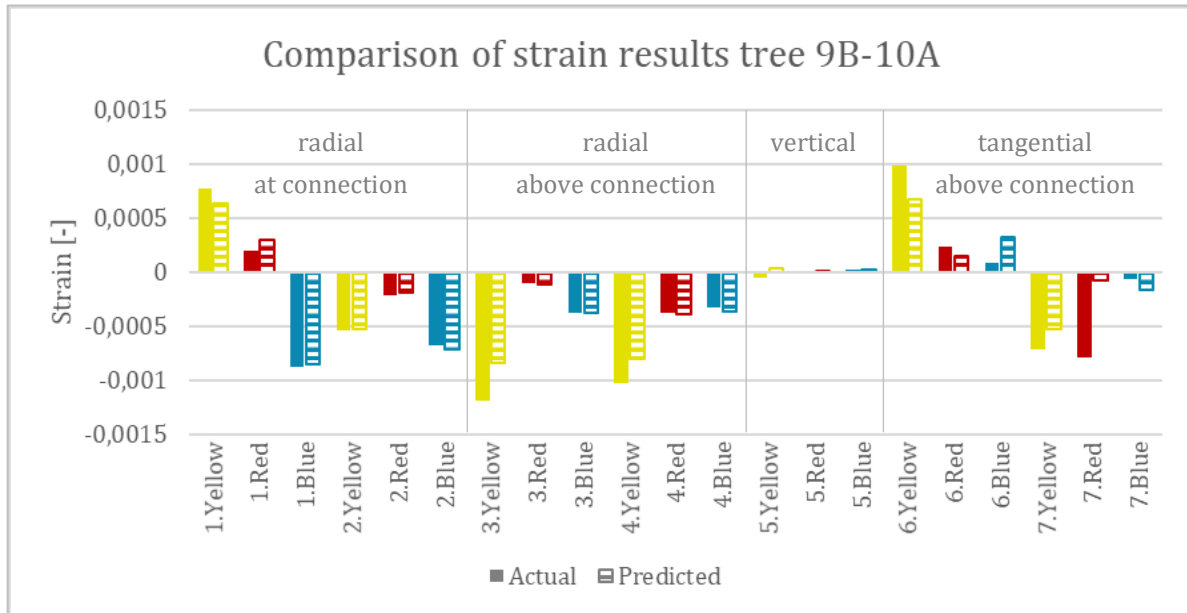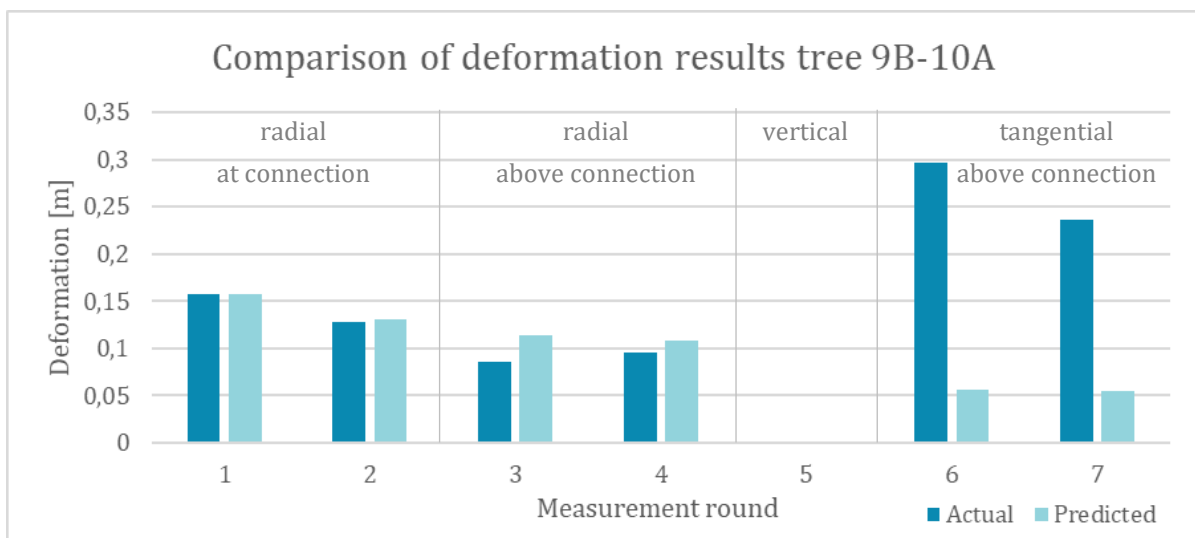

Figure 7.13 Histogram presenting the 'actual' strain results from the three elastometers during seven winching rounds on trees 9B-10A. These are compared with the 'predicted' strain results from the finite element model.

Figure 7.14 shows a comparison between the measured displacements of trees 9B and 10A during the winching tests and the predicted displacements of the finite element model. The displacements are measured in horizontal direction at the location where the cable is attached to the tree. Appendix C.3.2 contains figures of the finite element model with numerical results, indicated at the locations of the measurements.

Figure 7.14 Histogram presenting the 'actual' deformation results at the location of the cable application during seven winching rounds on trees 9B-10A. These are compared with the 'predicted' deformation results from the finite element model.

Figure 7.13 shows that if the force is applied in radial direction, the strains of the model and the measured strains are similar. The same can be concluded for the deformations in figure 7.14 for the first four measurement rounds. This validates the way of modelling the trees and the connection when they are subjected to a radial force.

The placement of the elastometers during the application of a vertical force was incorrect. They should have been placed in the same direction as during the tangential force measurements, but they ware placed in the perpendicular direction. Figure 7.16 on the top left shows that the elastometers have been placed on locations with minimal strains. This makes a comparison between the measurements and the model difficult. The measurement of the red elastometer cannot be used as the measured strain is smaller than the accuracy value of the elastometers.

In measurement rounds six and seven, the force is applied in tangential direction. Figure 7.13 shows that the measured strains differ from the strains resulting from the model. Figure 7.16 on the top right and bottom shows that there is a higher strain found in the finite element model than measured with the blue elastometer on tree 9B. At the red elastometers on tree 10A, the opposite is found, the model gives less strain than is measured. The force transfer from tree 9B, which is pulled, to tree 10A may, in reality, be larger than in the model.

Furthermore, figure 7.14 shows that the displacements in tangential direction are five to six times larger than the results from the model. One explanation for this incongruity is the lift of the winch, that has already been discussed in paragraph 7.2.3. By correcting the measured deformation based on an estimated winch lift, the deformation diminishes from 0,30m to 0,19m in measurement round 6 and from 0,24m to 0,13m in measurement round 7. Although this improves the similarity with the model results, the measured deformations are still about three times larger. The method for modelling the trees and the connection when they are subjected to a tangential force can therefore not be verified.

The existence of lost parenchyma cells within the connection could be an explanation of why the force transfer is not the same in both directions. It is highly likely that the connection is similar to the connections observed with the CT-scans, as shown in paragraph 4.2. This implies that the connection contains lost parenchyma cells in between the two original stems which do not contribute to the bending strength. The shape of the area of these cells, illustrated in figure 7.15, results in a different influence in radial and tangential direction. This difference in fibre qualities has not been included in the connection model.
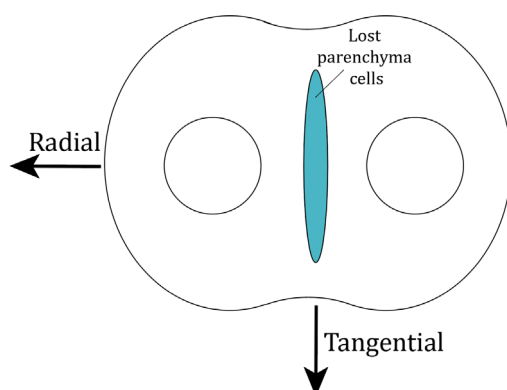

Figure 7.15 Connection of two trees with lost parenchyma cells indicated in blue in between the stems. With arrows a radial and tangential force direction is indicated.
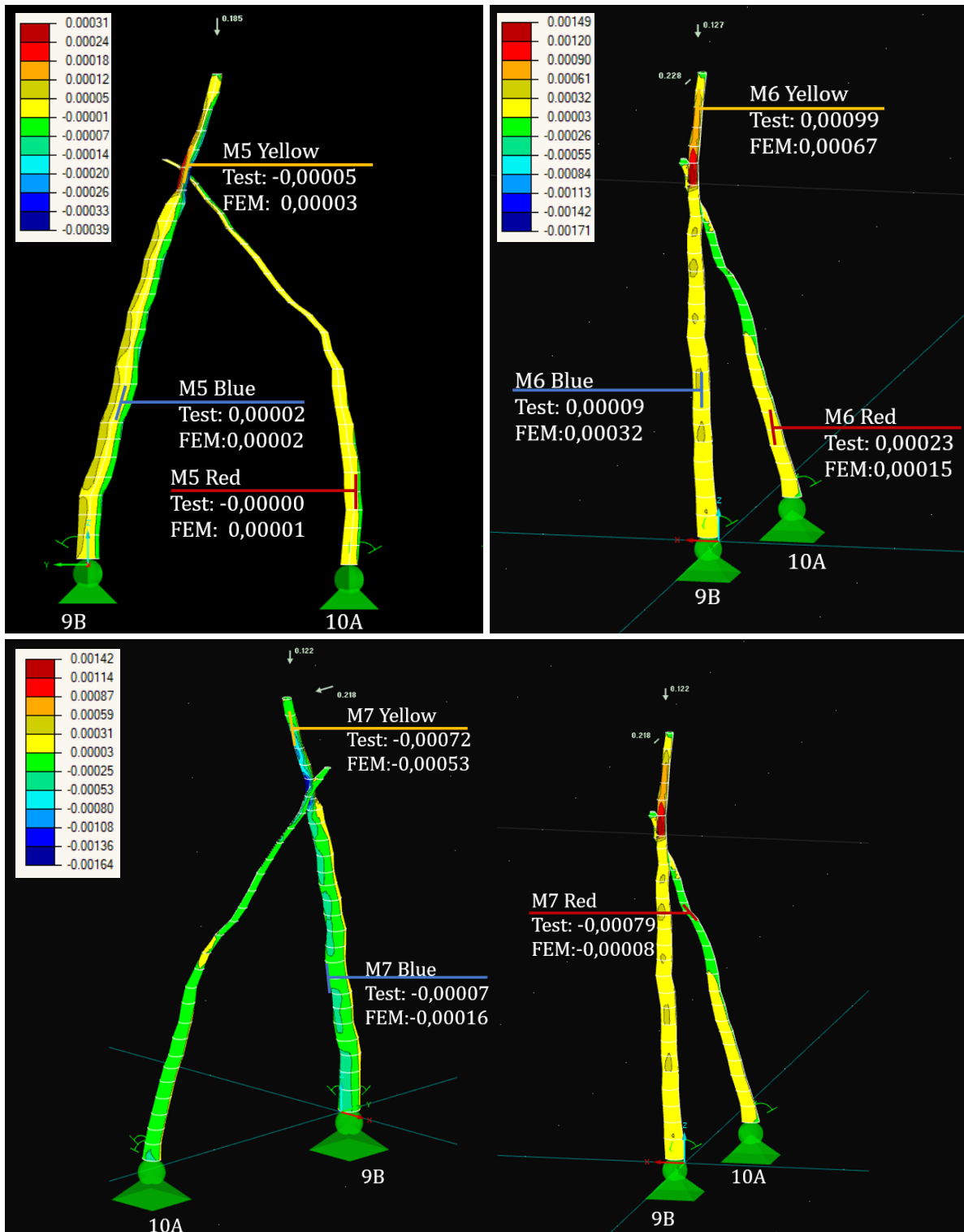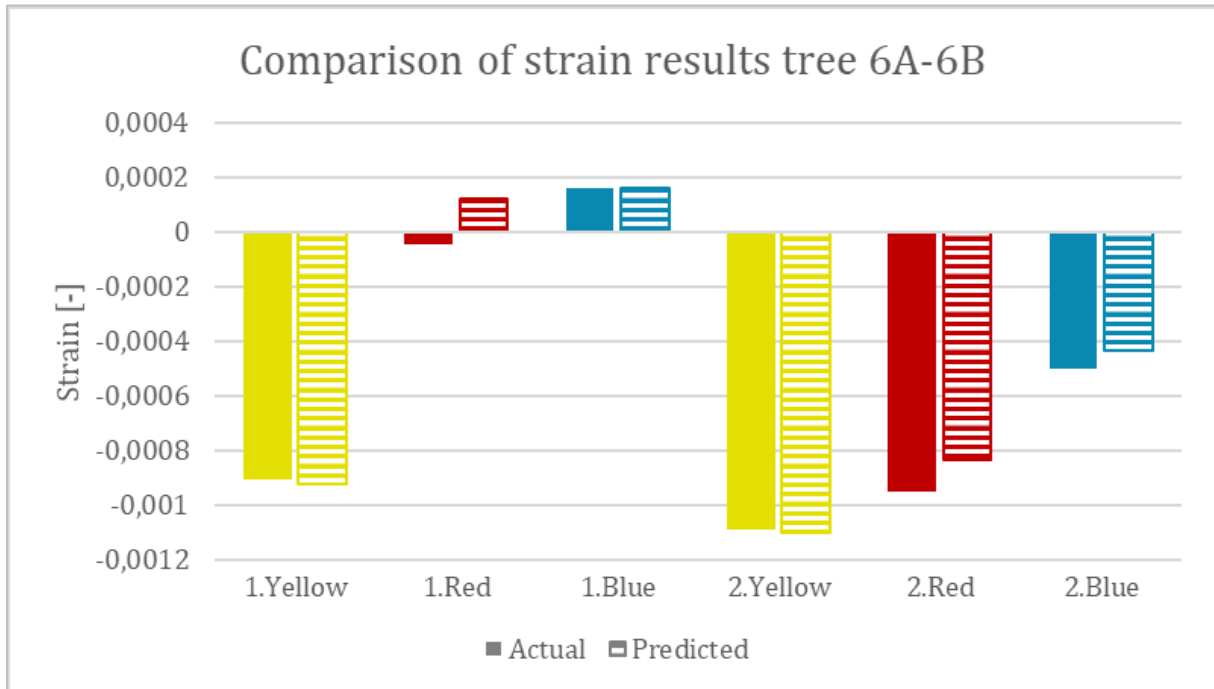
Figure 7.16 Strains in finite element model at the position of the elastometers on tree 9B and 10A. Top left: Measurement round 5. Top right: Measurement round 6. Bottom: Measurement round 7 front side (compression) and back side (tension).

7.3.3 Stress distribution due to connection – parallel connection

Figure 7.17 shows a comparison between the actual measured strain results and the prediction of strain results by the finite element model for parallel-connected trees 6A and 6B. Appendix C.3.3 contains figures of the finite element model with numerical results, indicated at the locations of the elastometers.
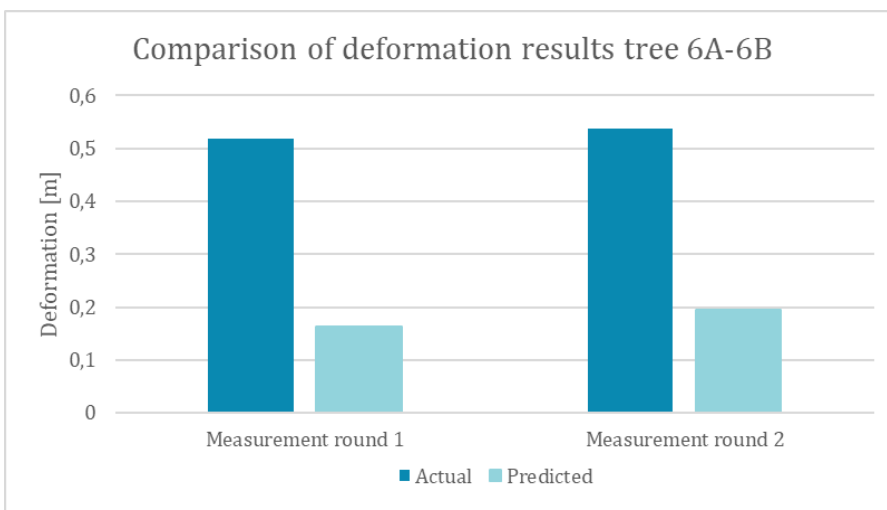

Figure 7.17 Histogram presenting the 'actual' strain results from the three elastometers during two winching rounds on trees 6A-6B. These are compared with the 'predicted' strain results from the finite element model.

Figure 7.18 shows a comparison between the measured displacements of trees 6A and 6B during the winching tests and the predicted displacements of the finite element model. The displacements are measured in horizontal direction at the location where the cable is attached to the tree. Appendix C.3.2 contains figures of the finite element model with numerical results, indicated at the locations of the measurements.

Figure 7.18 Histogram presenting the 'actual' deformation results at the location of the cable application during two winching rounds on trees 6A-6B. These are compared with the 'predicted' deformation results from the finite element model.

62

Figure 7.18 shows that the measured deformations do not coincide with the deformations from the model. As previously explained in paragraph 7.2.3, the measured deformation is influenced by the lifting of the winch. By correcting the measured deformation based on an estimated winch lift, the deformation diminishes from 0,52m to 0,39m in measurement round 1 and from 0,54m to 0,41m in measurement round 2. Although this improves the similarity with the model results, the measured deformations are still about two times larger.

Figure 7.17 shows that the elastometer measurements coincide with the strain results from the model. To get a better understanding of the distributions of strains through the connection, figure 7.19 shows a close-up of the finite element model in which the colour scale is adjusted to the limits of strains around the connection. Comparing the results from the winching tests with the results from the finite element model, it can be reasoned that the model gives a good representation of reality.
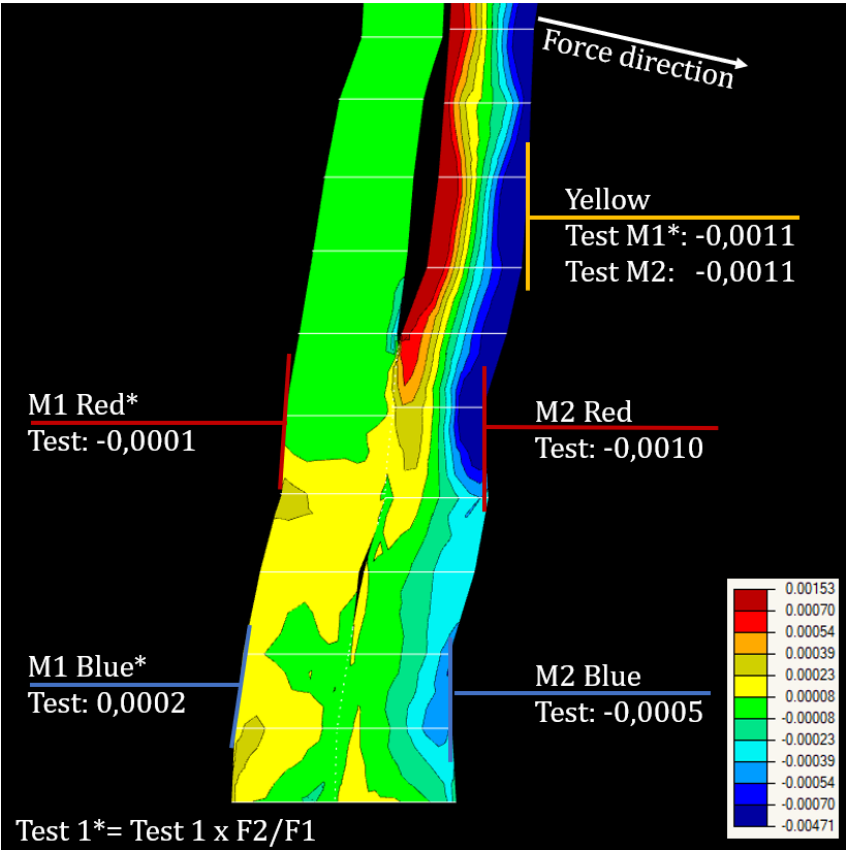
Figure 7.19 Close-up of strains in finite element model around the connection between trees 6A and 6B. At the position of the elastometers the measured strains are indicated, of which the strains of measurement round 1 are scaled to fit the measurements of round 2, based on the ratio of applied forces in round 1 and 2. Scale of strains ε_z [-]

8 APPLICATION TO WONDERWOODS

For this study, a case study is chosen in which the principle of interconnected living tree elements can be applied. This helps to create a clear vision of the possibilities and to get a better understanding of how to design with this concept.

Although it would be interesting to investigate all the possibilities of using living trees as structural elements, this would be too broad to study in a thesis report. Therefore, the question is not: What is possible? But: Is this specific design possible?

8.1 WONDERWOODS CASE STUDY

The chosen case study is *Wonderwoods*, a residential tower in Utrecht on which the vertical forest principle is applied, as can be seen in figure 8.1. Pieter Timmerman, one of the supervisors of this research project, has worked on the preliminary design of this building and therefore has some valuable information about the construction. The construction of the tower will start in the autumn of 2020.

To apply load-carrying living tree elements in this building, the structure can be adjusted as desired. In the following paragraphs, a quick design scan is given.

Figure 8.1 Left: Design Wonderwoods (Stefano Boeri Architetti, 2020). Right: Cut-out of design drawing Wonderwoods (Stefano Boeri Architetti, 2018)

8.1.1 Current Wonderwoods design

In the *Wonderwoods* building, two types of vegetation are used: plants and small trees. They both have different container systems and ways of connecting to the building. As can be seen in figure 8.1, the plants are placed on every balcony level. The trees with a minimum height of 4,5m, are planted in containers which have a height of one storey. They are allowed to grow up to a maximum height of two storeys (Koninklijke Ginkel Groep, 2018). Cut-outs are made in the balconies at the location of the trees.

8.1.1.1 Plants container system

The plants are placed in prefabricated concrete containers of 700x700mm which are placed at the end of cantilevering balconies. Loads of these containers and plants are not carried by the balcony decks but by consoles which are placed in a grid of 6900mm. These consoles are either made of 250x580mm concrete or HE300B steel beams. A technical drawing of this system can be seen in figure 8.2.
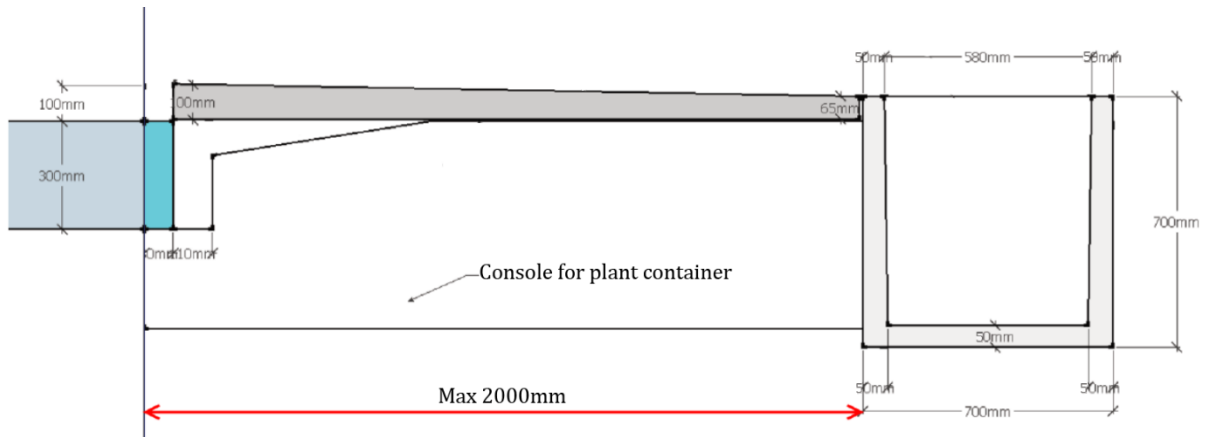
Figure 8.2 Drawing of the Wonderwoods plant containers (Telgen, 2018)

The added consoles to carry the plant containers are an undesired element in the structural design. Loads of the plant containers are transferred via the consoles and the floors to the load-bearing walls, which requires extra reinforcement in the floors. Ideally, the high-rise tower is built with a tunnel formwork which makes it possible to pour the concrete walls and floors of a single apartment in one day. Due to the extra reinforcement at the outer edge of the floors, this makes it more challenging to create and pour such a tunnel in a single day.

8.1.1.2   Trees container system

Although the containers of the trees have a height of one storey, the substratum is only one meter deep for weight reduction purposes. The weight of the trees and the containers are carried by extended load-bearing walls, which are positioned underneath the substratum containers. This can be seen in figure 8.3.
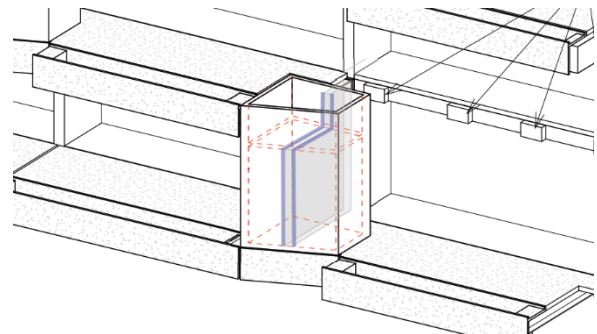
Figure 8.3 Drawing of the Wonderwoods tree containers (Telgen, 2018)

8.2   REQUIREMENTS

The design should demonstrate the possibilities of designing with living trees as a structural element, which should be visible for the residents of the tower.

Tree specifications at planting (Cents T. , et al., 2018):

- Height of at least 4,5 meters
- At least two years pre cultivated in a tree nursery
- Delivered on-site in airpots
- Life expectancy of at least 30 years
- The trees should naturally grow in The Netherlands

Tree specifications over their life-time (Cents T. , et al., 2018):

- Maximum growth up to two stories high, which is about six meters.
- The expected age of the trees depends on the tree species. For example, birch has a life expectancy of 30 years, and a field maple has a life expectancy of 60 years (Cents, 2020).

Building specifications (Telgen, 2018):

- The building has a design life expectancy of 50 years

8.3 DESIGN PROPOSAL

As explained in paragraph 8.1, the usage of consoles to carry the plant containers has some challenges. A more optimal design would be to transfer the forces of the plant containers via the tree containers directly to the load-bearing walls. This would make the use of extra consoles and reinforcement unnecessary and would create 'regular' balcony systems, which are common practice in residential towers. Therefore, it would be valuable to investigate whether the planted trees could carry the loads of these plant containers. The first design proposals are:

A. Single standing tree
B. Parallel interconnected trees – parallel to façade
C. Parallel interconnected trees – perpendicular to façade
D. Cross interconnected trees – parallel to façade
E. Cross interconnected trees – perpendicular to façade

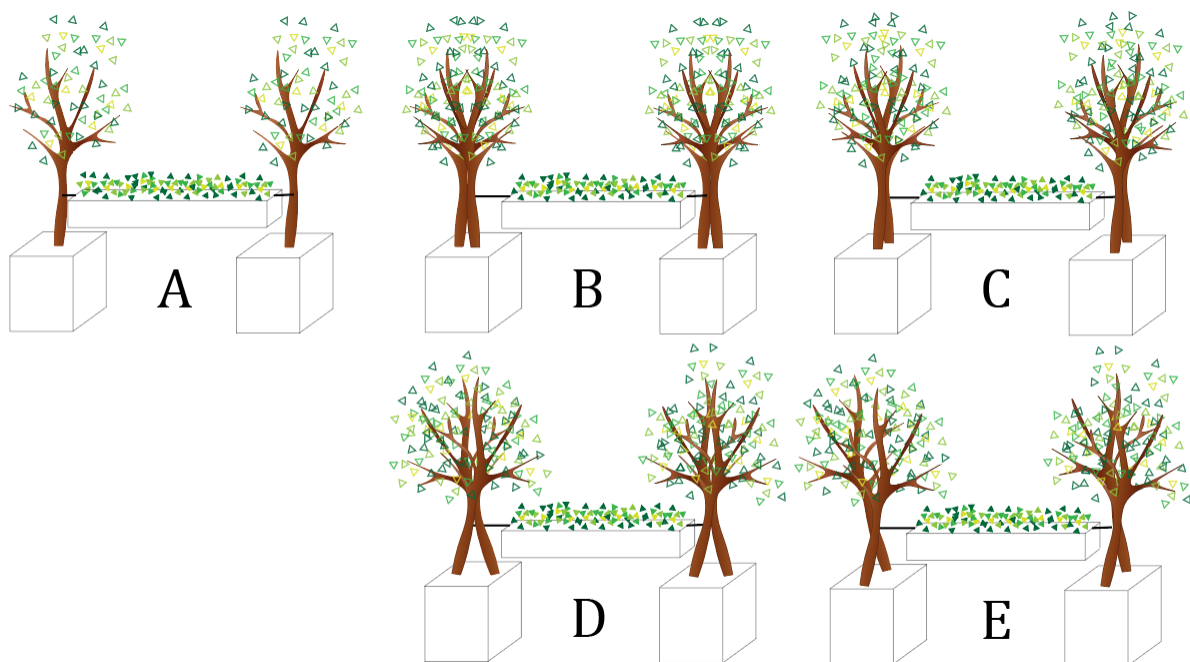Figure 8.4 shows small sketches of these proposals.

Figure 8.4 Overview of Wonderwoods sketch proposals

Placing the trees parallel to the façade has the advantage that both trees get the same amount of sunlight, but it takes up a lot of balcony space. Placing the trees perpendicular to the façade solves this problem but increases the chance of unequal tree growth due to the unequal amount of sunlight they receive. Therefore, it is chosen to make a combination of proposal D and E and to place the trees under an angle to the façade.

Additionally, proposal A is chosen to enable for a comparison between single and interconnected trees.

Figures 13 and 14 show how the design with the single standing tree could be applied to *Wonderwoods*. The tree containers are lowered a little bit so the residents of *Wonderwoods* can see that the trees carry the plant containers.

Figure 8.5 Front view of Wonderwoods facade with plant containers connected to single trees

Steel beams will transfer the loads from the plant containers to the trees. The beams are rigidly connected to the plant containers with an endplate with anchored at the top and bottom. Paragraph 8.8 examines several systems to create a connection between the steel beams and the tree. It is ensured that this connection is free to rotate, and that translation is only restricted in the vertical axis. In this way, the movement of one tree and move in horizontal direction.

In case of a sudden tree failure, a redundant load path is necessary. For this, the steel cables can be used that are installed to guide the growth direction of the trees. These cables span from the bottom of the tree to the tree container above. In normal circumstances, these cables are not stressed, but in the case of tree failure, they can make sure the plant containers do not fall. It is not a problem in such emergency cases that the plant containers displace.
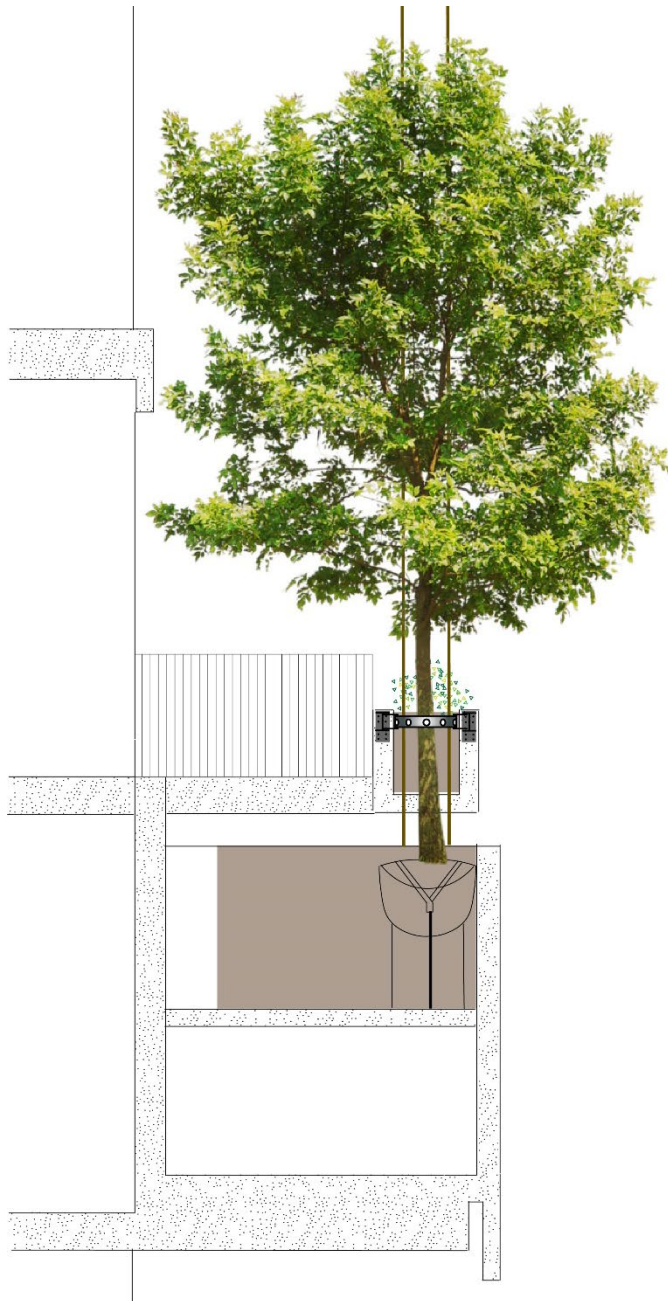
Figure 8.6 Side view of a single tree in a tree container with root ball anchoring. The tree is connected to a plant container with a ring system.

The plant containers are connected to the balconies by vertically slotted connections. In this way, horizontal (wind) forces are transferred to the balconies, reducing the amount of bending stress on the trees. In the balcony design, the tension and compression stress are not critical, so it is expected that the balconies can resist the additional load.

Proposal D&E - Interconnected trees

Figure 8.7 and figure 8.8 show a design with crosswise interconnected trees, applied to *Wonderwoods*. The tree containers are lowered a little so that *Wonderwoods'* residents can see the trees carrying the plant containers. The tree container is made a little deeper, so two trees can fit. The same steel beams, redundant load paths, and slotted balcony connections are used as in the single tree design.

Figure 8.7 Front view of Wonderwoods facade with plant containers connected to interconnected trees

Figure 8.8 Side view of interconnected trees in a tree container with root ball anchoring. The trees are connected to a plant container with brackets and a cable.

8.4 Tree species selection

Certain tree species are better able to form connections than others. In general, needled-leaved trees have more difficulties in creating connections because of the balm they produce when they are wounded. This balm flow hardens into a resin to protect the wound. Tree species with toxic substances such as the Eucalyptus and the Taxus are also more difficult to connect (Nuijten, 2011).

In general, it is advantageous if the trees have the same growth speed, size, and type of bark. To explain the latter, most of the trees have bark that falls off with vertical cracks, but there are some species as the birch that create cracks in horizontal direction. Threes with the same crack direction in their bark can more easily be connected, of which trees with both vertical cracks are the best (Nuijten, 2011).

Furthermore, it is an advantage if trees have a long, single, straight and unbranched main stem (Ludwig, 2012). Depending on the design, it is advantageous if the trees are easily bendable. If so, a low E-modulus and small diameter are preferred. In the *Wonderwoods* design, however, the trees must be able to carry a weight, which opts for stronger and stiffer tree species.

In appendix A, a list of tree species considered in this research is included. The composition of this list is based on the following studies and recommendations:

- As geometry measurements and winching tests are carried out on the Ash trees of the *Living Tree Pavilion*, there is much knowledge about the growth and behaviour of these trees and their connections. Therefore, this tree species might be useful in the design.
- Bob Ursem (2020), scientific director of the Botanical Garden of the TU Delft, has recommended several tree species like oaks, linden, and beeches that can grow well in pots, are suitable to prune regularly and can easily inosculate. Furthermore, the recommended species have a long life-expectancy and grow slowly, which results in stronger wood properties and makes them suitable to have a bearing function.
- In the PhD paper *Botanische Grundlagen der Baubotanik und deren Anwendung im Entwurf*, Ferdinand Ludwig (2012) has investigated several tree species for their capability to create connections and their applicability in *Baubotanik* structures. According to Ludwig, mostly planes, birches, and willows are suitable for inosculations.
- Xiuli Wang is a PhD candidate at the research group of *Bio-based Structures and Materials* at the *Delft University of Technology*. She studies the impact of self-growing connections on the stability of tree systems under wind loads. She has chosen to investigate three tree species: the willow because of its fast growth, the olive because of its high strength and the fig. The fig is a tree which grows fast and inosculates easily but does not grow naturally in Europe, so is out of the scope of this research.
- *Arcadis Landschapsarchitectuur & Stedenbouw* has made a selection of trees and plants that are suitable for the *Wonderwoods* towers (Cents T. , et al., 2018). This selection is based on vegetation that naturally grows in the nearby nature area *Utrechtse Heuvelrug*. The trees that are placed in the containers along the façade are chosen because they are not sensitive for sickness, are frost-resistant, do not carry fruit, and can thrive in an environment with much wind.

From the longlist in Appendix A a shortlist is made for which the pros and cons are summarized in table 8.1. Important to note is that this list is mostly based on expert opinions.

Table 8.1 Shortlist of tree species selection and their qualities

Tree species	Opinion Bob Ursem	Suitable for great height (Wim Beining)	Suitable for SGC (Ferdinand Ludwig)	Wonderwoods design
White Willow	No: too weak and short life expectancy	Yes	Very suitable, no screws	No
Silver Birch	Definitely no: not drought resistant, difficult in pots, bark not suitable for connections	Yes	Yes	Yes
London Plane	Good	No: not wind resistant	Very suitable	No
Common Ash	Good	No: ash dieback	Yes, with screws	No
Common Hornbeam	Good	No	Very suitable	Yes
Field Maple	Good	Yes	?	Yes

From the list, the Field Maple (*Acer campestre*) is chosen as most promising for this design. This tree species has the following advantages:

- According to Bob Ursem, it can grow well in containers, is suitable to prune regularly and can easily inosculate. Furthermore, Field Maples are strong, so suitable for a bearing function (Ursem, 2020).
- The Field Maple is included in the design of *Wonderwoods*, made by *Arcadis Landschapsarchitectuur & Stedenbouw*. Field Maples, therefore, have all the favourable qualities as described in the bullet points above (Cents T. , et al., 2018).
- Wim Beining is planting advisor for tree nursery *Ebben*, specialised in roof garden trees. He is part of a committee, set up by *BuGG - Bundesverband GebäudeGrün e. V.*, which exchanges knowledge about shrubs and trees on high roof terraces. This committee consists of selected specialists from tree nurseries, researchers, and landscape designers. They acknowledge that the Field Maple is suitable to grow on roofs of great height if a minimum root space thickness of 60-70cm is provided (Beining, 2020). Because of the large wind load on roof garden trees, they must be standing, breaking, frost and drought resistant. The *BuGG* scored several tree qualities of the Field Maple on a scale from zero to four (Beining, 2020):
    - Standing resistance (stability): 4/4. This is the capability of a tree to resist high wind forces due to its root structure, the growth behaviour, and its shape.

- Breaking resistance: 3/4. This is the breaking resistance of a stem or branch due to snow or wind load.
- Frost resistance: 4/4. This is acknowledged by Wessolly and Erb (2016), who mention that Maples are diffuse-porous. Due to their lack of big water vessels, they are less susceptible to frost damage.
- Draught resistance: 3/4. This is favourable as the water buffer in tree containers is small.
- Prune tolerance: 4/4. This corresponds with the statement of Bob Ursem (2020).
- Industrial resistance: 4/4. This means it can grow in polluted areas with nitrogen oxides and fine dust. This is of benefit in a polluted area such as the city centre of Utrecht.
- Light conditions: sunny or half-shaded areas. This is applicable to the south-west façade of *Wonderwoods*.

8.5 TREE GROWTH BEHAVIOUR OF FIELD MAPLE

In nature, Field Maples reach a height of twelve meters and a width of about seven or eight meters (Boomkwekerij Ebben, 2020).

A quality of the Field Maple is the fact that it is resistant to pruning. It can be pruned in a variety of shapes like spheres, blocks and even bonsais. As for 'regular' tree shapes, you can choose to have a multi-stemmed or single-stemmed shape. For simplicity, it is chosen to use a high single stem in this project. Its natural crown shape is then egg round; examples can be seen in figure 8.9 (Boomkwekerij Ebben, 2020).

Figure 8.9 Photos of a younger and older Field Maple to illustrate the shape of the crown (Boomkwekerij Ebben, 2020)

Wim Beining, tree expert for roof gardens at tree nursery *Ebben*, gave an indication for the growth of a Field Maple. At the time of planting, the tree is 4,5 meters high; this means its circumference at one meter above the ground is 16 to 18cm. The tree nursery has measured and gathered many data on the growth of tree species. In normal conditions, the diameter of the stem at one-meter height increases with three centimetres per three years. The growth in height is about 40cm per year, and the width of the crown grows with 40cm per year. However, depending on external influences, this growth can be influenced by 10 to 25% (Beining, 2020).

Because the height of the trees on *Wonderwoods* will not exceed eight meters, the trees can be categorized in the third size category according to *Normeninstituut Bomen* (2018). This corresponds with a necessary substrate volume of about ten square meters, applicable to trees which are not in contact with groundwater. From this can be concluded that the substrate volume of 2,25 square meters of the *Wonderwoods* containers is not enough to let the trees grow in natural conditions. Additional help is necessary, like root anchoring and a watering system. The growth of the trees will probably be negatively influenced. To take a conservative value, Wim Beining (2020) advised to reduce the growth prediction with 25%:

Diameter at one-meter height = 75% x 1 cm/year = 0,75 cm/year

Height = 75% x 40 cm/year = 30 cm/year

Crown width = 75% x 40 cm/year = 30 cm/year

In the design of *Wonderwoods* is expected that the Field Maples on the building will live for sixty years (Cents, 2020).

8.6 MATERIAL PROPERTIES OF FIELD MAPLE

Within species, material properties can differ between trees, between parts of a tree and even within a cross-section (Sterken, 2005). So, it is not that easy to assign general material properties to living Field Maple trees, but an attempt is made to choose these properties as accurately as possible.

Three methods to determine the material properties of Field Maple have been followed. These methods will be described hereafter, followed by a conclusion about the reliability and usability of each method.

8.6.1 Wessolly and Erb - greenwood

Wessolly and Erb (2016) reported the material properties of Field Maple, as stated in table 8.2. These are greenwood values, based on old thick trees which just failed or had to be logged. The stated values are mean values with the standard deviation subtracted, to avoid too optimistic results.

Table 8.2 Properties of Field Maple according to Wessolly and Erb (2016)

Parameter	Mean value – standard deviation
Elastic modulus [N/mm²]	6.000
Elastic limit [%]	0,43
Compressive strength [N/mm²] Parallel to the grain primary failure	25,5
Compressive strength [N/mm²] Perpendicular to the grain primary failure	11
Compressive strength [N/mm²] Tangent to the grain	8,7

As mentioned earlier, the modulus of elasticity increases over the lifetime of a tree. Rais, Van de Kuilen, and Pretzsch (2020) carried out a study on the cambial age of beech trees and found a linear increase of 14N/mm^2 per year, from 13.700N/mm^2 at 20 years till 15.500N/mm^2 at 140 years. This means an increase of 0,103% per year. It could be assumed that a similar relationship can be found in maple trees, which is also a hardwood species.

Unfortunately, the mean age of the trees from the table of Wessolly and Erb is unknown. If the tested wood pieces are for example 100 years old (they tested old, thick trees), then the elastic modulus of a ten-year-old tree is 5.500N/mm^2.

8.6.2   Kovryga – dry boards

In 2019 a study was carried out to the mechanical properties of 381 Maple boards. This study claims to apply to European Maple species, to which the Field Maple belongs. The results were adjusted to 12% moisture content based on EN384:2016 (Kovryga, Schlotzhauer, Stapel, Militz, & van de Kuilen, 2019). The tests contained boards both with and without pith. The results can be seen in the table below.

Table 8.3 Properties of Maple boards as tested by Kovryga et al. (2019)

Parameter	Mean	Coefficient of variation= Standard deviation/mean	5th percentile value
MOE dynamic [N/mm^2]	14.500	0,118	
MOE static [N/mm^2]	13.800	0,16	
Tensile strength [N/mm^2]	53,4	0,49	18,9
Density [kg/m^3]	664	0,067	569

To convert these values to greenwood, they have to be adjusted from 12% moisture content to 28% moisture content, as explained in paragraph 5.3.3. The code EN384 gives guidelines for adjustments for parallel compression strength, MOE, and density (NEN, 2018). The tensile strength is therefore first converted to compression strength, based on the same code for T-classes. This compression strength and the MOE are adjusted to 28% moisture content. It should be noted that the code describes this adjustment to be correct within a range of 8 to 18%. Whether the adjustment outside of this range is still a good approximation is debatable. From the adjusted compression strength, the remaining properties are calculated based on the EN384 code for D-classes.
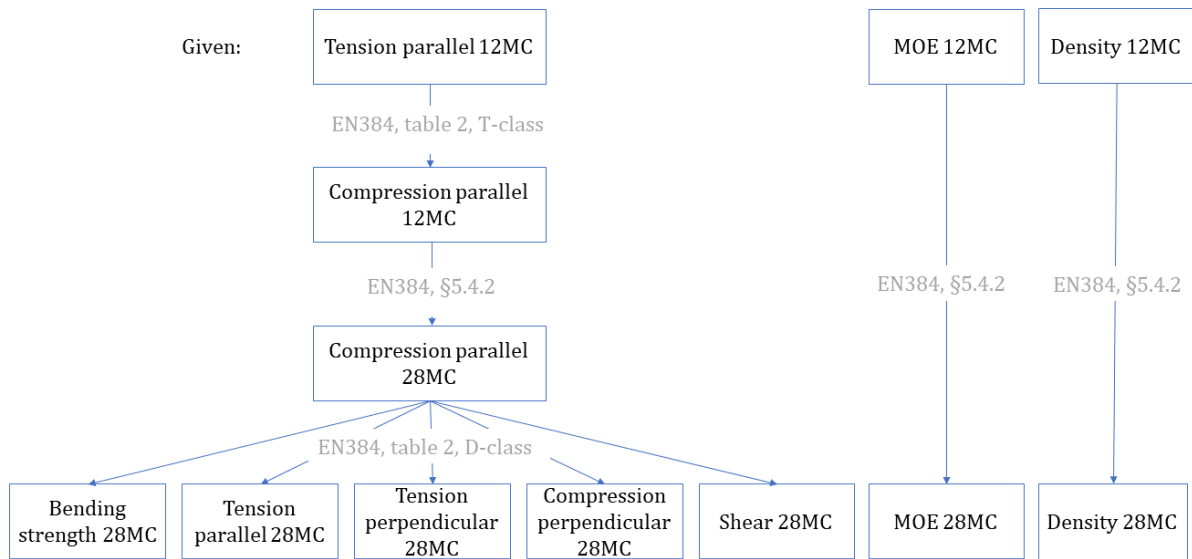
Figure 8.10 Adjustment procedure for Field Maple results from Kovryga (2019) to greenwood results

This gives the following results:

Table 8.4 Adjusted Kovryga (2019) properties Field Maple to greenwood

Parameter	Adjusted values 28MC
Bending strength [N/mm²]	29,7
Tension strength parallel [N/mm²]	14,2
Tension strength perpendicular [N/mm²]	0,6
Compression strength parallel [N/mm²]	20,9
Compression strength perpendicular [N/mm²]	6,0
Shear strength [N/mm²]	3,7
MOE dynamic [N/mm²]	12.200
MOE static [N/mm²]	11.600
Density [kg/m³]	600

8.6.3 Nuijten - clear dry wood

In the reports of Nuijten (2011) and Borská (2018), the wood properties are estimated based on the *Houtvademecum*. Because the *Houtvademecum* gives the properties of dry, small, and defect-free wood, an adjustment is made to convert the values into living tree values. They estimated that the bending strength of hardwood living trees is 25% of the bending strength of clear wood specimens. This value is based on studies to find a simplified assessment procedure for tropical hardwoods. Based on tests on several tropical hardwood species, a factor between 0,20 and 0,35 was found to adjust the mean value of small clear wood to the characteristic value of full-size beams (Ravenshorst, Kuilen, & Lanvin, 2011). A compromise is made, and a factor 0,25 is used (FCBA, Delft University of Technology, CIRAD, 2010).

Based on the adjusted bending strength and the original modulus of elasticity as found in the *Houtvademecum*, the wood properties are assigned to a strength class as described in the Eurocode 5 (NEN, 2011).
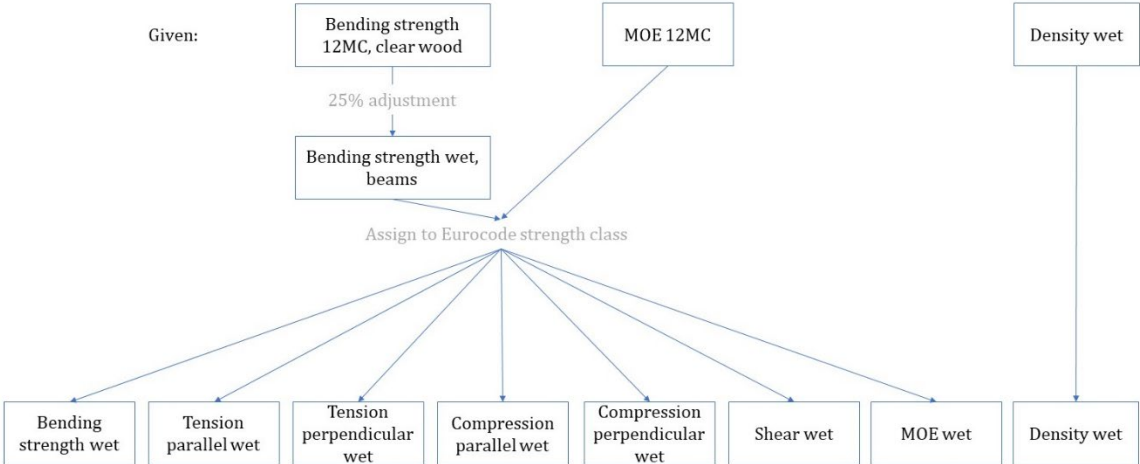
Figure 8.11 Adjustment procedure Houtvademecum Maple values to living tree values according to Nuijten (2011)

The *Houtvademecum* describes a bending strength for Maple of 94N/mm^2 and a modulus of elasticity of 10.100N/mm^2 (Klaassen, 2018). The adjusted bending strength to 25% is 24N/mm^2 which fits in strength class D24 with the properties, as shown in table 8.5. The prescribed modulus of elasticity of the D24 strength class corresponds to the one found in the *Houtvademecum*.

Table 8.5 Properties of D24 timber

Parameter	Class D24
Bending strength [N/mm^2]	24
Tension strength parallel [N/mm^2]	14
Tension strength perpendicular [N/mm^2]	0,6
Compression strength parallel [N/mm^2]	21
Compression strength perpendicular [N/mm^2]	7,8
Shear strength [N/mm^2]	4
MOE [N/mm^2]	10.000
Density [kg/m^3]	484

8.6.4 Conclusion

The three methods show similar results regarding material strengths. The magnitudes of the modulus of elasticity, however, vary greatly. From the winching tests can be concluded that the modulus of elasticity parallel to the grain is similar to, or a bit lower than, the modulus of elasticity stated in the *Stuttgarter Festigkeitskatalog*. Regarding the *Wonderwoods* design, it is therefore advised to use the modulus of elasticity from the method of Wessolly and Erb (2016), which makes use of the *Stuttgarter Festigkeitskatalog*.

Regarding the other material properties, it is advised to use the most unfavourable properties of the three methods, due to many uncertainties and not having the possibility to test the strength of the trees while placed on *Wonderwoods.* This results in:

Table 8.6 Material properties to be used for Field Maple trees in Wonderwoods

Parameter	Value
Bending strength [N/mm²]	24
Modulus of elasticity parallel [N/mm²]	5.500
Modulus of elasticity perpendicular[1] [N/mm²]	337
Tension strength parallel [N/mm²]	14
Tension strength perpendicular [N/mm²]	0,6
Compression strength parallel [N/mm²]	21
Compression strength perpendicular [N/mm²]	6,0
Shear strength [N/mm²]	4
Shear modulus[1] [N/mm²]	344

[1]From table 2 of EN384 hardwood timber (NEN, 2018)

8.6.5 Design values

According to the Eurocode 1995, the characteristic material properties should be adjusted with correction factors for size effects, moisture content and load duration. De Vries and Gard (1998) state that this, described for sawn timber, is also suitable for roundwood. They, however, argue that the corrections factors have to be revised. The partial factor for material properties could, for example, be more favourable, as living wood can react to external forces (Nuijten, 2011). Unfortunately, no studies could be found proposing revised values, so the design values of the *Wonderwoods* trees are based on regulations for sawn timber (NEN, 2011):

$$X_d = k_h \times k_{mod} \times \frac{X_k}{\gamma_M}$$

With:

k_h (Volumetric weight of Field Maple 840kg/m³ ≥ 700kg/m³)

         1,0

k_{mod} (Sawn timber, service class 3, trees are outdoors)

- Permanent load duration: 0,50
- Long-term load duration: 0,55
- Medium-term load duration: 0,65
- Short-term load duration: 0,70
- Instantaneous load duration: 0,90

γ_M (Sawn timber)

         1,3

8.7 DESIGN GEOMETRY

Figure 8.12 shows the dimensions of the single standing trees as is used in the structural verification. The dimensions are based on growth information, as described in paragraph 8.5. The trees at the time of planting (t=0) are 4,5 meters high, with a growth speed of 40cm per year they are about eleven years old. The crown of the trees starts at the height of two meters; this can be created by pruning before they are placed. This height is chosen to create an outside view for the residents. The tree crown is naturally egg-shaped (Boomkwekerij Ebben, 2020), which means it has a ratio of width over height of 0,8 (Altuntas & Sekeroglu, 2010). The tree will maintain this

shape index until it has reached is maximum allowed crown width of 3,5m (Cents, 2020) to which it will be pruned.

The area of the crown is approximated as oval-shaped; the horizontal and vertical areas of the crown are calculated, as shown in figure 8.12. As the tree is standing 1,75 meters away from the façade, the crown width perpendicular to the façade is maximal 3,5 meters. Following the example of Nuijten (2011), the shape of the stem is simplified as a cone with a diameter of zero at the top.

This plausibility of this simplification is checked by comparing it with the geometry measurements of the *Living Tree Pavilion*, as shown in figure 7.3. On average, the circumference of the pavilion trees decreases with 70mm per meter length, as is measured for the bottom 2,5 meters. If the cone shape simplification would be applied, in which the height of the tree and the circumference at one-meter height of the tree is included, then the circumference would decrease with 63mm per meter length. This shows that the cone assumption is plausible.

Figure 8.12 shows the diameter of the trees at the height of one meter and the vertical area of the stem up to two meters, which is used in wind load calculations.
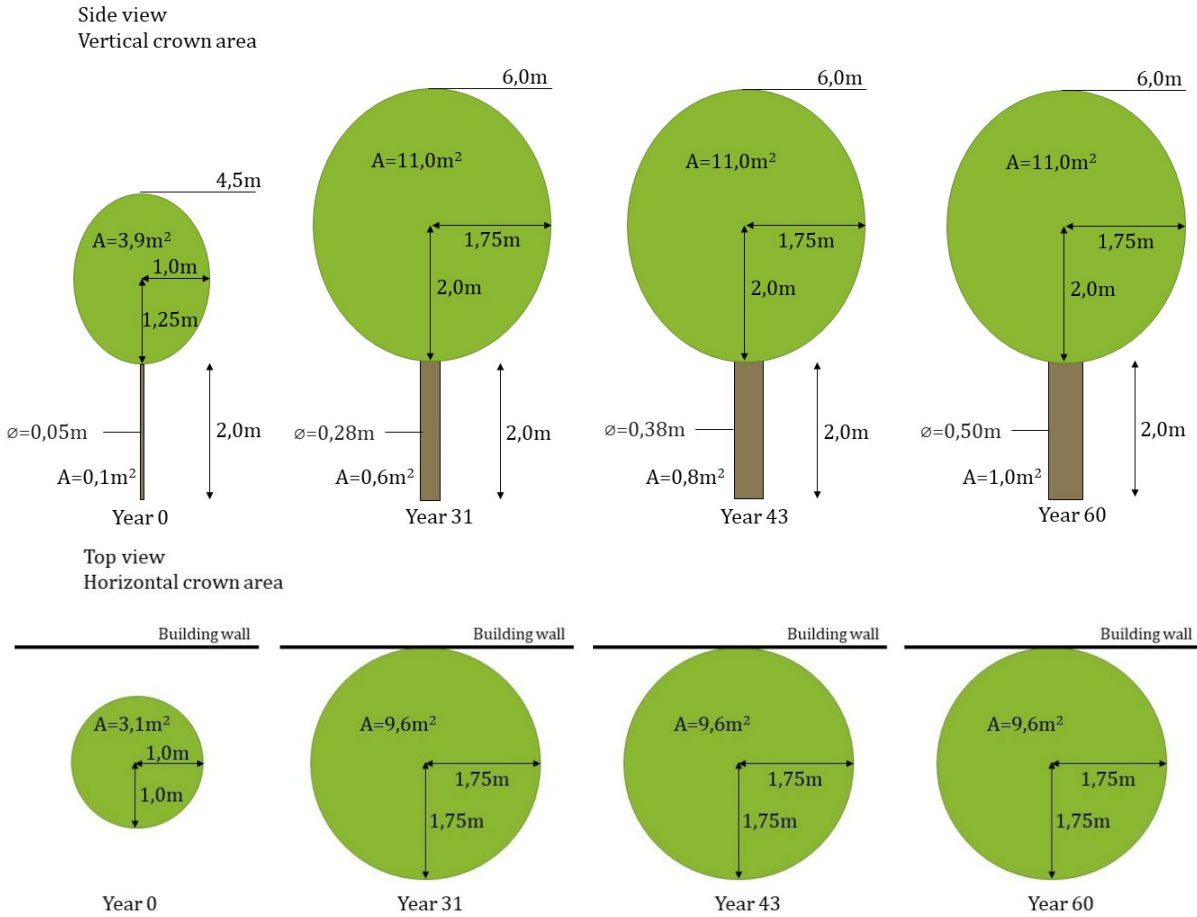
Figure 8.12 Top: Side view of the single trees including the height of the tree and the stem, the vertical crown area, the diameter of the stem at 1m height and the vertical area of the stem up till 2m. Bottom: Top view of the single trees including the horizontal crown area.

It is estimated that the interconnected trees have the same horizontal and vertical areas of the crown and stem, but then spread over a larger length because they are standing under an angle. Figure 8.13 shows the geometry of the interconnected trees that are standing on *Wonderwoods*

for 43 years. The trees are placed one meter apart, diagonally in the tree containers. They are connected at the height of two meters.
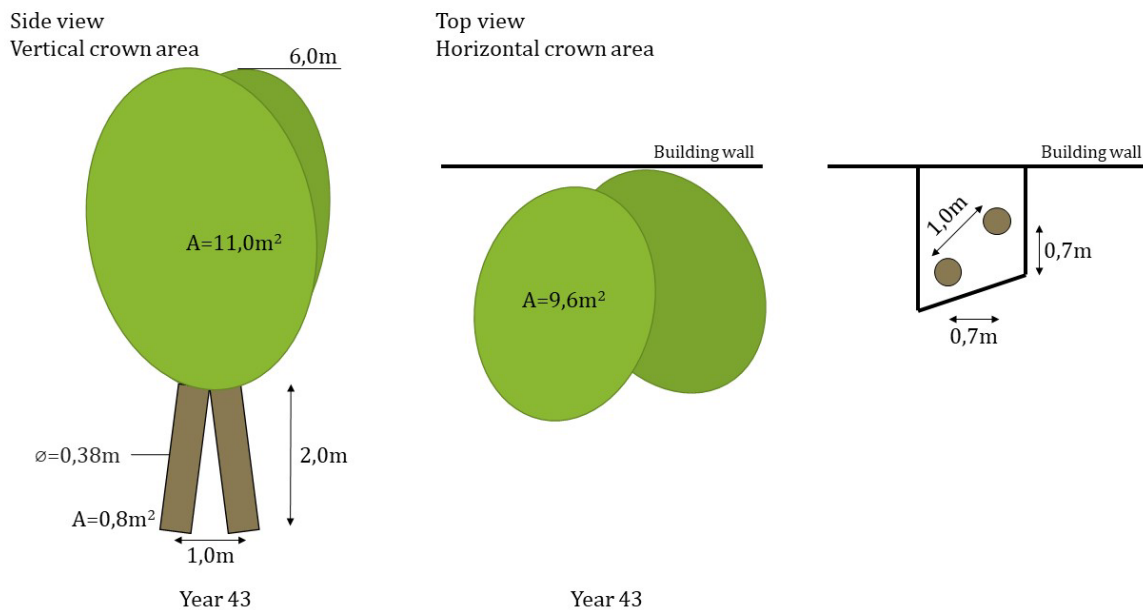
Figure 8.13 Left: Side view of interconnected trees year 43 including the height of the tree and the stem, the vertical crown area, the diameter of the stem at 1m height and the vertical area of the stem up till 2m. Right: Top view of interconnected trees including the horizontal crown area and the distances of the stems in the tree container.

8.8 CONNECTIONS TO NON-LIVING ELEMENTS

In both designs, the plant containers are connected to the trees at the height of one meter. Because of the popularity of building treehouses, several systems are on the market for connecting non-living elements to trees. Five possible systems and their feasibility for *Wonderwoods* will be discussed.

Favourable characteristics of systems are:

- A sufficient load-bearing capacity. In vertical direction, the system should be able to carry the weight of the plant containers, including rain load. This is about 1800kg on both sides of the tree. In horizontal direction, it must transfer a wind load of two times 4,3kN, which is about 900kg in total.
- Minimal tree intrusion. Tree intrusion influences a tree's growth, for example, by restricting its growth in thickness, or by drilling through its tissue. A tree can respond to this and minimize the consequences, but this costs energy which a tree will consequently be lacking in other places. Besides, it is possible that a tree does not fully recover so that the connection remains a weaker point.
- High aesthetical value. It is favourable if the system is minimalistic and does not block the inhabitants' view.
- Reliable. Either the system is repeatedly successfully used, or extensively tested.
- Maintenance. The system is low in maintenance if it does not have to be replaced or inspected regularly.

Osnabrück Double Belt System

Hanging constructions upon trees by cables allows the tree to move freely. The connection between the cable and the tree is often realized by using steel bands. These bands should be replaced every three to five years by wider bands to prevent strangling of the trees due to

secondary growth (Wahlländer, 2020), see figure 8.14. If this is not performed, the too-tight bands can constrict water-carrying vessels resulting in the death of tree parts (Wessolly & Erb, 2016).

Figure 8.15 shows a solution: the Osnabrück Double Belt System, consisting of two belts. An inner belt, made of a hollow polyester rope, is fastened to the tree. Due to its elasticity, it adapts automatically to secondary tree growth, preventing strangulation. The outer belt is larger and stronger, able to carry the load. Stobbe, Dujesiefken and Schröder (2000) investigated beech trees that had been secured with this system for six years and concluded that this system did not give the trees decolourisations nor fungal attack within the stem and on the bark.
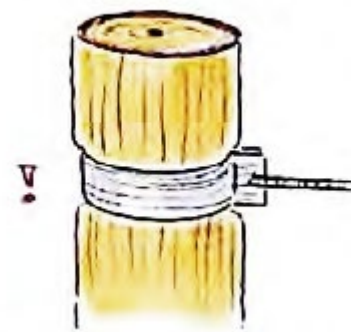
Figure 8.14 Strangling a tree by too tight steel bands (Wessolly & Erb, 2016)

A bandwidth of 4cm is strong enough to retain 2000kg; using two of these would be enough to retain the *Wonderwoods* plant containers (Wessolly & Erb, 2016). Whether this would work is, however, questionable. The belt system is designed to retain horizontal forces, while the weight of the plaint container gives significant vertical forces. If the plant container is not tightly strung between the trees, the vertical forces might result in sagging of the belt.
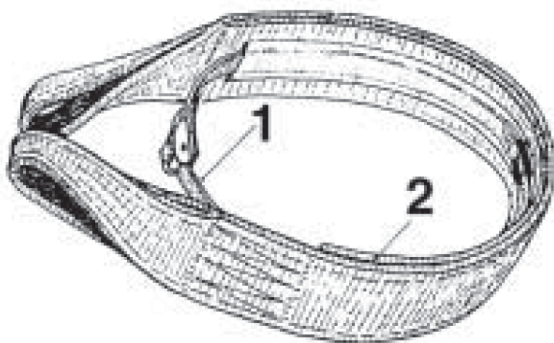
Figure 8.15 Left: Drawing of Osnabrück Double Belt System with an inner belt fixed to the stem (1) and a strong retaining outer belt (2). Right: Photo of the Osnabrück Double Belt System (Stobbe, Dujesiefken, & Schröder, 2000)

A solution to this could be to attach the belt around a stable branch or above a fully-grown cross-connection. The belt should be positioned as close to the main trunk as possible, to prevent large lever arms and directly introduce the force into the main trunk.

A disadvantage of this system is the lack of a failure warning system, as the cable or anchor point can abruptly fail. As this system has to be replaced every eight years, maintenance is less intensive than using steel bands (Wahlländer, 2020).

Ring system

Another solution to prevent strangulation of too tight steel bands is a ring system designed by an architecture student of the Iuav University of Venice (Gozzi, 2011). Hard plastic feet are placed on the bark, transferring compression forces. The outer ring is made of steel, is 12 cm wide, and has a thickness of 0,8 cm. Favourable for this system is that it can be adjusted along with the growth of the tree. It is, therefore, a tree-friendly system which does not have to be replaced regularly. However, maintenance investments are high because the system needs to be adjusted every couple of years. Another advantage compared to a regular steel ring, is that the tree does not have

to be perfectly round. Unfortunately, this system is still in its design phase and not yet tested; its strength is therefore unknown.
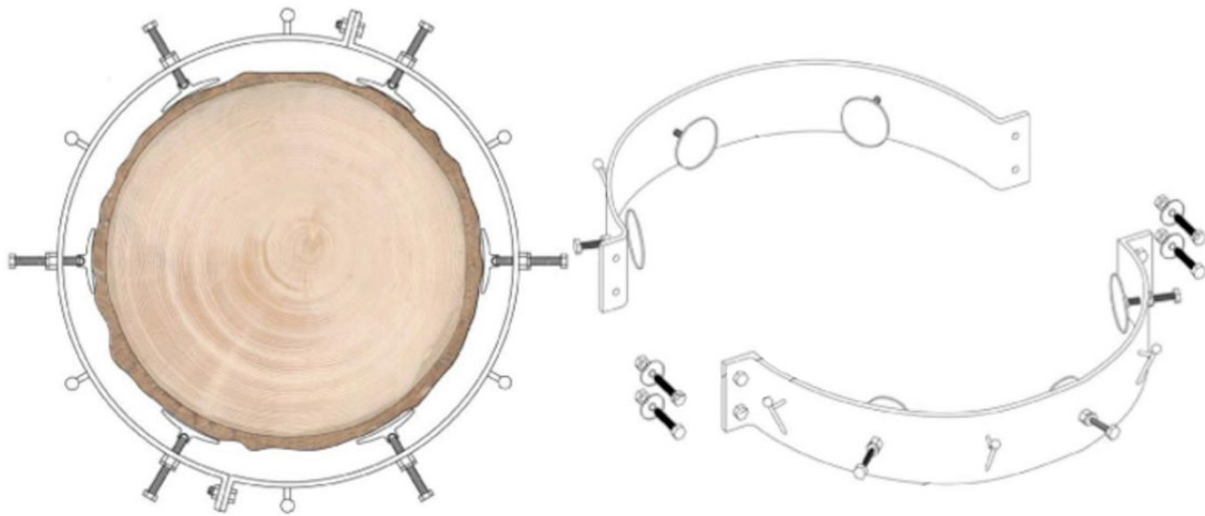

Figure 8.16 Ring system (Gozzi, 2011)

Metal brackets with Treehouse Attachment Bolt

It is crucial to allow the trees to move relative to the plant container. A bracket system, shown in figure 8.17, can fulfil this requirement. These are connected to a tree, and a beam can slide in it in one direction. If the tree moves perpendicular to this direction, this movement has to be accounted for somewhere else in the support system.
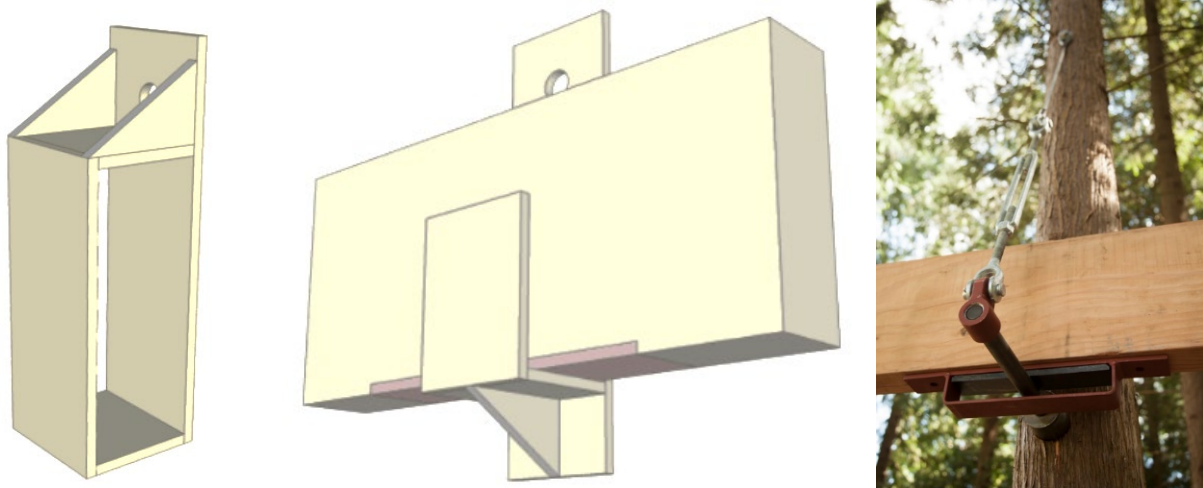
Figure 8.17 Left and middle: Metal brackets (Fulton, 2020). Right: Example of combining metal brackets and cables (Nelson, 2020)

The brackets can be fixed to the tree with two types of bolts. The first is a bolt that goes through the entire stem. First, a hole is drilled after which a rod is pushed through it. This rod is connected at both sides of the stem with washers and nuts. Advantages are the high pull-out resistance and the possibility of a tree overgrowing it, making it barely visible (Wahlländer, 2020). The main disadvantage of the bolt going through the kern of the tree is the chance of creating rot on the inside of the tree. The centre of the tree is not able to respond to injuries, so discolouration and fungi can quickly spread (Stobbe, Dujesiefken, & Schröder, 2000). See figure 8.18.

Figure 8.18 Left: Illustration of bolt going through the stem (Wahlländer, 2020). Right: Bolt created discolouration and white rot some years after installation (Stobbe, Dujesiefken, & Schröder, 2000)

Another type of bolt is the especially designed *Treehouse Attachment Bolt*, placed in pre-drilled holes which do not go all the way through the stem, see figure 8.19. Wahlländer (2020) points out the similarities with a branch, as the trees react to the intrusion of the bolt by creating reaction wood and thus increasing the connection's strength over time. However, a large difference is the lack of interlocking fibres, which adequate stem-branch connections have, as explained in paragraph 5.4.1

The connection is rigid if the wood tissue around the bolt does not deform. This can be achieved by a stiff wood tissue and an absence of cracks or holes.

Before drilling holes, it is essential to consult a tree specialist about the risk of biological degradation. This risk is decreased if a tree has an adequate compartmentalisation capacity, which is the tree's

Figure 8.19 Left: Illustration of Treehouse Attachment Bolt (Wahlländer, 2020). Right: Photo of Treehouse Attachment Bolt (Nelson, 2020)

mechanism to isolate a damaged part. Maple trees are diffuse-porous (Hacke & Sauter, 1996), which results in an adequate wound healing capacity (Ludwig, 2012; Neely, 1988). Therefore, it is expected that Field Maples are suitable for the *Treehouse Attachment Bolts*. Ideally, as the ability to compartmentalise is influenced by genetic factors (Shigo, Dorn, & Lee, 1982), the Field Maples are selected from nurseries that breed trees based on this quality. Wound healing tests could be performed by drilling bolts in living Field Maples. If the spread of discolouration is small, effective compartmentalisation took place (Ludwig, 2012). The spread can be observed by either sawing through the tree, or by tomographic methods (Roloff, 2016).

The bolts have a minimum shaft diameter of 3cm and use a collar of about 8cm wide to spread the load over a larger area of the tree surface (Fulton, 2020). A *Treehouse Attachment Bolt* can carry weights in a range of 900 till 4500kg, depending on the tree in which it is placed. This is sufficient for *Wonderwoods*. Other advantages are the low maintenance and the failure warning system, as a tree shows plastic deformation before it fails (Wahlländer, 2020). The tree needs to have a diameter of at least 30cm at the location of installation.

It is advised to use a single bolt. If several bolts are placed close to each other, less than 30cm apart from each other, compartmentalisation problems can occur as the tree can create one large
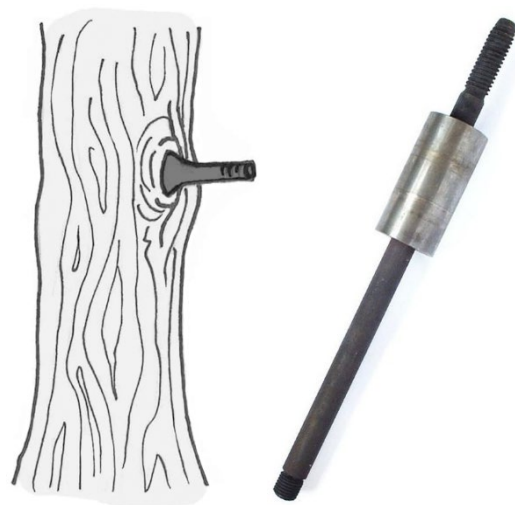
compartment around all the bolts. After some years, this compartment dies and will not be able anymore to hold the bolts' loads (Fulton, 2020).

Knee bracing

Knee bracing is a well-known system in treehouse design, favourable because of its high load-bearing capacity. Just as for the metal brackets, this system is connected to the tree with bolts, accompanying the same complications. The upper beam has to transfer a tension force to the tree via a metal bracket. The lower brace transfers compression forces so a metal bracket is not necessary, but can still be used. This support is rigid. Some freedom of movement should be integrated elsewhere in the support system to allow movement of the trees.
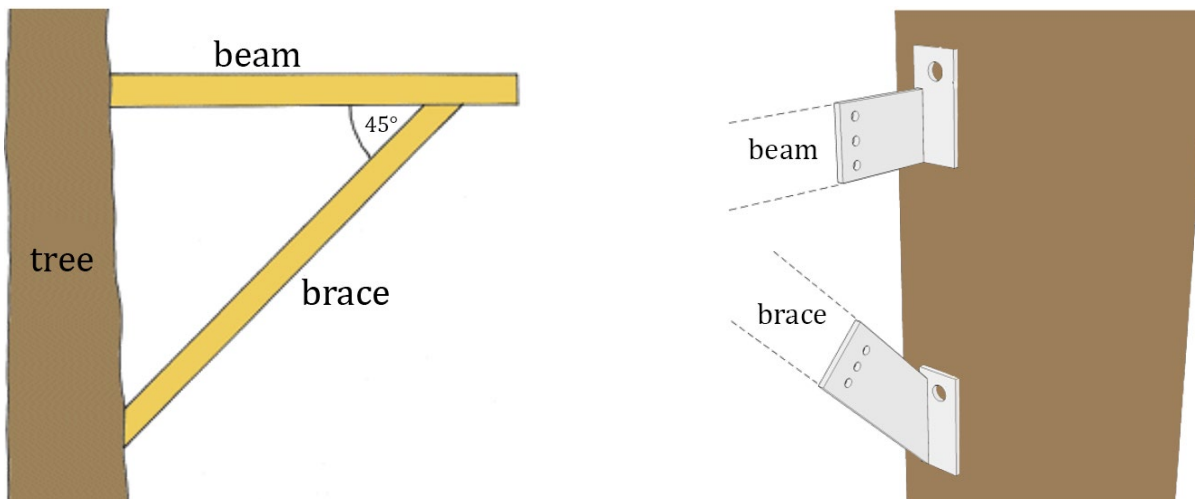
Figure 8.20 Knee bracing system (Fulton, 2020)

Natural joint

A tree can grow around objects and thus create a connection between the tree and the object. See figure 8.21 for an example. This could work in *Wonderwoods* if bars are placed against the trees in the nursery. When the trees have to be planted on the construction, a selection can be made of trees that show promising signs of incorporating the bar into their stems. Once placed on the tower, the trees can strengthen this connection with the bars until it is strong enough to carry the plant containers. Unfortunately, this technique accompanies a significant tree intrusion which can create breaking points if the tree is not able to strengthen its tissue around it. Furthermore, water can accumulate in between the connection, making it vulnerable to rot (Wahlländer, 2020).

Figure 8.21 Tree growing around a fence (Covey, 2020)

Conclusion

Table 8.7 shows an overview of the advantages and disadvantages of the compared systems. From this can be concluded that a system with brackets is most favourable, regarding the system with the *Treehouse Attachment Bolt*. Noteworthy, the stem diameter needs to be at least 30cm, which the trees have when they are standing on *Wonderwoods* for 33 years.

The bracket system could be used for the interconnected trees, in which both stems can hold one bracket. For the single tree system, however, placing a bracket on one side of the tree introduces

considerable bending stress. Placing two brackets, one on each side of the tree, is not possible because of the explained compartmentalisation problems. Therefore, it is advised to do more research into the ring system, as this system has a high potential for the single trees.

Table 8.7 Overview of systems to connect the plant container to the tree compared by sufficient load-bearing capacity, minimal tree intrusion, high aesthetical value, high reliability, and low maintenance

	Double belt	Ring system	Brackets	Knee bracing	Natural joint
Bearing capacity	+/-	?	+	+	?
Tree intrusion	+	+	+/-	+/-	-
Aesthetical	+/-	+/-	+/-	-	+
Reliability	-	?	+	+	-
Maintenance	-	+/-	+	+	+

Because the *Treehouse Attachment Bolt* introduces large stresses in the tree, an extra cable is attached to the bolt and connected higher up in the tree with another bolt. Like the system in the right picture of figure 8.17.

Eurocode 5 (NEN, 2011) describes that all connection systems need to be corrosion resistant.

8.9   DESIGN LOADS

The loads that need to be carried by the trees consist of the self-weight, the plant containers, and the variable loads from wind, rain, and snow.

8.9.1   Loads on the trees

Self-Weight

The self-weight of the trees can be calculated with:

$$F_{self-weight.i} = \rho_{maple} \times V_{tree.i} \times 9,81$$

In which "i" is the number of years after planting.

$$V_{tree,i} = (V_{stem,i} + V_{branch,1,i} + V_{branch,2,i} + V_{branch,3,i} + V_{branch,4,i} + V_{branch,5,i}) \times 1,2$$

$$V_{stem,i} = 0,7 \times \pi \times r_{chest,i}^2 \times h_i$$

$$V_{branch,j,i} = 0,7 \times \pi \times r_{branch,j,i}^2 \times l_{j,i}$$

See paragraph 8.7 for the dimensions of the tree stems. The volumetric weight of green maple trees is 840kg/m³ (Wessolly & Erb, 2016).

Figure 8.22 Overview of loads on the single tree

The diameters of the five largest branches are based on measurements on the trees of the *Living Tree Pavilion* that have similar heights and stem diameters. Although the pavilion trees are Common Ash trees, it gives a first impression of the volumes of Field Maple trees on *Wonderwoods*. Appendix D.1 contains the complete calculation.
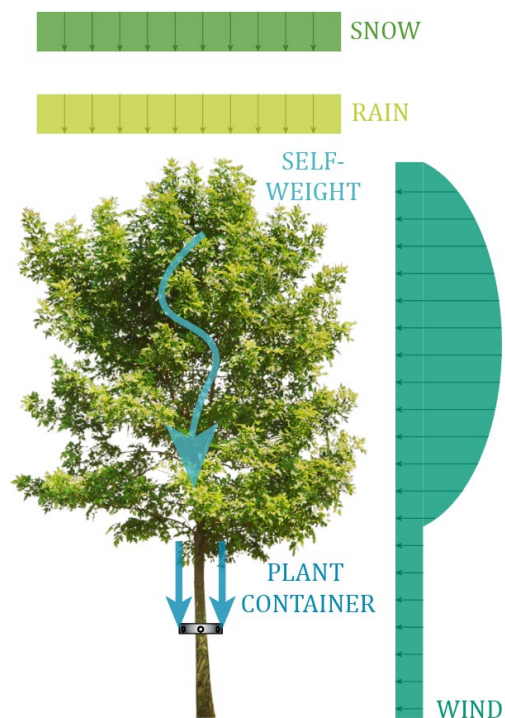
This gives the following results:

$$F_{self-weight.0} = 0,09 kN; \; F_{self-weight,31} = 2,2 kN; \; F_{self-weight,43} = 3,8 kN; \; F_{self-weight,60} = 6,9 kN$$

Wind

As explained in paragraphs 5.2.1 and 5.2.2, a tree's reaction to wind load is a challenging field of study. In this model, the crown is simplified as a rigid body on which a static wind load is applied. According to Gatti and Ruck (2019), the maximum gust wind can then be calculated with:

$$F_{wind,j,i} = 0,5 \times \rho \times c_{D,j} \times A_{j,i} \times (c_A \times v_p)^2$$

With "j" is the object exposed to wind and "i" is the number of years after planting.

In which:

ρ = density of air, usually taken as 1,25kg/m³.

$c_{D,j}$ = mean drag coefficient of the object in flow direction in free flow. This value should be based on literature, in which wind tunnel tests on trees are carried out. For the tree crown, it could range in between 0,2 to 0,6 (Gatti & Ruck, 2019). According to Wessolly and Erb (2016), the crown of the Field Maple has a drag coefficient of 0,25. The stem has a drag coefficient of 0,7 (Sinn & Wessolly, 1989).

$A_{j,i}$ = projected area of the object in flow direction in free flow.

Figure 8.23 Amplification factor at Wonderwoods south-west elevation (Gatti & Ruck, 2019)

c_A = amplification factor due to the velocity increase due to the building. This is determined for the *Wonderwoods* façade with a wind tunnel test. The largest amplification factor for the trees in the façade is 1,5. Figure 8.23 shows that this applies to the corner trees (Gatti & Ruck, 2019).

v_p = wind speed, the maximum is 44,15m/s at 100 meters height. This is based on Eurocode NEN-EN 1991-1-4+A1+C2:2010 and the Dutch national annexe NEN-EN 1991-1-4+A1+C2:2011/NB:2011. Utrecht belongs to wind zone category III, and also the terrain belongs to category III (Gatti & Ruck, 2019).

This results in a maximum horizontal drag force [kN] for every tree's location, see for the calculation appendix D.2. For the trees at the corners of the building, the following wind forces apply:

$F_{wind,crown,0} = 2,7kN;$ $\quad\quad\quad$ $F_{wind,stem,0} = 0,2kN;$

$F_{wind,crown,31} = 7,5kN;$ $\quad\quad\quad$ $F_{wind,stem,31} = 1,1kN;$

$F_{wind,crown,43} = 7,5kN;$ $\quad\quad\quad$ $F_{wind,stem,43} = 1,4kN;$

$F_{wind,crown,60} = 7,5kN$ $\quad\quad\quad$ $F_{wind,stem,60} = 1,9kN$

Snow

The snow load on the trees will not be governing in the design because the load of the leaves during a shower is larger. Due to the seasons, the trees will not have leaves at the same time as snow load (Gatti & Ruck, 2019). However, to get a better understanding of the magnitudes of the loads, the calculation is still shown.

The snow load on the plant containers must be considered.

The snow load can be calculated as follows:

$F_{snow,j,i} = q_{snow} \times A_{j,i}$

In which "j" is the object exposed to snow and "i" is the number of years after planting.

$q_{snow} = 0,7 \times 0,8 = 0,56kN/m^2$ (Eurocode 1991-1-3 Dutch National Annex)

See appendix D.3 for the calculation.

The results for the snow load on the crown and the plant containers are as follows:

$F_{snow,crown,0} = 0,9kN;$ $F_{snow,crown,31} = 2,7kN;$ $F_{snow,crown,43} = 2,7kN;$ $F_{snow,crown,60} = 2,7kN$

$F_{snow,plantcontainer} = 0,9kN$

Rain

The rain load can with this information be estimated as follows:

$F_{rain,j,i} = \rho_{water} \times 9,81 \times \max rain \times A_{j,i}$

In which "j" is the object exposed to snow and "i" is the number of years after planting.

$\rho_{water} = 997kg/m^3$

The maximum amount of rain that fell in one day since 1960 is 63,9mm. This is measured in the Bilt, close to Utrecht, at the 13th of October in 2013 (Koninklijk Nederlands Meteorologisch Instituut, 2020).

See appendix D.4 for the calculation. The rain loads are:

$F_{rain,crown,0} = 1,0kN;$ $F_{rain,crown,31} = 3,0kN; F_{rain,crown,43} = 3,0kN; F_{rain,crown,60} = 3,0kN$

$F_{rain,plantcontainer} = 1,0kN$

<u>Plant containers</u>

Figure 8.24 shows the dimensions of the plant containers. It is made of ultra-high-strength concrete with a volumetric weight of 27kN/m³. This results in a dead load of 2,8kN per meter container. The load of the mature plants and the fully saturated soil is 4,8kN per meter container (Telgen, 2018). Snow and rain load are not included in this load.

The length of the containers varies from 3,6 to 4,5 meters. If a container of 4,5 meters has two supports, this gives a load of 17,1kN per support.

$$F_{plantcontainer} = 17,1kN$$
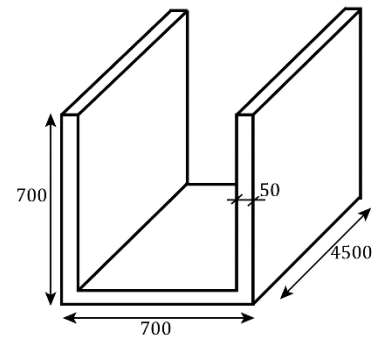
Figure 8.24 Dimensions of the plant containers in mm

8.9.2 Load combinations

The load combinations are generated according to Eurocode 1990 (NEN, 2019).

ULS1:
$$1,2 \times \left(F_{self-weight} + F_{plantcontainer}\right) + 1,5 \times (F_{wind,crown,0} + F_{wind,stem,0})$$

ULS2:
$$1,2 \times \left(F_{self-weight} + F_{plantcontainer}\right) + 1,5 \times (F_{wind,crown,90} + F_{wind,stem,90})$$

ULS3:
$$1,2 \times \left(F_{self-weight} + F_{plantcontainer}\right) + 1,5 \times (F_{snow,crown} + F_{snow,plantcontainer})$$

ULS4:
$$1,2 \times \left(F_{self-weight} + F_{plantcontainer}\right) + 1,5 \times (F_{rain,crown} + F_{rain,plantcontainer})$$

ULS5:
$$1,35 \times \left(F_{self-weight} + F_{plantcontainer}\right)$$

ULS special:
$$1,2 \times \left(F_{self-weight} + F_{plantcontainer}\right) + 1,5 \times (F_{wind,crown,0} + F_{wind,stem,0} + F_{wind,crown,180} + F_{wind,stem,180})$$

SLS1:
$$1,0 \times \left(F_{self-weight} + F_{plantcontainer}\right) + 1,5 \times (F_{wind,crown,0} + F_{wind,stem,0})$$

SLS2:
$$1,0 \times \left(F_{self-weight} + F_{plantcontainer}\right) + 1,5 \times (F_{wind,crown,90} + F_{wind,stem,90})$$

SLS3:
$$1,0 \times \left(F_{self-weight} + F_{plantcontainer}\right) + 1,5 \times (F_{snow,crown} + F_{snow,plantcontainer})$$

SLS4:
$$1,0 \times \left(F_{self-weight} + F_{plantcontainer}\right) + 1,5 \times (F_{rain,crown} + F_{rain,plantcontainer})$$

With "ULS special" is checked what happens if the two crowns of interconnected trees are subjected to wind loads in opposite directions.

Eccentricities are not included in the calculations. They could occur if, for example, an abseiling person doing maintenance stands on one of the plant containers.

8.9.3 Loads on the structure

The trees transfer the loads via the tree container to the console connected to the bearing walls of *Wonderwoods*. To get an idea of the increase of load due to the plant containers, estimations of the original loads and the loads in the new single tree design are made at 60 years after planting.

<u>Original bending moment</u>

The original bending moment is calculated at the bottom of the tree container, which is one meter deep. The bending moment is solely due to the wind load (Gatti & Ruck, 2019).

Arcadis does not consider the horizontal load or bending moments due to a possible angle of the trees. Under this assumption, they must make sure that trees are guided to grow upwards. A disadvantage is that trees cannot adapt to the climate around it, such as the sun and wind direction. This makes the tree weaker. If a tree is smaller than five meters, this overhang can be ignored in bending moment calculations (Gatti & Ruck, 2019).

The bending moment then becomes:

$$M = 1,5 \times (F_{wind,crown,60} \times 5m + F_{wind,stem,60} \times 3m) = 64,8kNm$$

<u>Original vertical force</u>

The original vertical force is the weight of the tree, the rain load on the crown, the weight of the soil, and the weight of the tree container.

The load of the soil can be calculated as:

$$F_{soil} = V_{soil} \times \rho_{soil+roots}$$

The volume of soil in the tree container is (Telgen, 2018):

$$V_{soil} = 1,5m \ \times 1,5m \ \times 1,0m = 2,25m^3$$

The volumetric weight of the soil and roots together is (Sinn & Wessolly, 1989):

$$\rho_{soil+roots} = \frac{2 \times \rho_{soil} + 1 \times \rho_{roots}}{3}$$

In which:

$$\rho_{soil} = 15,5kN/m^3 \text{ (Telgen, 2018)}$$

$$\rho_{roots} = 9,0kN/m^3 \text{ (Sinn & Wessolly, 1989)}$$

In total this gives $F_{soil} = 30,0kN$

The load of the tree container can be calculated as:

$$F_{treecontainer} = V_{treecontainer} \times \rho_{USHBconcrete}$$

The volume of the tree container is (Telgen, 2018):

$$V_{treecontainer} = 4 \times 1,5m \times 3,0m \times 0,08m + 1,5m \times 1,5m \times 0,08m = 1,62m^3$$

The volumetric weight of the concrete container is:

$$\rho_{USHBconcrete} = 27kN/m^3$$

In total this gives $F_{treecontainer} = 43{,}7kN$

The vertical force then becomes:

$F_v = 1{,}2 \times \left(F_{self-weight,60} + F_{soil} + F_{treecontainer}\right) + 1{,}5 \times F_{rain,crown,60} = 101{,}2kN$

New design bending moment

If eccentricities are ignored, no additional bending moments are resulting from the plant containers:

$M = 1{,}5 \times (F_{wind,crown,60} \times 5m + F_{wind,stem,60} \times 3m) = 64{,}8kNm$

This is an increase in bending moment of 0%.

New design vertical force

Additional vertical forces are given by the weight of the plant containers and the rain load on the plant containers. This weight is multiplied by two because there are two halves of the plant containers connected to one tree. This results in:

$F_v = 1{,}2 \times \left(F_{self-weight,60} + F_{soil} + F_{treecontainer} + F_{plantcontainer} \times 2\right) + 1{,}5 \times (F_{rain,crown,60}$
$+ F_{rain,plantcontainer} \times 2) = 145{,}3kN$

This is an increase in vertical force of 44%.

In the original design, the transfer of forces from the tree container to the load-bearing walls is far from reaching its limit. It is therefore expected that this increase in loads does not require extra strengthening of the load-bearing walls.

8.10 DESIGN STRUCTURAL MODEL
Both the designs with the single trees and the interconnected trees have to be structurally verified. They are checked on uprooting, breaking and deformation. Based on the outcomes of this, an expectation is given how old the trees need to be to carry the plant containers.

8.10.1 Uprooting check
In 1989, Sinn and Wessolly proposed a method to perform a quick uprooting check for trees. This is carried out for the trees on *Wonderwoods* just after planting and when they are standing there for 60 years. Sinn and Wessolly stated that a tree should have a sufficient uprooting resistance if the following is true:

$M_s \geq 1{,}5 \times M_k$

In which M_s is the standing moment, which is the self-weight of the tree and roots times the width of the root area. This should be larger
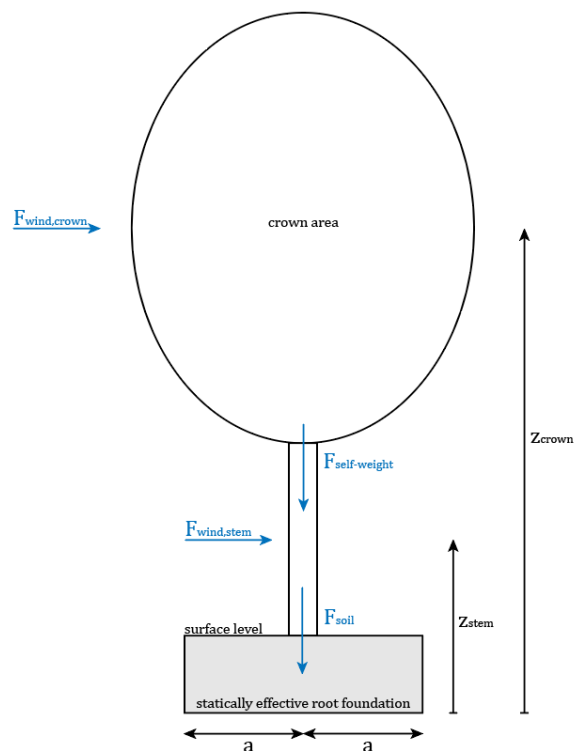
Figure 8.25 Uprooting calculation according to Sinn and Wessolly (1989)

than 1,5 times M_k, which is the tipping moment due to the wind force. For the *Wonderwoods* trees, this can be calculated with:

$$\left(F_{self-weight} + F_{soil}\right) \times a \geq 1,5 \times \left(F_{wind,crown} \times z_{crown} + F_{wind,stem} \times z_{stem}\right)$$

This is illustrated in figure 8.25. Table 8.8 shows the resulting unity check of the uprooting resistance. A unity-check larger than 1,0 means failure, which is the case for both time indications. This means that without additional measures, the single trees are prone to uprooting if they get exposed to the maximum wind load.

Table 8.8 Uprooting resistance of Wonderwoods (single) trees at the time of planting and 60 years after planting

	Year 0	Year 60
$F_{self-weight}$ [kN]	0,1	3,9
F_{soil} [kN]	3,1	3,1
a [m]	1,25	1,25
M_s [kNm]	4	8,8
$F_{wind,crown}$ [kN]	2,7	7,5
$F_{wind,stem}$ [kN]	0,2	2,0
z_{crown} [m]	3,25	4,0
z_{stem} [m]	1,0	1,0
M_k [kNm]	9	32
U.C. ($\mathbf{1,5} \times M_k/M_s$)	3,4	5,5

8.10.2 Breaking check – Ultimate Limit State

The tree breaks if the stresses exceed the maximum allowable stresses as defined in paragraph 8.6. With Eurocode 1990 and Eurocode 1995 is checked if sufficient breaking safety can be guaranteed. With a simplified calculation in appendix D.5, an estimation is given for the minimum amount of years the trees need to stand on *Wonderwoods* before they are big enough to hold the plant containers.

It takes 31 years for the single trees to be big enough and 43 years for the interconnected trees. The main reason the interconnected trees need to be bigger are the large bending moments acting around the connection.

To get a better insight into the distribution of stresses, a 3D finite element model is created with the same procedure as the winching test models. See appendix D.6 for the input values and the ULS checks of the models. The single tree of 31 years is modelled with a ring system, as explained in paragraph 8.8. The interconnected trees of 43 years are modelled with a bracket system, connected to the tree with *Treehouse Attachment Bolts*.

In the single tree, the maximum allowable bending stress is not exceeded for the largest part of the stem. Just above and below the ring system connection, there are tiny spots where the maximum bending stress is exceeded for ULS 1 and ULS 2. This is the result of introduced bending moments due to the way of modelling the ring system with rigid elements. It is expected that in reality, the bending stress around the ring system is smaller because the ring feet are not entirely stiff. Additionally, bending stresses will be smaller as the tree can adapt to applied loads by creating secondary growth. ULS 3, ULS 4, and ULS 5 do not exceed the maximum allowable bending stress.

In the model with interconnected trees, the maximum bending stress is also exceeded for ULS 1 and ULS 2. This is, however, only the case for a small area around the inosculation. It can be argued

that this is the result of incorrect modelling of the inosculation. The sudden change in slope gives bending stress. In reality, the tree will create a smoother inosculation, so the stresses become smaller. In the rest of the tree, the maximum bending stress is not exceeded. Likewise, for ULS 3, ULS 4, and ULS 5, the bending stresses are not exceeded. Also, for ULS special, in which the wind load is oppositely directed on the two crowns, the bending stresses are not exceeded.

8.10.3 Deformation check – Serviceability Limit State

The tree crown does not have a limitation for the allowed deformation. The plant containers are, in principle, allowed to move freely; however, it is expected that residents of the tower will not be relaxed if the plant containers move a lot. It is, therefore, up to the reader to determine whether the deformation is acceptable.

The deformations of the trees are checked at the height of one meter, where the connection with the plant containers is located. Models are created with both a rigid support stiffness and with a rotational spring stiffness of 24,4kNm/rad, according to the root stiffness results of the tested airpot tree in paragraph 7.2.2.

Appendix D.6 contains figures of the SLS checks.

The maximum displacement of the single tree with a rigid foundation is 7,0mm, which is due to SLS2, containing self-weight and perpendicular wind. The deformations due to wind load on the single tree with a spring support are too large for the finite element software to calculate, from which can be concluded that the tree will fall over.

The maximum displacement of the interconnected trees with a rigid foundation is 5,9mm, likewise due to SLS2, containing self-weight and perpendicular wind. If the interconnected trees with a spring support are subjected to wind load, the deformations are huge, up to 1,5m due to SLS2. As this deformation occurs at a tree height of only one meter, it is expected that the trees fall over.

Deformations due to SLS3 and SLS4, self-weight with respectively snow or rain, are neglectable small, with a maximum of 1mm.

The results show that if the *Wonderwoods* Field Maple trees have the same root stiffness as determined for the Elm tree in an airpot, the risk of uprooting is too large. It can, however, be argued that the root system of the Field Maple is stiffer than of the Elm. In paragraph 8.4, the *BuGG* committee is introduced, which composed a list of trees suitable for placing on buildings with great height. Elm is not stated on this list while Field Maple is.

Nevertheless, additional root anchoring is necessary to reduce the risk of uprooting. In paragraph 8.11, several solutions will be discussed.

8.11 Tree anchoring

As is concluded from the structural design, the trees' root systems need anchoring to prevent uprooting. A tree can be anchored above ground or underground, with a rigid or flexible system. A rigid system can, for example, be created by staking the tree with steel cables or a pole, see figure 8.26 on the left. Loads are then mainly transferred through this system, not via the tree. This is undesired because the tree starts to rely on this, reducing its growth in thickness. The anchoring becomes part of the tree's structural system, so removing it after a couple of years is problematic (Wessolly & Erb, 2016). It is thus essential that the ties have certain flexibility; this way, the tree can move due to applied loads and develop its stiffness. Possible ways of creating flexibility are by using shock absorbers or using flexible plastic ropes.
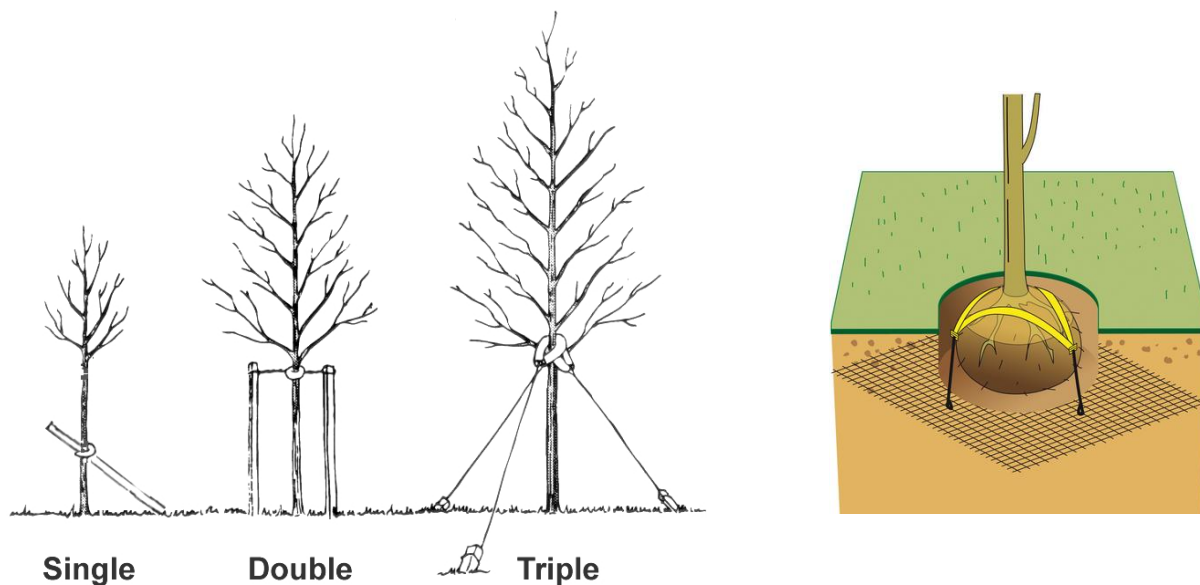
Figure 8.26 Left: Examples of staking a tree with cables or poles (Wilson B. , 2017). Right: Root ball anchored with straps to a wire net (Green Max, 2018)

Underground anchorage of the root ball does not restrict the movement of the tree, so a tree develops sufficient secondary growth of the stem and roots. Besides, aesthetically it is favourable as it is out of sight. The root ball can, for example, be anchored with straps, putting pressure on the root system (Green Max, 2018). Another method to anchor the root ball is by driving two dowels through the root ball into the soil. A longer dowel will act as an anchor below the root ball, simulating a taproot. A shorter dowel resists twisting of the tree (Phillips, 2020).

Terra Toggle   Brooks Tree Brace   2x2 Anchoring
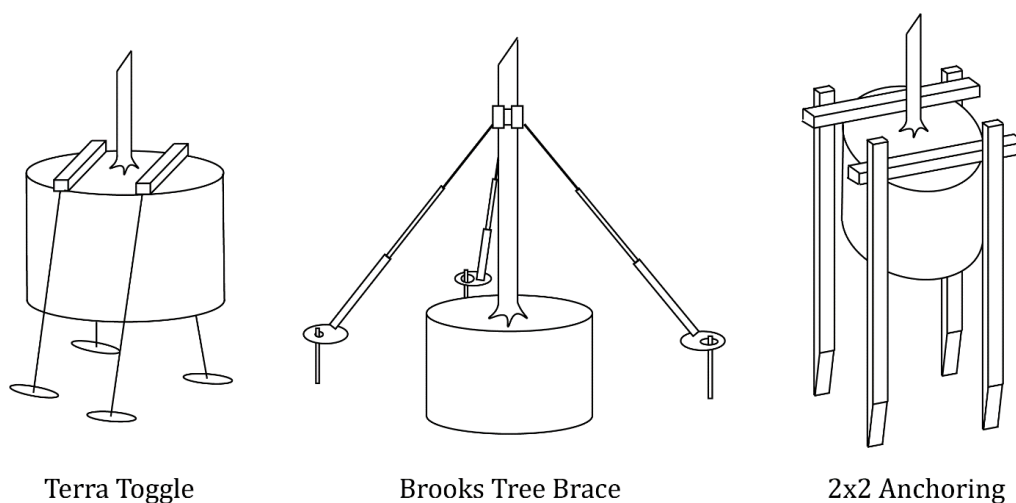
Figure 8.27 Examples of effective anchoring methods

In 2008 pulling tests were conducted on container-grown oak trees with different stabilizing systems, including the above-ground poles and cables and underground root ball anchoring with dowels or straps (Eckstein & Gilman, 2008). Anchoring methods that resulted in being very useful were the *Terra Toggle*, the *Brooks Tree Brace* and 2x2 anchoring. See figure 8.27. The *Terra Toggle* is a system with two timber pieces placed on top of the root ball, connected with low-stretch plastic strapping to plastic anchors that are driven into the soil. The *Brooks Tree Brace* uses telescoping metal braces that have a hinged connection to the stem, protected with rubber pads. The braces are connected to the soil with slotted plates and pegs. The third system is the 2x2 anchoring in which timber pieces are placed on top of the root ball and connected to sticks that are hammered into the soil.

93

Systems that turned out to not work effectively are poles, as shown in figure 8.26 on the left, and dowels and staples, connected to the root system and driven into the soil.

Because the trees of *Wonderwoods* are envisioned to fulfil a structural function, they must be stimulated to increase their thickness. An above soil anchoring system is therefore unfavourable. From the research by Eckstein and Gilman (2008) came evident that underground anchoring systems which are strapped over the root ball work best. Because the *Wonderwoods* trees are placed in a container, it is easy to fasten the straps to the bottom of the container. This system is included in the designs of figure 8.6 and figure 8.8.

8.12 TEMPORARY SUPPORT

Until the trees are old enough to carry the plant containers, they need to be carried by another support structure. In the design proposals, the console underneath the tree container transfers the plant container's load to the main *Wonderwoods* structure. So, it is practical if the temporary support structure also transfers the load via the tree container.

This is ensured by placing the plant containers on top of the tree containers with a support, as indicated in blue in figure 8.28. Ideally, the support dissolves slowly, so the tree can get used to the applied load and adapt its growth behaviour. This could be achieved by jacks which can either be adjusted automatically or manually, according to the growth of the tree.

In case the risk of failure of the tree increases, for example, due to sickness, the temporary supports can be placed again.

Figure 8.28 Front view of the Wonderwoods design, the blue blocks indicate the temporary support system

8.13 MAINTENANCE

The process from young till mature tree

Two years before the trees are planted on *Wonderwoods*, they are placed in airpots in the nursery. This way, the roots of the trees can grow very dense, which is necessary if they are placed in the small containers along the façade.

For the trees that need to be interconnected, it is advised to place them crosswise together in a single airpot and to stimulate them to grow the inosculation. Although in paragraph 4.3 Ludwig (2012) suggests that using screws is the most reliable method for stimulating inosculations, it is advised to use rubber bands. One reason is that it is unknown how the trees react to the screws on the long term and another reason is that the rubber bands can be removed once the inosculation is mature. By then, the connection consists of no materials other than the tree itself. After two years in the nursery, a selection can be made of trees that show signs of inosculation growth. These trees will be transported together in one container to *Wonderwoods*. In this way, the chance of breaking the young connection is small.

The *Treehouse Attachment Bolt* can be drilled into the interconnected trees when they have a diameter of 30cm; it is expected that this will take 33 years. The tree then has ten years to integrate this bolt before it must carry the plant containers.

The ring system can anytime be placed around the single trees. It is advised to place the system at least ten years before the trees need to carry the plant containers. The load can then gradually be increased, allowing the tree to adjust to the extra load.

Inspection

In the treehouse industry, it is advised to have a routine inspection every three years in which the health of the trees and the status of the connection between the trees and the structure is checked. This would be a good guideline for the *Wonderwoods* trees. If the single trees with the ring system are used, the feet of the system should also be adjusted every three years. It is advised to do additional inspections after large storms.

Arcadis has proposed that maintenance along the façade of the tower can be carried out by abseiling. Rope access specialists can attach themselves to portable davits, which are small cranes that can be installed on the roofs (Koninklijke Ginkel Groep, 2018). Reaching the plants and trees via the apartments is according to Arcadis undesired because of the large intrusion of the residents' living quality (Cents T. , et al., 2019).

Pruning

Either particular protection layers or the composition of the concrete prevents root penetration through the tree container. Pruning of the roots is therefore not necessary (Cents, 2020; Koninklijke Ginkel Groep, 2018).

Due to the small tree containers, the trees cannot grow huge, which works like bonsai trees (Cents T. , et al., 2019). Intensive pruning is thus not necessary. Occasionally, branches hindering sight for the residents need to be removed. Additionally, it is essential to select the desired branches and stems and remove others. This makes sure that the trees put energy in the growth of the stem that needs to carry the plant containers. For the interconnected trees, this requires extra maintenance because the trees are placed under an angle. A tree then naturally wants to select an upward growing branch as its main stem, reducing the growth in thickness of the envisioned, angled, main stem. Figure 8.29 shows an illustration of this.
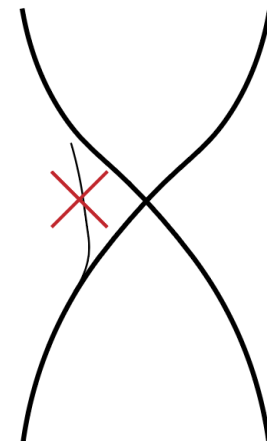
Figure 8.29 Two cross connected trees with a branch growing upright which should be removed

Furthermore, pruning needs to ensure an equal crown size of two interconnected trees. Else, one of the two trees can grow more vigorous and win the competition for space.

Death of trees

If trees die, the temporary support system of the plant containers should be used again. A decision should be made whether to replace the tree or not. Hoisting the trees can be carried out via the portable davits. If one of two interconnected trees dies, the remaining tree should be supported because it has optimised its secondary growth based on the dead tree.

Surroundings

The surrounding area of the tree must not suddenly change, for example by building another tower in front of it, or by giving the façade a much darker or lighter colour (Wessolly & Erb, 2016). The tree is optimised for specific wind, temperature, and light conditions. Changing these abruptly can weaken the tree.

<u>Watering</u>

The trees are watered naturally during showers. Underneath the soil layer, retention crates are placed that fill slowly with rainwater. Via capillary cones, the water is transported vertically to the roots. In dry periods the trees are watered from above with water coming from a water storage on the roof (Cents T. , et al., 2019).

Fire safety

Arcadis states that trees and plants do not give additional fire safety risks. The trees and plants are planted in incombustible steel containers. The chance of the greenery catching fire is small due to the lack of ignition sources and the moisture content of the greenery. A fire that starts within the building will not spread via the façade because of the installed sprinkler system (Haas & Riet, 2018).

8.14 COMPARISON OF DESIGNS

The two systems with single trees or with interconnected trees will be compared based on their botanical and structural feasibility.

8.14.1 Botanical

Both systems make use of the same tree species, the Field Maple, which shows favourable qualities for both designs, like standing-, breaking-, frost- and drought-resistance. For the interconnected design, in particular, favourable qualities of this tree species are the high strength perpendicular to the grain and the ability to create inosculations.

From a botanical point of view, the design with single trees has a larger chance of success. The interconnected trees are shaped in unnatural directions, which costs the energy of the tree. Furthermore, the change of the trees not creating suitable inosculations is high.

In an ideal situation, the two trees are fully inosculated and behave like a single organism. They share water and nutrients and help each other to stay alive. This is necessary because the two trees rely on each other for their structural stability. However, the chances are big that this ideal situation does not occur, and trees start competing for space. This will be fought both in the air, searching for light, and in the soil, searching for water, nutrients, and space to grow their roots. Due to the very little available space, this competition can become fierce. There is a considerable chance that this results in one tree lagging growth or even die.

8.14.2 Structural

Based on the ultimate limit state checks of paragraph 918.10.2, it is expected that single trees need to stand on *Wonderwoods* for 31 years before they can bear the plant container while this is 43 years for the interconnected trees. This opts for using the single tree. The largest stresses of the interconnected trees occur at the inosculation, which is the part of which the least is known. This makes it risky to rely on the structural capacity of interconnected trees.

The serviceability limit state checks of paragraph 8.10.3 show that the interconnected tree system is more favourable because of the smaller deformations. This is especially the case if the root

system is not rigid. However, the winching results of chapter 7 show contradictory results, in which the single tree deforms less than the interconnected trees. It is therefore difficult to draw conclusions from this.

8.14.3 Wonderwoods

Both systems have a high aesthetical value, as they both show residents of *Wonderwoods* the possibilities of using living trees as structural elements. The interconnected system, however, reveals a technique that most people have never heard of, which may excite the residents.

The disadvantage of using the interconnected system is that it brings higher loads on the building, firstly because there are two trees used instead of one, secondly because it is necessary to increase the size of the tree container.

8.15 FINAL DESIGN OPTIMISATION

Several solutions will be proposed to improve the single tree design and reduce the number of years before the trees can carry the plant containers.

The graphs of figure 8.30 show the change of the loads on the trees over time together with the change of resistance and the change in unity check over time. It shows that the wind load on the crown of the tree has the largest contribution to the maximum stress. In the proposed modifications, this is tried to be reduced. The calculations of the following paragraphs are carried out with the same procedure as used in paragraph 8.10. The input parameters will be described.
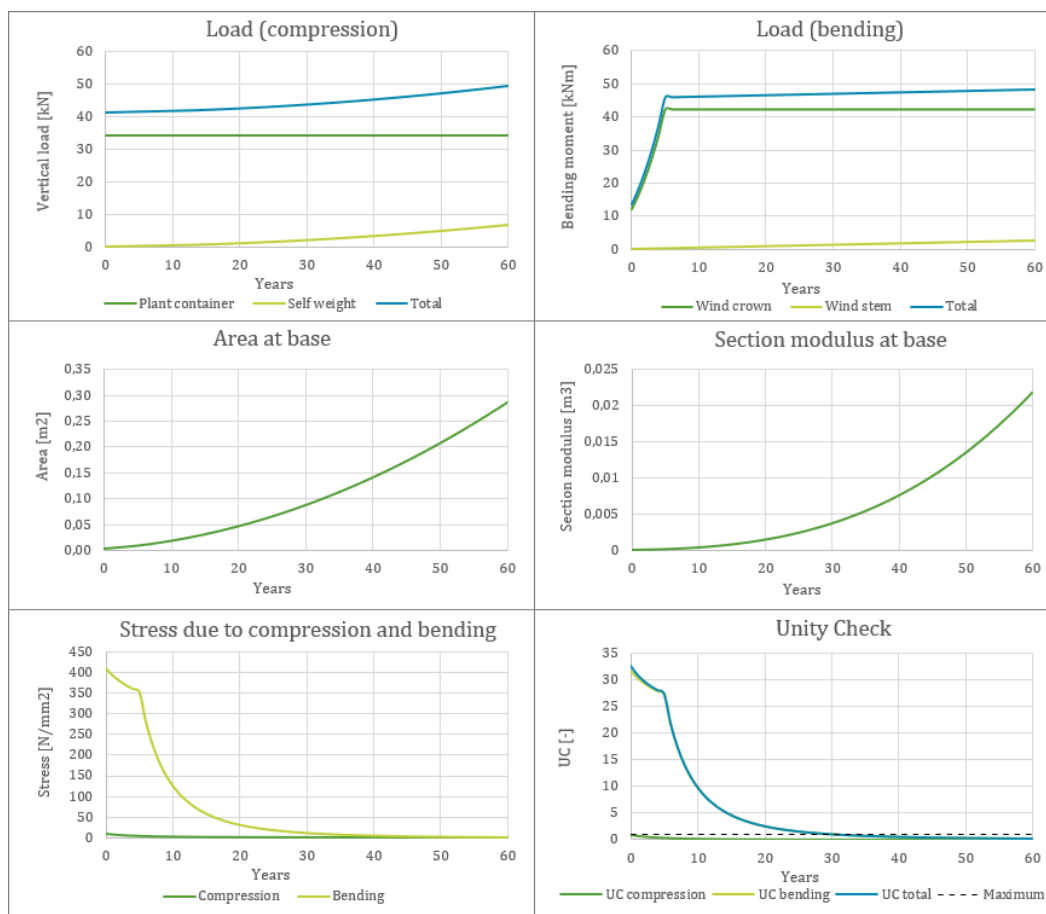
Figure 8.30 Change in load and resistance of the single tree over time, at the base of the tree. Top left: Compression load. Top right: Bending load. Middle left: Area of the cross-section. Middle right: Section modulus of the cross-section. Bottom left: Compression and bending stress. Bottom right: Unity check for compression, bending, and the combination. The maximum unity check is 1,0.

8.15.1 Pruning of the tree

The amount of wind load on a tree can be decreased by pruning the crown. Figure 8.31 shows the maximum sizes of Field Maples on *Wonderwoods*, as proposed by Gatti and Ruck (2019) based on their wind calculations. The maximum crown area is reduced from 11,0m^2 (see paragraph 8.7) to 7,8m^2. This reduces the number of years from 31 to 26.

Side view
Vertical crown area
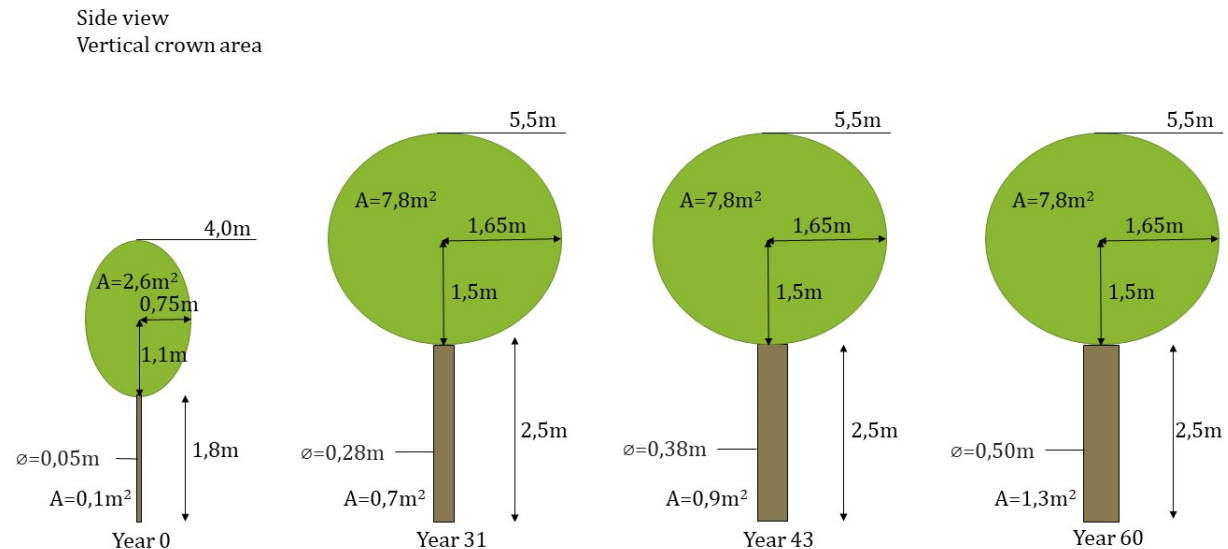
Figure 8.31 Smaller sizes of Field Maples as proposed by Gatti and Ruck (2019)

8.15.2 Position on the building

The wind load is calculated at the most unfavourable positions of the building, which are the corners. At these locations, the wind load is multiplied with an amplification factor of 1,5, as is explained in paragraph 8.9.1. In the middle of the building, however, the amplification factor is only 1,1. This reduces the number of years required for the smaller trees to be able to resist the loads from 26 to 20 years.

8.15.3 Second plant container

In the design, the trees carry the plant containers at the height of one meter. The consoles still carry the plant containers at the level above. In an ideal case, the trees can also carry the plant containers of the higher level, at four meters height of the tree.

Connecting the plant containers higher up in the tree, where it has many branches, brings some implications. The tree must be pruned carefully, creating a distinct main stem, and preventing branch growth around the connection. If assumed that this is possible, then the tree should be able to carry the plant containers after 23 years. Figure 8.32 shows the forces, acting at the location of the connection, on the (smaller) 23-year-old tree, standing in the middle of the façade.

Another complication of connecting a second plant container is the required temporary support system. It cannot, like the first plant container, elegantly be placed on the tree container below. It is therefore advised to temporarily hang the plant containers with cables to the tree container above.
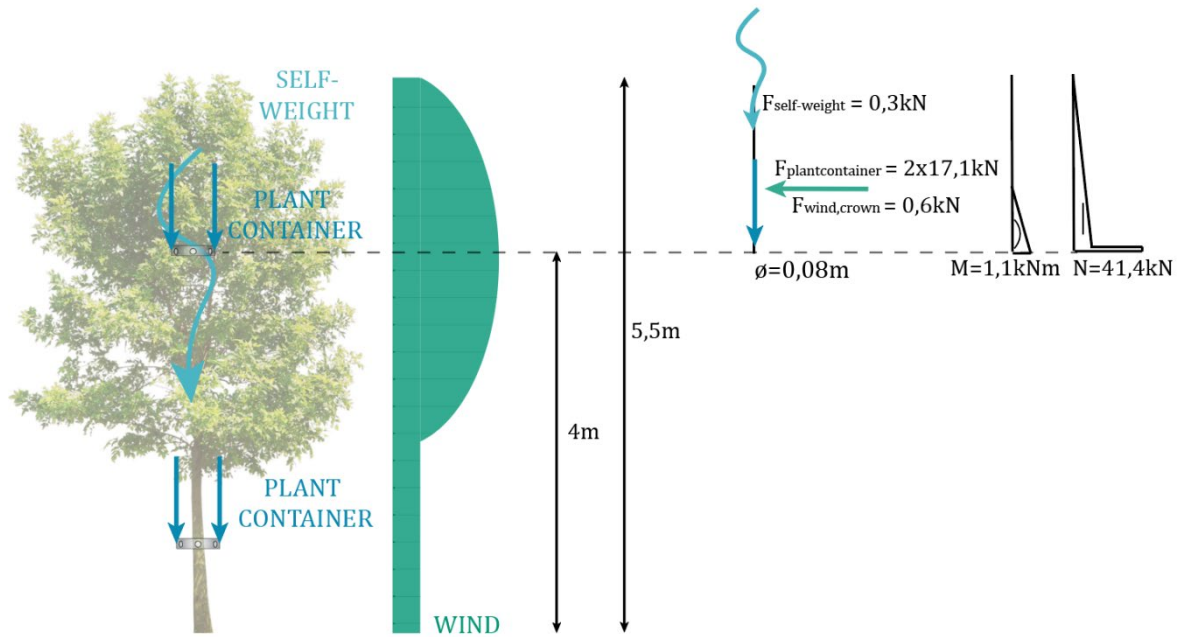
Figure 8.32 Calculation of the bending moment and compression force at 4m height of the tree. Calculated at year 23 for the smaller tree geometry as described in paragraph 8.15.1.

8.15.4 Cable

Figure 8.30 shows that even without the plant containers, the trees are not able to resist the wind load until they are standing on *Wonderwoods* for 31 years. They should, therefore, be assisted in carrying this wind load. This can be accomplished by connecting the tree to the vertical spanning cable. It is vital that the tree can still move during moderate winds so that it can develop reaction wood. However, during severe storms, the cable must be activated (Ludwig, 2012). To achieve this, more flexible synthetic cables are preferred over steel cables. Additionally, shock absorbers should be installed, so tightening of the cable during storms does not give shock loads. Such an absorber is placed in the cable of figure 8.33. According to the manufacturer, this system is made for a service life of twelve years (Freeworker, 2019).

Figure 8.33 Synthetic cable with a shock absorber (Freeworker, 2019)

Ideally, the tree is connected to the cable at the wind load centre of gravity. The top illustration in figure 8.34 shows the structural scheme of the original tree system for year 0, at which the wind load is the most critical. The illustration on the bottom shows the structural scheme if the tree is connected to a stressed cable. This reduces the bending moment such that the tree can resist the wind load with a unity check of 0,6. The plant container can then be connected to the tree after two years.

It is important to note that this is an estimation of a very favourable situation, without eccentricities and with the cable being able to take up all the wind load on the crown.

For a further design stage, it is recommended to consult an arborist about the placing of the cable. He or she can inform about the right equipment and position of the tree attachment.
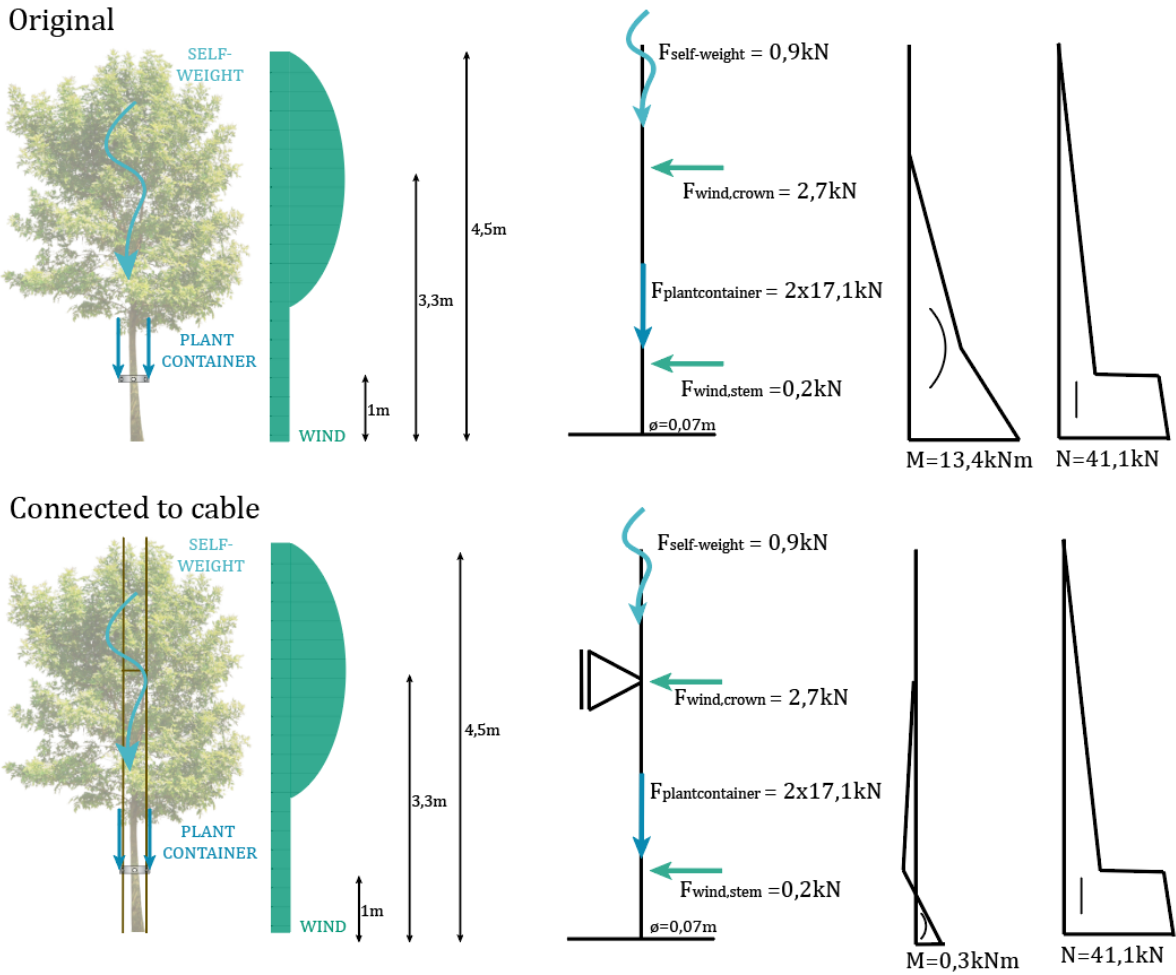
Figure 8.34 Calculation of the bending moment and compression force at the base of the tree with (bottom) and without (top) a connection to a steel cable. Calculated for the design at year 0 with a geometry as shown in paragraph 8.7.

9 DISCUSSION

Paragraph 9.1 discusses the findings of chapter 7 and 8 and compares them to the theory, as outlined in chapter 4 and 5. Furthermore, paragraph 9.2 discusses the methods of the tests on the *Living Tree Pavilion* and the *Airpot* tree, as outlined in chapter 6. This is followed by a discussion of the method used in the *Wonderwoods* design, as outlined in chapter 8.

9.1 DISCUSSION OF RESULTS

First, the results of the tree characteristic measurements will be discussed, followed by the results of the winching tests and the finite element model. Then, the results of the application to *Wonderwoods* will be discussed.

9.1.1 Living Tree Pavilion and Airpot Tests

Tree geometry measurements show indications of the trees adjusting their shape to certain loads, which was expected based on the literature study in paragraph 4.1. One of the indications is the sudden decrease in circumference just below the connection in the cross-connected trees. Another indication is the ovalisation of a tree in the direction in which it is leaning. Figure 7.4 shows that on average, the diameter in the leaning direction is 6% larger than the perpendicular diameter. Remarkably, the trees which are leaning the most, have a negative ovalisation in the leaning direction. Possibly, this is due to the cross-connection of these trees with another tree, which could take away the need of developing stiffness in the leaning direction. Furthermore, figure 6.3 illustrates that only seven inosculations can be observed in the *Living Tree Pavilion*, while the design contained 36. This shows that creating inosculations is not guaranteed to be a success, which was also concluded by the *Baubotanik* research group (Ludwig, 2012), introduced in paragraph 4.3.

The winching tests show that an open-soil root system is stiffer than a root system constrained by an airpot. Figure 7.5 and figure 7.6 show that in this experiment, the unconstrained root stiffness is about seven times larger. This result meets the expectations as an unconstrained tree can create a broader root system and thus withstand larger bending moments. Paragraph 7.2.1 shows that the moisture content around both the constrained and unconstrained tree is similar, which makes a comparison between the two legitimate. If the soil moisture content changes, the root system stiffnesses might change as well.

Furthermore, the system stiffness of (interconnected) trees is determined based on the measured displacement. Contradictory to the results obtained by Borská (2018), the system stiffness of a single tree is a lot higher than the stiffnesses of the interconnected trees. The trees that are pulled in tangential direction show the lowest stiffness. Paragraph 7.2.3 gives a partial explanation for the low tangential stiffness, in which a winch lift influences the displacement measurements. Additionally, cracks in the bark indicate that the trees are not used to loading in tangential direction, which can be the cause for the low tangential stiffness.

Additionally to the winching tests, the tested trees are modelled in a finite element software. The models are validated based on the measured strain and displacement results of the winching tests.

Figure 7.10 shows that the strain measurements on the single tree are comparable with the strain results in the model. Figure 7.11, however, shows that the measured deformation of the single tree is larger than the deformation found in the model, which suggests that the tree should be

modelled with a lower modulus of elasticity. Paragraph 7.3.1 explains that this is possible due to the change of elastic moduli within the tree's cross-section and over the tree's length in combination with a different area over which the strain and displacement measurements determine the elastic moduli. The strain results indicate the elastic moduli solely at the location of the elastometers. The deformation results, on the other hand, are influenced by the entire range of elastic moduli over the tree's length up to the measurement location at the force application, which is higher up in the tree. It is therefore expected that to fit both the strain and deformation measurements best; the tree should be modelled with an inhomogeneous modulus of elasticity. Figure 7.12 shows that no clear trend is found in the development of the modulus of elasticity over the height. In future research, it would be wise to increase the number of measurement points and the number of trees to gain a more thorough understanding of this development.

Furthermore, it is recommended to measure the displacements of the tree at several heights, to get a better insight into the relationship between the local and global elastic moduli. This could be carried out by filming the winching test with a fixed camera. Later, the tree deformation can be measured from the footage by comparing it with a reference length.

The model of the radially pulled cross-connected trees is a good representation of reality. This statement is based on figure 7.13 and figure 7.14 in which both the strain and displacement measurements fit the finite element model. Modelling the connection rigidly is in accordance with paragraph 5.4, which describes that a connection behaves rigidly once common rings have grown, which is the case in the cross-connection.

In the tangentially pulled cross-connected trees, the measured transfer of strains from the pulled tree to the connected tree is larger than seen in the model. An explanation for this incongruity is illustrated in figure 7.15, which shows an uneven distribution of lost parenchyma cells within the connection. It is recommended to do more research into the influence of these lost parenchyma cells on the behaviour of the connection and include potential results in the finite element model.

In the tangentially pulled parallel-connected trees, the measured strains coincide well with the strains found in the model. Modelling the trees with a fully rigid connection is thus a good representation of reality.

The measured deformations when the cross-connected and parallel-connected trees are pulled in tangential direction, do not coincide with the deformation results of the model. The cross-connected trees deform five to six times more than the corresponding model, and the parallel-connected trees deform about five times more. One explanation for this incongruity is the lift of the winch, as has been discussed in paragraph 7.2.3. By correcting the measured deformation based on the estimated winch lift, the deformation diminishes. However, the cross-connected trees still show a deformation three times larger than resulting from the model. The parallel-connected trees still show a deformation two times larger. It is not possible to deduct the cause for this effect from the gathered data. However, as is explained in paragraph 7.2.3, cracks in the bark indicate that the trees are not often subjected to a tangential force. Potentially, trees have diverging characteristics in directions that are not often subjected to loads, which are not included in the model. It is recommended to carry out more research into this phenomenon.

9.1.2 Application to Wonderwoods

The technique of using living trees as structural elements has been applied to the *Wonderwoods* case study by creating a design in which trees bear the loads of plant containers. From the tree species selected for the original *Wonderwoods* design, Field Maples are the best applicable as they are tolerant to the growth conditions in a vertical forest. Furthermore, they easily inosculate, and

they contain satisfactory material properties, particularly perpendicular to the grain. If the location of *Wonderwoods* changes, other tree species could be advantageous for the design.

The design shows that both single trees and cross-connected Field Maple trees can bear loads of the plant containers. Adequate systems are available to create a connection between the trees and the plant containers. Both designs failed when they were modelled with a root system stiffness as found by winching the airpot Elm tree. It can be argued that the root system of the Field Maple is stiffer as this tree species is chosen for its quality to resist high wind forces due to its root structure. Furthermore, Field Maple is listed by the *BuGG* committee as suitable for placing on buildings with great height, while Elm is not (Beining, 2020). Despite these qualities, the small root space results in a high uprooting risk. It is advised to mitigate this risk by anchoring the root-ball.

There are three reasons why cross-connected trees are not favourable over a design with single trees. First, because the single trees can bear the plant containers after 31 growth years, while it takes 43 years before the cross-connected trees can bear the plant containers. Second, due to the high risk of trees not creating suitable inosculations, and third, because of the possibility for space competition of interconnected trees.

The time it would take before the trees can bear the plant containers is long when the life expectancy for Field Maples on *Wonderwoods* is taken into account, which is 60 years. Several ideas are proposed to optimise the single tree design and reduce the required growing time. By reducing the size of the tree, the growth time reduces to 26 years. For the trees placed in the middle of the façade, where the wind loads are smaller, the time it takes to grow fully is further reduced to 20 years. For this situation, the possibilities of connecting a second plant container higher up in the tree are investigated. If the growth of a single main stem can be assured, this would be possible after 23 years.

The most significant time reduction could be accomplished by connecting the trees to a cable which relieves the trees from the extreme wind loads. An arborist should be consulted to help with designing this system.

9.2 METHODOLOGICAL LIMITATIONS AND IMPLICATIONS

This paragraph discusses the methods used, starting with the tests on the *Living Tree Pavilion* and Airpot tree and finishing with the application to *Wonderwoods*. Additionally, limitations are described, and suggestions for further research are given.

9.2.1 Living Tree Pavilion and Airpot Tests

Geometry characteristics of the *Living Tree Pavilion* trees were measured manually so that measurements can contain human errors. The results are compared with measurements of Borská (2018). Likely, the locations where she carried out the measurements are not exactly the same as in this research. Firstly, because she did not mention on which side of the tree she measured the length, which in this research is the side that faces the middle of the pavilion. Secondly, because the height of the ground level can change over time. This influences the trees' base height, which are reference points for the measurements in both Borská's and this research. For future research, it is advised to change the reference point to the concrete block in the middle of the pavilion and incorporate any height difference in comparisons and subsequent calculations.

The direction and amount in which a tree leans, based on the centre-of-gravity, is determined on eyesight. This is sufficient to get a rough indication for the ovalisation of trees in the leaning direction. However, the accuracy of this relationship can be improved, as it is challenging to find the tree's centre of gravity on eyesight. This could be achieved by measuring the total geometry of the tree and reconstructing this in a software program which calculates the centre of gravity. A vector, drawn between the centre of gravity and the stem base, then indicates the direction and amount in which the tree leans.

Winching tests were carried out in which the elongation on several locations of the tree was measured, giving insight into the strain distribution. Additionally, the displacement of the trees was measured. Finite element models of the trees were created on which the same winching load is applied. Results from the models were compared with the winching test results. The models have a modulus of elasticity parallel to the grain of 6.250N/mm², as is stated in the *Stuttgarter Festigkeitskatalog* (Wessolly & Erb, 2016) for Ash trees. Based on the reports of Nuijten (2011) and Borská (2018), it was assumed that the trees of the *Living Tree Pavilion* were Ash trees. The trees are, however, common Lime trees, which have a modulus of elasticity of 4.500N/mm² (Wessolly & Erb, 2016). Tree expert Dennis de Goederen (2020) knows from experience, that old common Lime trees fit the winching results better if they are modelled with an elastic modulus of 8.000N/mm². This is the elastic modulus of the parent trees of the hybrid common Lime, which are the large-leaved and small-leaved Limes (Wessolly & Erb, 2016). As no specific information on the stiffness of juvenile wood of Lime trees could be found, an average value of 6.250N/mm² has been assumed for the calculations.

The winching tests were carried out according to the standard procedure of *Pius Floris Boomverzorging*. In general, this method was applicable to this study. However, because the method is designed for large and old trees, some improvements can be made to make the method more suitable for young trees. The main difference between young and old trees is that young trees deform significantly more at a lower load. To stay within the elastic behaviour of trees, the winching test stops when a certain deformation is reached. This results in low force applications for young trees, which is not handled well by the equipment designed for older trees. This effect was noticeable in the force meter measurements. It showed fluctuating results, as the applied force was in a range of 0,2 to 1,2kN, while the force meter had an accuracy of 0,3kN. The influence of this inaccuracy is diminished by applying the average of the force development to the finite element model, as is explained in paragraph 6.4.

In contrast to the force meter, the inclinometers and elastometers had sufficient accuracy for measuring the rotation and strain of young trees. The inclinometer accuracy of 0,005° was precise enough for the rotation measurements, which were in a range of 0,1 to 0,6°. Except for one poorly placed elastometer, the elongation measurements were within a range of 40 to 2000 μm, for which the elastometer accuracy of 1μm was acceptable.

Another improvement for applying the winching tests to younger trees is to make sure the winch does not get lifted, for example by anchoring it to the ground. As explained in paragraph 7.2.3, lifting the winch influences the measurements of the deformation and the angle of the force. The influence on the deformation measurements is significant, as was explained in the discussion of results. The finite element model does not include the change in force angle since the height of the winching lift was not measured during the experiment. Estimations reveal that the effect is minor. The largest winch lift occurred during the tests of the parallel-connected trees. With an estimated winch lift of half a meter, the angle of the force changes from 19,2° to 13°. This increases the horizontal component of the force angle with only 3,2%.

After analysing the 'translation' of real trees to trees in the finite element model, several improvements were found. Firstly, the geometry measurements were carried out manually. Although performed carefully, this method contains inaccuracies and human errors. Carrying out the coordinate measurements (radial distance, tangential distance, and height) was sometimes difficult due to terrain inaccuracies. Furthermore, the geometry is measured discrete, with intervals of 10cm, instead of continuous. This is argued to be sufficient for this study. For future research, the accuracy could be improved by laser scanning the entire tree geometry, which should be done when the tree does not carry leaves.

A second inaccuracy in the 'translation' process, is the fact that the elastometers were placed in the same line as the force using purely eyesight, instead of a more exact method. The estimated deviation for this method is 2cm. In the finite element model, the strains are extracted at the locations of the elastometers. A 2cm deviation at this position in the finite element model results in a 10-15% difference in strain results. It is advised for future research to either make sure the elastometers are placed in the line of force or to measure the deviation of the elastometer positions. Figure 9.1 illustrates a method in which a line directed towards the middle of the
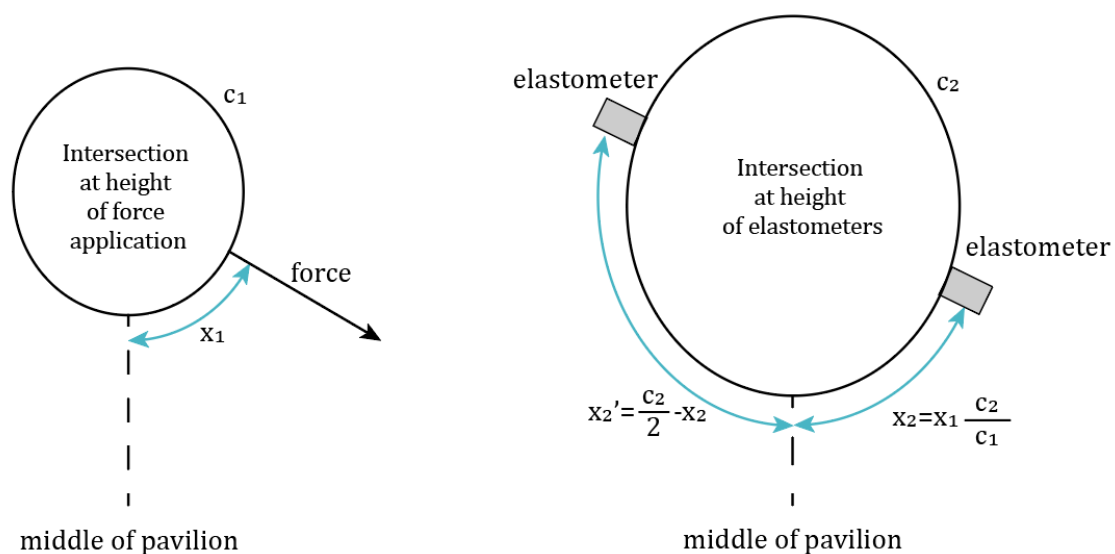
Figure 9.1 Method for determining the location of the force application and elastometers on the circumference of the tree at two different heights. The line directing the middle of the pavilion is used as a reference.

pavilion is used as a reference from which the location of the force and the elastometers can be determined on different heights of the tree.

For simplification, the finite element model has anisotropic and homogeneous material properties. Assigning inhomogeneous material properties would, in this stage of research, only increase the number of uncertainties, as no quantified course of material properties over the height and cross-section are available for (young) ash trees. Including such inhomogenisation improves the representation of reality.

By carrying out a geometrical linear analysis, no second-order effects are included in the finite element model. It is expected that the second-order effects are insignificant. This is based on research by Gatti and Ruck (2019) who state that the second-order effects can be ignored for trees smaller than 5m, as the moment induced by the overhanging mass is small compared to the moment caused by the horizontal load.

Lastly, the model geometry is created with steps of 10cm, resulting in sudden changes of slope in the model, especially around the connection. This gives stresses that would not appear in real trees, as these do not have such sudden changes in slope. It is suggested to improve the finite element models by creating a smoother tree surface.

9.2.2 Application to Wonderwoods
The structural behaviour of the trees in the *Wonderwoods* design is explored using simplified wireframe calculations and finite element models. These models follow the same procedure as used in the finite element models for the *Living Tree Pavilion* trees.

The growth behaviour of Field Maple trees, as described in paragraph 8.5, is based on experience data from a tree nursery. Based on their observations, a good estimate is made of the time required for the trees to be large enough to bear the desired loads. If the design is to be completed, more research should be carried out on the growth behaviour of Field Maples in tree containers which are placed on a great height. As a starting point, the growth of trees on completed vertical forests could be investigated, for example, from *Bosco Verticale* in Milan.

The material properties of Field Maples are estimated based on three different procedures from which the least favourable value for each property is chosen. This gives a conservative structural result which is believed to be necessary due to the many uncertainties of tree growth and material properties. Suppose tests could be carried out on both younger and older Field Maples. In that case, more realistic material properties, changing over the lifetime of a tree, could be used in the structural calculation.

The finite element models show peak stresses at the inosculations and the location of the non-living connections. The former can be explained by the sudden change in slope, which would not be the case in real trees. For future research, it is advised to model the connection more realistically by performing more geometry measurements around the connection and smoothing the surface. The peak stresses around non-living connections result from the force transmission from rigid elements (the non-living connections) to the solid (the tree). This gives some discrepancy in stress, which is partly solved by the *connecting cross* as recommended by the finite element software. Because of the small area of peak stresses, these are not considered in the breaking checks. To avoid such peak stresses, rigid elements should not be combined with solids in one finite element model.

10 CONCLUSIONS AND RECOMMENDATIONS

10.1 CONCLUSIONS

This research aimed to expand knowledge on the topic of using living trees as structural elements. In this context, three systems are investigated: single trees, cross-connected trees, and parallel connected trees. The latter two consist of two trees, connected either crosswise or parallel to one another by self-growing inosculations.

To investigate the effect of using interconnected trees as structural elements in comparison to single trees, the following sub-questions are answered:

What is the botanical behaviour of (interconnected) trees?

When building with living trees, it is crucial to respect their natural growth behaviour. Hindering the growth will not give the desired structural capability. The most important mechanism to understand is the optimisation of shape by secondary growth, which strengthens the tree at the locations with the highest stresses. If a tree is supported, it incorporates this support in its structural scheme, minimizing secondary growth. To prevent this, movement should not be restricted. Additionally, trees should not deviate much from their natural upright position.

If interconnected trees are used, both trees must be equally triggered to grow. Else, the risk arises that one of the trees takes over the functions of the other, hindering the growth of the other tree. The inner workings into the way that the connection is formed are still up for debate. First, the bark tissue in the trees merge, which is followed by the xylem tissue. Once common growth rings are created, the inosculation has mechanical strength.

What is the structural behaviour of (interconnected) trees?

A tree can fail either by uprooting or breakage of the stem or branches. The most critical loads acting on a tree are due to wind, precipitation, and self-weight. Additionally, dynamic loads and diverging tree shapes can give stresses in the tree.

The mechanical properties of living trees could be compared with standardized properties for structural timber. The most remarkable difference, however, is that a living tree can adapt to the applied loads. Furthermore, living trees contain a higher moisture content than structural timber which causes lower material properties. An advantage of this is that a tree, subjected to compression, shows plastic deformation before failure. Other essential aspects of living trees are their inhomogeneous material properties that change over their lifetime.

There is not much known about the strength of self-growing connections. If assumed that they behave similarly to branch and stem unions, then their strength depends on the interlocking of fibres and the inclusion of bark. A well-grown connection is likely to be as strong as the branches or stem around it. Winching tests, carried out on interconnected trees, show a good exchange of stress from the pulled tree, via the inosculation, to the connected tree.

How could (interconnected) trees be structurally modelled?

In this research, a method is proposed on how to model trees and, if applicable, their connection. The trees are modelled as 3D solids in a finite element software, which allows for including changing circumferences over the tree's height and gives insight in the distribution of stress in trees and around connections. Interconnected trees are first created as two intersecting separate solids. Then, one compound solid is created, which behaves as a single solid.

This method is proven to be adequate for single trees as the results from the model match with the winching test results. Similarly, this method is proven to be adequate for modelling out-of-plane pulled cross-connected, and in-plane pulled parallel-connected trees. For in-plane pulled cross-connected trees, more research is needed to determine whether diverging tree characteristics, in a direction rarely subjected to load, could explain the discrepancy in measured and modelled behaviour.

How could (interconnected) trees be used as structural elements in Wonderwoods?

A design is proposed in which either single or cross-connected trees are carrying the plant containers in *Wonderwoods*. The design includes an underground anchoring system and connections between the trees and the plant containers. The version with the single tree is favourable because of the shorter time needed for the tree to be able to function as a structural element. Additionally, there is no risk of a single tree competing for space or creating unsuitable inosculations. Several promising adjustments have been proposed to reduce the number of years needed before the single trees can bear the plant containers, among which a reduction of the tree size, the location of the trees on the building and the use of a cable to transfer extreme wind loads.

With the answers on the sub-questions, the main question can be answered:

What is the effect of using interconnected trees as structural elements compared to using single trees?

Interconnecting the trees has botanical implications as the trees deviate much from their natural upright position. Furthermore, interconnected trees can compete for space, and the risk of not creating suitable inosculations is high. These implications are not related to single trees.

Structurally, no signs of increased stability of interconnected trees were found during winching tests, because cross- and parallel-connected trees deformed more than a single tree. Furthermore, finite element models show that interconnected trees have an unfavourable force distribution. When the same force is applied, cross-connected trees experience larger stresses than single trees. This is the result of a concentration of bending moments higher up in connected trees as opposed to single trees. Because of the smaller cross-section, higher stresses are measured at this point.

Based on this research, it can be concluded that a system of interconnected trees as structural elements is not favourable over a system of single trees.

10.2 Recommendations

In this last paragraph, we will provide a list of recommendations for future research based on our findings.

This research provided the groundwork on how to approach a living tree design. Three subjects came up, regarding the structural behaviour of living trees, for which we recommend carrying out more research. The first is a quantification of change in mechanical properties within a stem and over the height of a tree. This could be researched by performing mechanical tests on wood pieces, extracted from several locations within one tree. Additionally, the winching deformation on several heights of the tree could be studied by filming the winching tests and measure the deformation from the footage.

A second subject is a quantification of change of mechanical properties over the lifetime of a tree, which could be investigated by performing winching on trees of the same species with a different age. Thirdly, it is recommended to do more research on the mechanical properties of inosculations, focussed on their breaking strength and their rigid versus hinged behaviour. For this, mechanical laboratory tests are advised on cut inosculations.

The tree characteristic measurements gave indications that inosculations and the leaning of a tree influence the secondary growth. To investigate this relationship more thoroughly, we recommended performing measurements on a larger number of trees and increase the accuracy of determining the centre-of-gravity, by measuring the total geometry of the trees.

Additionally, in this research, only one possibility of using living trees as structural elements was investigated, namely by letting them bear the plant containers in *Wonderwoods*. To explore the full capability of threes, we recommend searching for other possibilities. One way is to choose other case studies in which living trees are subjected to a variety of circumstances and loads. Another way is to take the trees as a starting point for the design, instead of trying to use the trees as traditional structural elements. This could open new possibilities. It can, for example, turn out that a system of three or more interconnected trees has favourable qualities over a system of two trees, to which this research is limited.

The scope of this research did not include costs and environmental impact calculations. However, we recommend incorporating these in a next design stage, when considering the value for implementing a living tree design in the building industry.

Lastly, this research focused on vertical forests. Using these trees as structural elements is challenging due to the harsh environment regarding wind loads and root space. To start with a more realistic case, we recommend exploring the structural possibilities of living trees that are standing in open soil, for example, for housing or low-rise buildings. This allows for gathering practical insights that can be incorporated in vertical forest designs.

11 BIBLIOGRAPHY

Altuntas, E., & Sekeroglu, A. (2010). Mechanical behavior and physical properties of chicken egg as affected by different egg weights. *Journal of Food Process Engineering, 33*, pp. 115-127. doi:10.1111/j.1745-4530.2008.00263.x

Bao, F. C., Jiang, Z. H., Jiang, X. M., Lu, X. X., Luo, X. Q., & Zhang, S. Y. (2001). Differences in wood properties between juvenile wood and mature wood in 10 species grown in China. *Wood Science and Technology*(35), pp. 363-375. doi:10.1007/s002260100099

Beining, W. (2020, May 13). Vragen groeigegevens en lijst daktuin bomen. (T. Lievestro, Interviewer)

Blaß, H. J., & Sandhaas, C. (2017). *Timber Engineering - Principles for design.* (R. Mort, Trans.) Karlsruhe: Karlsruher Institut für Technologie scientific publishing. doi:10.5445/KSP/1000069616

Boeri, S. (2016). *A vertical forest.* Mantova, Italy: Maurizio Corraini s.r.l.

Boomkwekerij Ebben. (2020, May 8). *Acer campestre, Veldesdoorn, Spaanse Aak*. Retrieved from TreeEbb: https://www.ebben.nl/nl/treeebb/accampes-acer-campestre/

Borská, H. (2018). *Living Tree Structures.* Prague: Czech Technical University in Prague.

Brahmatewari, S. (2020, January 9). Mail: Constructie The Valley. Amsterdam: VanRossum.

Cents, T. (2020, May 26). Afstudeeropdracht Wonderwoods. Amersfoort.

Cents, T., Heldens, L., Kloet, J. v., Kruijt, R., Pel, M., & Bouman, H. (2018). *Wonderwoods Tuinplan.* Amersfoort: Arcadis Landschapsarchitectuur & stedenbouw.

Cents, T., Heldens, L., Kloet, J., Kruijt, R., Hoogenraad, J., & Bouman, H. (2019). *Wonderwoods Tuinplan Definitief Ontwerp.* Amersfoort: Arcadis Landschapsarchitectuur & stedenbouw.

Ciftci, C., Brena, S. F., Kane, B., & Arwade, S. R. (2013). The effect of crown architecture on dynamic amplification factor of an open-grown sugar maple (Acer saccharum L.). *Trees, 27*(4), 1175-1189. doi:10.1007/s00468-013-0867-z

Ciftci, C., Kane, B., Brena, S. F., & Arwade, S. R. (2013, December 29). Loss in moment capacity of tree stems induced by decay. *Trees, 28*, pp. 517-529. doi:10.1007/s00468-013-0968-8

Clair, B., Fournier, M., Prevost, M. F., Beauchene, J., & Bardet, S. (2003). Biomechanics of buttressed trees: bending strains and stresses. *American Journal of Botany, 90*(9), pp. 1349-1356. doi:10.3732/ajb.90.9.1349

Coder, K. D. (1989). Should you or shouldn't you fill tree hollows? *Grounds Maintenance, 24*(9), pp. 70-73.

Covey, A. (2020, September 16). *Trees growing through objects*. Retrieved from Pinterest: https://nl.pinterest.com/pin/716213146960981802/

Dahle, G. A., James, K. R., Kane, B., Grabosky, J. C., & Detter, A. (2017, May). A review of factors that affect the static load-bearing capacity of urban trees. *Arboriculture and Urban Forestry, 43*(3), pp. 89-106.

Duchesne, I., Vincent, M., Wang, X., Ung, C.-H., & Swift, D. (2016). Wood mechanical properties and discoloured heartwood proportion in Sugar maple and Yellow birch grown in New Brunswick. *BioResources, 11*(1), 2007-2019.

Eckstein, R., & Gilman, E. F. (2008). Evaluation of landscape tree stabilization systems. *Journal of Arboriculture & Urban Forestry, 34*(4), 216-221.

Encyclopaedia Britannica. (2012). *Encyclopædia Britannica.* Retrieved March 6, 2020, from https://www.britannica.com/science/sieve-element#/media/1/543478/380

FCBA, Delft University of Technology, CIRAD. (2010, November 03). Simplified strength properties assessment for tropical hardwoods in view to CE marking - Conclusions. 1-4. Paris.

Forest Products Laboratory. (2010). *Wood handbook—Wood as an engineering material.* Madison: United States Department of Agriculture.

Freeworker. (2019, March 26). *Tree bracing: materials, types, models, manufacturers.* Retrieved October 14, 2020, from Freeworker Fachhandel für Baumpflege: https://www.freeworker.de/en/2019/03/26/tree-bracing/

Fulton, P. (2020, September 16). *Flexible supports.* Retrieved from The Treehouse Guide: http://www.thetreehouseguide.com/constructiontutorials/flexiblejoints.htm

Gardiner, B., Peltola, H., & Kellomäki, S. (2000, May). Comparison of two models for predicting the critical wind speeds required to damage coniferous trees. *Ecological Modelling, 129*(1), 1-23. doi:10.1016/S0304-3800(00)00220-9

Gatti, L., & Ruck, B. (2019). *Wonderwoods - tree dimensioning after wind test.* Milan: Laura Gatti Studio.

Glass, S. V., & Zelinka, S. L. (2010). Moisture Relations and Physical Properties of Wood. In R. J. Ross, *Wood handbook-Wood as an engineering material* (Centennial Edition ed., pp. 4.1-4.19). Madison: United States Department of Agriculture - Forest Service - Forest Products Laboratory.

Gozzi, J. (2011). *A tree-house village - Respect the environment.* Venezia: Universita Iuav di Venezia.

Green Max. (2018). *Root Ball Anchoring.* Retrieved from Green Max: https://www.greenmax.eu/en/rootballanchoring/

Haas, C., & Riet, R. (2018). *Memorandum Voorlopig Ontwerp.* Bilthoven: European Fire Protection Consultants N.V.

Hacke, U., & Sauter, J. J. (1996). Xylem dysfunction during winter and recovery of hydraulic conductivity in diffuse-porous and ring-porous trees. *Oecologia, 105*, pp. 435-439.

Hannema, K. (2019). Bos in aanbouw. *De Volkskrant*, V8-V9.

Hartsuijker, C. (2014). *Toegepaste Mechanica - Deel 2 Spanningen, vervormingen, verplaatsingen* (9 ed.). Den Haag: BIM Media B.V. Academic Service. ISBN: 90 395 0594 2.

Heräjärvi, H. (2004). Variation of basic density and Brinell hardness within mature Finnish Betula pendula and B. pubescent stems. *Wood and Fiber Science, 36*(2), 216-227.

Höpfl, L. (2020, February 2). Mail: Research structural use of living wood. Munich.

Hundert, M., & Pfeiffer, S. (2019). *Rethinking Wood - Future Dimensions of Timber Assembly.* Berlin, Germany: Birkhäuser. doi:978-3-0356-1689-7

James, K. (2003, May). Dynamic loading of trees. *Journal of Arboriculture, 29*(3), pp. 165-171.

James, K. R., Dahle, G. A., Grabosky, J., Kane, B., & Detter, A. (2014, January). Tree Biomechanics Literature Review: Dynamics. *Arboriculture and Urban Forestry, 40*(1), pp. 1-15.

Kane, B. (2014). Determining parameters related to the likelihood of failure of red oak (Quercus rubra L.) from winching tests. *Trees, 28*, 1667-1677. doi:10.1007/s00468-014-1076-0

Kane, B., Farrell, R., Zedaker, S. M., Loferski, J. R., & Smith, D. W. (2008). Failure mode and prediction of the strength of branch attachments. *Arboriculture and Urban Forestry, 34*(5), pp. 308-316.

Klaassen, R. (2018). *Houtvademecum.* Zwolle: Vakbladen.com & Smartwave. ISBN: 978 90 828 172 94.

Koninklijk Nederlands Meteorologisch Instituut. (2020, August 31). *Neerslag 29 KNMI weerstations*. Retrieved from Weerdata: https://weerdata.nl/

Koninklijke Ginkel Groep. (2018). *Wonderwoods Groeidocument.* Veenendaal: Koninklijke Ginkel Groep.

Kovryga, A., Schlotzhauer, P., Stapel, P., Militz, H., & van de Kuilen, J.-W. (2019). Visual and machine strength grading of European ash and maple for glulam application. *Holzforschung*, 1-15. doi:10.1515/hf-2018-0142

Kretschmann, D. E. (2010). Mechanical Properties of Wood. In R. J. Ross, *Wood handbook-Wood as an engineering material* (pp. 5.1-5.46). Madison: United States Department of Agriculture - Forest Service - Forest Products Laboratory.

Larson, P. R. (1965, December 01). Stem Form of Young Larix As Influenced by Wind and Pruning. *Forest Science, 11*(4), pp. 412-424. doi:10.1093/forestscience/11.4.412

Lehnebach, R., Beyer, R., Letort, V., & Heuret, P. (2018, January 23). The pipe model theory half a century on: a review. *Annals of Botany, 121*, pp. 773-795. doi:10.1093/aob/mcx194

Ludwig, F. (2012). *Botanische Grundlagen der Baubotanik und deren Anwendung im Entwurf.* Stuttgart: Institut Grundlagen Moderner Architektur und Entwerfen der Universität Stuttgart.

Ludwig, F. (2014). BAUBOTANIK - Designing Growth Processes. *Symposium "Form-Rule | Rule-Form 2014".* Innsbruck: University of Innsbruck.

Lundström, T., Jonsson, M., & Kalberer, M. (2007). The root–soil system of Norway spruce subjected to turning moment: resistance as a function of rotation. *Plant Soil, 300*(1-2), 35-49. doi:10.1007/s11104-007-9386-2

Mattheck, C. (1998). *Design in Nature - Learning from trees.* (W. Linnard, Trans.) Karlsruhe, Germany: Springer-Verlag Berlin Heidelberg GmbH. doi: 10.1007/978-3-642-58747-4

Mattheck, C., & Breloer, H. (1994). *The body language of trees - A handbook for failure analysis.* (D. Lonsdale, Ed., & R. Strouts, Trans.) London: HMSO. ISBN: 978-0117530676.

Miesbauer, J. W., Gilman, E. F., & Giurcanu, M. (2014). Effects of Tree Crown Structure on Dynamic Properties of Acer rubrum L. 'Florida Flame'. *Arboriculture and Urban Forestry, 40*(4), 218-229.

Millner, E. M. (1932). *Natural grafting in Hedera helix.* New Phytologist.

Neely, D. (1988). Wound closure rates on trees. *Journal of Arboriculture, 14*(10), pp. 250-254.

Nelson, P. (2020, September 16). *SL TAB*. Retrieved from Nelson Treehouse and Supply: https://store.beinatree.com/collections/treehouse-hardware/products/tab-treehouse-attachment-bolt

NEN. (2006, October 30). Houtconstructies - Hout met ronde doorsnede voor constructieve toepassingen - Eisen. Delft.

NEN. (2011). NEN-EN 1995-1-1+C1+A1:2011. *Eurocode 5: Ontwerp en berekening van houtconstructies*. Delft.

NEN. (2018). NEN-EN 384:2016+A1:2018. *Structural timber - Determination of characteristic values of mechanical properties and density*. Delft.

NEN. (2019). NEN-EN 1990+A1+A1/C2:2019 nl. *Eurocode: Grondslagen van het constructief ontwerp*. Delft.

Niklas, K. J. (1997, May). Size- and Age-dependent Variation in the Properties of Sap- and Heartwood in Black Locust (Robinia pseudoacacia L.). *Annals of Botany, 79*(5), 473-478. doi:10.1006/anbo/79.5.473

Niklas, K. J., & Spatz, H.-C. (2010). Worldwide correlations of mechanical properties and greenwood density. *American Journal of Botany, 97*(10), 1597-1594. doi:10.3732/ajb.1000150

Norminstituut Bomen. (2018). *Handboek Bomen.* Gouda: Norminstituut Bomen.

Nuijten, A. (2011). *Living Tree Buildings - A research into the possibilities and the load bearing capacity of living tree structures.* Delft: TU Delft.

Phillips, L. (2020, September 15). *Tree Stabilization*. Retrieved from Gibney Continuing Education: https://gibneyce.com/tree-stabilization---classics.html

Rais, A., van de Kuilen, J.-W., & Pretzsch, H. (2020). Impact of species mixture on the stiffness of European beech (Fagus sylvatica L.) sawn timber. *Forest Ecology and Management, 461*, 1-8. doi:10.1016/j.foreco.2020.117935

Ranta-Maunus, A. (2000). Bending and compression properties of small diameter round timber. *WCTE2000 Conference.* Whistler: Vancouver, B.C. : Conference Secretariat, 2000.

Ravenshorst, G. (2019). Failure mechanisms wood based on straw model. *CIE4110 Timber Structures and Wood Technology*. Delft.

Ravenshorst, G., Kuilen, J.-W., & Lanvin, J.-D. (2011). *Tropical hardwood species to be included in EN 1912 according to the simplified method.* Timber Structures and Wood Technology. Delft: Delft University of Technology.

Roloff, A. (2016). *Urban Tree Management for the Sustainable Development of Green Cities.* Tharandt, Germany: John Wiley & Sons, Ltd. ISBN: 978-1-118-95458-4.

Ruel, J.-C., Achim, A., Herrera, R. E., & Cloutier, A. (2010). Relating mechanical strength at the stem level to values obtained from defect-free wood samples. *Trees, 24*(6), 1127-1135. doi:10.1007/s00468-010-0485-y

Shigo, A. L., Dorn, D. E., & Lee, H. C. (1982). Selections of Maple and Birch Trees with High Resistance to Spread of Decay Associated with Wounds. *Tree Improvement and Genetics - Northeastern Forest Tree Improvement Conference*, (pp. 110-115). Durham.

Sinn, G., & Wessolly, L. (1989). A contribution to the proper assessment of the strength and stability of trees. *Arboricultural Journal, 13*, pp. 45-65.

Slater, D. (2016). An argument against the axiom of uniform stress being applicable to trees. *Arboricultural Journal, 38:3*, 143-162. doi:10.1080/03071375.2016.1202699

Slater, D., & Ennos, A. R. (2013). Determining the mechanical properties of hazel forks by testing their components. *Trees*(27), pp. 1515-1524. doi:10.1007/s00468-013-0898-5

Smiley, T. E., & Fraedrich, B. R. (1992). Determining strength loss from decay. *Journal of Arboriculture, 18*(4), 201-204.

Stefano Boeri Architetti. (2018). Design Drawings Architecture Z02 South and West Elevations. *WW -SBA-Z02-ZZ-DR-AR-4001*.

Stefano Boeri Architetti. (2019, December 18). *Vertical ForestING*. Retrieved from Stefano Boeri Architetti: https://www.stefanoboeriarchitetti.net/en/vertical-foresting/

Stefano Boeri Architetti. (2020, January 24). *wonderwoods*. Retrieved from Stefano Boeri Architetti: https://www.stefanoboeriarchitetti.net/en/project/wonderwoods/

Sterken, P. (2005). *A Guide For Tree-stability Analysis.* ISBN: 9090193774.

Stobbe, H., Dujesiefken, D., & Schröder, K. (2000). Tree Crown Stabilization with the Double-Belt System Osnabrück. *Journal of Arboriculture, 26*(5), 270-274.

Telgen, M. v. (2018). *Wonderwoods Utrecht, Uitgangspunten constructief ontwerp VO-fase Ontwerpdeel Boeri.* Rotterdam: Arcadis.

The Editors of Encyclopaedia Britannica. (2018, April 14). *Gravimetric analysis.* Retrieved from Encyclopaedia Britannica: https://www.britannica.com/science/gravimetric-analysis

Ursem, B. (2020, April 14). Afstudeerproject boom eigenschappen. (T. Lievestro, Interviewer)

Van Tieghem, P. (1884). *Traité de botanique.* Paris: Librairie F. Savy. doi:10.5962/bhl.title.33254

Viguier, J., Jehl, A., Collet, R., Bleron, L., & Meriaudeau, F. (2015). Improving strength grading of timber by grain angle measurement and mechanical modelling. *Wood Material Science and Engineering, 10*(1), 145-156. doi:10.1080/17480272.2014.951071

Vries, P. A., & Gard, W. (1998). *The development of a strength grading system for small diameter roundwood.* Delft: Delft University of Technology. Retrieved 3 17, 2020, from https://repository.tudelft.nl/view/tno/uuid:d05b38dc-2678-4d3d-bc97-c4f99c4cbec9

Wahlländer, V. (2020, September 17). *How to attach a treehouse platform safely in the tree without harming it?* Retrieved from The Treehouse Shop: https://thetreehouse.shop/how-to-attach-tree-house/treehouse-attachment-fastening-mounting/?lang=en

Wang, Q., Fu, W., Yu, S., Allan, L., Garg, A., & Gu, M. (2018). Mathematical model and case study of wind-induced responses for vertical forest. *Journal of Wind Engineering and Industrial Aerodynamics, 179*, 260-272. doi:10.1016/j.jweia.2018.06.007

Wessolly, L., & Erb, M. (2016). *Manual of Tree Statics and Tree Inspection.* (K. Faust, Trans.) Berlin - Hannover: Patzer Verlag. ISBN: 978-3-87617-143-2.

Wilson, B. (2017, August 18). *How to stake a newly planted tree & how long to leave it staked*. Retrieved September 15, 2020, from Wilson Bros Gardens: https://www.wilsonbrosgardens.com/staking-a-new-tree.html

Wilson, B. F., & Archer, R. R. (1977). Reaction Wood: Induction and Mechanical Action. *Annual Review of Plant Physiology, 28*(1), 23-42. doi:10.1146/annurev.pp.28.060177.000323

Winterman, C. (2020). *The description of anatomic features of self-growing connection in ficus trees to be able to determine mechanical properties.* Delft: TU Delft.

Wohlleben, P. (2016). *Het verborgen leven van bomen.* Amsterdam: Bruna. ISBN: 978-94-005-0732-6.

Appendix A   INVESTIGATED TREE SPECIES

In the following table, the tree species that have been considered in the design are listed, including the source, as is mentioned in paragraph 8.4.

Table A.1 Selection of tree species, longlist

		F. Ludwig	X. Wang	Wonder woods	Botanical Garden	B. Ursem
White willow	*Salix alba*	*Baubotanik*				
Black alder	*Alnus glutinosa*					
Silver birch	*Betula pendula*					
False acacia	*Robinia pseudoacacia*					
London plane	*Platanus acerifolia*					
Norway maple	*Acer platanoides*					
Common ash	*Fraxinus excelsior*				*Tree Pavilion*	
Common (summer) oak	*Quercus robur*					
Common hornbeam	*Carpinus betulus*					
European beech	*Fagus sylvatica*					
Olive	*Olea europaea*					
Fig	*Ficus benjamina*		CT scan			
Field maple	*Acer campestre*					
Willow oak	*Quercus phellos*					
European white elm	*Ulmus laevis*					
Juneberry	*Amelanchier lamarckii*					
Cornelian cherry	*Cornus mas*					
Linden	*Tilia*					
Evergreen oak	*Quercus iles*					
Poplar	*Populus*					

Appendix B   METHODOLOGY

B.1   STUDY AREA

<u>Overview photos</u>
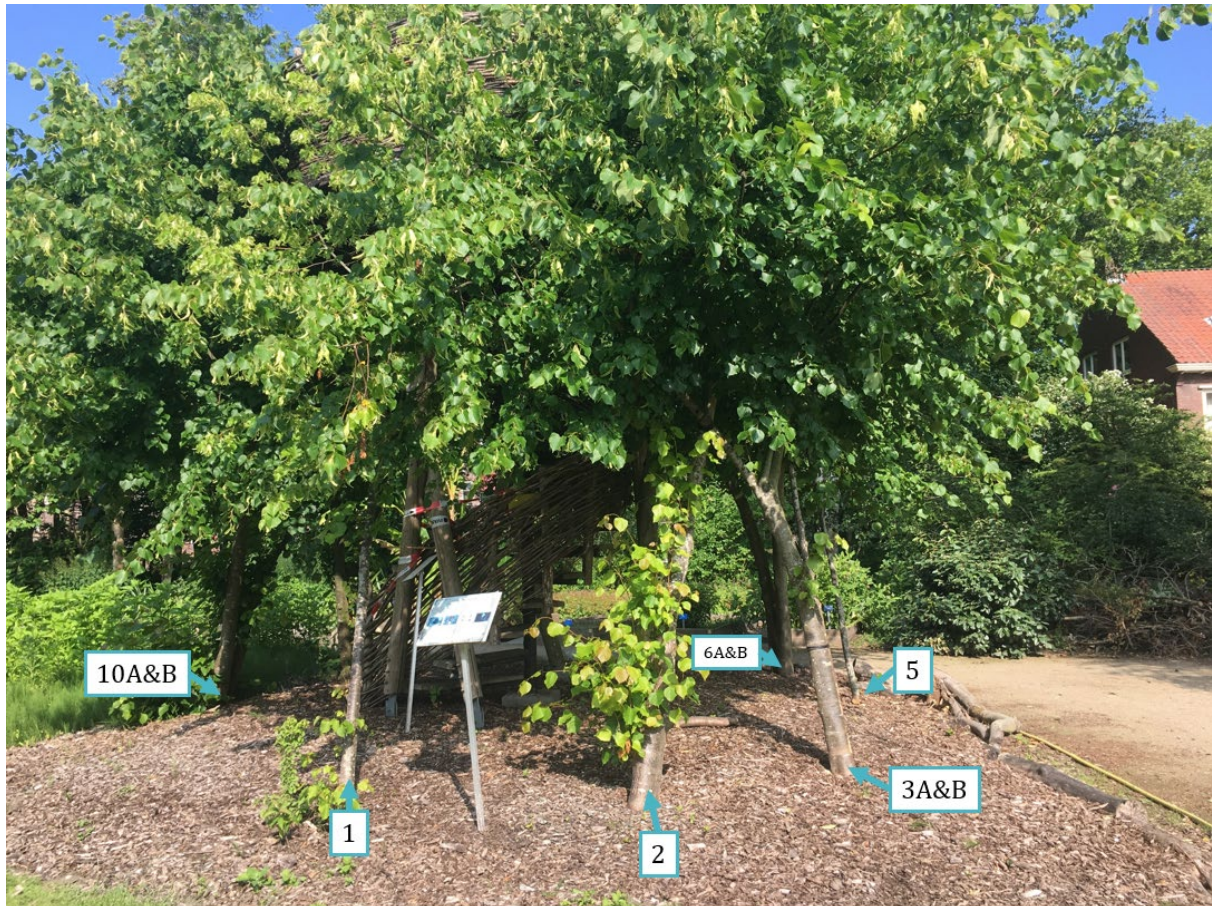
Figure B.1 Trees of the Living Tree Pavilion and their assigned names
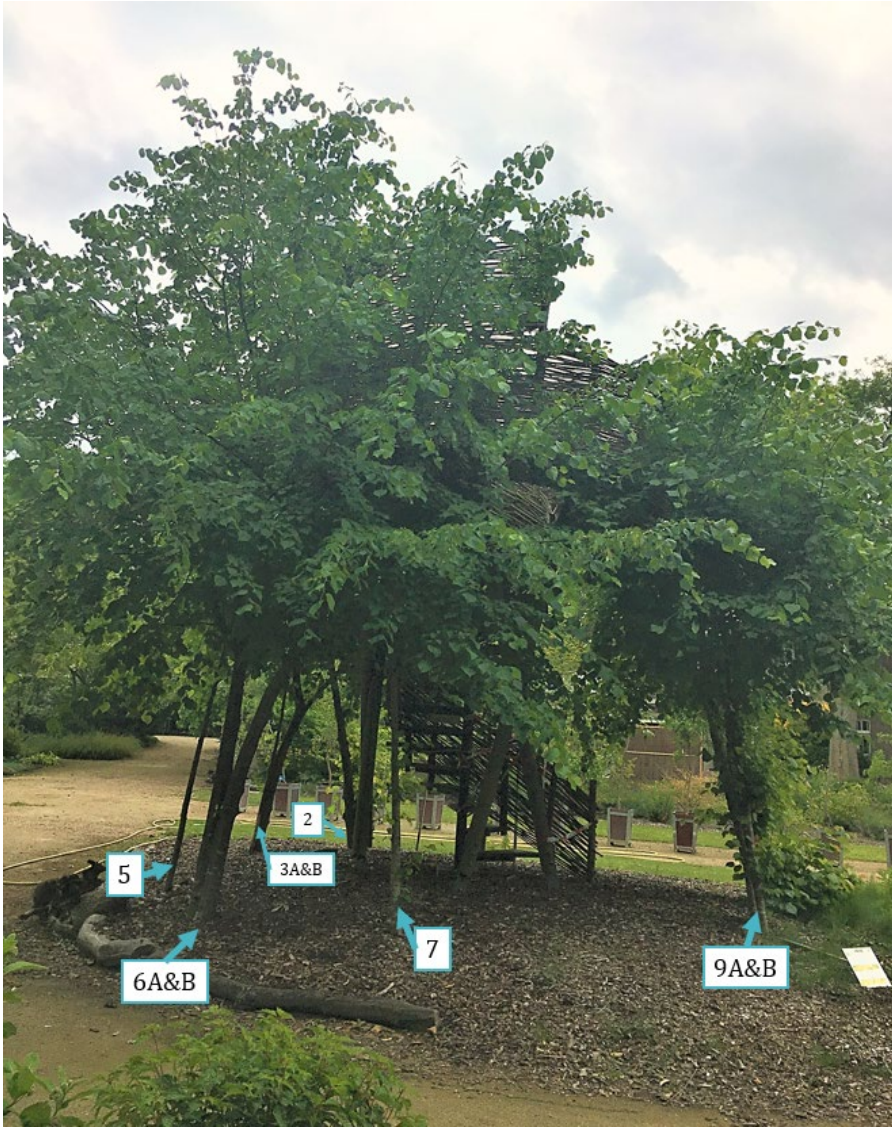
Figure B.2 Trees of the Living Tree Pavilion and their assigned names

Connections trees 2, 3A, and 3B
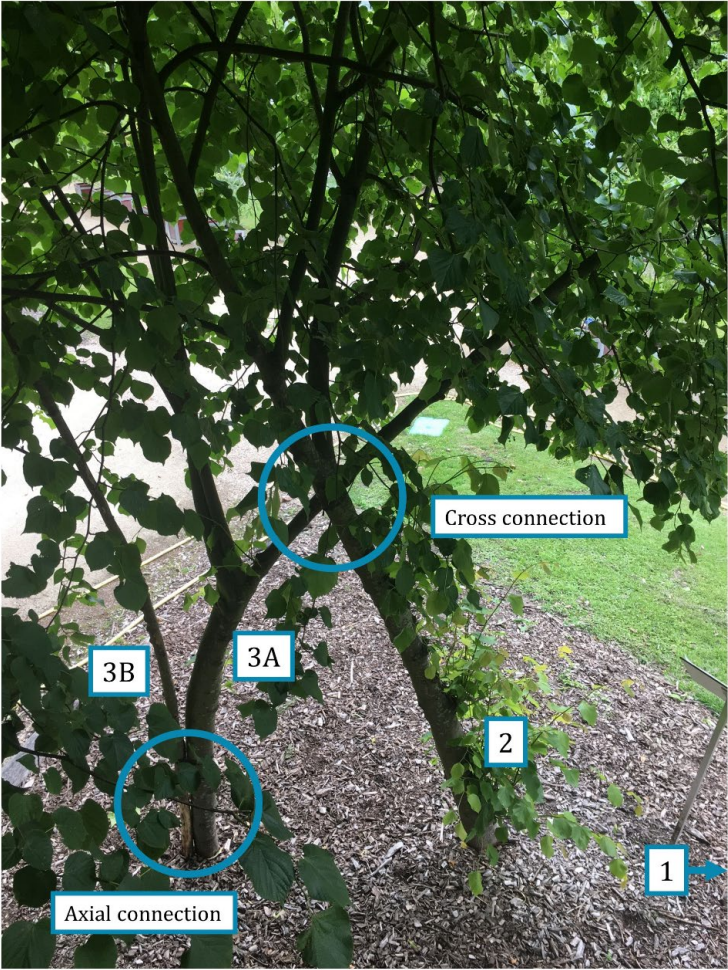
Figure B.3 Overview of connections between trees 2, 3A, and 3B

A more detailed picture of the cross-connection between tree 2 and 3A can be seen in Figure B.4. The trees show a change in bark texture around the connection, but the connection is not fully grown.

Between tree 3A and 3B signs of an axial connection could be seen, as shown in Figure B.5. This connection is not fully grown. Furthermore, it is visible that tree 3B is dead.

Figure B.4 Detailed photos of cross connection tree 2-3A

Figure B.5 Detailed photos of axial connection tree 3A-3B

Connections trees 6A and 6B
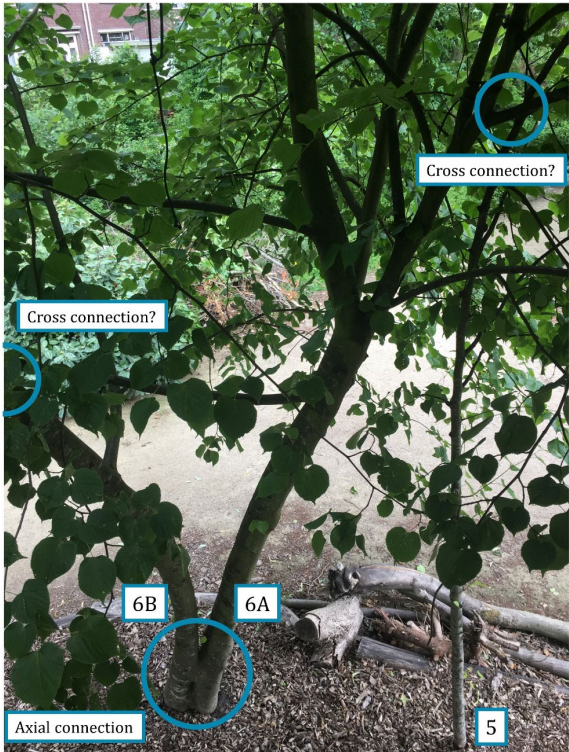
Figure B.6 Overview of connections between trees 6A and 6B

A detailed picture of the two axial connections between trees 6A and 6B can be seen in Figure B.7. These connections are fully grown.

Figure B.7 Detailed photos of axial connection tree 6A-6B

Connections trees 9A, 9B, and 10A
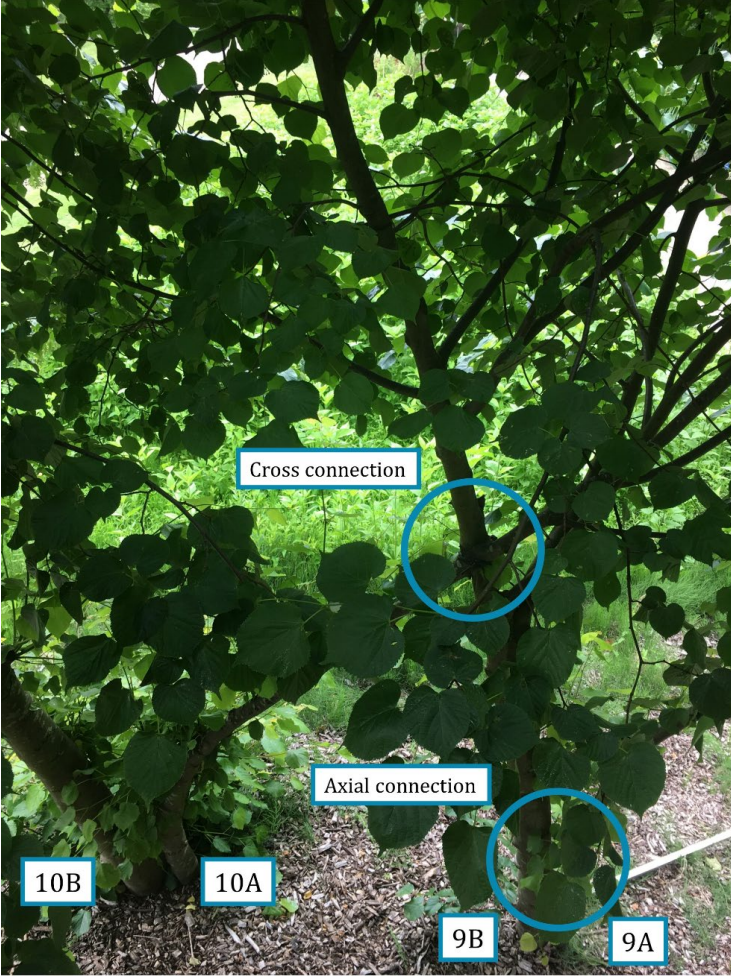
Figure B.8 Overview of connections between trees 9A, 9B, and 10A

Between 9A and 9B, the start of an axial connection is visible, see Figure B.9.

Figure B.9 Detailed view of axial connection tree 9A-9B

Pictures of the fully grown cross-connection of tree 9B and 10A can be seen in Figure B.10.

Figure B.10 Detailed photos of cross connection tree 9B-10A

B.2 MATERIALS USED

B.2.1 Tree characteristic measurements

Tree growth – circumference increase

- Sewing tailor measure ruler soft tape
- Waterproof marker

Connection growth

- Sewing tailor measure ruler soft tape, used for measuring the circumference of the stems below and above the connection, and for measuring the total circumference at the spot of the connection.
- Rope, used to wrap around the circumference of a connection.
- Steel retractable meter measuring tape, used to measure the length of the rope that was wrapped around the connections.

Influence of connection on stem circumference

- Sewing tailor measure ruler soft tape
- Waterproof marker

Ovalisation due to leaning of trees

- Calliper

Tree geometry as input for the finite element model

- Sewing tailor measure ruler soft tape
- Rope with weight
- Steel retractable meter measuring tape
- Calliper
- Triangle ruler
- Waterproof marker
- Two laths of 1.5m length
- Two thin laths, glued perpendicular to each other

B.2.2   Winching tests

Winching tests

- 3x *TreeQinetic* Elastometer (measuring the strain of the marginal fibres of a tree)
  - Resolution 0,1 µm
  - Accuracy 1 µm
  - Measuring range +/- 2 mm
  - Distance between measuring tips 198-202 mm
  - Diameter of measuring pins 2-4 mm
- 2x *TreeQinetic* Inclinometer (measuring the rotation of the root plate)
  - Resolution 0,002°
  - Accuracy 0,005°
  - Measuring range +/- 15°
- *TreeQinetic* Force meter
  - Resolution 0,01 kN
  - Accuracy 0,3 kN
  - Measuring range 0-40 kN
- Winch
- Steel cable
- *Nikon Forestry Pro* Laser hypsometer with a build-in inclinometer (measuring the angle of the cable)
- Communication Unit
- Portable Computer
- Soft ruler
- Ruler lath

Soil moisture content

- Shovel
- Plastic bags
- Waterproof marker
- Scale
- Aluminium containers
- Oven at 105°C

B.3 Winching test overview

B.3.1 Tree 10B – Single tree
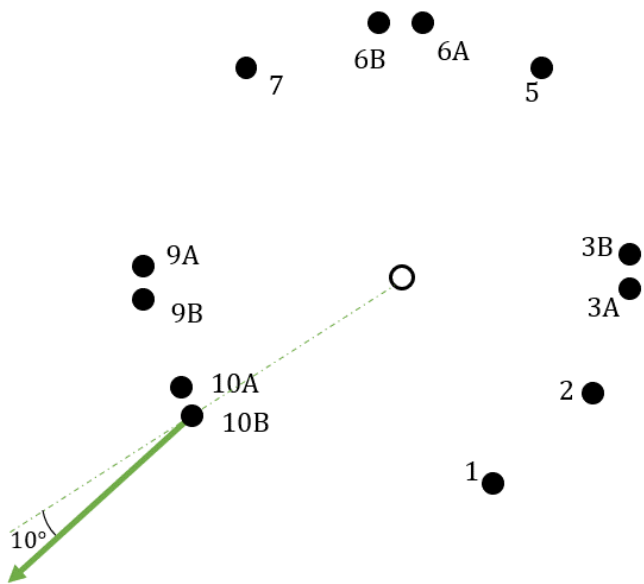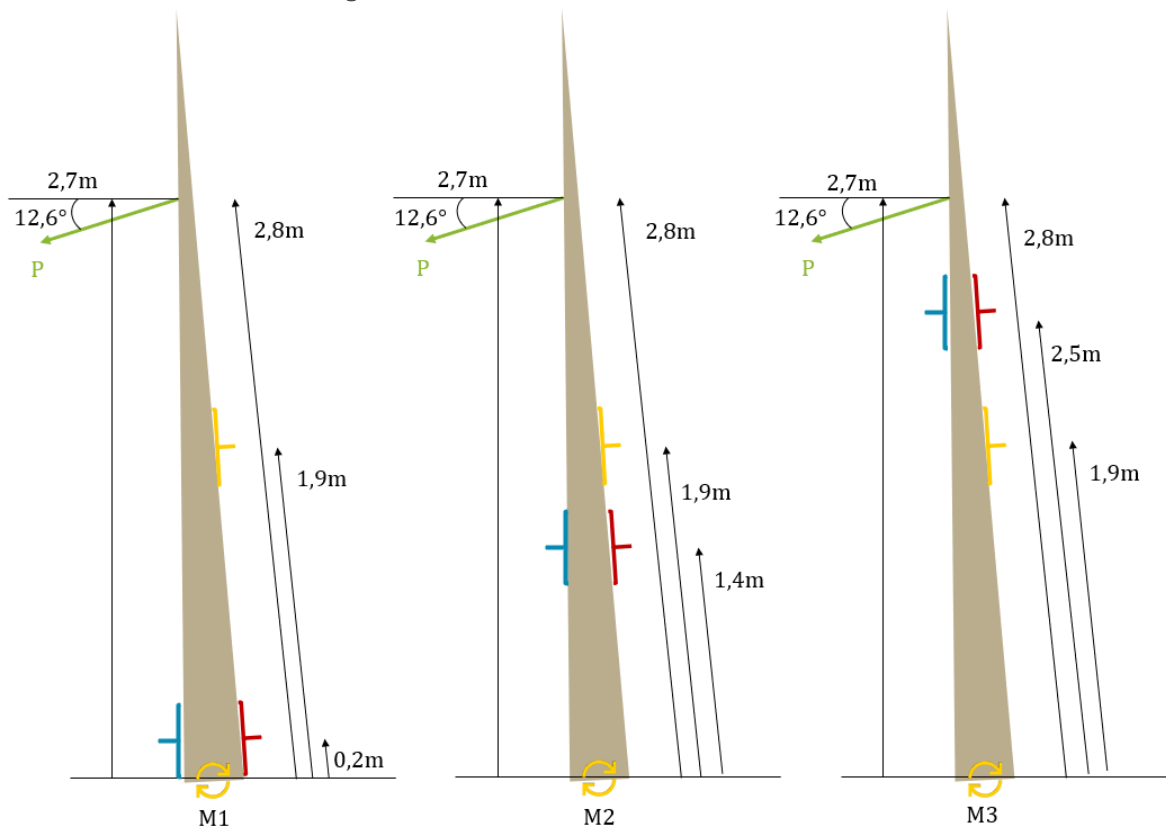
Figure B.11 Winching test set-up tree 10B. Top: Three measurement rounds and their elastometer locations. Bottom left: Top view with winching direction. Bottom right: Photo of tree 10B set-up.
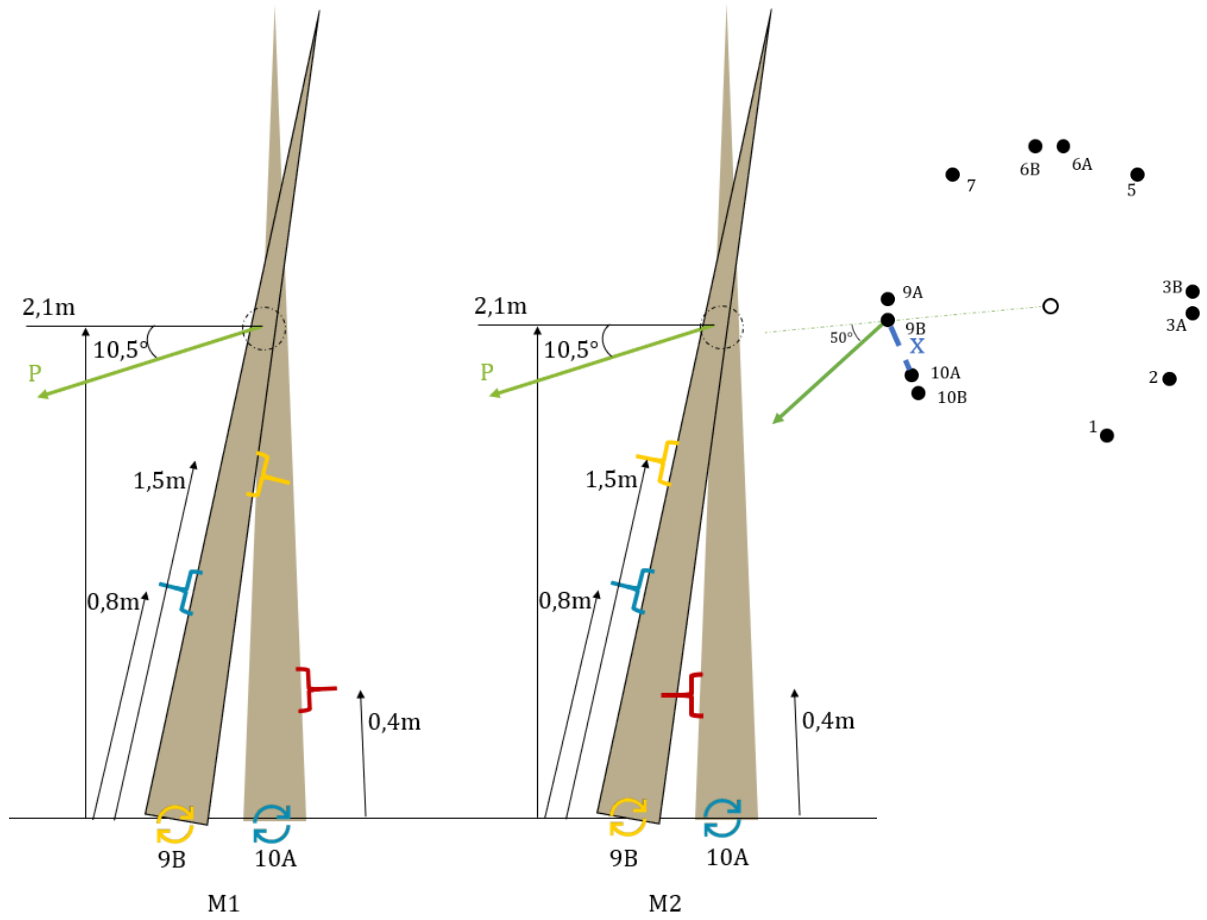
Figure B.12 Winching test set-up tree 9B-10A. Top left: Two measurement rounds and their elastometer locations. Top right: Top view with winching direction. Bottom left: Force is applied at the connection. Bottom right: Photo of set-up.

Note 1: Placed on tree 9B over the connection
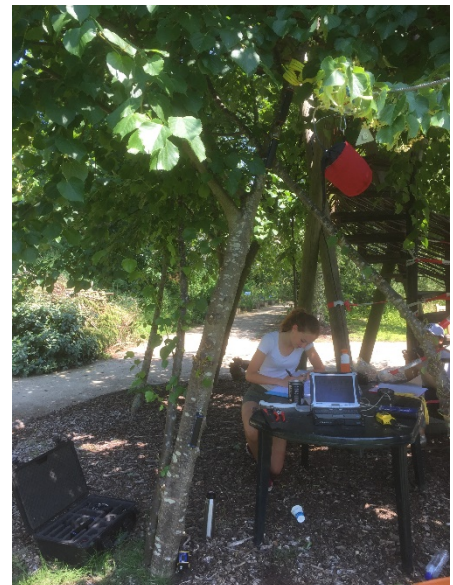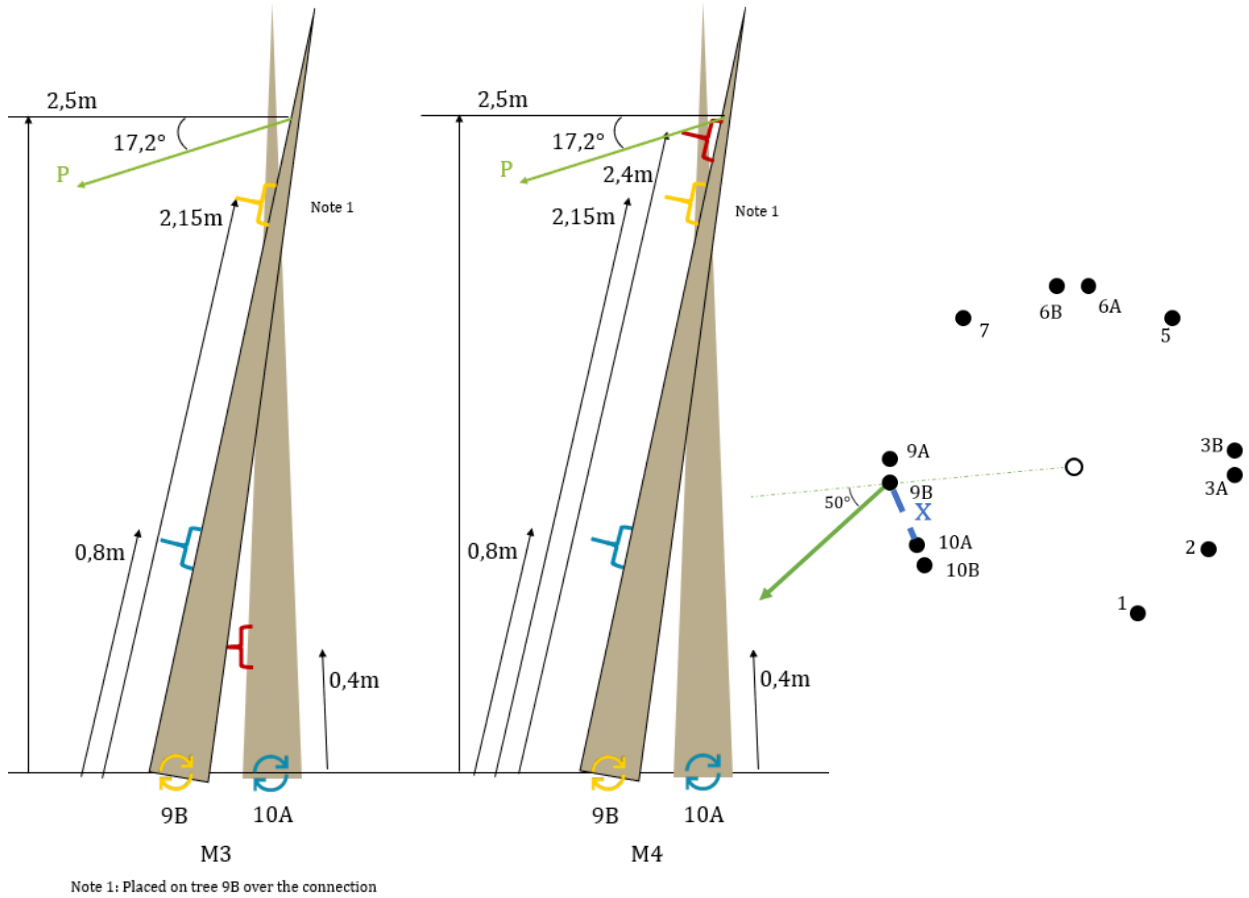
Figure B.13 Winching test set-up tree 9B-10A. Top left: Two measurement rounds and their elastometer locations. Top right: Top view with winching direction. Bottom left: Force is applied above the connection. Bottom right: Photo of set-up.
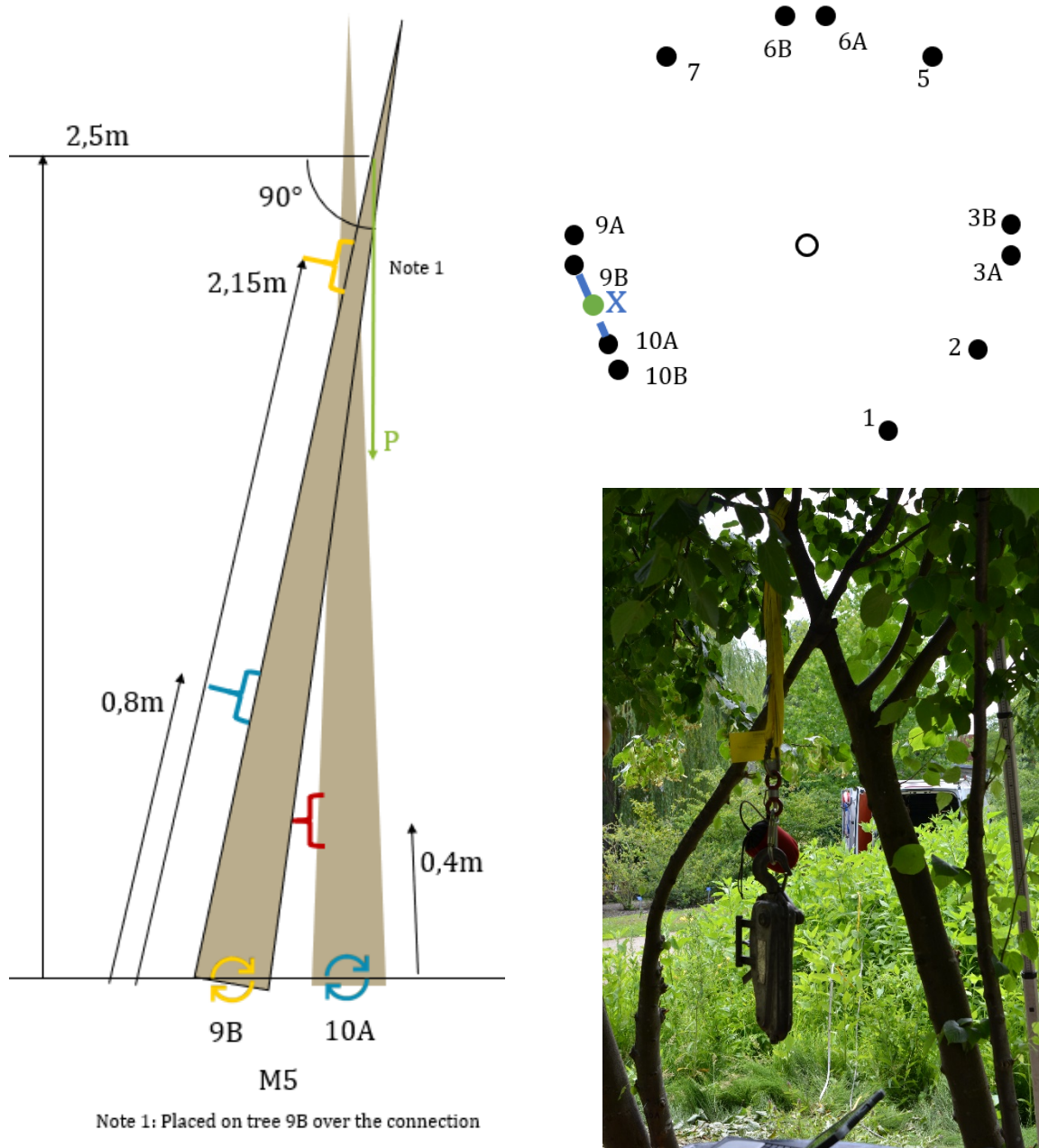
Figure B.14 Winching test set-up tree 9B-10A. Left: One measurement round and its elastometer locations. Top right: Top view with winching direction. Bottom right: Photo of set-up.
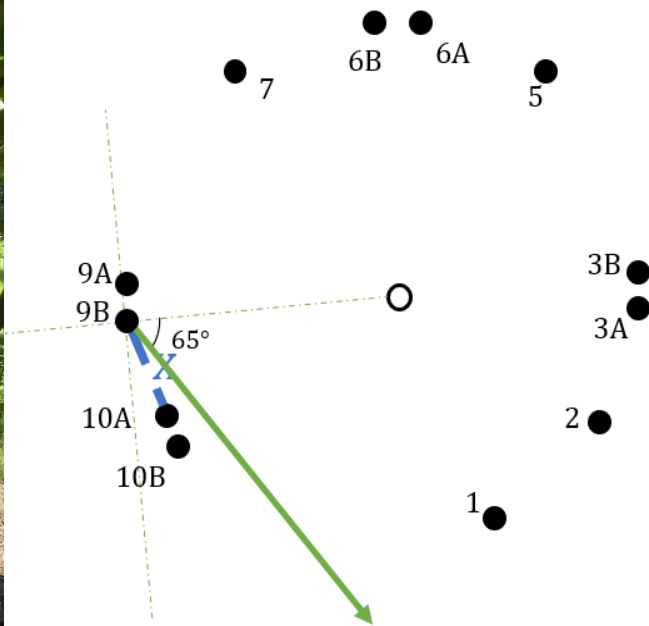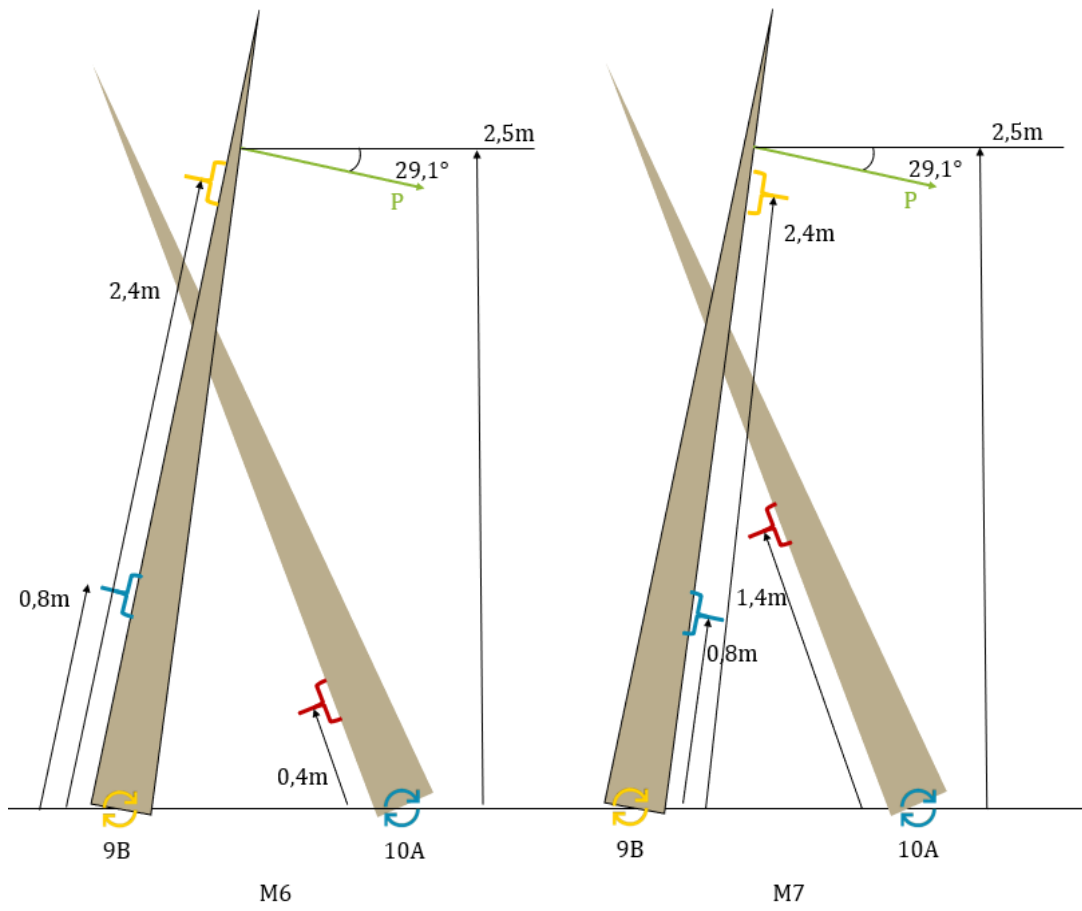
Figure B.15 Winching test set-up tree 9B-10A. Top: Two measurement rounds and their elastometer locations. Bottom left: Photo of set-up. Bottom right: Top view with winching direction.
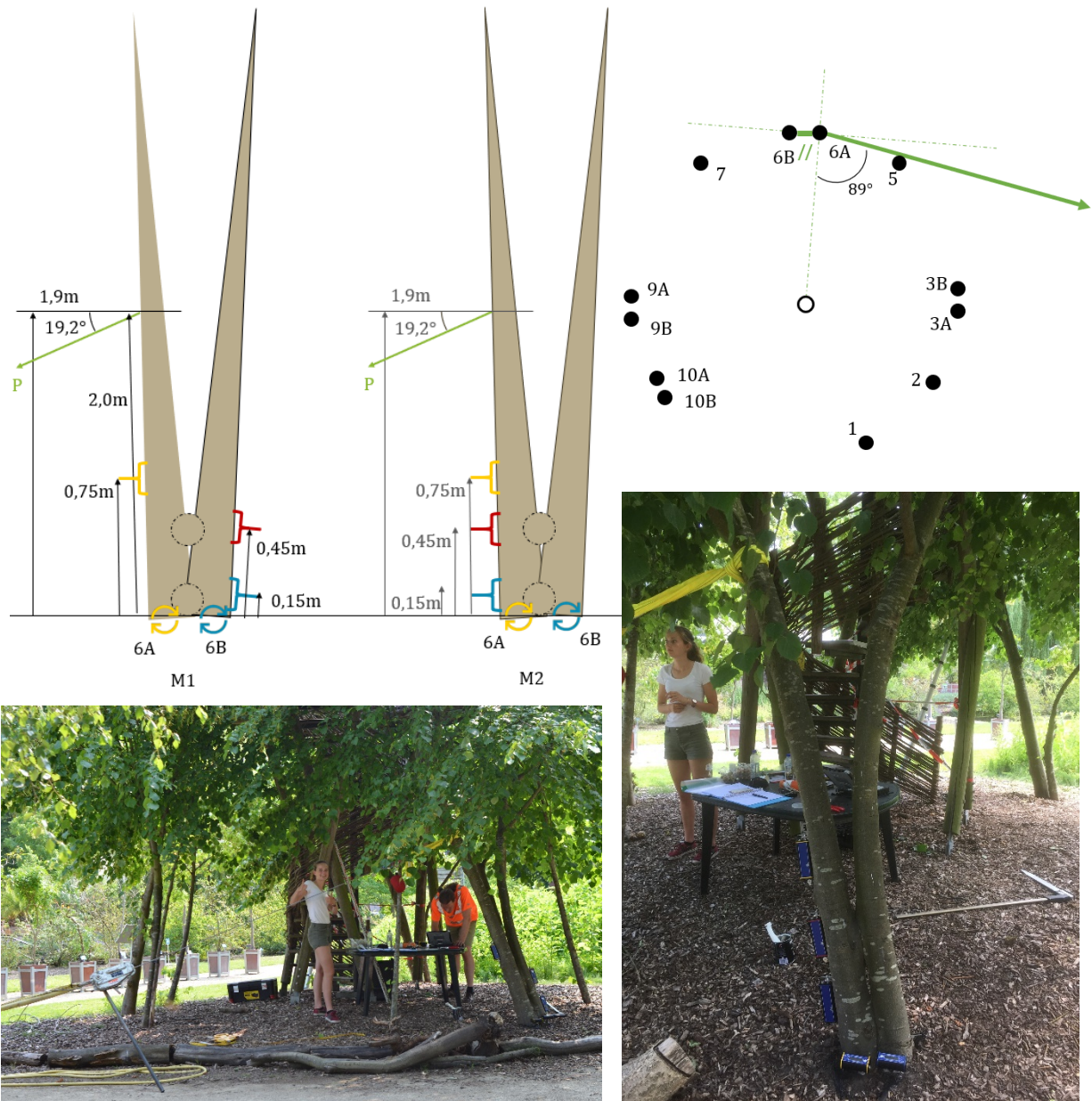
Figure B.16 Winching test set-up tree 6A-6B. Top left: Two measurement rounds and their elastometer locations. Top right: Top view with winching direction. Bottom left and right: Photo of set-up.
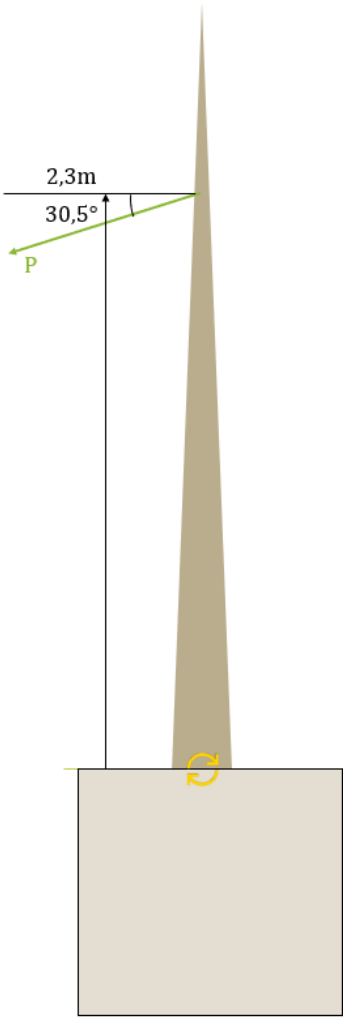
Figure Appendix B.17 Winching test set-up tree 6A-6B. Left: One measurement round and its inclinometer location. Right: Photo of set-up.

Appendix C   RESULTS

C.1   TREE CHARACTERISTIC MEASUREMENTS

C.1.1   Tree growth – circumference increase

Table C.1 shows the results of the circumference measurements in the right-most column; this is measured ten years after planting of the trees. Measurement results from Borská (2018) are listed in column 't=6 years'. The column 't=0 years' shows the prognosis of Nuijten (2011). If the circumference increased, it is coloured green; otherwise, it is coloured red.

Table C.1 Prognosis (Nuijten, 2011) and results of circumference [mm] of trees in Living Tree Pavilion at 1m length, measured 6 years after planting (Borská, 2018) and 10 years after planting. Red indicates a decrease in circumference; green indicates an increase.

		t=0 years [mm]	t=6 years [mm] (Borská, 2018)	t=10 years [mm]
Prognosis (Nuijten, 2011)	All trees	100	220	300
Results	Tree 1A	100	154	X
	Tree 1B	100	200	209
	Tree 2B	100	384	365
	Tree 2A	100	X	X
	Tree 3A	100	282	342
	Tree 3B	100	157	152
	Tree 4A	100	129	X
	Tree 4B	100	157	X
	Tree 5A	100	154	160
	Tree 5B	100	125	X
	Tree 6A	100	380	422
	Tree 6B	100	308	370
	Tree 7A	100	182	202
	Tree 7B	100	X	X
	Tree 8?	100	143	X
	Tree 8?	100	X	X
	Tree 9A	100	148	144
	Tree 9B	100	326	369
	Tree 10A	100	214	241
	Tree 10B	100	386	430
	Tree 11A	100	X	X
	Tree 11B	100	X	X
	Tree 12A	100	X	X
	Tree 12B	100	X	X

C.1.2   Connection growth

Winter 2011

Table C.2 shows the expected horizontal circumferences of the connections at the time of planting (Nuijten, 2011). The vertical circumference at the time of planting is 0mm.

Table C.2 Connections Living Tree Pavilion year 0 (Nuijten, 2011)

Level	Height [m]	Type of connection	Circumference [mm]
I	0-1.3	12 axial welds	92.5
II	2.8	6 axial welds and 6 grafts	46.25
III	4	12 axial welds	~0

Winter 2017, after 6 growing seasons

Table C.3 shows the measurements of Borská (2018), carried out in December 2017.

Table C.3 Results connection measurements 2017 (Borská, 2018)

| Tree | Joint type | Height [mm] | Circumference [mm] | | | | | |
| | | | Vertical | Horizontal | Stems below | | Stems above | |
					A	B	A	B
2-3A	Cross	1900	32	397	245	147	275	159
3A-3B	Axial	2	70	435	311	178	303	174
3A-3B	Axial	216	172	509	371	202	342	190
6A-6B	Axial	0	-	796	-	-	471	387
6A-6B	Axial	224	383	694	461	369	411	339
9B-10A	Cross	2100	242	281	119	169	181	125

Next to these fully grown joints, Borská mentioned some locations where the trees are connected by tape, but a connection has not grown yet. These are:

- 4A-4B, axial weld just above the ground
- 5A-5B, axial weld just above the ground
- 5B-6A, cross weld
- 6B-7, cross weld
- 8-9A, cross weld

Winter 2020, after 9 growing seasons

Table C.4 shows the measurements taken in March 2020. All sizes that have increased are coloured green. Decreasing measurements are coloured red. Values that are the same or were not measured in the previous measurements are coloured black.

Table C.4 Results connection measurements March 2020

| Tree | Joint type | Height [mm] | Circumference [mm] | | | | | |
| | | | Vertical | Horizontal | Stems below | | Stems above | |
					A	B	A	B
2-3A	Cross	1900	115	410	265	160	290	175
3A-3B	Axial	90	85	490	375	170	350	170
3A-3B	Axial	216	190	450	350	165	345	160
6A-6B	Axial	0	-	790	-	-	500	402
6A-6B	Axial	340	540	740	490	400	450	392
9A-9B	Axial	380	80	545	162	405	162	385
9B-10A	Cross	2100	330	270	130	175	200	115

<u>Summer 2020, during the 10th growing season</u>

Table C.5 shows the measurements taken in June 2020. After removing the rubber bands from connections 2-3A and 9A-9B, it was observed that these connections are not fully grown yet. Focussed is on measuring the connections that are fully grown.

Table C.5 Results connection measurements June 2020

Tree	Joint type	Height [mm]	Circumference [mm]					
			Vertical	Horizontal	Stems below		Stems above	
					A	B	A	B
2-3A	Cross	1900						
3A-3B	Axial	216						
6A-6B	Axial	0	-	800	-	-	500	414
6A-6B	Axial	340	580	740	495	414	485	405
9A-9B	Axial	380						
9B-10A	Cross	2100	340	295	145	205	210	120

C.2   WINCHING TESTS

Date: 25th June 2020

Location:
Botanische tuin TU Delft
Poortlandplein 6
2628 BM Delft

Winching tests performed by Dennis de Goederen, part of *Pius Floris Boomverzorging*. Soil tests performed by Marc Friebel, part of the laboratory of Geoscience TU Delft.

Weather conditions, by Royal Netherlands Meteorological Institute (KNMI), registration at Rotterdam Airport:

Daily mean windspeed	3,3m/s
Maximum hourly mean windspeed	6,0m/s (between 10.00 and 11.00 a.m.)
Average wind direction	127° (SE)
Daily mean temperature	24,3 °Celsius
Maximum temperature	30,9 °Celsius (between 13.00 and 14.00 p.m.)

No precipitation during the tests

The soil moisture content at 15cm below the surface tested with gravimetric method:

Around tree 10A	30,98%
Around tree 6A	16,74%
Around Airpot tree *Ulmus 'Clusius'*	27,70%

C.2.1   Tree 10B – Single tree
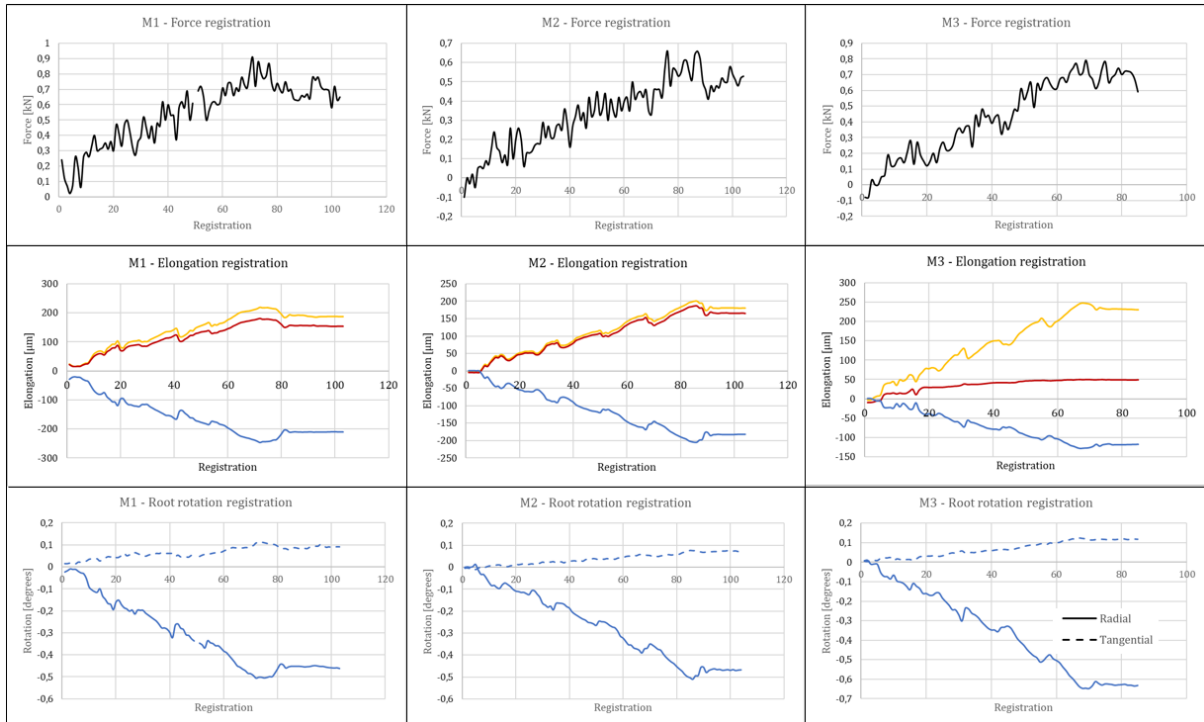
Figure C.1 Winching results tree 10B. Force in radial direction

Shortening of winching cable M1: 0,23m
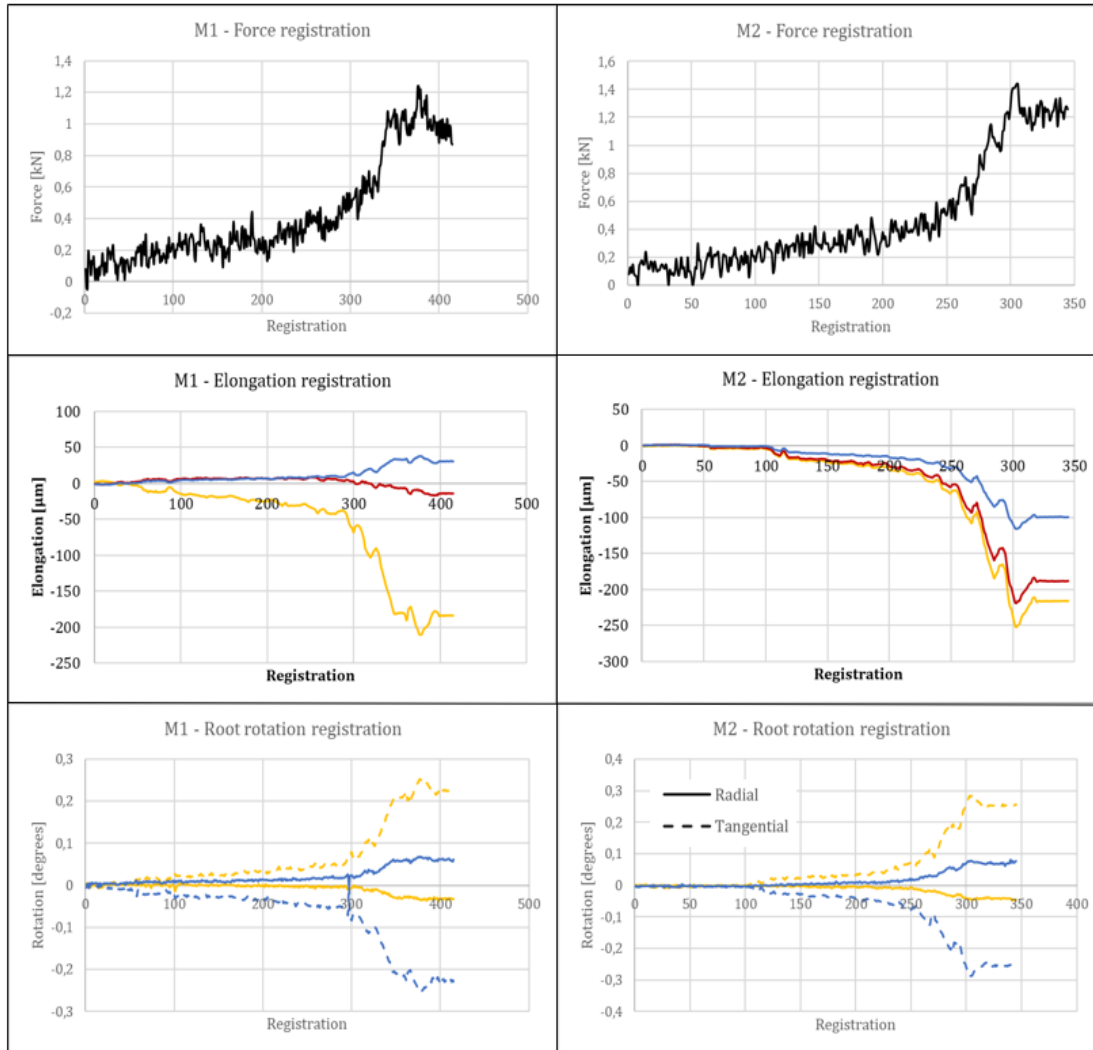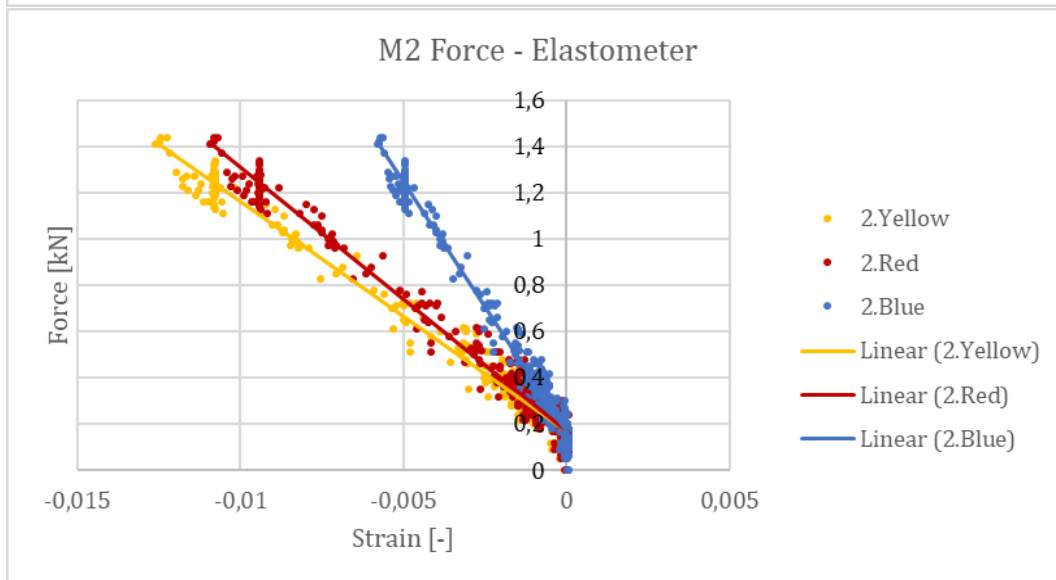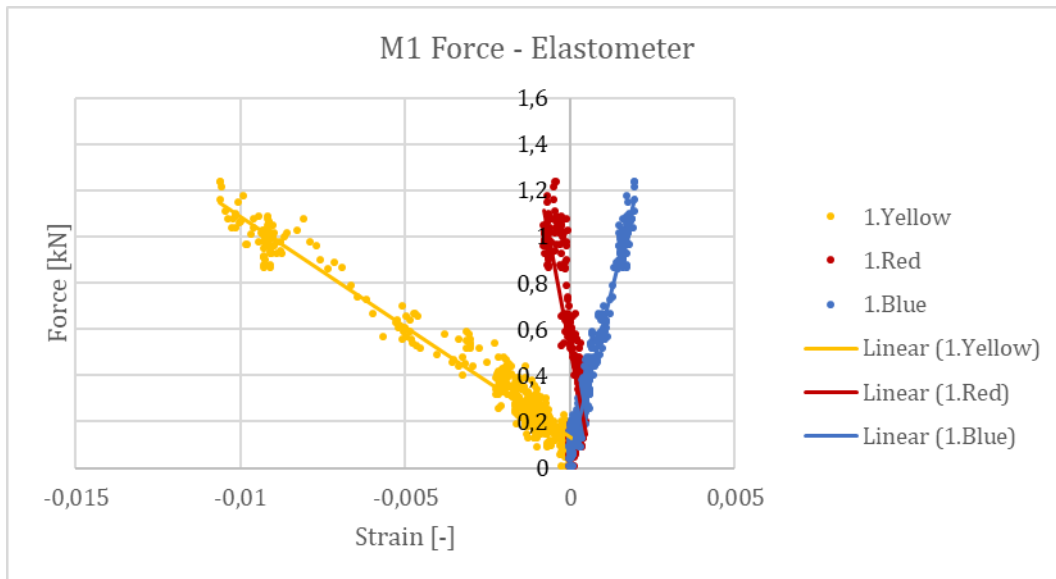
Shortening of winching cable M2: 0,26m

Shortening of winching cable M3: 0,30m
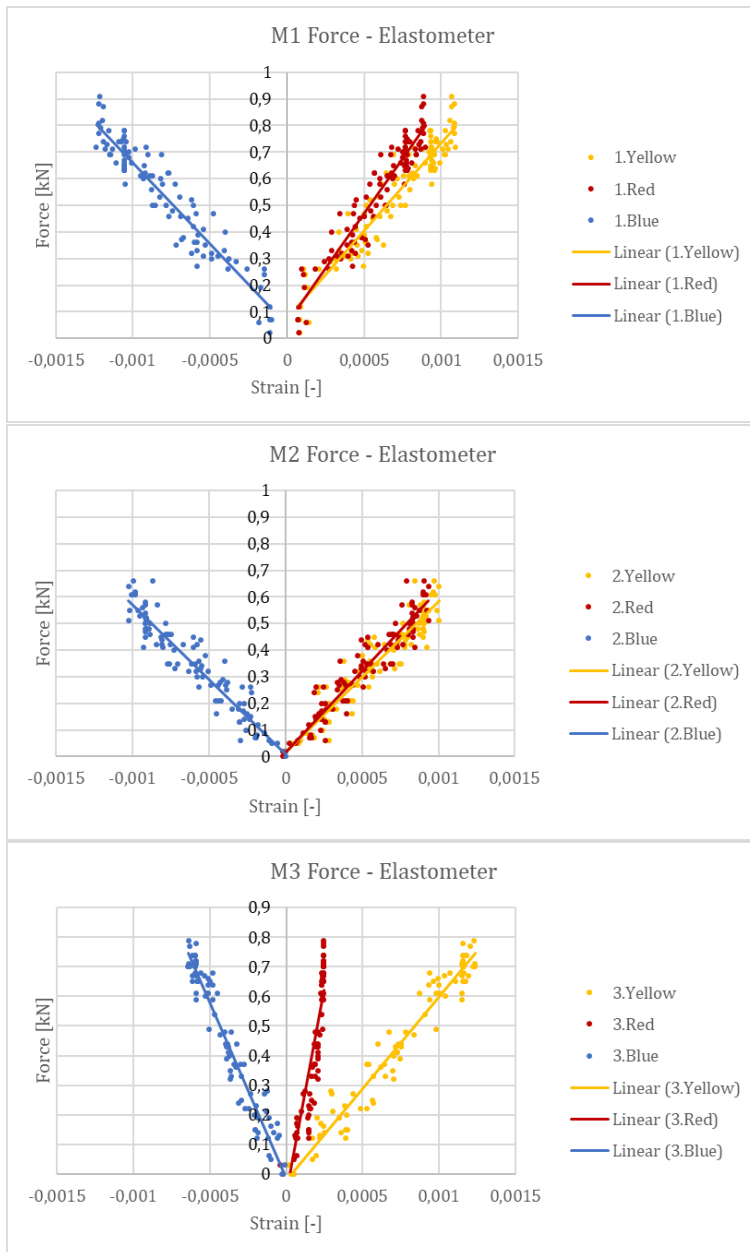
Figure C.2 Registration of force and strain for tree 10B. Top: Measurement round 1. Middle: Measurement round 2. Bottom: Measurement round 3
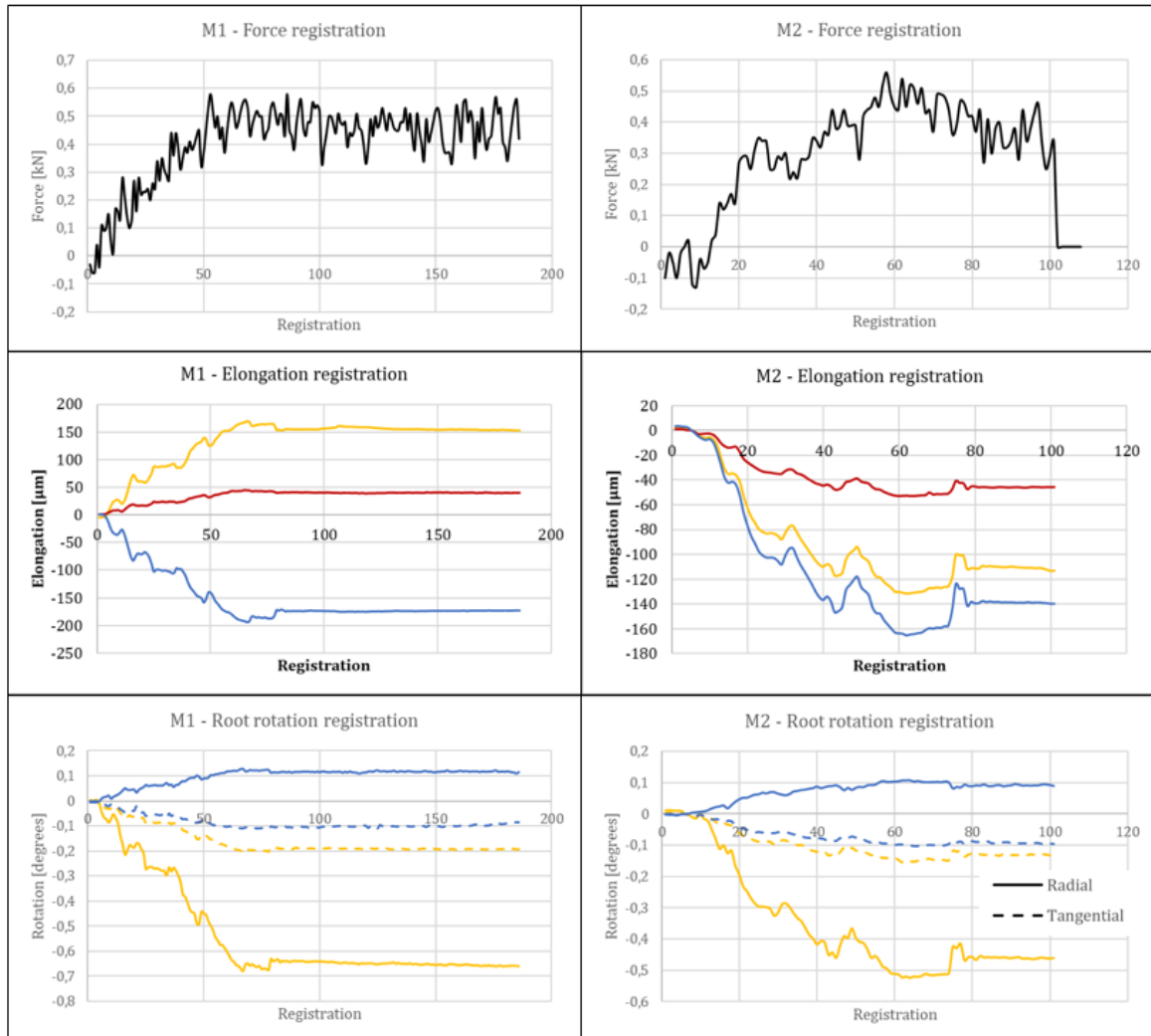
Figure C.3 Winching results tree 9B-10A. Force in radial direction, rope tied around the connection

Shortening of winching cable M1: 0,16m

Shortening of winching cable M2: 0,13m
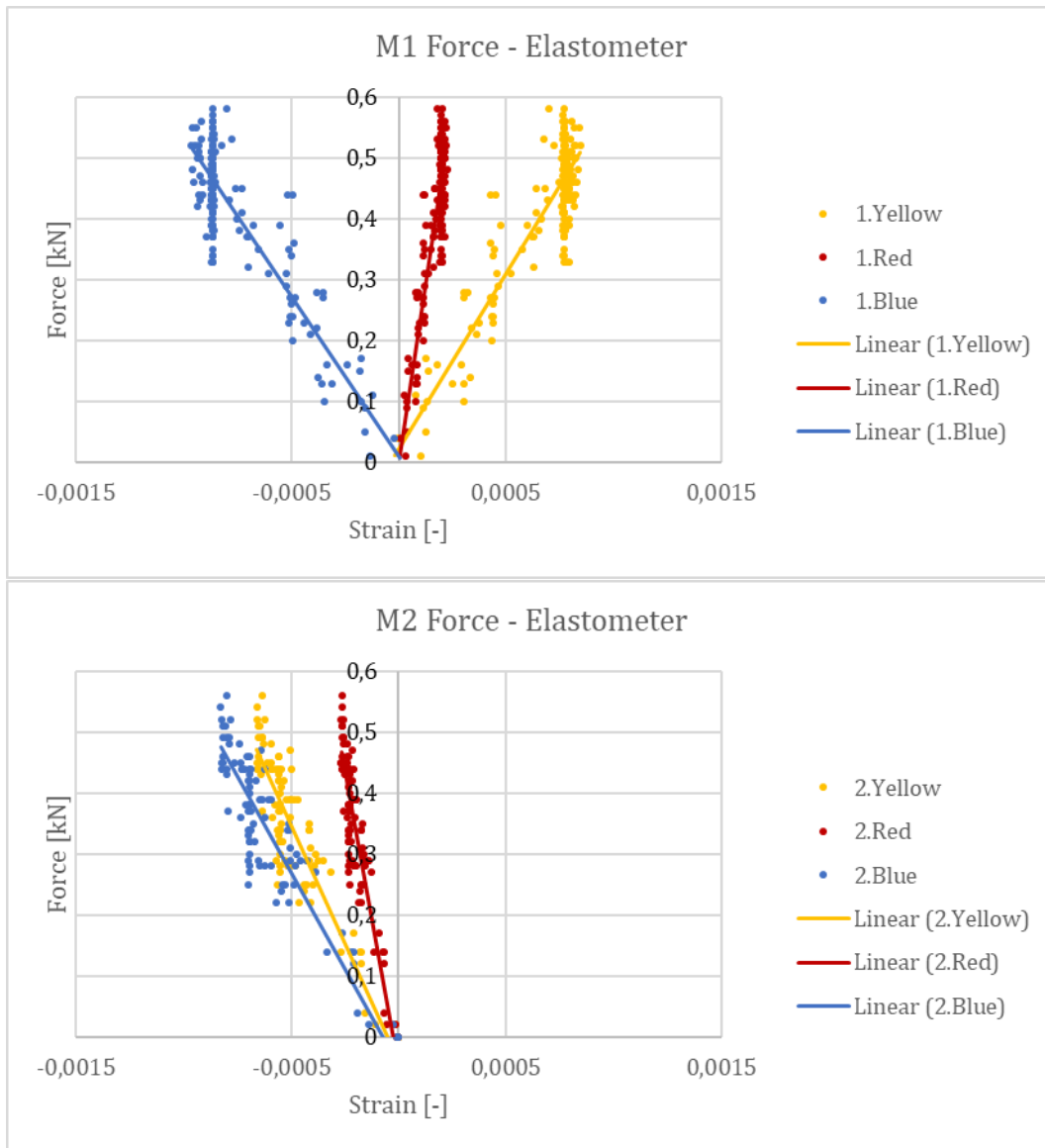
Figure C.4 Registration of force and strain for trees 9B and 10A. Top: Measurement round 1. Bottom: Measurement round 2
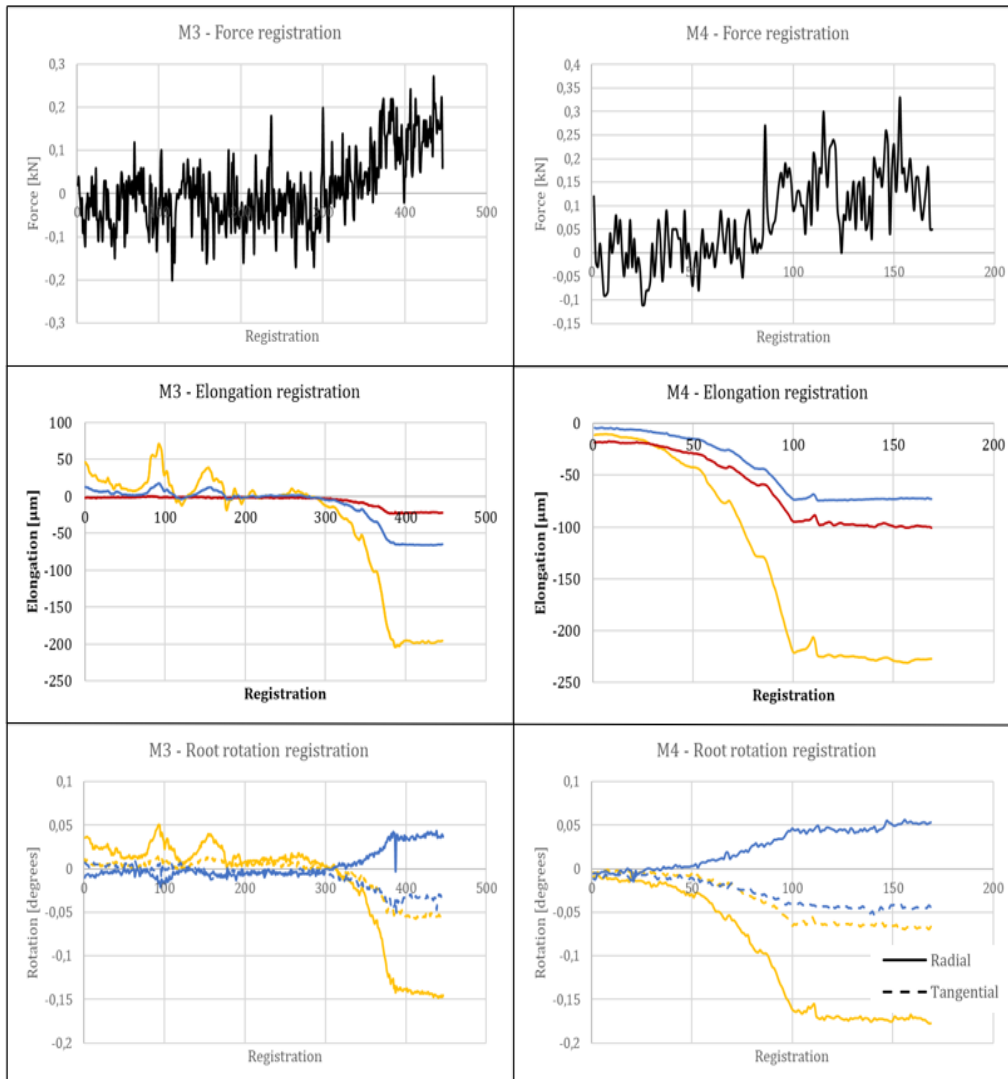
Figure C.5 Winching results tree 9B-10A. Force in radial direction, rope tied above the connection

Shortening of winching cable M3: 0,09m

Shortening of winching cable M4: 0,10m
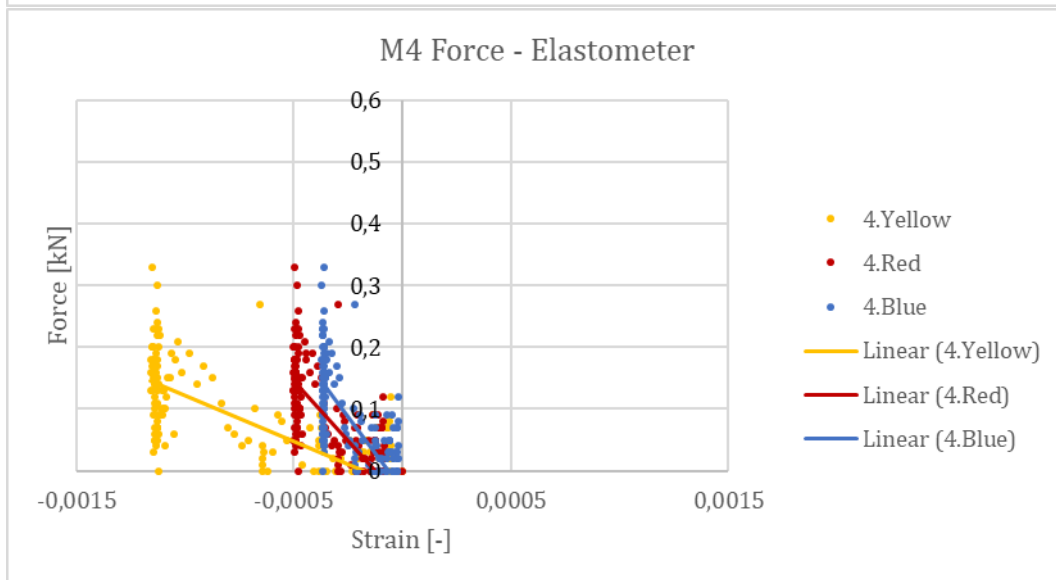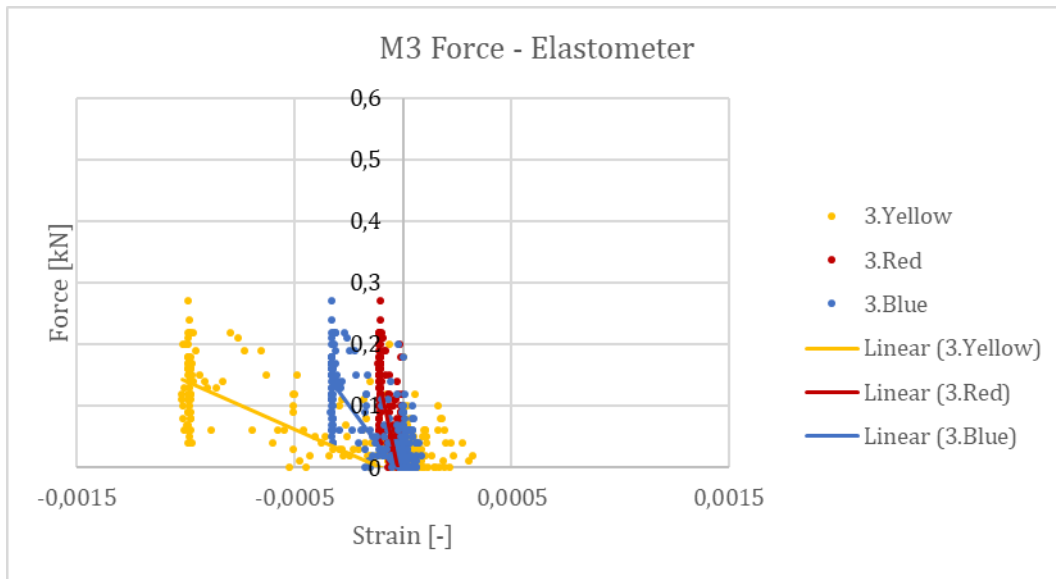
Figure C.6 Registration of force and strain for trees 9B and 10A. Top: Measurement round 3. Bottom: Measurement round 4
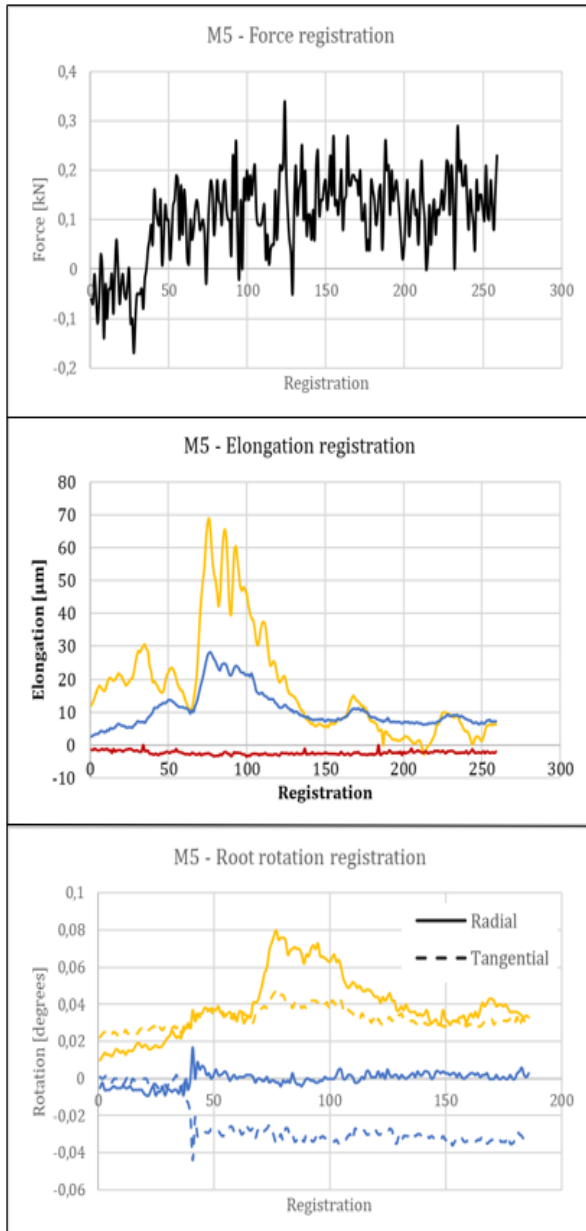
Figure C.7 Winching results tree 9B-10A. Force in vertical direction, rope tied above the connection

Shortening of winching cable M5: not applicable
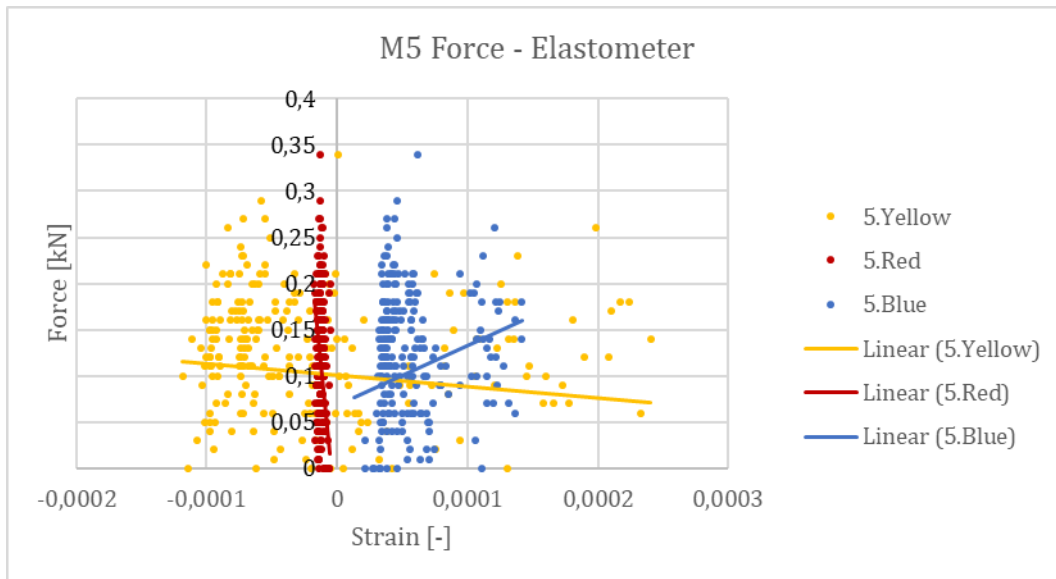
Figure C.8 Registration of force and strain for trees 9B and 10A. Measurement round 5.
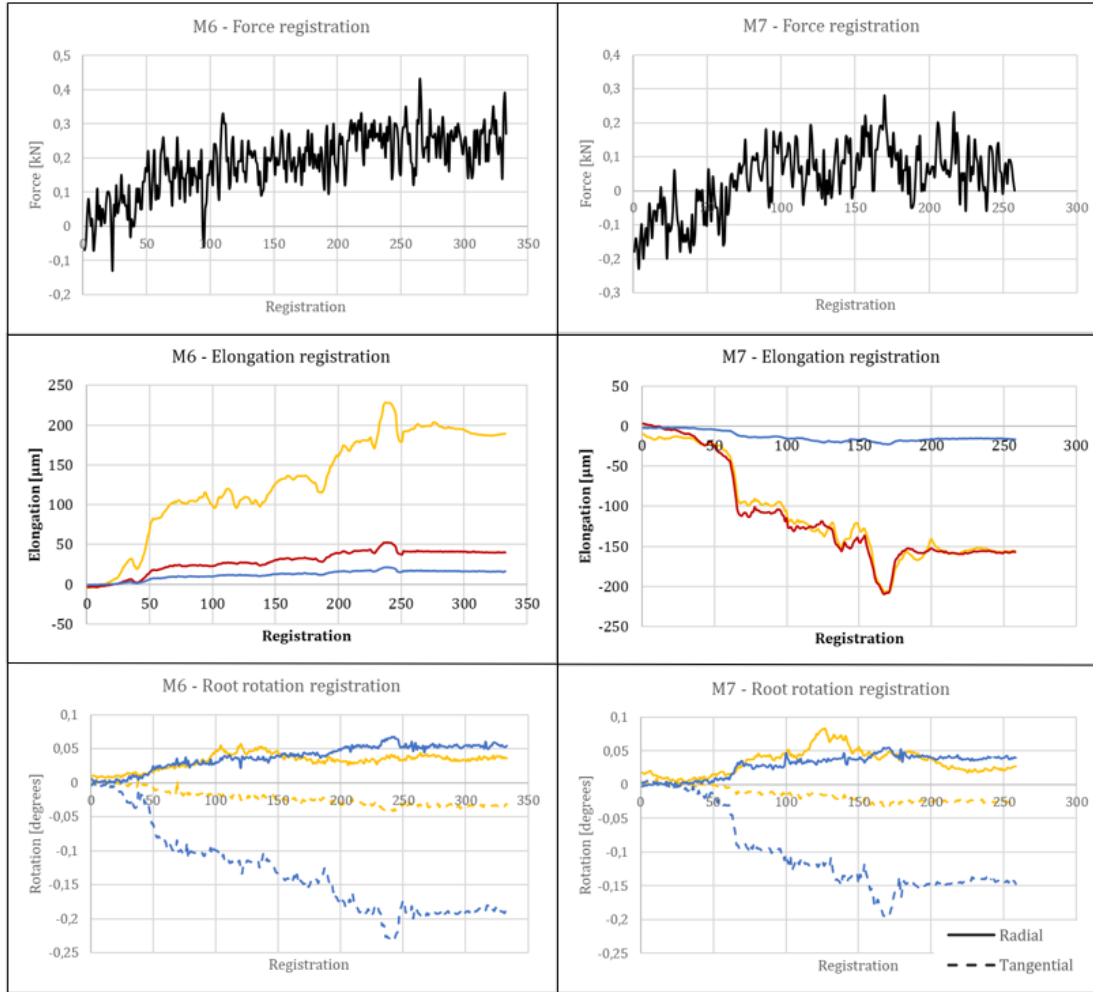
Figure C.9 Winching results tree 9B-10A. Force in tangential direction, rope tied above the connection

Shortening of winching cable M6: 0,34m

Shortening of winching cable M7: 0,27m

Note: The force registration of measurement round 7 is not calibrated at zero, see Figure C.9. A correction is applied to the force magnitude in the graph of Figure C.10.
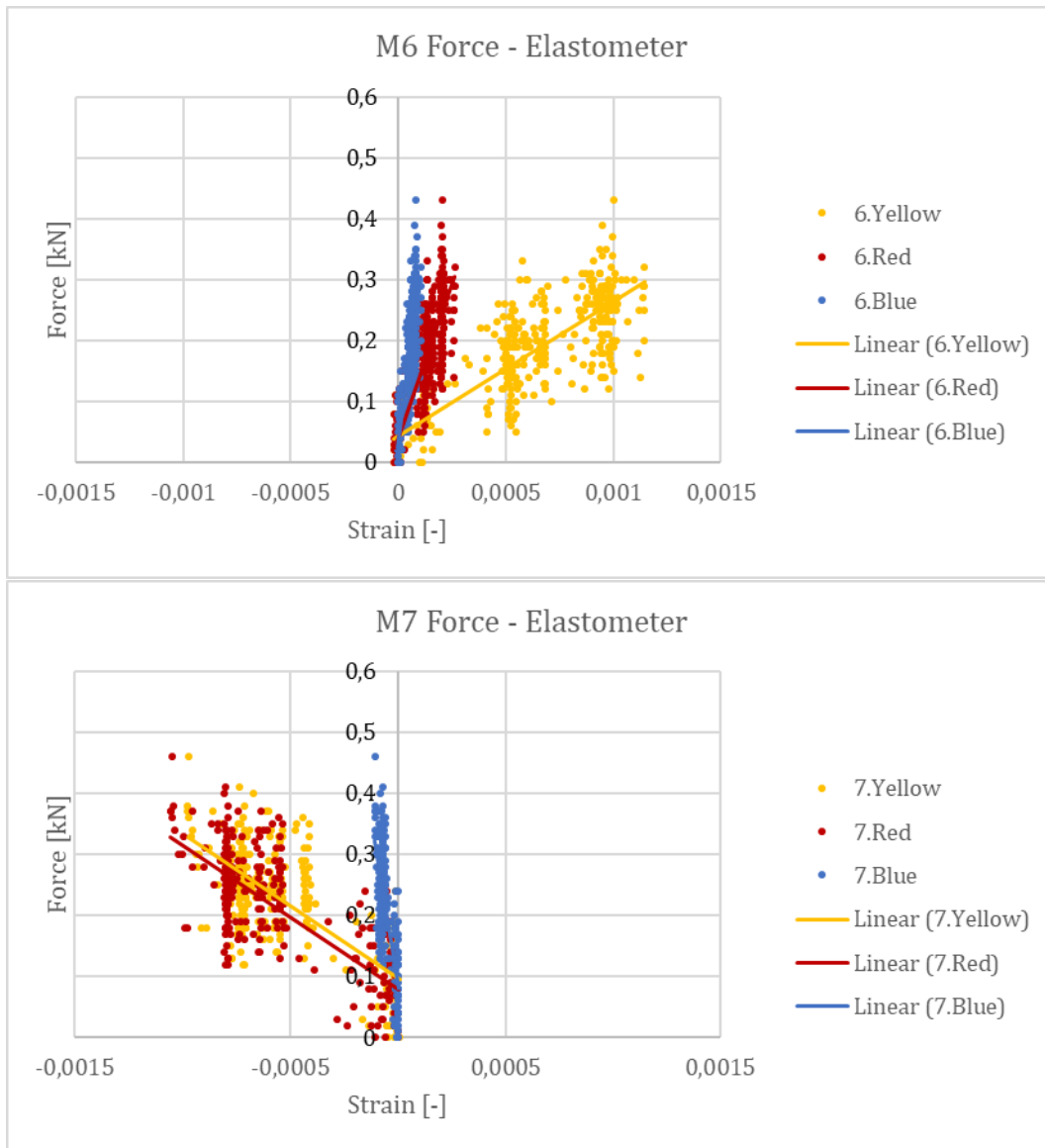
Figure C.10 Registration of force and strain for trees 9B and 10A. Top: Measurement round 6. Bottom: Measurement round 7. The force registration of round 7 is lifted to start at 0.

C.2.6 Tree 6A-6B – Parallel connection

Figure Appendix C.11 Winching results tree 6A-6B. Force in tangential direction.

Shortening of winching cable M1: 0,55m

Shortening of winching cable M2: 0,57m

Figure C.12 Registration of force and strain for trees 6A and 6B. Top: Measurement round 1. Bottom: Measurement round 2
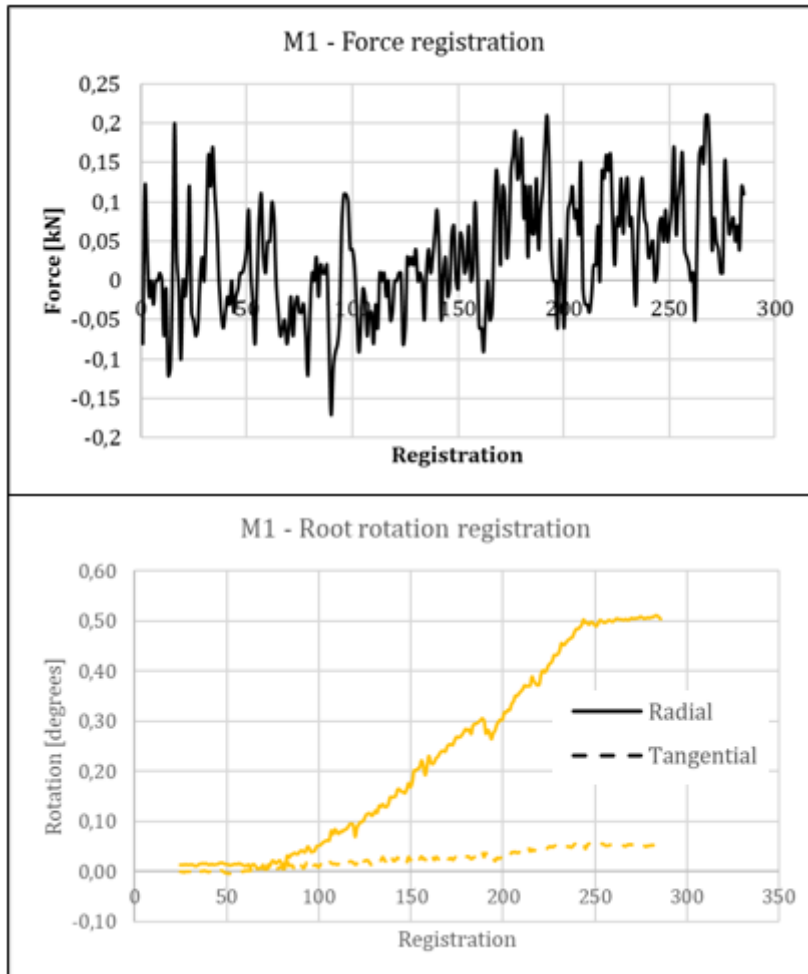
Figure C.13 Winching results tree Ulmus 'Clusius'. Force in radial direction.

Shortening of winching cable: not applicable

C.3   FINITE ELEMENT MODEL

C.3.1   Modulus of elasticity single tree

The following figures compare the strain and deformation results from the winching tests with the results from the finite element model of the single tree 10B. In the figures, the location of the elastometers is indicated for all the measurement rounds.
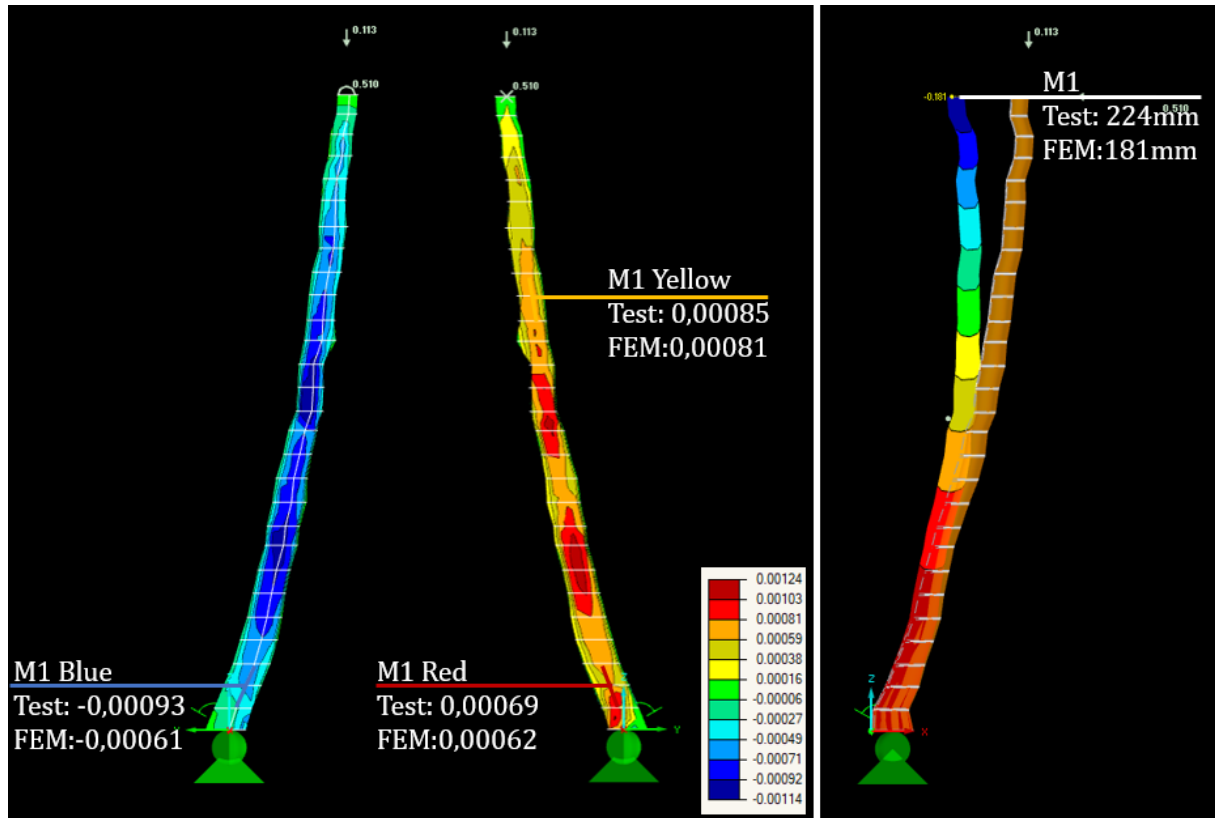
Figure C.14 Left: Strains in finite element model at the position of the elastometers on tree 10B during measurement round 1. Shown are the front side (compression) and back side (tension). Scale of strains ε_z [-]. Right: Displacement in finite element model at the position of the force application, in the direction of the force (U_x) on tree 10B during measurement round 1.
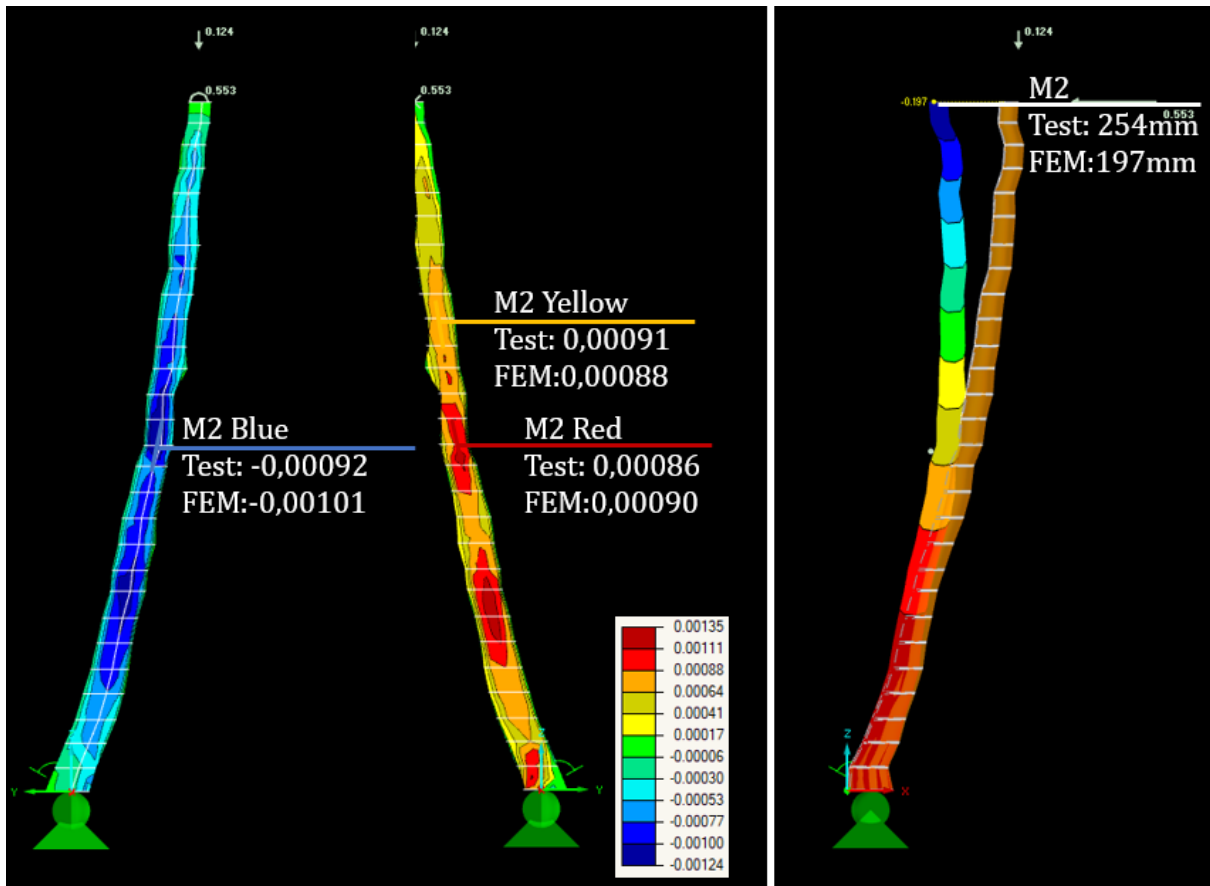
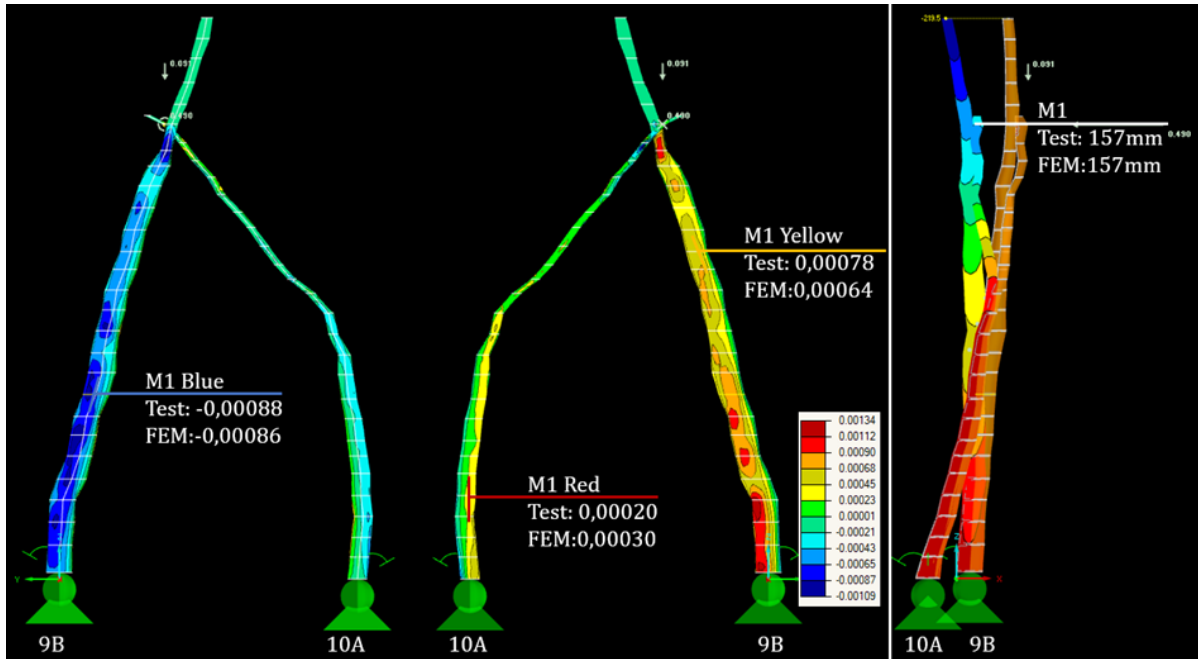*Figure C.15 Left: Strains in finite element model at the position of the elastometers on tree 10B during measurement round 2. Shown are the front side (compression) and back side (tension). Scale of strains ε_z [-]. Right: Displacement in finite element model at the position of the force application, in the direction of the force (U_x) on tree 10B during measurement round 2.*
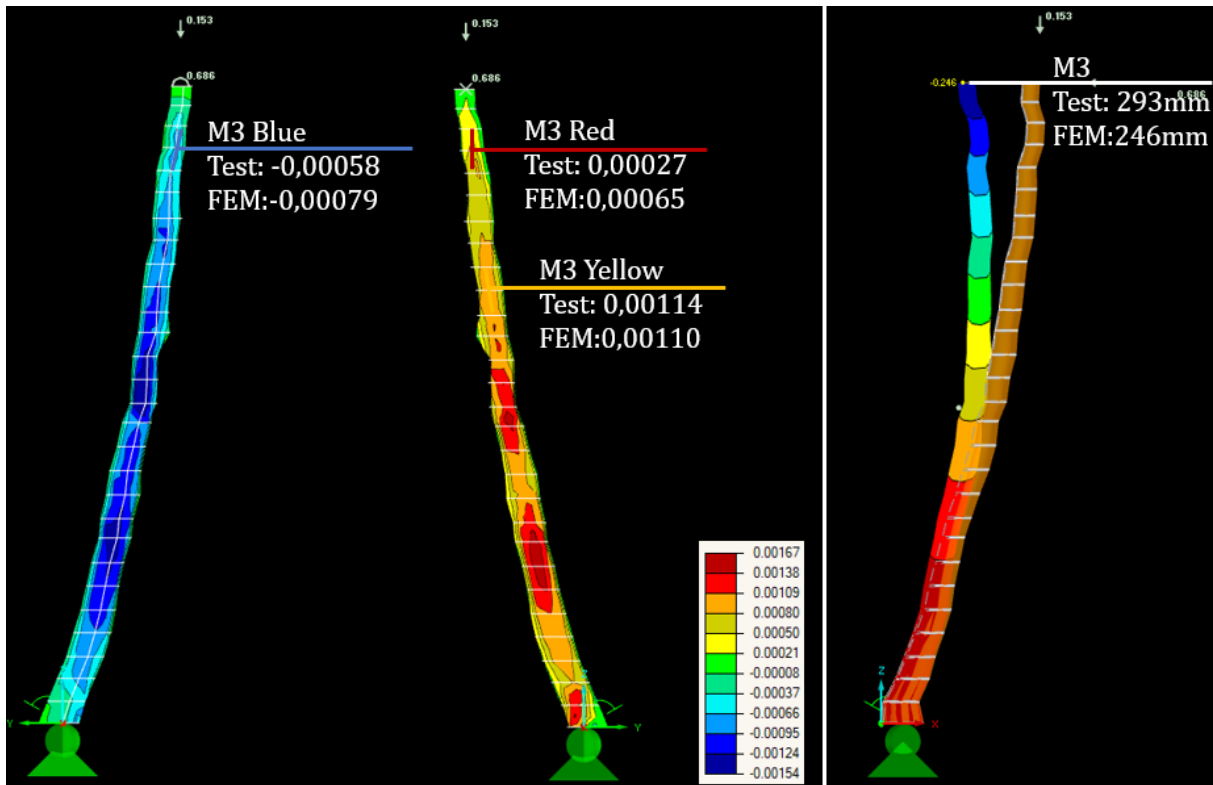
Figure C.16 Left: Strains in finite element model at the position of the elastometers on tree 10B during measurement round 3. Shown are the front side (compression) and back side (tension). Scale of strains ε_z [-]. Right: Displacement in finite element model at the position of the force application, in the direction of the force (U_x) on tree 10B during measurement round 3.

Table C.6 shows the distribution of the modulus of elasticity over the height of tree 10B.

Table C.6 Distribution of MOE over the height of tree 10B, based on stress results from the FE model ($MOE_{parallel}$=6.250N/mm²) and strain measurements from the winching tests

	Position	Height [mm]	Result FE model stress σ_z [N/mm²]	Results winching tests strain [-]	MOE = σ_z / strain [N/mm²]
Measurement 1					
Yellow elastometer	Back	1900	5,28	0,00085	6.227
Red elastometer	Back	200	4,55	0,00069	6.611
Blue elastometer	Front	200	-4,52	-0,00093	4.847
Measurement 2					
Yellow elastometer	Back	1900	5,75	0,00091	6.295
Red elastometer	Back	1400	6,52	0,00086	7.620
Blue elastometer	Front	1400	-8,89	-0,00092	9.677
Measurement 3					
Yellow elastometer	Back	1900	7,19	0,00114	6.330
Red elastometer	Back	2500	4,32	0,00027	16.314
Blue elastometer	Front	2500	-5,59	-0,00058	9.662

C.3.2 Stress distribution due to connection – cross connection

The following figures compare the strain and deformation results from the winching tests with the results from the finite element model of the cross-connected trees 9B and 10A. In the figures, the location of the elastometers is indicated for all the measurement rounds.
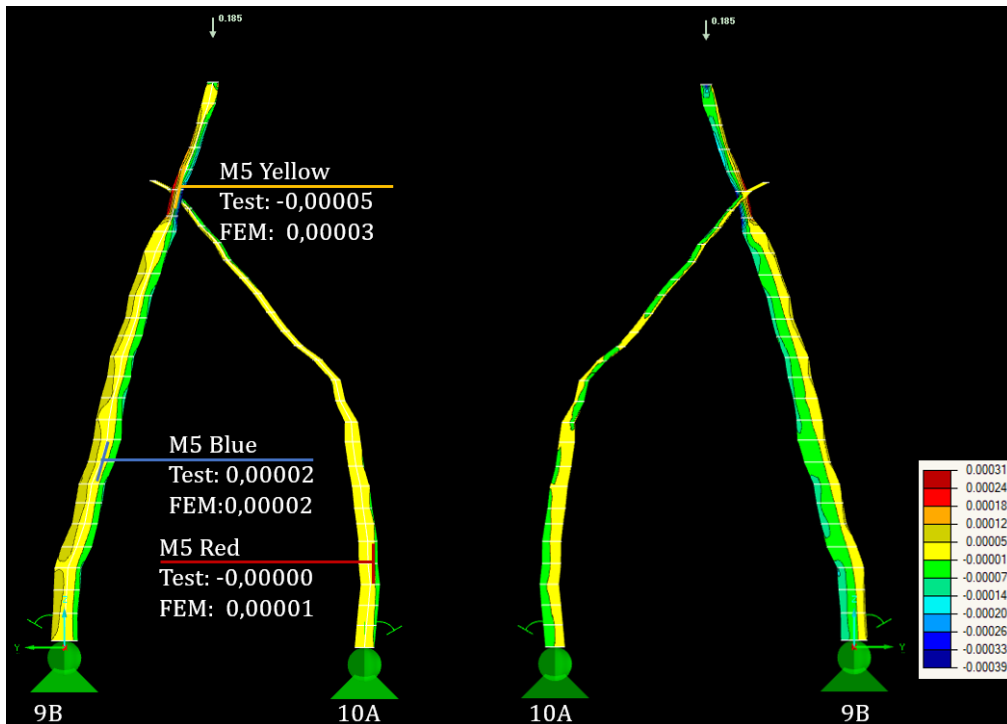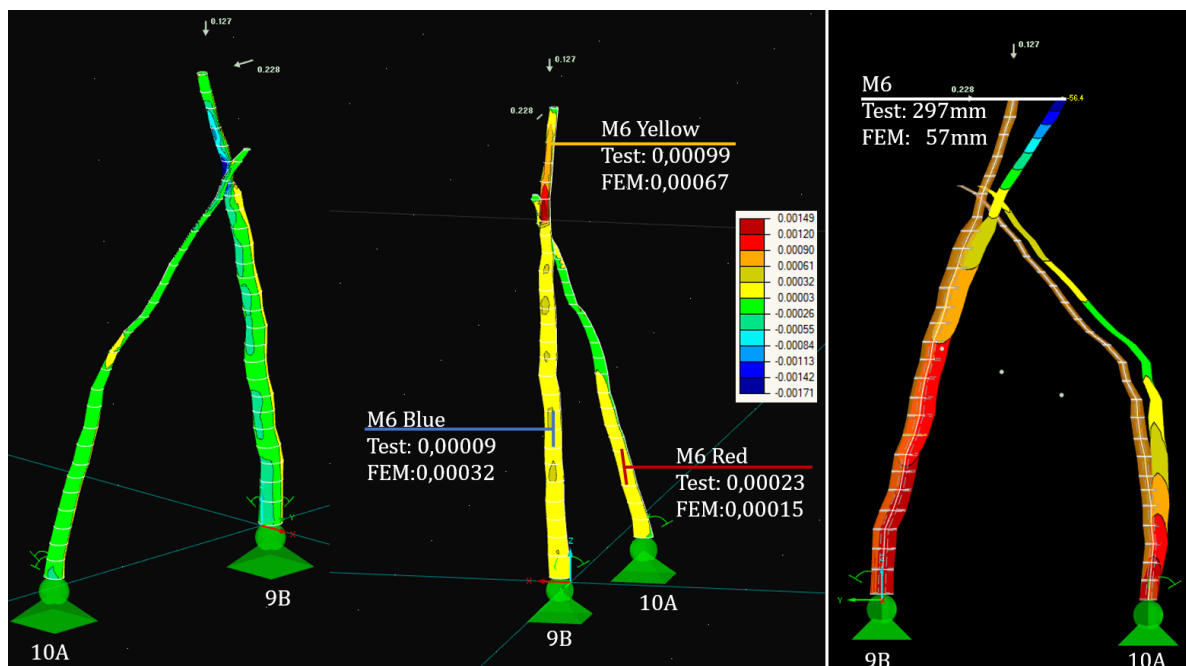

Figure C.17 Left: Strains in finite element model at the position of the elastometers on tree 9B and 10A during measurement round 1. Shown are the front side (compression) and back side (tension). Scale of strains ε_z [-]. Right: Displacement in finite element model at the position of the force application, in the direction of the force (U_x) on tree 9B and 10A during measurement round 1.
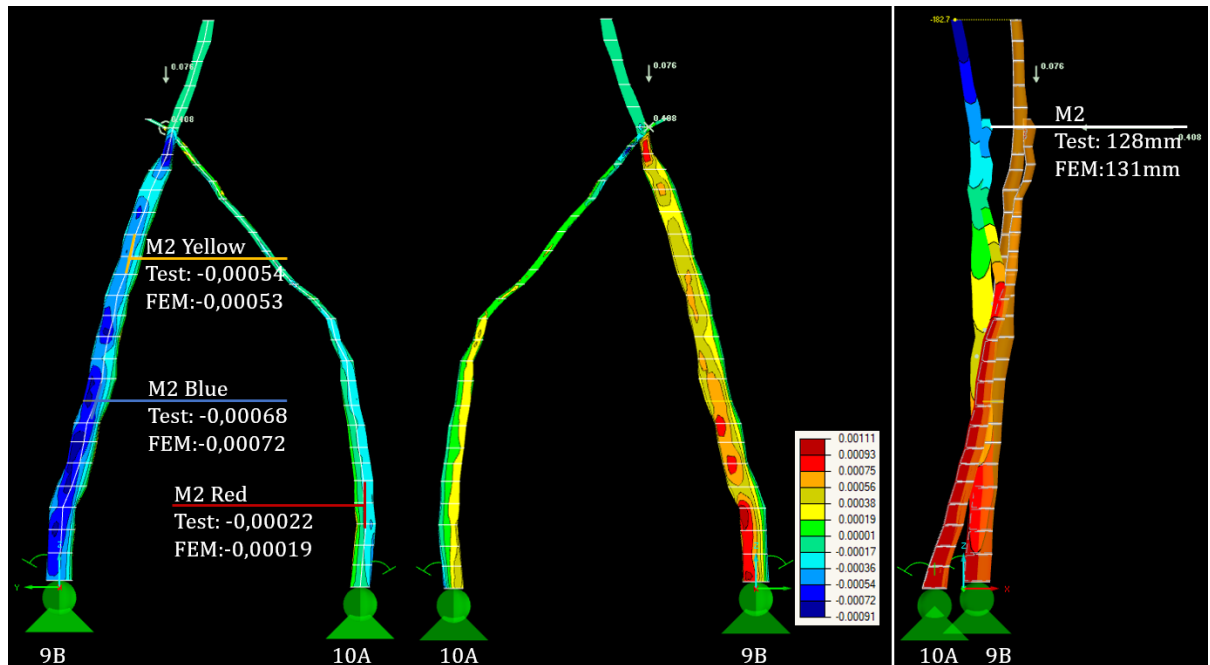
Figure C.18 Left: Strains in finite element model at the position of the elastometers on tree 9B and 10A during measurement round 2. Shown are the front side (compression) and back side (tension). Scale of strains ε_z [-]. Right: Displacement in finite element model at the position of the force application, in the direction of the force (U_x) on tree 9B and 10A during measurement round 2.
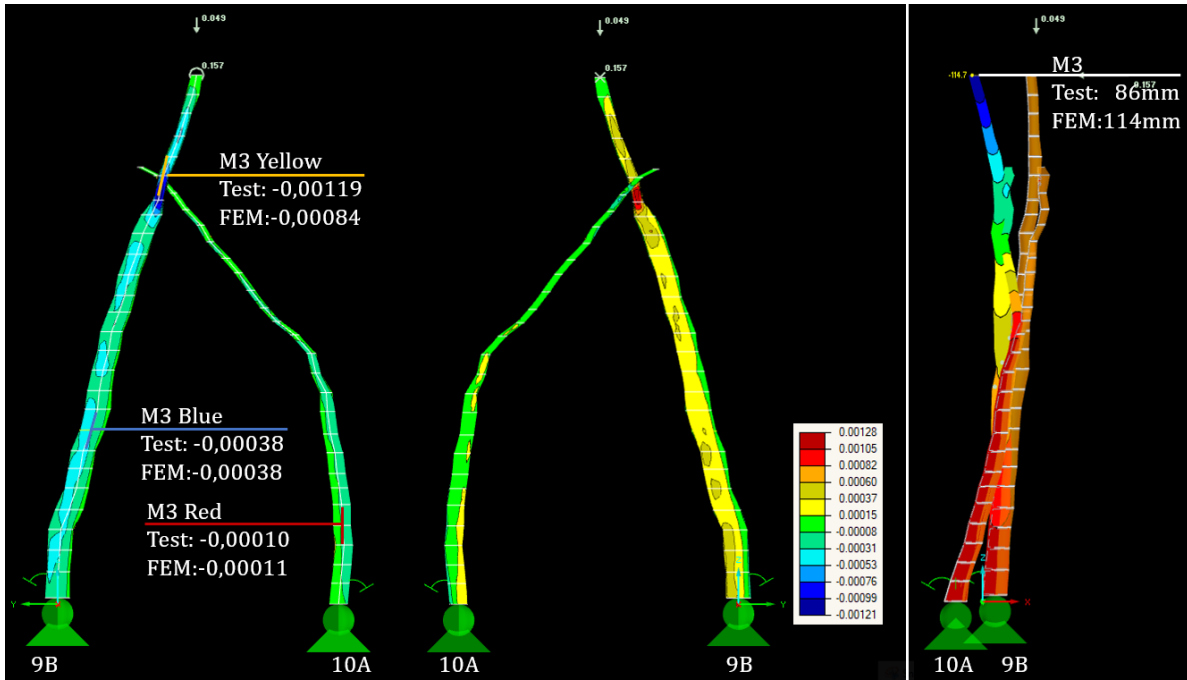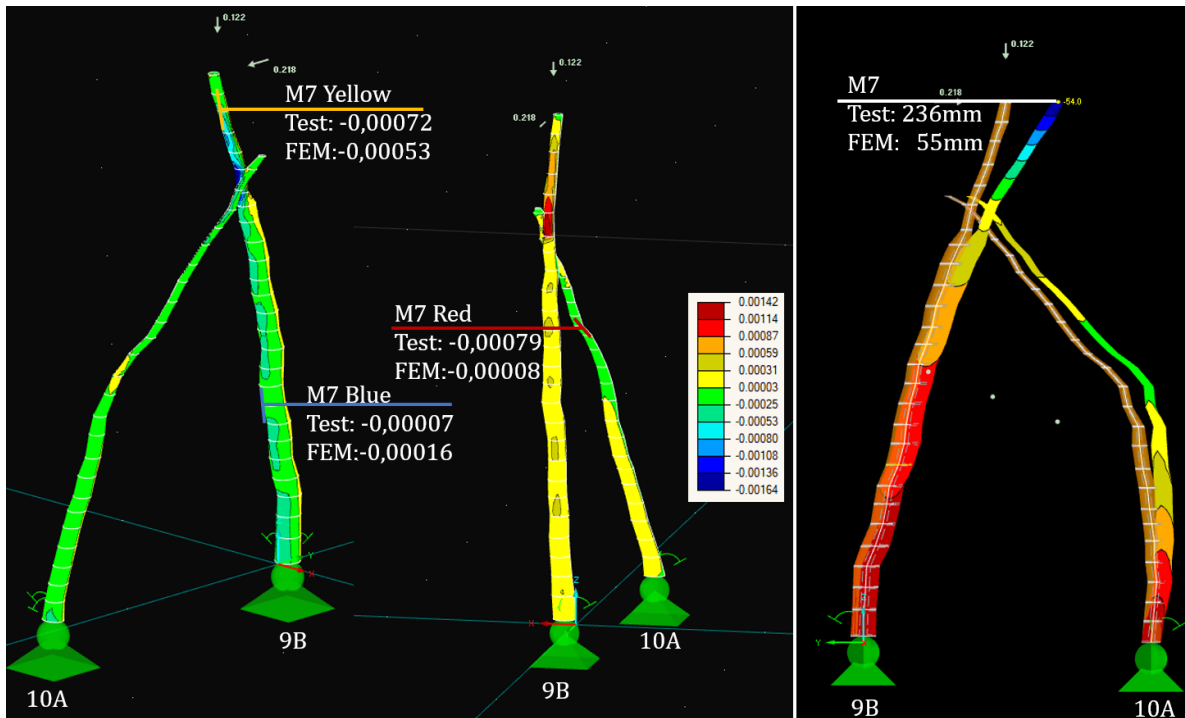
Figure C.19 Left: Strains in finite element model at the position of the elastometers on tree 9B and 10A during measurement round 3. Shown are the front side (compression) and back side (tension). Scale of strains ε_z [-]. Right: Displacement in finite element model at the position of the force application, in the direction of the force (U_x) on tree 9B and 10A during measurement round 3.
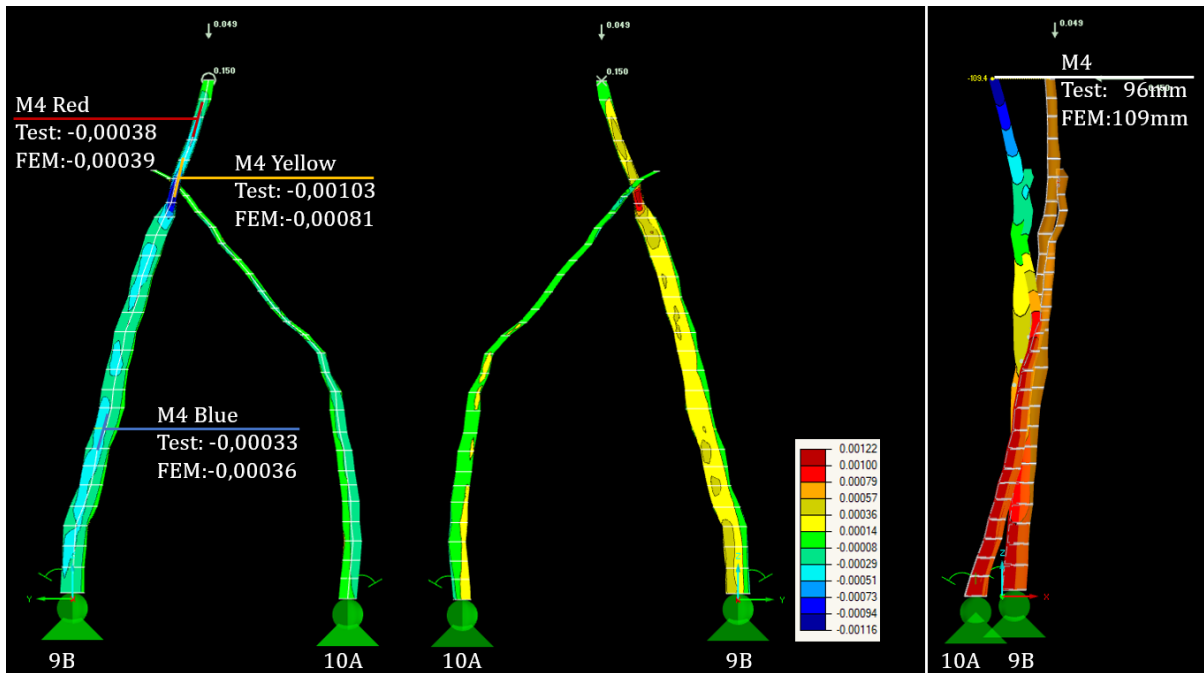
Figure C.20 Left: Strains in finite element model at the position of the elastometers on tree 9B and 10A during measurement round 4. Shown are the front side (compression) and back side (tension). Scale of strains ε_z [-]. Right: Displacement in finite element model at the position of the force application, in the direction of the force (U_x) on tree 9B and 10A during measurement round 4.
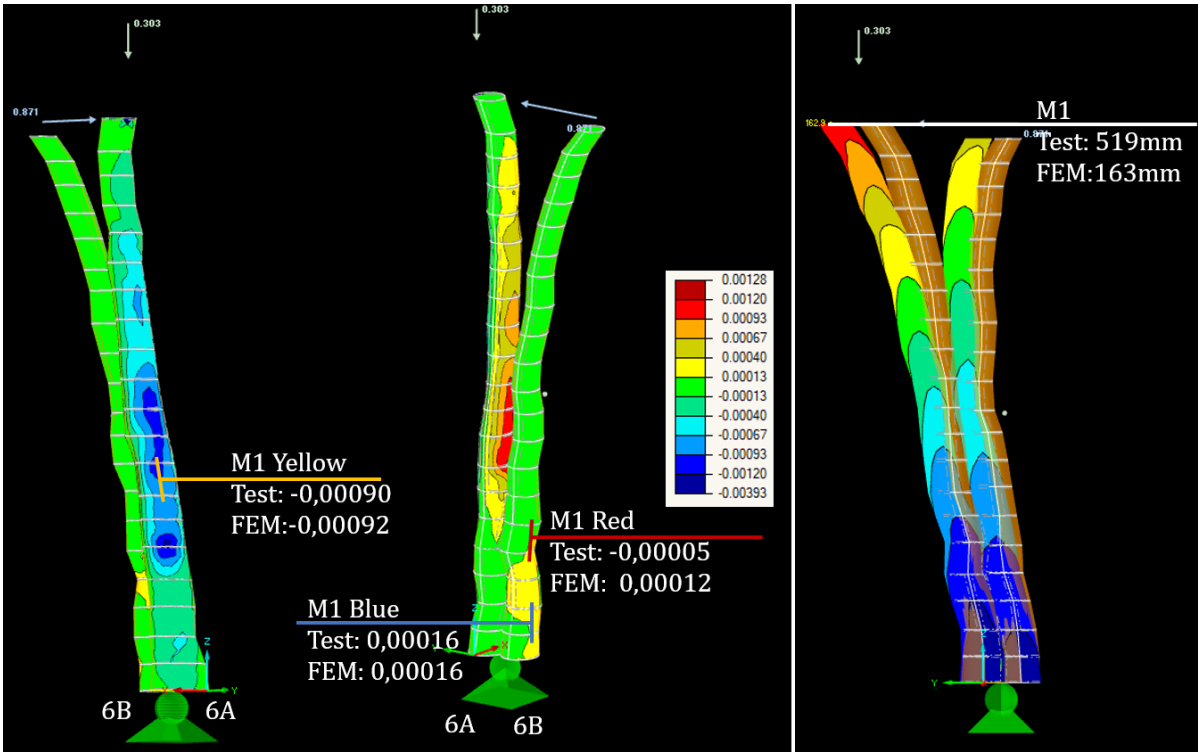
152

Figure C.21 Left: Strains in finite element model at the position of the elastometers on tree 9B and 10A during measurement round 5. Shown are the front side (compression) and back side (tension). Scale of strains ε_z [-].
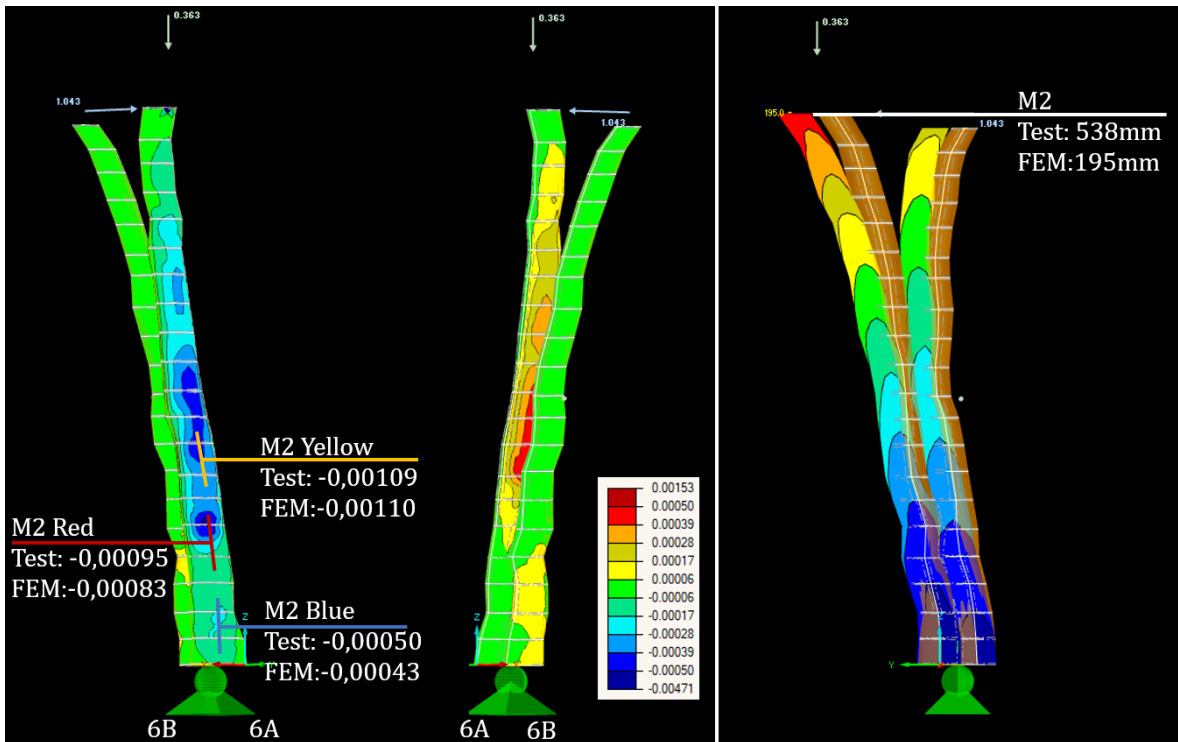

Figure C.22 Left: Strains in finite element model at the position of the elastometers on tree 9B and 10A during measurement round 6. Shown are the front side (compression) and back side (tension). Scale of strains ε_z [-]. Right: Displacement in finite element model at the position of the force application, in the direction of the force (U_y) on tree 9B and 10A during measurement round 6.

Figure C.23 Left: Strains in finite element model at the position of the elastometers on tree 9B and 10A during measurement round 7. Shown are the front side (compression) and back side (tension). Scale of strains ε_z [-]. Right: Displacement in finite element model at the position of the force application, in the direction of the force (U_y) on tree 9B and 10A during measurement round 7.

C.3.3   Stress distribution due to connection – parallel connection

The following figures compare the strain and deformation results from the winching tests with the results from the finite element model of the parallel-connected trees 6A and 6B. In the figures, the location of the elastometers is indicated for all the measurement rounds.

154

Figure C.24 Left: Strains in finite element model at the position of the elastometers on tree 6A and 6B during measurement round 1. Shown are the front side (compression) and back side (tension). Scale of strains ε_z [-]. Right: Displacement in finite element model at the position of the force application, in the direction of the force (U_y) on tree 6A and 6B during measurement round 1.

Figure C.25 Left: Strains in finite element model at the position of the elastometers on tree 6A and 6B during measurement round 2. Shown are the front side (compression) and back side (tension). Scale of strains ε_z [-]. Right: Displacement in finite element model at the position of the force application, in the direction of the force (U_y) on tree 6A and 6B during measurement round 2.

155

Appendix D   WONDERWOODS STRUCTURAL DESIGN

D.1   SELF-WEIGHT

The self-weight of the trees can be calculated with:

$$F_{self-weight.i} = \rho_{maple} \times V_{tree.i} \times 9,81$$

In which "i" is the number of years after planting.

If the diameter at breast height is larger than 15cm, the volume of the tree can be estimated with (Wessolly & Erb, 2016):

$$V_{tree,i} = 0,7 \times \pi \times r_{chest,i}^2 \times h_i$$

This gives the following results:

Table D.1 Input values for self-weight calculation year 33 and 60

	Year 31	Year 43	Year 60
h_i [m]	6,0	6,0	6,0
$r_{chest,i}$ [cm]	14,3	18,8	25,2
ρ_{maple} [kg/m³]	840	840	840

$F_{self-weight,31} = 2,2kN; \ F_{self-weight,43} = 3,8kN; \ F_{self-weight,60} = 6,9kN$

At the time of planting, the trees have a diameter of 5,4cm. Their volume is estimated as recommended by Dennis de Goederen:

$$V_{tree,i} = (V_{stem,i} + V_{branch,1,i} + V_{branch,2,i} + V_{branch,3,i} + V_{branch,4,i} + V_{branch,5,i}) \times 1,2$$

$$V_{stem,i} = 0,7 \times \pi \times r_{chest,i}^2 \times h_i$$

$$V_{branch,j,i} = 0,7 \times \pi \times r_{branch,j,i}^2 \times l_{j,i}$$

The volume of the branches is estimated by using the volumes of a comparable tree of the *Living Tree Pavilion*, tree number 1B. This tree has a height of 4,9m and a chest radius of 3,3 cm. This should give a good estimation because the growth behaviour of Ash trees (*Living Tree Pavilion*) is comparable with the growth behaviour of Field Maples (*Wonderwoods*) (Beining, 2020).

Table D.2 Input values for self-weight calculation year 0

	Year 0
h_i [m]	4,5
$r_{chest,i}$ [cm]	2,7
$l_{1,i}$ [cm]	160
$r_{branch,1,i}$ [cm]	1,8
$l_{2,i}$ [cm]	120
$r_{branch,2,i}$ [cm]	1,3
$l_{3,i}$ [cm]	70
$r_{branch,3,i}$ [cm]	0,7
$l_{4,i}$ [cm]	60
$r_{branch,4,i}$ [cm]	0,6
$l_{5,i}$ [cm]	40
$r_{branch,5,i}$ [cm]	0,6
ρ_{maple} [kg/m³]	840

This gives the following results:

$$F_{self-weight,0} = 0,09kN$$

D.2 WIND

The maximum gust wind can be calculated with (Gatti & Ruck, 2019):

$$F_{wind,j,i} = 0,5 \times \rho \times c_{D,j} \times A_{j,i} \times (c_A \times v_p)^2$$

The input values for the tree crown can be seen in Table D.3.

Table D.3 Input values for wind calculation tree crown

	Year 0	Year 31	Year 43	Year 60
ρ [kg/m³]	1,25	1,25	1,25	1,25
$c_{D,crown}$ [-]	0,25	0,25	0,25	0,25
$A_{crown,i}$ [m²]	3,9	11,0	11,0	11,0
c_A [-]	1,5	1,5	1,5	1,5
v_p [m/s]	44,15	44,15	44,15	44,15

This gives the following results:

$$F_{wind,crown,0} = 2,7kN; F_{wind,crown,31} = 7,5kN; F_{wind,crown,43} = 7,5kN; F_{wind,crown,60} = 7,5kN$$

The input values for the tree stem can be seen in Table D.4. The area of the stem is calculated up till 2m at which the crown starts.

Table D.4 Input values for wind calculation tree stem

	Year 0	Year 31	Year 43	Year 60
ρ [kg/m³]	1,25	1,25	1,25	1,25
$c_{D,stem}$ [-]	0,7	0,7	0,7	0,7
$A_{stem,i}$ [m²]	0,1	0,6	0,8	1,0
c_A [-]	1,5	1,5	1,5	1,5
v_p [m/s]	44,15	44,15	44,15	44,15

This gives the following results:

$$F_{wind,stem,0} = 0,2kN; F_{wind,stem,31} = 1,1kN; F_{wind,stem,43} = 1,4kN; F_{wind,stem,60} = 1,9kN$$

D.3 SNOW

The snow load can be calculated with:

$$F_{snow,j,i} = q_{snow} \times A_{j,i}$$

In which "j" is the object exposed to snow and "i" is the number of years after planting.

The input values for the tree crown can be seen in Table D.5. Only 50% of the precipitation stays on the tree canopy, therefore, the crown area is divided by two (Ursem, 2020).

Table D.5 Input values for snow calculation tree crown

	Year 0	Year 43	Year 31	Year 60
q_{snow} [kN/m²]	0,56	0,56	0,56	0,56
$A_{crown,i}$ [m²]	3,1/2=1,6	9,6/2=4,8	9,6/2=4,8	9,6/2=4,8

This gives the following results:

$$F_{snow,crown,0} = 0,9kN; F_{snow,crown,31} = 2,7kN; F_{snow,crown,43} = 2,7kN; F_{snow,crown,60} = 2,7kN$$

The input values for the plant container can be seen in Table D.6. The area of the plant container is divided by two because the plant container has two supports.

Table D.6 Input values for snow calculation plant container

	All years
q_{snow} [kN/m²]	0,56
$A_{plantcontainer}$ [m²]	3,2/2=1,6

This gives the following results:

$$F_{snow,plantcontainer} = 0,9kN$$

D.4 RAIN

The rain load can be calculated with:

$$F_{rain,j,i} = \rho_{water} \times 9,81 \times \max rain \times A_{j,i}$$

In which "j" is the object exposed to snow and "i" is the number of years after planting.

The input values for the tree crown can be seen in Table D.7. Only 50% of the precipitation stays on the tree canopy; therefore, the crown area is divided by two (Ursem, 2020).

Table D.7 Input values for rain calculation tree crown

	Year 0	Year 31	Year 43	Year 60
ρ_{water} [kg/m³]	997	997	997	997
max rain [mm]	63,9	63,9	63,9	63,9
$A_{crown,i}$ [m²]	3,1/2=1,6	9,6/2=4,8	9,6/2=4,8	9,6/2=4,8

This gives the following results:

$$F_{rain,crown,0} = 1,0kN; F_{rain,crown,31} = 3,0kN; F_{rain,crown,43} = 3,0kN; F_{rain,crown,60} = 3,0kN$$

The input values for the plant container can be seen in Table D.8. The area of the plant container is divided by two because the plant container has two supports.

Table D.8 Input values for rain calculation plant container

	All years
ρ_{water} [kg/m³]	997
max rain [mm]	63,9
$A_{plantcontainer}$ [m²]	3,2/2=1,6

This gives the following results:

$$F_{rain,plantcontainer} = 1,0kN$$

D.5 SIMPLIFIED CALCULATION

D.5.1 ULS of single tree, after 31 years

Ultimate limit state checks are performed according to Eurocode 1990 (NEN, 2019) and Eurocode 1995 (NEN, 2011).

Governing load combination: ULS 2
$$1,2 \times \left(F_{self-weight} + F_{plantcontainer}\right) + 1,5 \times \left(F_{wind,crown,90} + F_{wind,stem,90}\right)$$
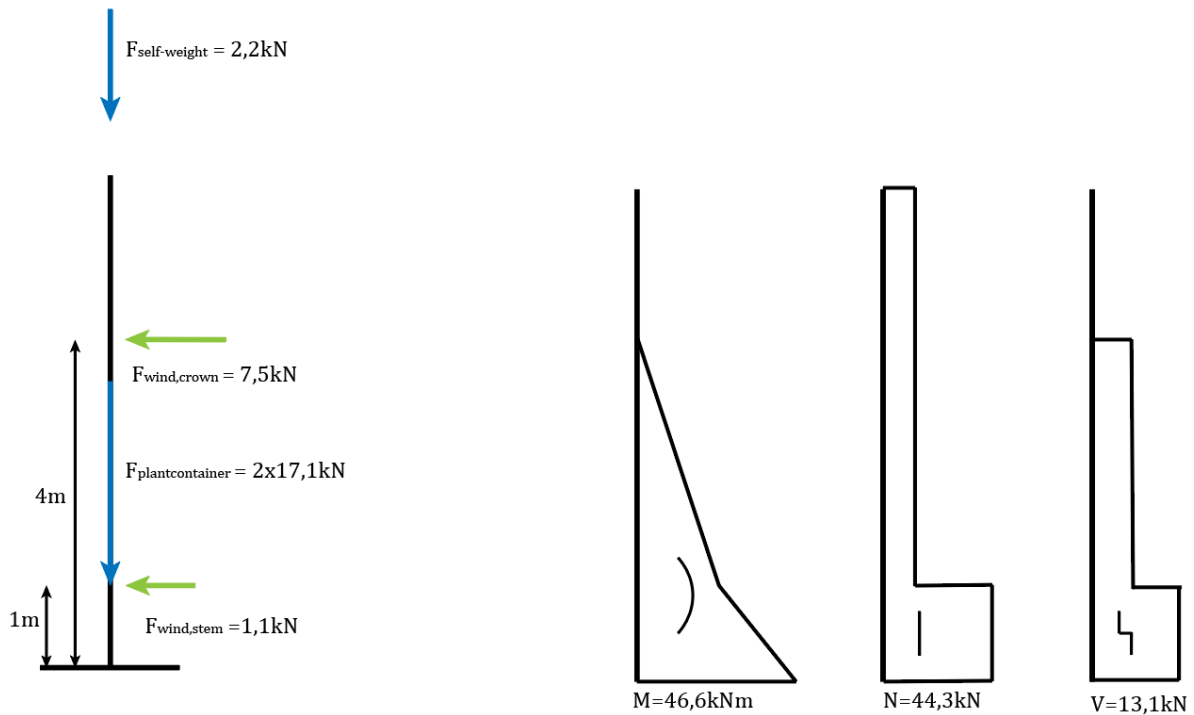
Figure D.1 Loads, bending moment, normal force and shear force of a single tree that is standing on Wonderwoods for 31 years

$$M_{max} = 1,5 \times \left(F_{wind,crown,90} \times 4m + F_{wind,stem,90} \times 1m\right) = 46,6kNm$$

$$N_{max} = 1,2 \times \left(F_{self-weight} + 2 \times F_{plantcontainer}\right) = 44,3kN$$

$$V_{max} = 1,5 \times \left(F_{wind,crown,90} + F_{wind,stem,90}\right) = 13,1kN$$

Checks:

Compression parallel to the grain:

$$\sigma_{c,0,d} = \frac{N_{max}}{A} = \frac{44,3\ kN}{0,1\ m^2} = 0,4\ N/mm^2$$

$$f_{c,0,d} = k_{mod} * \frac{f_{c,0,k}}{\gamma_M} = 0,7 * \frac{21\ N/mm^2}{1,3} = 11,3\ N/mm^2$$

$$U.C. = \frac{\sigma_{c,0,d}}{f_{c,0,d}} = 0,04 \qquad\qquad \text{Requirement is fulfilled}$$

Bending:

$$\sigma_{m,y,d} = \frac{M_{y,max}}{W} = \frac{46,6\ kNm}{\frac{1}{32}\pi * (0,33m)^3} = 12,8\ N/mm^2$$

$$\sigma_{m,z,d} = 0\ N/mm^2$$

$$f_{m,d} = k_{mod} * \frac{f_{m,k}}{\gamma_M} = 0,7 * \frac{24\frac{N}{mm^2}}{1,3} = 12,9\ N/mm^2$$

$$k_m = 1 \qquad \text{Circular cross section}$$

$$U.C. = \frac{\sigma_{m,y,d}}{f_{m,d}} + k_m * \frac{\sigma_{m,z,d}}{f_{m,d}} = 0{,}99 \qquad \text{Requirement is fulfilled}$$

$$U.C. = k_m * \frac{\sigma_{m,y,d}}{f_{m,d}} + \frac{\sigma_{m,z,d}}{f_{m,d}} = 0{,}99 \qquad \text{Requirement is fulfilled}$$

Combined bending and compression:

$$U.C. = \left(\frac{\sigma_{c,0,d}}{f_{c,0,d}}\right)^2 + \frac{\sigma_{m,y,d}}{f_{m,d}} + k_m * \frac{\sigma_{m,z,d}}{f_{m,d}} = 0{,}99 \qquad \text{Requirement is fulfilled}$$

$$U.C. = \left(\frac{\sigma_{c,0,d}}{f_{c,0,d}}\right)^2 + k_m * \frac{\sigma_{m,y,d}}{f_{m,d}} + \frac{\sigma_{m,z,d}}{f_{m,d}} = 0{,}99 \qquad \text{Requirement is fulfilled}$$

Shear:

$$\tau_{max} = \frac{4*V_{max}}{3\pi*r_{base}^2} = \frac{4*26{,}0kN}{3\pi*(0{,}2m)^2} = 0{,}20 \ N/mm^2 \quad \text{(Hartsuijker, 2014)}$$

$$f_{v,d} = k_{mod} * \frac{f_{v,k}}{\gamma_M} = 0{,}7 * \frac{4\frac{N}{mm^2}}{1{,}3} = 2{,}15 \ N/mm^2$$

$$U.C. = \frac{\tau_{max}}{f_{v,d}} = 0{,}09 \qquad \text{Requirement is fulfilled}$$

D.5.2 ULS of interconnected tree, after 43 years

Ultimate limit state checks are performed according to Eurocode 1990 (NEN, 2019) and Eurocode 1995 (NEN, 2011).

Governing load combination: ULS 2

$$1{,}2 \times \left(F_{self-weight} + F_{plantcontainer}\right) + 1{,}5 \times \left(F_{wind,crown,90} + F_{wind,stem,90}\right)$$

The interconnected trees have an angle of 45° with the wind direction. The wind load is therefore decomposed in the directions parallel (y) and perpendicular (x) to the interconnected trees. See Figure D.2, top.
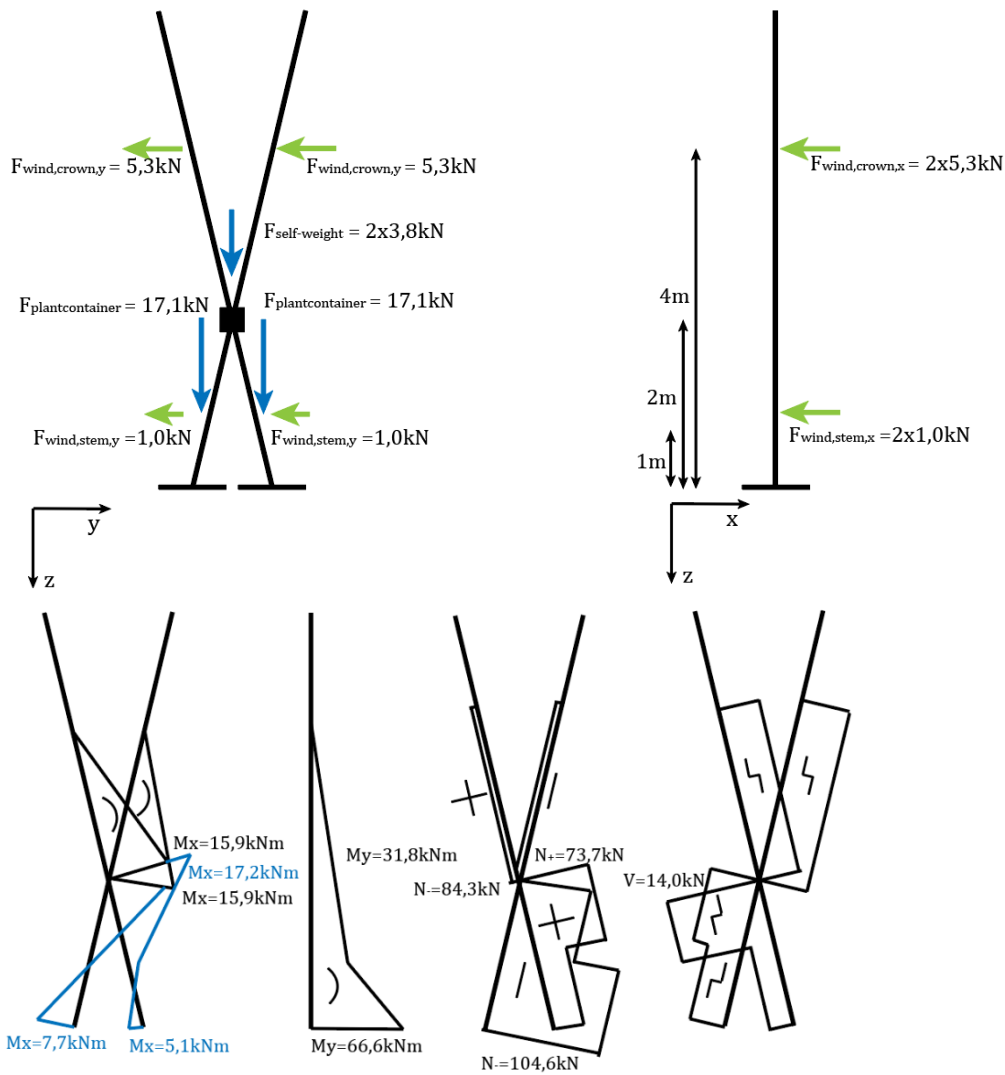
Figure D.2 Top: Loads on interconnected trees that are standing on Wonderwoods for 43 years decomposed in x and y direction. Bottom: Results of bending moment, normal force and shear force.

Above the connection, the bending moment does not depend on the bending stiffness of the members. Below the connection, the system is statically undetermined. The internal forces are calculated with the *MatrixFrame* wireframe software. The members below the connection are modelled with single profile parameters, being the average of the parameters at the bottom and the top of the member:

A =   0,106 m²

I = $8,91*10^{-4}$ m⁴

E =   5.500.000 kN/m²

This results in the following internal forces that need to be checked:

At connection:

$M_{x,max} = 17,2 kNm$

$M_{y,max} = 31,8 kNm$

$N_{+,max} = 73,7 kN$

$N_{-,max} = 84,3 kN$

$V_{max} = 14,0 kN$

At root system:

$M_{x,max} = 7,7 kNm$

$M_{y,max} = 66,6 kNm$

$N_{-,max} = 104,6 kN$

Checks at stems around connection:

Compression parallel to the grain:

$$\sigma_{c,0,d} = \frac{N_{-,max}}{A} = \frac{84,3 \ kN}{0,07 \ m^2} = 1,18 \ N/mm^2$$

$$f_{c,0,d} = k_{mod} * \frac{f_{c,0,k}}{\gamma_M} = 0,7 * \frac{21 \ N/mm^2}{1,3} = 11,3 \ N/mm^2$$

$$U.C. = \frac{\sigma_{c,0,d}}{f_{c,0,d}} = 0,11 \qquad \text{Requirement is fulfilled}$$

Tension parallel to the grain:

$$\sigma_{t,0,d} = \frac{N_{+,max}}{A} = \frac{73,7 \ kN}{0,07 \ m^2} = 1,03 \ N/mm^2$$

$$f_{t,0,d} = k_{mod} * \frac{f_{c,0,k}}{\gamma_M} = 0,7 * \frac{14 \frac{N}{mm^2}}{1,3} = 7,54 \ N/mm^2$$

$$U.C. = \frac{\sigma_{t,0,d}}{f_{t,0,d}} = 0,14 \qquad \text{Requirement is fulfilled}$$

Bending:

$$\sigma_{m,y,d} = \frac{M_{y,max}/2}{W} = \frac{31,8 \ kNm/2}{\frac{1}{32}\pi*(0,30m)^3} = 5,93 \ N/mm^2 \qquad \text{Due to symmetry 50/50 divided}$$
over two stems

$$\sigma_{m,x,d} = \frac{M_{x,max}}{W} = \frac{17,2 \ kNm}{\frac{1}{32}\pi*(0,30m)^3} = 6,41 \ N/mm^2$$

$$f_{m,d} = k_{mod} * \frac{f_{m,k}}{\gamma_M} = 0,7 * \frac{24\frac{N}{mm^2}}{1,3} = 12,9 \ N/mm^2$$

$$k_m = 1 \qquad \text{Circular cross section}$$

$$U.C. = \frac{\sigma_{m,y,d}}{f_{m,d}} + k_m * \frac{\sigma_{m,x,d}}{f_{m,d}} = 0,96 \qquad \text{Requirement is fulfilled}$$

$$U.C. = k_m * \frac{\sigma_{m,y,d}}{f_{m,d}} + \frac{\sigma_{m,x,d}}{f_{m,d}} = 0,96 \qquad \text{Requirement is fulfilled}$$

Combined bending and compression:

$$U.C. = \left(\frac{\sigma_{c,0,d}}{f_{c,0,d}}\right)^2 + \frac{\sigma_{m,y,d}}{f_{m,d}} + k_m * \frac{\sigma_{m,x,d}}{f_{m,d}} = 0,97 \qquad \text{Requirement is fulfilled}$$

$$U.C. = \left(\frac{\sigma_{c,0,d}}{f_{c,0,d}}\right)^2 + k_m * \frac{\sigma_{m,y,d}}{f_{m,d}} + \frac{\sigma_{m,x,d}}{f_{m,d}} = 0,97 \quad \text{Requirement is fulfilled}$$

Combined bending and tension:

$$U.C. = \left(\frac{\sigma_{t,0,d}}{f_{t,0,d}}\right)^2 + \frac{\sigma_{m,y,d}}{f_{m,d}} + k_m * \frac{\sigma_{m,x,d}}{f_{m,d}} = 0,97 \quad \text{Requirement is fulfilled}$$

$$U.C. = \left(\frac{\sigma_{t,0,d}}{f_{t,0,d}}\right)^2 + k_m * \frac{\sigma_{m,y,d}}{f_{m,d}} + \frac{\sigma_{m,x,d}}{f_{m,d}} = 0,97 \quad \text{Requirement is fulfilled}$$

Shear:

$$\tau_{max} = \frac{4*V_{max}}{3\pi*r_{atconnection}^2} = \frac{4*14,0kN}{3\pi*(0,15m)^2} = 0,26 \; N/mm^2 \quad \text{(Hartsuijker, 2014)}$$

$$f_{v,d} = k_{mod} * \frac{f_{v,k}}{\gamma_M} = 0,7 * \frac{4\frac{N}{mm^2}}{1,3} = 2,15 \; N/mm^2$$

$$U.C. = \frac{\tau_{max}}{f_{v,d}} = 0,12 \qquad \qquad \text{Requirement is fulfilled}$$

Checks at root system:

Compression parallel to the grain:

$$\sigma_{c,0,d} = \frac{N_{-,max}}{A} = \frac{104,6 \; kN}{0,16 \; m^2} = 0,65 \; N/mm^2$$

$$f_{c,0,d} = k_{mod} * \frac{f_{c,0,k}}{\gamma_M} = 0,7 * \frac{21 \; N/mm^2}{1,3} = 11,3 \; N/mm^2$$

$$U.C. = \frac{\sigma_{c,0,d}}{f_{c,0,d}} = 0,06 \qquad \qquad \text{Requirement is fulfilled}$$

Bending:

$$\sigma_{m,y,d} = \frac{M_{y,max}/2}{W} = \frac{66,6 \; kNm/2}{\frac{1}{32}\pi*(0,45m)^3} = 3,68 \; N/mm^2 \qquad \text{Due to symmetry 50/50 divided}$$
over two stems

$$\sigma_{m,x,d} = \frac{M_{x,max}}{W} = \frac{7,7 \; kNm}{\frac{1}{32}\pi*(0,45m)^3} = 0,85 \; N/mm^2$$

$$f_{m,d} = k_{mod} * \frac{f_{m,k}}{\gamma_M} = 0,7 * \frac{24\frac{N}{mm^2}}{1,3} = 12,9 \; N/mm^2$$

$$k_m = 1 \qquad \qquad \text{Circular cross section}$$

$$U.C. = \frac{\sigma_{m,y,d}}{f_{m,d}} + k_m * \frac{\sigma_{m,x,d}}{f_{m,d}} = 0,35 \qquad \text{Requirement is fulfilled}$$

$$U.C. = k_m * \frac{\sigma_{m,y,d}}{f_{m,d}} + \frac{\sigma_{m,x,d}}{f_{m,d}} = 0,35 \qquad \text{Requirement is fulfilled}$$

Combined bending and compression:

$$U.C. = \left(\frac{\sigma_{c,0,d}}{f_{c,0,d}}\right)^2 + \frac{\sigma_{m,y,d}}{f_{m,d}} + k_m * \frac{\sigma_{m,x,d}}{f_{m,d}} = 0,35 \quad \text{Requirement is fulfilled}$$

$$U.C. = \left(\frac{\sigma_{c,0,d}}{f_{c,0,d}}\right)^2 + k_m * \frac{\sigma_{m,y,d}}{f_{m,d}} + \frac{\sigma_{m,x,d}}{f_{m,d}} = 0,35 \quad \text{Requirement is fulfilled}$$

D.6 FINITE ELEMENT MODEL

D.6.1 Single tree, after 31 years

Table D.9 Input parameters of FE model single tree

	Year 31
Material properties	
Modulus of elasticity parallel [N/mm²]	5.500
Modulus of elasticity perpendicular [1] [N/mm²]	367
Shear modulus [1] [N/mm²]	344
Poisson's ratio	0,0625
Geometrical properties	
Nodal support stiffness [kNm/rad]	Rigid
Height [m]	6,0
Circumference at bottom [m]	1,1
Circumference at top [m]	0,1
Angle with vertical [°]	0

The connection is modelled as a fully rigid circle with eight rigid members connected to the solid. The connection between the members and the solid is created, according to Dlubal RFEM recommendations, with a connecting cross. This consists of two crossing rigid members of 7cm, which is the size of the plastic feet of the designed connection. These feet can transfer in-plane forces due to the pressure and the friction between the tree and the feet. Out of plane, the feet can only transfer pressure forces. Figure D.3 illustrates how one of these connections is modelled. In total, the ring system has eight of these feet.
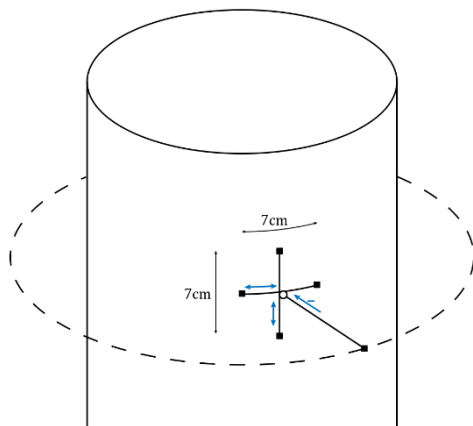
Figure D.3 Illustration of one connecting cross in ring system including the forces that can be transferred. In total there are eight of these connecting crosses in the ring system.

The results from the model should only be considered below a height of 2m. Above this height, a real tree starts branching, so the model does not correspond to reality.

ULS Checks

ULS 1 (self-weight and wind parallel):

Maximum allowable bending stress: $f_{m,d} = k_{mod} * \frac{f_{m,k}}{\gamma_M} = 0,7 * \frac{24\frac{N}{mm^2}}{1,3} = 12,9 \ N/mm^2$

Figure D.4 shows the bending stress due to the ULS 1 load. As explained, only the stem below a height of 2m should be considered, which is indicated with a dashed line. In general, the maximum bending stress is not exceeded. Just above and below the ring system connection, there are small spots where the maximum bending stress is exceeded. This is the result of introduced bending moments which are there due to the stiff connecting cross. It is expected that in the 'real' trees, the bending stress around the ring system is smaller because the ring feet are not entirely stiff, and the tree can adapt to applied loads by creating secondary growth.
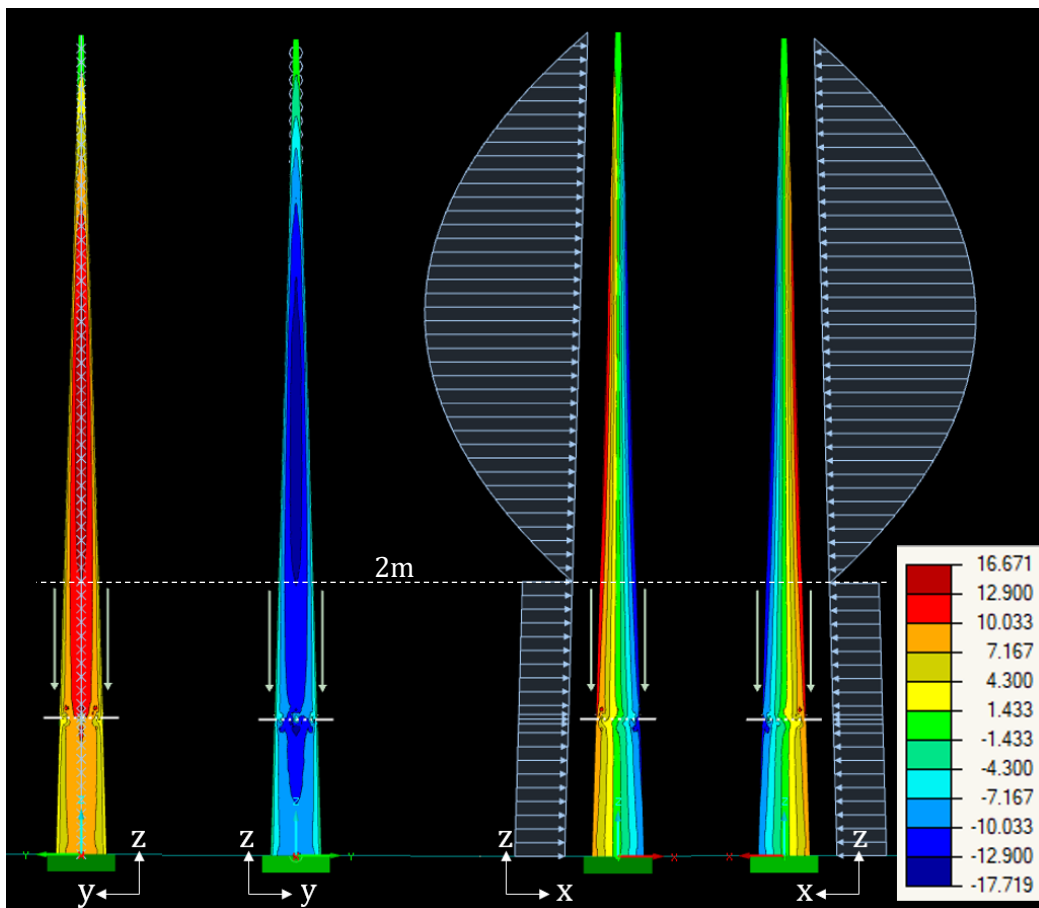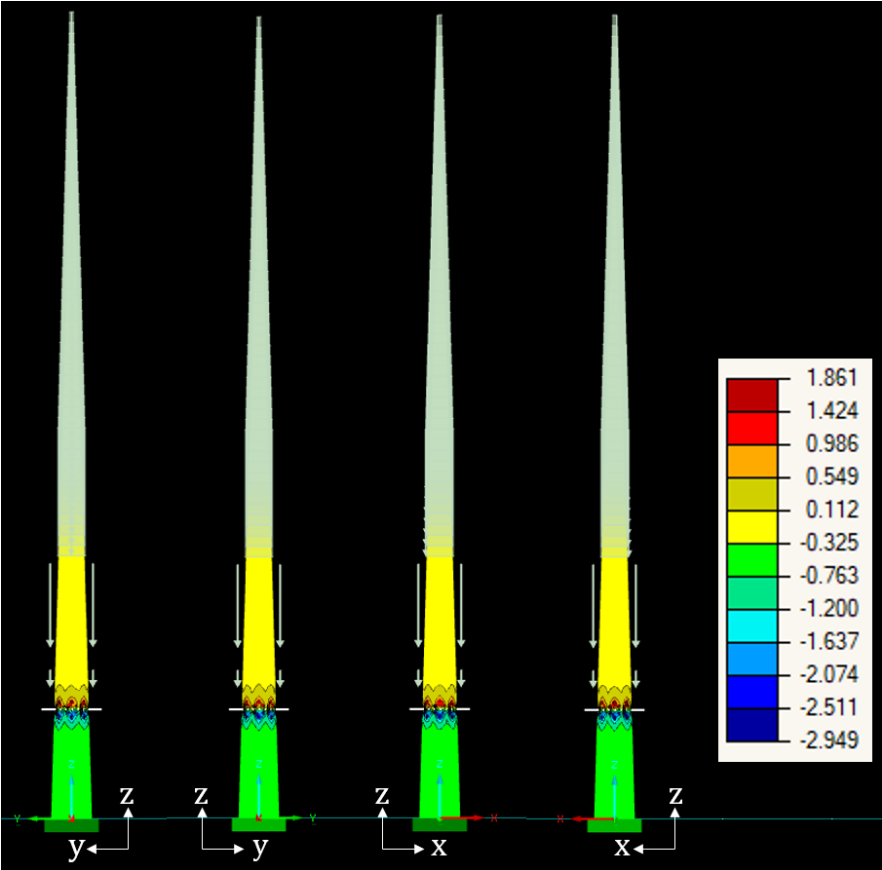

Figure D.4 FE results of bending stress due to ULS 1 (self-weight and wind parallel), shown for single tree year 31

ULS 2 (self-weight and wind perpendicular):

Maximum allowable bending stress: $f_{m,d} = k_{mod} * \frac{f_{m,k}}{\gamma_M} = 0,7 * \frac{24\frac{N}{mm^2}}{1,3} = 12,9 \, N/mm^2$

Figure D.5 shows the bending stress due to the ULS 2 load. Just as for ULS 1, the maximum bending stress is only exceeded at small locations around the ring system.
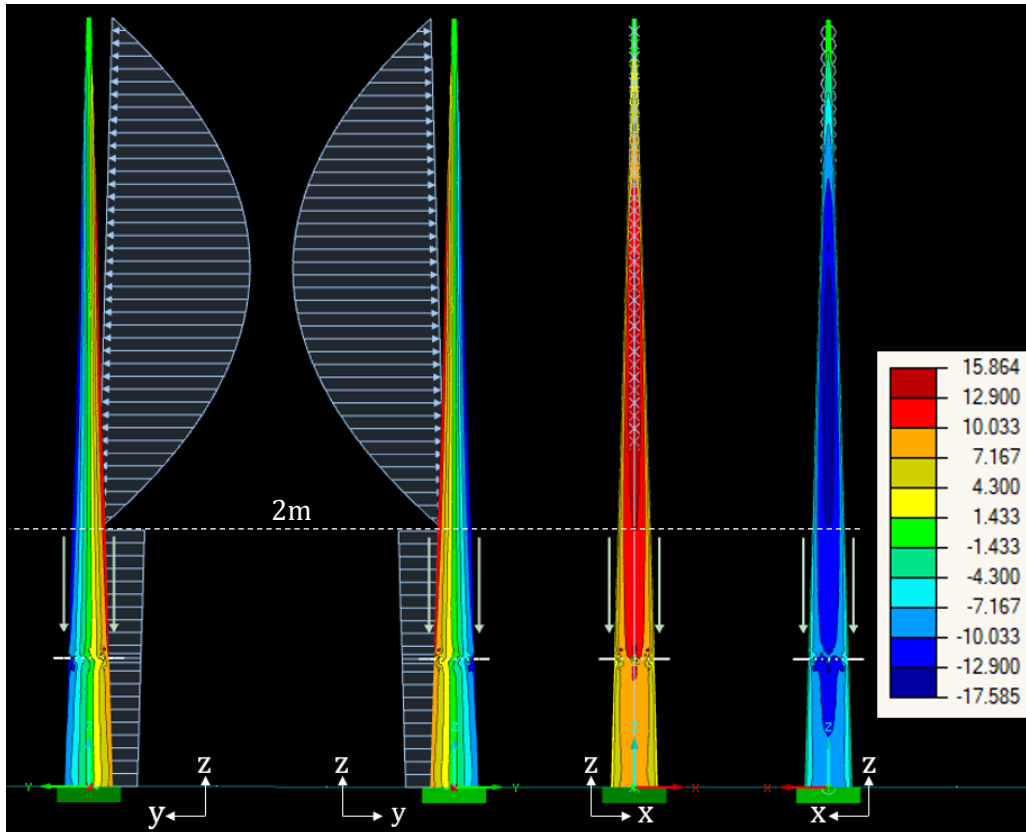
Figure D.5 FE results of bending stress due to ULS 2 (self-weight and wind perpendicular), shown for single tree year 31

ULS 3 (self-weight and snow):

Maximum allowable bending stress: $f_{m,d} = k_{mod} * \frac{f_{m,k}}{\gamma_M} = 0,7 * \frac{24\frac{N}{mm^2}}{1,3} = 12,9 \; N/mm^2$

Figure D.6 shows that the maximum allowable bending stress is not exceeded for ULS3.
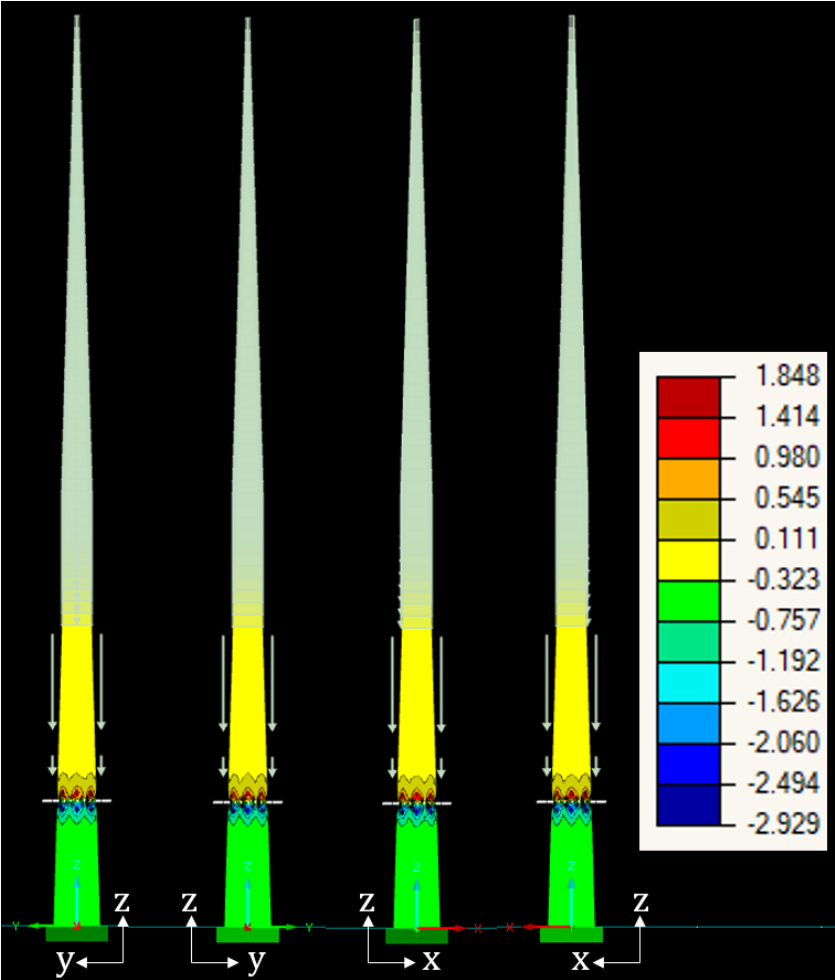
Figure D.6 FE results of bending stress due to ULS 3 (self-weight and snow), shown for single tree year 31

ULS 4 (self-weight and rain):

Maximum allowable bending stress: $f_{m,d} = k_{mod} * \frac{f_{m,k}}{\gamma_M} = 0,7 * \frac{24\frac{N}{mm^2}}{1,3} = 12,9\ N/mm^2$

Figure D.7 shows that the maximum allowable bending stress is not exceeded for ULS4.

Figure D.7 FE results of bending stress due to ULS 4 (self-weight and rain), shown for single tree year 31

ULS 5 (self-weight):

Maximum allowable bending stress: $f_{m,d} = k_{mod} * \frac{f_{m,k}}{\gamma_M} = 0,5 * \frac{24\frac{N}{mm^2}}{1,3} = 9,2\ N/mm^2$

Figure D.8 shows that the maximum allowable bending stress is not exceeded for ULS5.
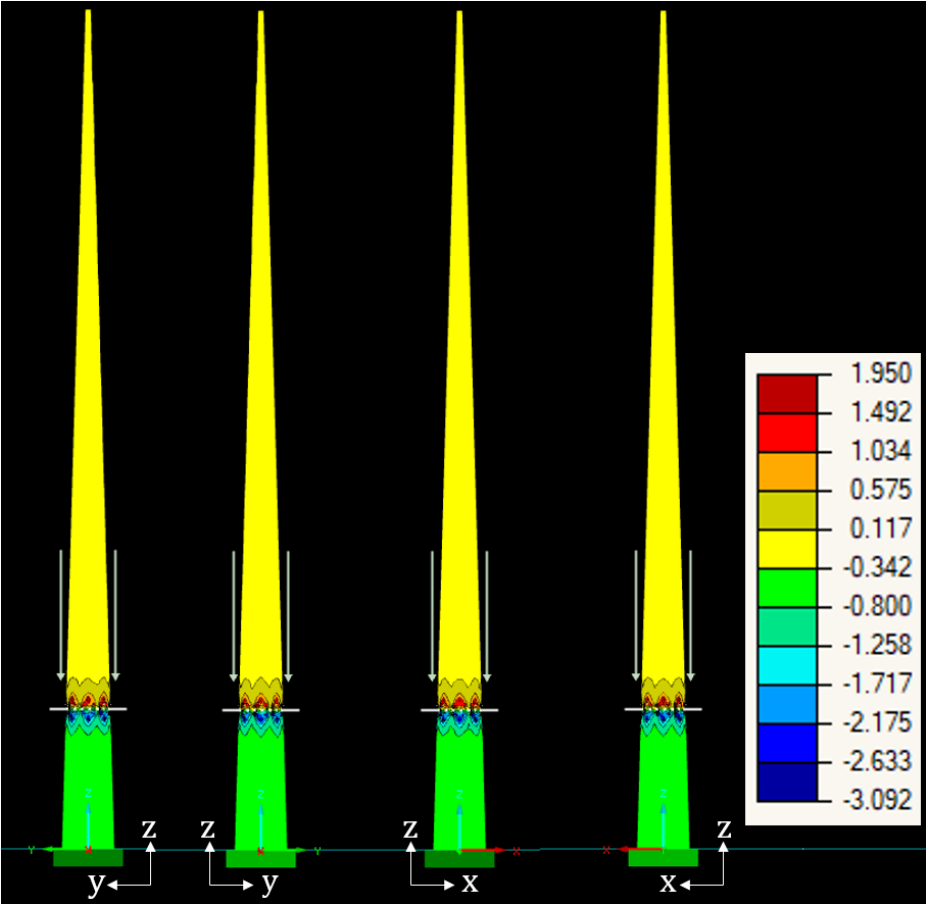
Figure D.8 FE results of bending stress due to ULS 5 (self-weight), shown for single tree year 31

SLS 1 (self-weight and wind parallel):

The deformation of the single tree with a rigid support is 5,6mm at the height of 1m. The model with a support stiffness of 24,4kNm/rad gives an error that the maximum number of iterations is performed without finding a stable result. At the last iteration, a deformation of 3,9m was shown at the height of 1m. This means that the tree would fall over if the SLS 1 load is applied.
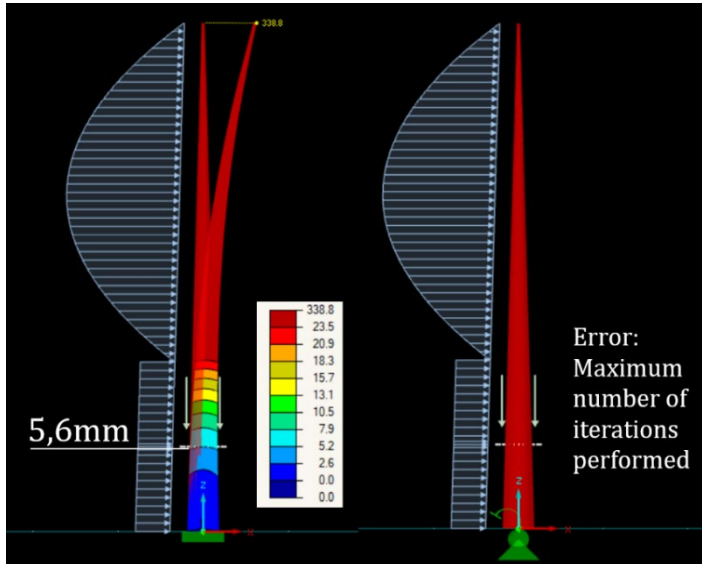
Figure D.9 FE results of deformation due to SLS 1 (self-weight and wind parallel), shown for single tree year 31. Left: rigid support. Right: Spring support with a stiffness of 24,4kNm/rad.

SLS 2 (self-weight and wind perpendicular):

The largest deformation is found for SLS 2. At 1m height, the deformation is 7mm if the tree has a rigid support. The model with a spring support shows the same error as for SLS 1, with a minimal displacement at 1m height of 4,9m.
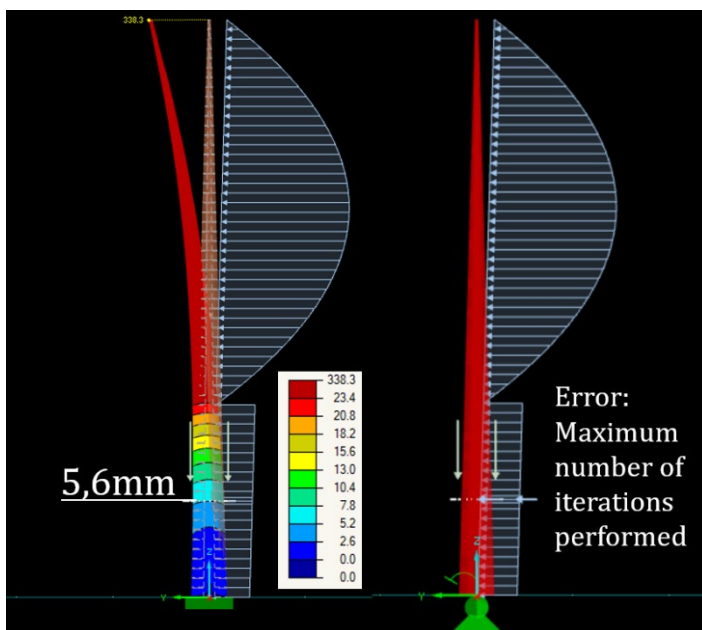
Figure D.10 FE results of deformation due to SLS 2 (self-weight and wind perpendicular), shown for single tree year 31. Left: rigid support. Right: Spring support with a stiffness of 24,4kNm/rad.

SLS 3 (self-weight and snow):

SLS 3 gives neglectable deformations for both models with a rigid support and with a rotational spring support.
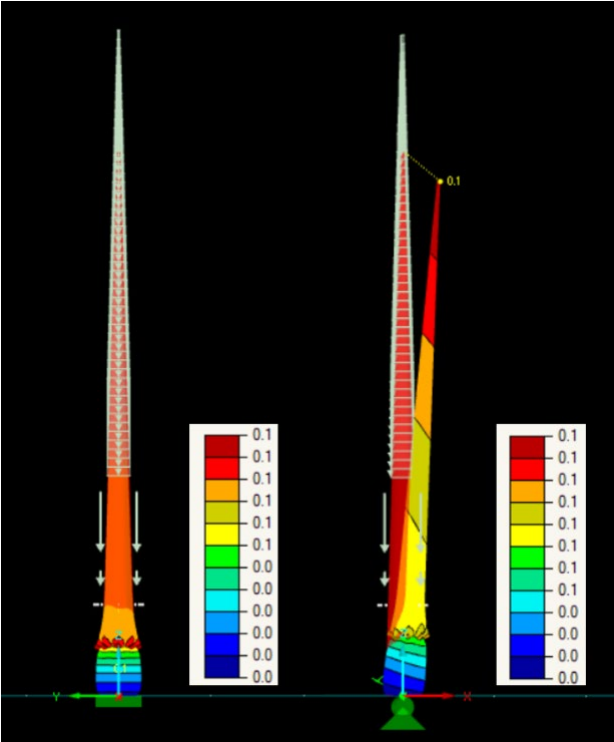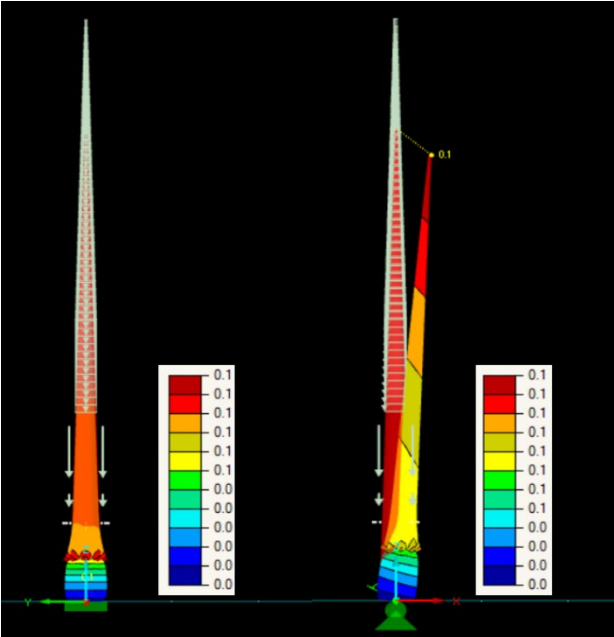

Figure D.11 FE results of deformation due to SLS 3 (self-weight and snow), shown for single tree year 31. Left: rigid support. Right: Spring support with a stiffness of 24,4kNm/rad.

SLS 4 (self-weight and rain):

SLS 4 gives neglectable deformations for both models with a rigid support and with a rotational spring support.

Figure D.12 FE results of deformation due to SLS 4 (self-weight and rain), shown for single tree year 31. Left: rigid support. Right: Spring support with a stiffness of 24,4kNm/rad.

D.6.2 Interconnected trees, after 43 years

Table D.10 Input parameters of FE model interconnected trees

	Year 43
Material properties	
Modulus of elasticity parallel [N/mm²]	5.500
Modulus of elasticity perpendicular [1] [N/mm²]	367
Shear modulus [1] [N/mm²]	344
Poisson's ratio	0,0625
Geometrical properties	
Nodal support stiffness [kNm/rad]	Rigid
Height [m]	6,0
Circumference at bottom [m]	0,43
Circumference at top [m]	1,33
Angle with vertical [°]	12,1
Distance between trees [m]	1,0

The two trees are modelled as solids and then, just like the finite element models of the *Living Tree Pavilion* trees, merged into a single solid.

A *Treehouse Attachment Bolt* ensures the connection of the trees with the plant containers. In the FE model, this is modelled with a rigid member of 20cm long, rigidly connected to the trees with a connecting cross. The loads from the plant containers are applied at this rigid member at 5cm distance from the tree.

To reduce the stress introduced in the tree by the rigid member, a cable is attached to the end of the bolt. 50 cm above the rod the cable is attached to the tree. An example of such system is shown in Figure 8.17 on the right.

The results from the model should only be considered below a height of 2m. Above this height, a real tree starts branching, so the model does not correspond to reality.

ULS Checks

ULS 1 (self-weight and wind parallel):

Maximum allowable bending stress: $f_{m,d} = k_{mod} * \frac{f_{m,k}}{\gamma_M} = 0,7 * \frac{24\frac{N}{mm^2}}{1,3} = 12,9 \; N/mm^2$

Figure D.13 shows that the maximum allowable bending stress is exceeded around the interconnection of the trees (darkest red and darkest blue). Argued can be that this is the result of incorrect modelling of the inosculation. The sudden change in slope gives bending stress. In real life, the tree will create a smoother inosculation, so the stresses become smaller. In the rest of the tree, the maximum bending stress is not exceeded.
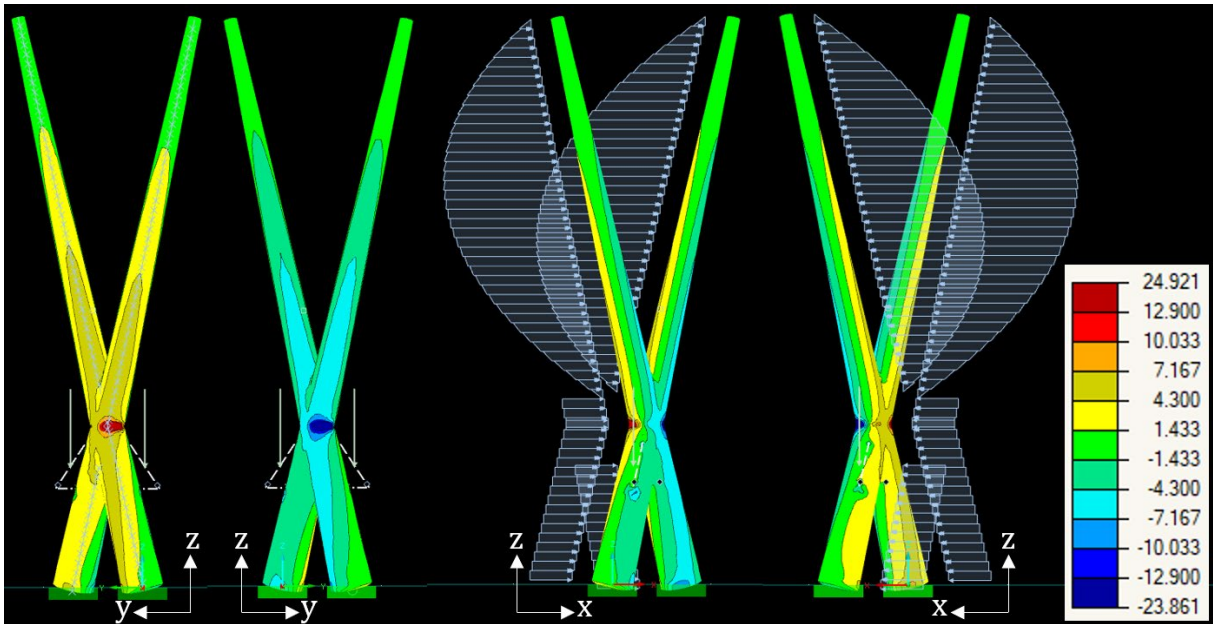
Figure D.13 FE results of bending stress due to ULS 1 (self-weight and wind parallel), shown for interconnected trees year 43

ULS 2 (self-weight and wind perpendicular):

Maximum allowable bending stress: $f_{m,d} = k_{mod} * \frac{f_{m,k}}{\gamma_M} = 0,7 * \frac{24\frac{N}{mm^2}}{1,3} = 12,9 \ N/mm^2$

Figure D.14 shows that the maximum allowable bending stress is exceeded around the inosculation of the trees (darkest red and darkest blue). The same discussion as for ULS1 holds.
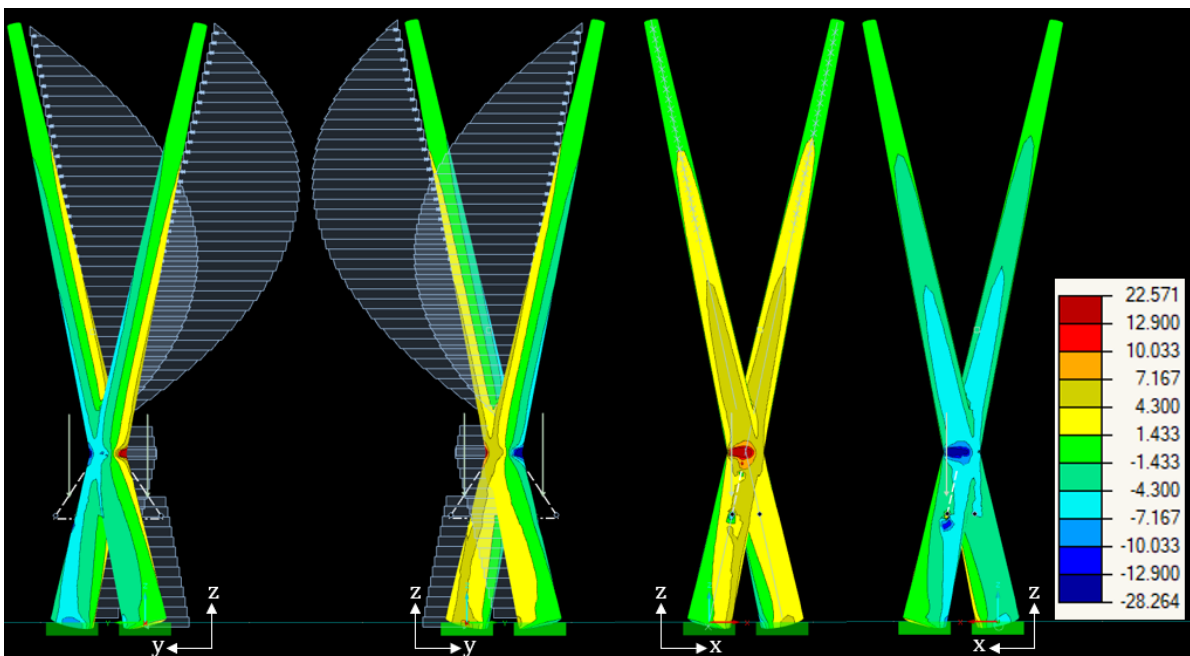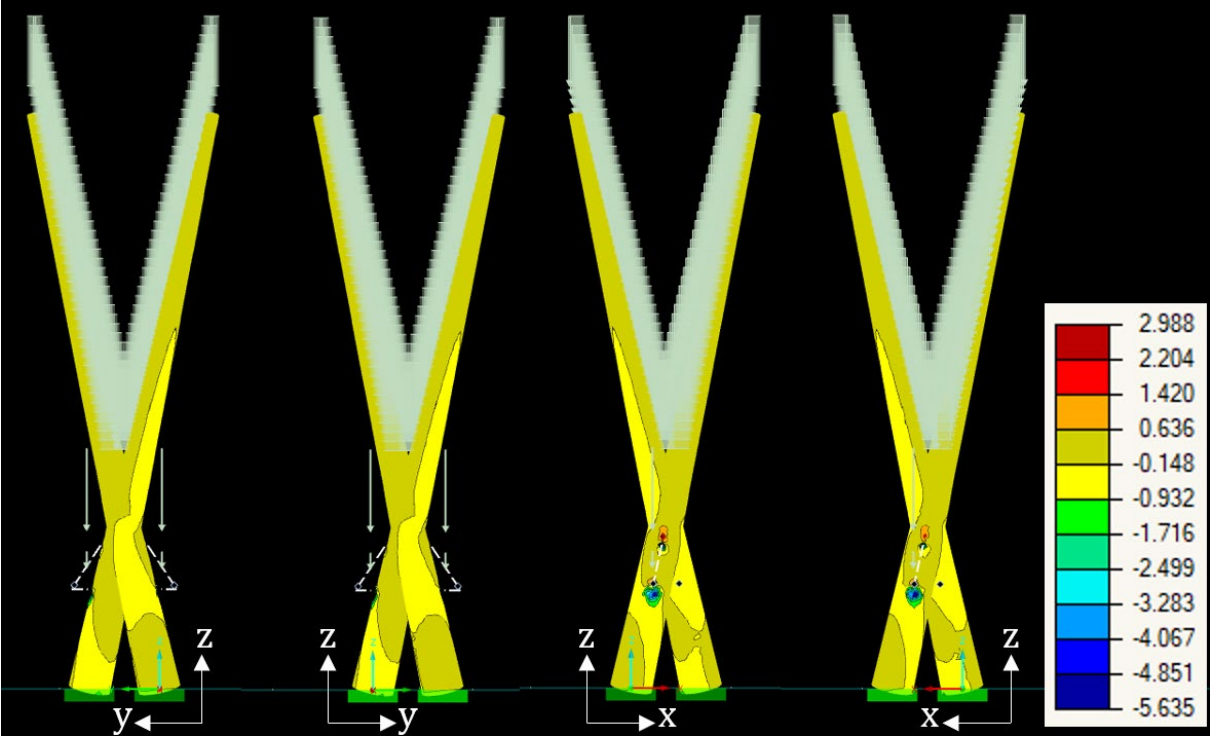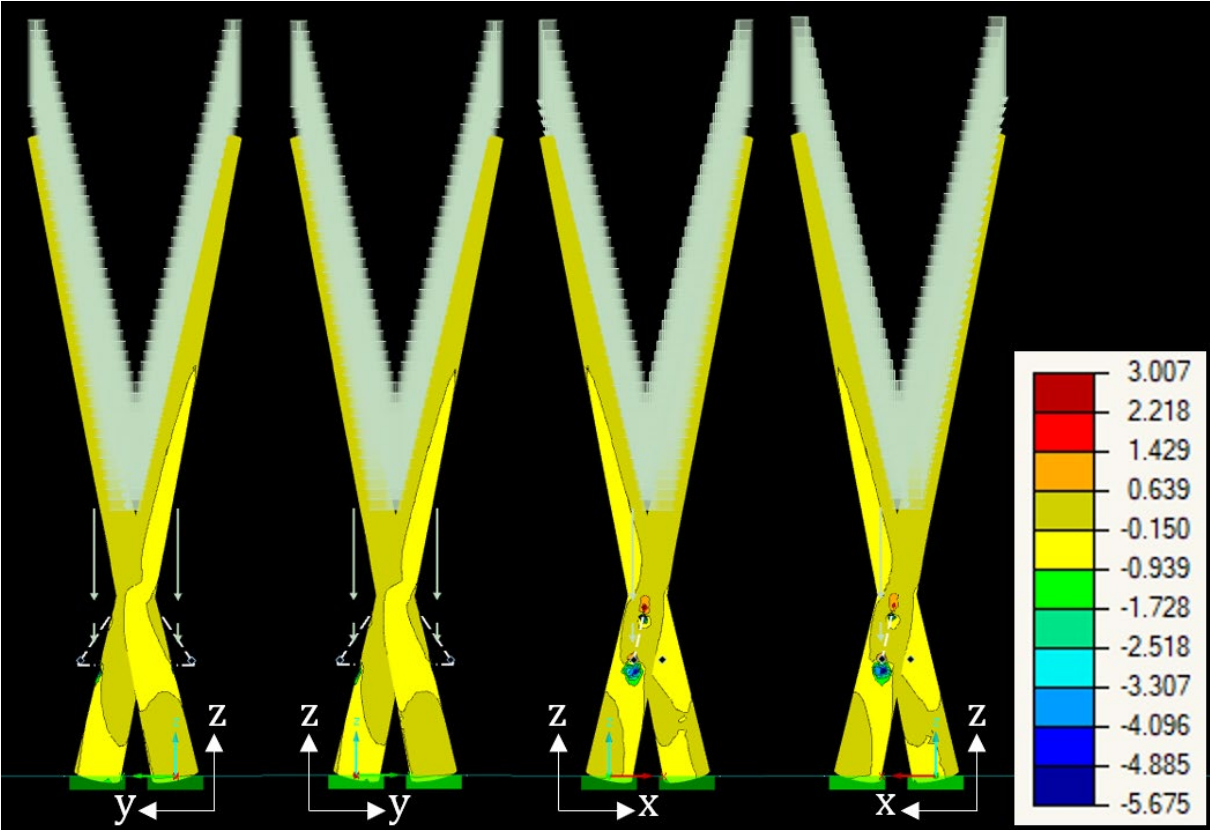

Figure D.14 FE results of bending stress due to ULS 2 (self-weight and wind perpendicular), shown for interconnected trees year 43

ULS 3 (self-weight and snow):

Maximum allowable bending stress: $f_{m,d} = k_{mod} * \dfrac{f_{m,k}}{\gamma_M} = 0{,}7 * \dfrac{24\frac{N}{mm^2}}{1{,}3} = 12{,}9 \; N/mm^2$

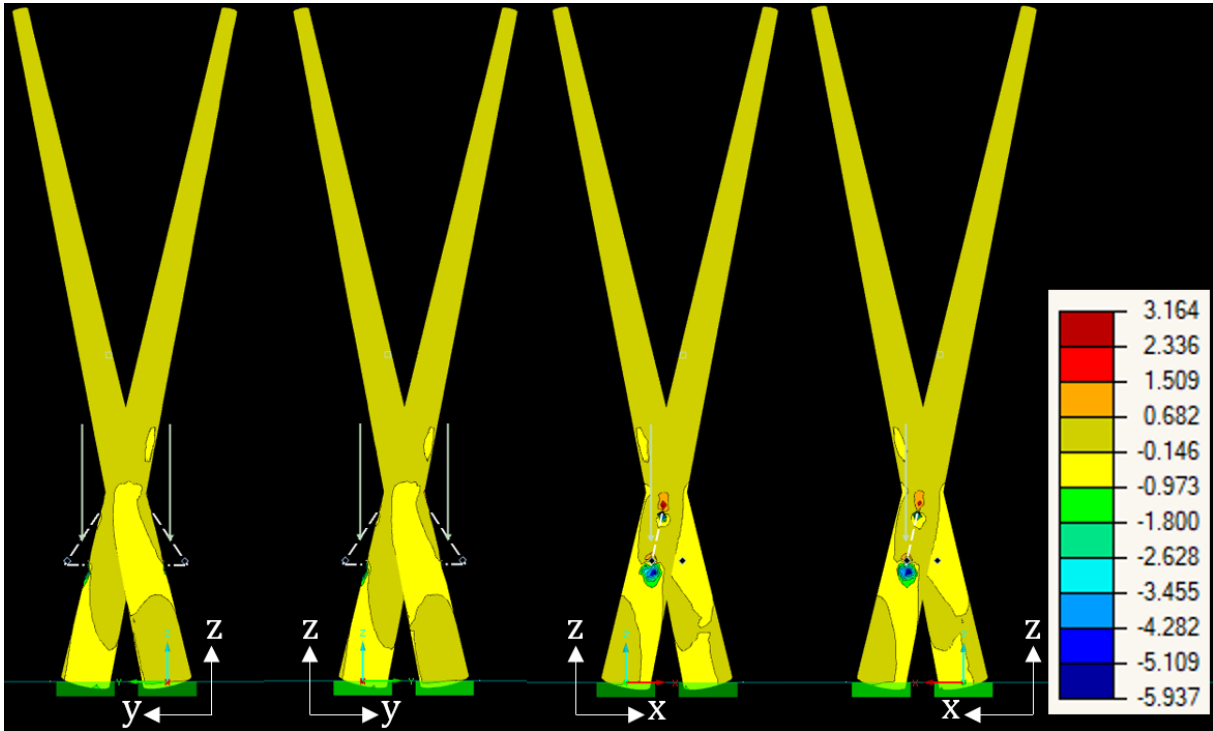Figure D.15 shows that the maximum allowable bending stress is not exceeded for ULS3.

Figure D.15 FE results of bending stress due to ULS 3 (self-weight and snow), shown for interconnected trees year 43

ULS 4 (self-weight and rain):

Maximum allowable bending stress: $f_{m,d} = k_{mod} * \frac{f_{m,k}}{\gamma_M} = 0,7 * \frac{24\frac{N}{mm^2}}{1,3} = 12,9 \ N/mm^2$

Figure D.16 shows that the maximum allowable bending stress is not exceeded for ULS4.

Figure D.16 FE results of bending stress due to ULS 4 (self-weight and rain), shown for interconnected trees year 43

ULS 5 (self-weight):

Maximum allowable bending stress: $f_{m,d} = k_{mod} * \frac{f_{m,k}}{\gamma_M} = 0.5 * \frac{24\frac{N}{mm^2}}{1.3} = 9.2 \ N/mm^2$

Figure D.17 shows that the maximum allowable bending stress is not exceeded for ULS5.

Figure D.17 FE results of bending stress due to ULS 5 (self-weight), shown for interconnected trees year 43

ULS special (self-weight and wind in opposite directions):

Maximum allowable bending stress: $f_{m,d} = k_{mod} * \frac{f_{m,k}}{\gamma_M} = 0.7 * \frac{24\frac{N}{mm^2}}{1.3} = 12.9 \ N/mm^2$

Figure D.18 shows that the maximum allowable bending stress is not exceeded for ULS special.
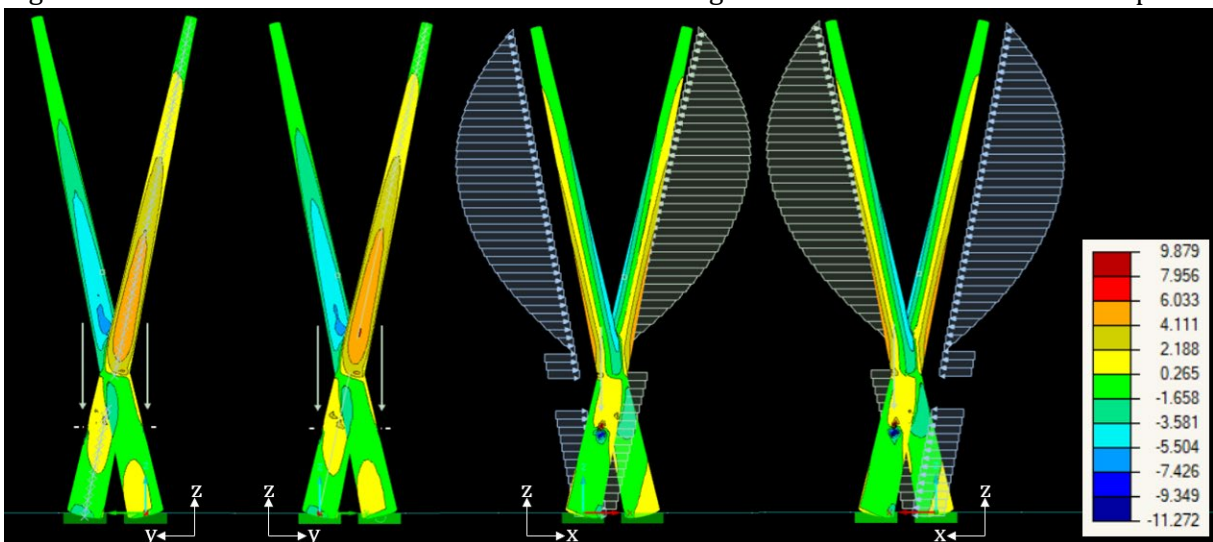
Figure D.18 FE results of bending stress due to ULS special (self-weight and wind in opposite directions), shown for interconnected trees year 43

SLS1 (self-weight and wind parallel):

The interconnected trees with a rigid support have a deformation of 4,5mm at the height of one meter. The model with a rotational spring support with a stiffness of 24,4kNm/rad has a deformation of 1,3 meters at the height of one meter.
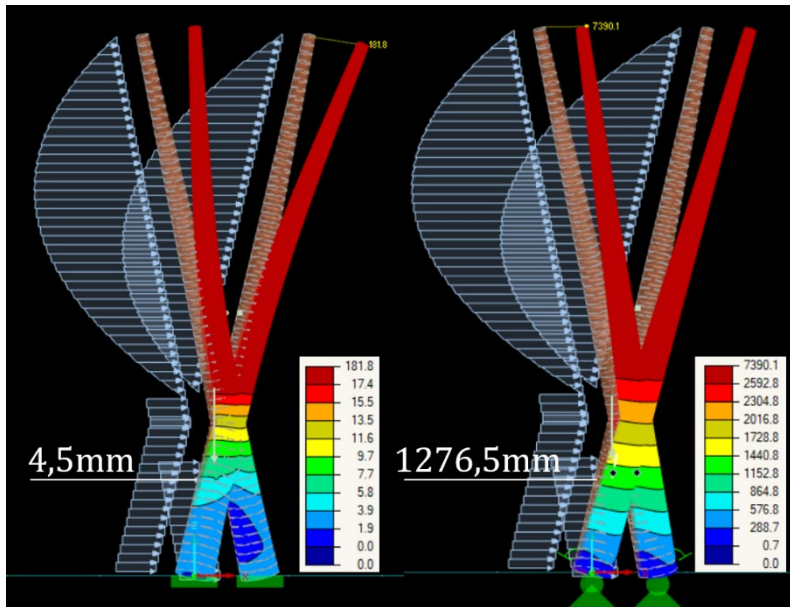

Figure D.19 FE results of deformation due to SLS 1 (self-weight and wind parallel), shown for interconnected trees year 43. Left: rigid support. Right: Spring support with a stiffness of 24,4kNm/rad.

SLS2 (self-weight and wind perpendicular):

The deformation at the connection to the plant container is 5,8mm in the model with a rigid support and almost 1,5m in the model with the spring support.
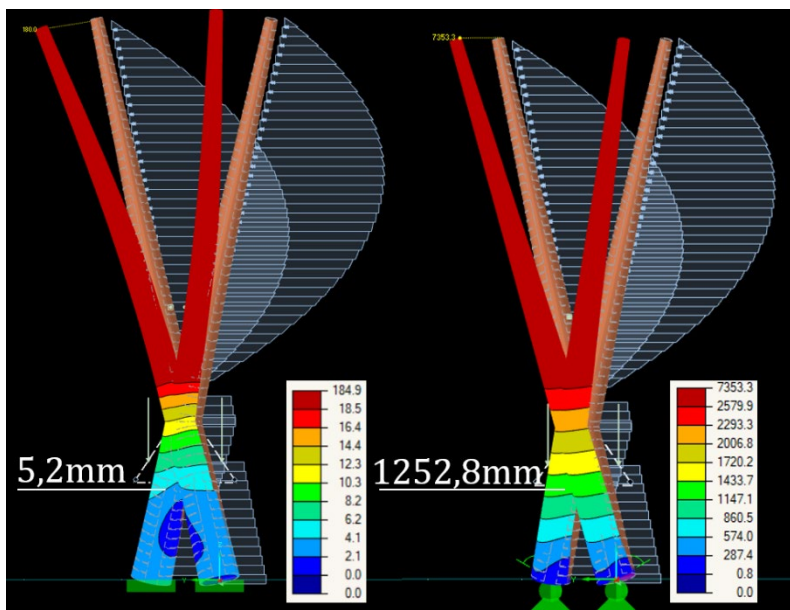

Figure D.20 FE results of deformation due to SLS 2 (self-weight and wind perpendicular), shown for interconnected trees year 43. Left: rigid support. Right: Spring support with a stiffness of 24,4kNm/rad.

SLS3 (self-weight and snow):

The deformation at one-meter height due to SLS3 is 0,4mm in the model with a rigid support and 0,9mm in the model with a spring support.
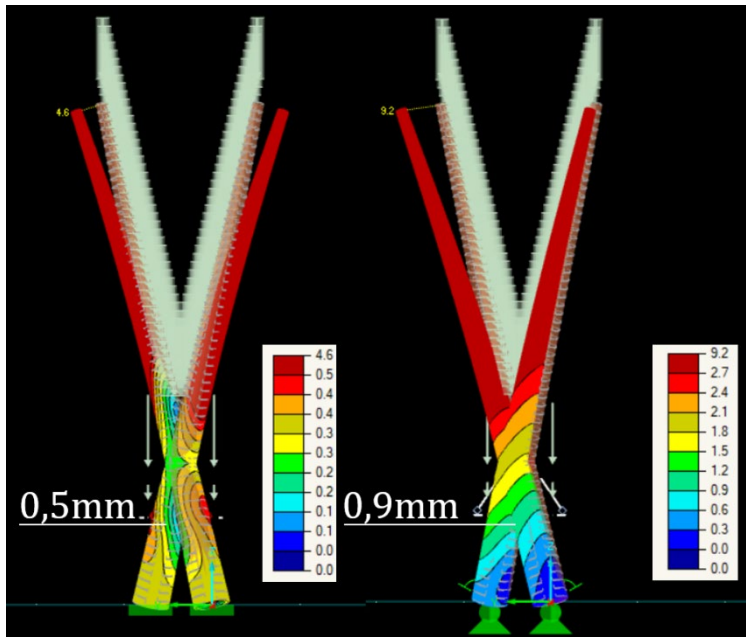

Figure D.21 FE results of deformation due to SLS 3 (self-weight and snow), shown for interconnected trees year 43. Left: rigid support. Right: Spring support with a stiffness of 24,4kNm/rad.

SLS4 (self-weight and rain):

The deformation at one-meter height due to SLS4 is 0,5mm in the model with a rigid support and 1,0mm in the model with a spring support.
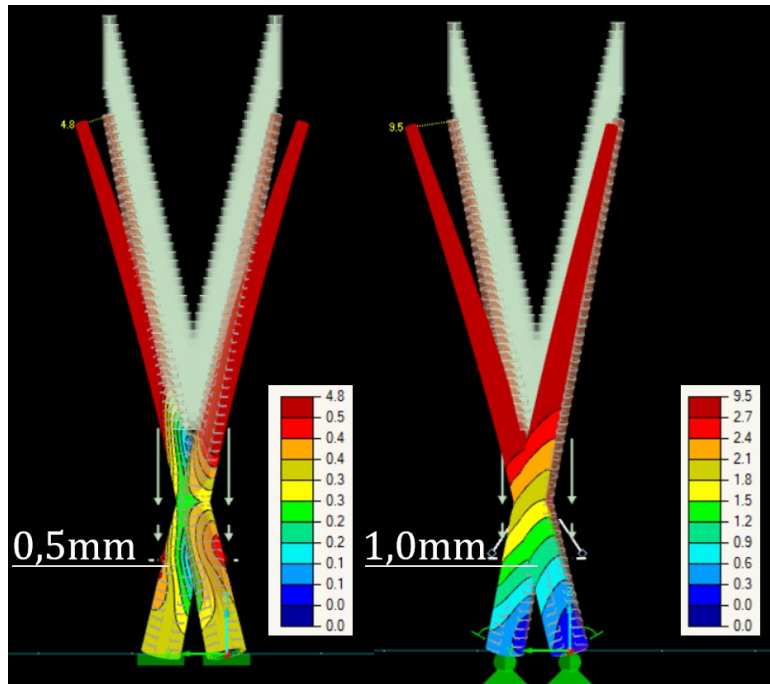

Figure D.22 FE results of deformation due to SLS 4 (self-weight and rain), shown for interconnected trees year 43. Left: rigid support. Right: Spring support with a stiffness of 24,4kNm/rad.